The University of Nottingham

UNITED KINGDOM · CHINA · MALAYSIA

Combining root architecture, root function and soil management to improve production efficiency and quality of apples

Magdalena Cobo Medina

Thesis submitted to the University of Nottingham for the degree of Doctor of Philosophy

November 2023

Abstract

Rootstock-induced dwarfing is a complex mechanism that causes a reduction in the size of the grafted scion by altering the floral and vegetative balance. Dwarfing rootstocks are essential to intensive production methods since they crop more and earlier. The impact of rootstock-induced dwarfing has previously been widely studied in scions but little is known about the role of dwarfing on root architecture. With the increase in food demand and climate change, it is essential to understand the impact of dwarfing on root architecture and how rootstocks can be optimised for both productivity and resilience to better adapt to future climate conditions.

Several QTL mapping studies have been conducted in apples to identify QTL linked to rootstock-induced dwarfing. However, the genetic basis of this complex trait remains unknown. A previous study which performed QTL mapping for root bark percentage, a trait associated with rootstock-induced dwarfing, identified three QTL named *Rb1*, *Rb2* and *Rb3* in Chromosomes 5, 11 and 13, respectively. In this thesis, fourteen SSR markers spanning *Rb1* and *Rb2* QTL were developed to fine-map these large QTL areas. The *Rb1* QTL region has been successfully reduced from 4.4 Mb to 2.2 Mb. Regarding *Rb2*, the analysis interestingly suggested that there were actually two QTL in that region, located between 6.9 Mb and 7.5 Mb, and between 10.9 Mb and 12.7 Mb. In addition, this thesis has generated useful markers linked to dwarfing that are currently used by breeders to accelerate the breeding process.

Another aspect of this thesis identified QTL for rooting ability using stoolbeds that colocalized with the dwarfing QTL. However, when winter hardwood cuttings were utilised no QTL were identified for rooting ability. This revealed that rooting ability in apples is impacted by dwarfing and/or the physiologically active processes associated with dwarfing. Furthermore, seedling root architecture was studied to determine if early selection of deep-rooted (and therefore more climate resilient) varieties is feasible. In this study, three QTL linked to primary root length in rootstock seedlings were identified. However, no correlation was found between the seedling root architecture and the grafted rootstocks propagated using stoolbeds. This indicates that for apples, seedlings are not a good tool for predicting future root architecture.

Lastly, a selection of these rootstocks with different levels of dwarfing were collected from stoolbeds, grafted with Gala and planted in rhizotrons to analyse root system architecture changes over a season. It was found that dwarfing rootstocks exhibited a reduced maximum root system depth and convex hull area compared to vigorous rootstocks at the end of the first growing season. The great variability of data, especially in the dwarfing group, suggested that either dwarfing genotypes are more susceptible to environmental factors or that there are other genes influencing root architecture, opening the possibility of decoupling dwarfing and root system architecture.

Root bark QTL fine mapping, together with the identification of rooting ability QTL colocalizing with the dwarfing QTL, and the root architectural responses to dwarfing, have advanced our understanding of the genetics and physiological processes occurring in dwarfing rootstocks and their root systems. In future investigations, more genetic markers spanning the refined QTL could be tested in the key genotypes generated in this study to further reduce the size of these areas. Moreover, the advances in the physiological understanding of dwarfing root systems will help to better design future experiments for QTL mapping of relevant root traits that will improve rootstock resilience in a changing climate.

Acknowledgements

First of all, I would like to thank my supervisors Dr Amanda Rasmussen at the University of Nottingham, Felicidad Fernandez at NIAB, Dr Richard Harrison formerly at NIAB and Dr Nicola Harrison at NIAB for giving me the opportunity to undertake this PhD. I am especially grateful to Dr Amanda Rasmussen for her continuous support during these years and for all the “virtual hugs” that have helped me better cope with the ups and downs of the PhD.

I would also like to thank Dr Amanda Karlstrom for all her help with the genetics and for her support not only as a colleague but as a friend. I additionally would like to thank all the temporary students who helped me with the phenotyping of thousands of roots.

A mis padres, Juan y Manoli, gracias por confiar siempre en mí y por vuestra inestimable ayuda. No me alcanzará la vida para agradeceros todo lo que hacéis por mí. Os quiero infinitamente. A mi hermano y cuñada, Juan Manuel y Mónica, por su apoyo y ánimo en los momentos difíciles, y en especial por darme a Adrián, el sobrino más maravilloso del mundo, cuya sonrisa ha animado mis tardes tristes.

Quiero dedicar un agradecimiento especial a mi marido, Antonio, por su apoyo incondicional, por estar a mi lado en cada paso y por alentarme a perseguir mis sueños. Gracias por cuidarme y motivarme en los días difíciles. Eres el compañero de vida perfecto.

Y por último, pero no menos importante, a mi hija, Claudia. Eres la alegría de mi vida y la que me da fuerzas para todo. La vida es mucho más bonita desde que llegaste.

Table of Contents

Chapter 1. General introduction 1

1.1 Apple and apple rootstocks 1

1.1.1 Overview of apple production 1

1.1.2 Origin of modern apples 1

1.1.3. Genomic resources in apple 2

1.1.4 Apple rootstocks 3

1.1.4.1 Benefits of the use of rootstocks 3

1.1.4.2 Rootstock-induced dwarfing 3

1.1.4.3 Main breeding programs and commonly used rootstocks 3

1.1.5 Rootstock-scion mechanisms that regulate dwarfing in apple rootstocks .. 5

1.1.5.1 Hormonal regulation 6

1.1.5.2 Water uptake and anatomical characteristics 10

1.1.5.3 Assimilates production and distribution 10

1.1.5.4 Nutrient uptake and distribution 12

1.1.6 Genetic control of rootstock-induced dwarfing in apples 13

1.2. Propagation methods in apple rootstocks 14

1.2.1 Sexual propagation method 14

1.2.2 Asexual propagation methods 15

1.2.2.1 Softwood cuttings 15

1.2.2.2 Hardwood cuttings 16

1.2.2.3 Micropropagation 17

1.2.2.4 Stooling and Layering 17

1.3. Root architecture 18

1.3.1 The impact of dwarfing rootstocks on root system architecture 19

1.3.2 Root systems as a breeding target for climate resilience 19

1.4. Challenges in understanding rootstock-induced dwarfing, root system architecture and breeding for resilience: Knowledge gaps 21

Chapter 2. Fine mapping the root bark QTL associated with rootstock-induced dwarfing in apple rootstocks 23

2.1 Introduction 23

2.2 Methods 25

2.2.1. Primers development and identification of dwarfing alleles 25

2.2.1.1. Single Sequence Repeat (SSR) detection 25

2.2.1.2. Primer design 27

2.2.1.3. DNA extraction, PCR amplification and DNA genotyping by capillary electrophoresis 28

2.2.1.4. Dwarfing allele identification using the M432 population (Dataset 1) 29

2.2.2. Primer selection and screening on interrelated apple rootstock families. 30

2.2.2.1 MCM rootstock families (Dataset 2) 30

2.2.2.2. Final primer selection and screening 31

2.2.2.3. Second batch of primers and screening 34

2.2.3. MCM families phenotyping and data analysis 36

2.2.3.1. Canopy and root bark measurements 36

2.2.3.2. Data analysis using MCM families 37

2.2.4 Process to identify the recombination event that occurred during the cross that generated M.27 38

2.2.4.1 MDX132 (Dataset 3) 38

2.2.4.2 SNP calling of rootstocks related to M.9 or M.27 (Dataset 4) 39

2.2.5. Rootstock material from breeding trials to further fine map the RB QTL. 39

2.2.5.1 Rootstocks from breeding trials (Dataset 5) 39

2.2.5.2 NH rootstock families (Dataset 6) 42

2.2.5.3 Data analysis for genotypes in datasets 5 and 6 43

2.3 Results 45

2.3.1. Identifying haplotypes linked to root bark using the M432 population (Dataset 1) 45

2.3.2. Fine mapping Step 1 - Recombination in M9 gamete in the M.13 x M.9 cross that generated M27 (Datasets 1, 3 and 4) 48

2.3.2.1 M.9 and M.27 dwarfing haplotypes 48

2.3.2.2 Using commercial rootstocks derived from M.9 or M.27 to confirm the M.9 to M.27 recombination hypothesis (Dataset 4) 50

2.3.3. Fine mapping Step 2 - MCM rootstock families (Dataset 2) 53

2.3.3.1 Dwarfing haplotype determination in the parents of the MCM families 53
2.3.3.2 Identification of recombinant genotypes in MCM rootstocks families 54
2.3.3.3 Useful recombinants in MCM rootstocks families 57
2.3.3.4 Fine mapping of Rb1 using MCM families 58
2.3.3.5 Fine mapping of Rb2 using MCM families 62
2.3.4 Fine mapping Step 3 - Rootstocks from the breeding trials (Dataset 5) ... 66
2.3.4.1 Fine mapping Rb1 and Rb2 using the recombinant genotypes found in the breeding trials 66
2.3.4.2 Recombination locations in the rootstocks from breeding trials 70
2.3.4.3 Summary of the recombinants in the breeding trials 74
2.3.5 Fine mapping Step 4 - NH families (Dataset 6) 75
2.3.5.1 Identification of recombinant genotypes in the NH families 75
2.3.5.2 Fine mapping Rb1 and Rb2 QTL using NH progenies 77
2.3.6 Marker validation using rootstocks from the breeding trials 80
2.3.7 Effect of scion on root bark percentage 82
2.4 Discussion 85
2.4.1 Fine mapping of RB QTL associated with rootstock-induced dwarfing 85
2.4.1.1 Fine mapping Rb1 QTL 85
2.4.1.2 Fine mapping Rb2 QTL 88
2.4.2 Validation of the dwarfing markers developed for this study 92
2.4.3 Effect of scion on root bark percentage 94
2.5 Conclusion 94
Chapter 3. Investigating links between seedling roots, adventitious rooting and dwarfing using QTL mapping 95
3.1 Introduction 95
3.2 Methods 97
3.2.1. Plant material and genotypic data 97
3.2.3. Floating seedlings experiment 97
3.2.4. Rootstock propagation experiment 99
3.2.5. Hardwood cuttings experiment 100
3.2.6. QTL analysis 102

3.2.7. Haploblock analysis 102
3.2.8. Correlation analysis 103
3.2.9. Analysis of the root bark QTL effects on root traits 103

3.3 Results 104

3.3.1 QTL identification 104

3.3.1.1 Identification of QTL associated with root architecture in floating seedlings 104

3.3.1.2 Identification of QTL associated with rooting ability in stoolbeds 104

3.3.1.3 Identification of QTL associated with rooting ability in hardwood cuttings 104

3.3.2 Haploblock analysis 105

3.3.2.1 Haploblock analysis for primary root length in floating seedlings 105

3.3.2.2 Haploblock analysis for rooting ability in the stoolbeds 106

3.3.3 Correlation between rooting traits in the MDX132 progeny 108

3.3.4 Effect of RB QTL on rooting ability in the seedlings' root architecture and the hardwood cuttings experiment 110

3.4 Discussion 112

3.4.1. *Rb1* QTL associated with rootstock-induced dwarfing colocalizes with a QTL identified for rooting ability in the stoolbeds 112

3.4.2. Identification of QTL associated with primary root length in rootstock seedlings 113

3.4.3. Impact of dwarfing on seedlings root architecture, stoolbeds rooting ability and hardwood cutting propagation 114

3.4.4. Other factors influencing rooting in the different propagation methods . 116

3.5 Conclusion 116

Chapter 4. Effect of dwarfing on root system architecture in apple rootstocks 117

4.1 Introduction 117

4.2 Methods 119

4.2.1. Genotyping 119

4.2.2. Lifting stoolbeds and rooting phenotyping in 2020 119

4.2.3. Genotype selection for root architecture experiment 119

4.2.4. Root system architecture rhizoboxes 120
4.2.5. Initial phenotyping 120
4.2.6. Canopy phenotyping and imaging 121
4.2.7. Final phenotyping 121
4.2.8. Imaging analysis 123
4.2.9. Statistical analysis 126
4.3. Results 128
4.3.1. Effect of RB QTL on rootstock traits before planting 128
4.3.2. Effect of RB QTL on canopy traits during the first growing season 129
4.3.2.1. Tree height 129
4.3.2.2. Trunk diameter above the graft union 131
4.3.2.3. Trunk diameter below the graft union 133
4.3.3. Effect of root bark QTL on root traits 137
4.3.3.1. Effect of RB QTL on total root length (TRL) 137
4.3.3.2. Effect of RB QTL on maximum root diameter 138
3.3.3.3. Effect of RB QTL on mean root diameter 140
4.3.3.4. Effect of RB QTL on the total root system depth 142
4.3.3.5. Effect of RB QTL on convex hull area (chull area) 143
4.3.4. Principal component analysis 146
4.3.5. Root bark percentage, canopy and root wet weight and root-to-shoot wet ratio 151
4.3.6. Correlation analysis 155
4.4 Discussion 157
4.4.1. Initial root surface area 157
4.4.2. Canopy traits analysis 157
4.4.3. Root traits analysis 158
4.4.4. Final phenotyping analysis 162
4.4.5. Correlation analysis 163
4.5 Conclusion 164
Chapter 5. General discussion 165
5.1 Key findings 165
5.2 Future directions 169

5.2.1. Use of SNP markers and *Rb3* to further fine map the root bark QTL 169
5.2.2. QTLseq analysis to further fine map the root bark QTL 170
5.2.3. QTL mapping for rooting ability in apple rootstocks 170
5.2.4. QTL mapping for root traits in apple rootstocks..... 170
5.2.5. Investigating how the scion-rootstock interaction impacts root morphology and physiology in apple rootstocks in the context of dwarfing..... 171
5.2.6. Impact of mycorrhizal inoculation on nutrient uptake and root system architecture..... 172

References 173

Supplementary data 206

List of Figures

Chapter 1

Figure 1.1 Apple rootstocks classified in the six traditionally used dwarfing categories……page 5
Figure 1.2 Diagram describing the hormonal interactions between rootstock and scion that may explain rootstock-induced dwarfing ……..…page 9

Chapter 2

Figure 2.1 Diagram summarising the six datasets used in the fine mapping of the RB QTL and details about the main use of each dataset.…..…page 25
Figure 2.2 Rootstock pedigree used for variant calling ……..…page 25
Figure 2.3 Root bark percentage QTL map using M432 population (M.27 x M.116). Markers found to be most significantly linked by are shown in bold……..…page 27
Figure 2.4 Root segments after removing a ring of bark. Green arrow pointing to the area where the stele of the root remains.……..……..page 36
Figure 2.5 Diagram showing key SNP distribution delimiting the *Rb1* and *Rb2* QTL original regions (blue) and the reduced regions (purple) after visually inspecting recombinant genotypes from M432 population. ……. page 46
Figure 2.6 Summary of allele sizes in 6 non-recombinant individuals with unambiguous dwarfing (top) vs non-dwarfing (bottom) phenotypes from the M432 (M.27 x M.116) population for the five SSR markers in the *Rb1* region (Chr5) developed in this study. ……..... page 47
Figure 2.7 Summary of allele sizes in 6 non-recombinant individuals with unambiguous phenotypes, dwarfing (top) vs non-dwarfing (bottom) from the M432 (M.27 x M.116) population for the three SSR markers in the *Rb2* region (Chr11) developed in this study…..……..…page 48
Figure 2.8 Allele segregation, phase and position in the genome of the SNPs from the M432 and MDX132 populations in the *Rb1* QTL region. SNPs in common highlighted in blue……..…page 49

Figure 2.9 Expected haplotypes for M.16 and M.9, parents of M.26. In blue, the section that matches the M27 dwarfing haplotype estimated from the M432 population……..……..….page 51
Figure 2.10 Expected haplotypes for R5 and Ottawa 3, parents of M.200. In blue, the section that matches the M.27 dwarfing haplotype estimated from the M432 population……..……..….page 51
Figure 2.11 Expected haplotypes for R5 and M.9, parents of G.30. In blue, the section that matches the M.27 dwarfing haplotype estimated from the M432 population……..……..….page 52
Figure 2.12 Expected haplotypes for M.27 and R5, parents of G.41. In blue, the section that matches the M.27 dwarfing haplotype estimated from the M432 population……..……..….page 53
Figure 2.13 Estimated haplotypes in the parents of MCM families showing allele sizes for all the markers used in this study…..……..……..….page 54
Figure 2.14 Drawing showing genotypes with a recombination event in the *Rb1* QTL region, the RB % at a 7.5 mm root, trunk diameter, tree height, number of roots collected and their estimated dwarfing level based on all the phenotypic information.……..……..….page 61
Figure 2.15 . Drawing showing genotypes with a recombination event in the *Rb2* QTL region, the RB % at a 7.5 mm root, trunk diameter, tree height, number of roots collected and their estimated dwarfing level based on all the phenotypic information..……..……..….page 65
Figure 2.16 Root bark percentage of recombinant genotypes and controls from plot RF185……..……..……..….page 67
Figure 2.17 Root bark percentage of recombinant genotypes and controls from plot EE207……..……..……..….page 68
Figure 2.18 Root bark percentage of recombinant genotypes and controls from plot SP250……..……..……..….page 70
Figure 2.19 Estimated haplotypes of the recombinant rootstocks identified in plots RF185 and SP250 showing allele sizes for all the markers used in this study……..page 72
Figure 2.20 Estimated haplotypes of the recombinant rootstocks identified in the EE207 plot showing allele sizes for all the markers used in this study……..….page 73

Figure 2.21 Fine mapping summary using the recombinant genotypes from breeding trials……..……..……..….page 75
Figure 2.22 Drawing showing genotypes with a recombination event in the *Rb1* QTL region (top) and *Rb2* QTL region (bottom), the RB % at a 7.5 mm root, tree height, number of roots collected and their estimated dwarfing level based on all the phenotypic information……page 79
Figure 2.23 Effect of scion on root bark percentage in rootstocks planted at the breeding plot EE207…….……..….page 82
Figure 2.24 Effect of scion on root bark percentage in rootstocks planted at the breeding plot EE207……..……..….page 83
Figure 2.25 Diagram showing the approximate location of *Dw2/Rb2* according to different authors……...……..……..….page 91

Chapter 3

Figure 3.1 A and B: Two MDX132 floating seedlings with different root architecture. C: Cropped seedling image with the main root highlighted in yellow. D: Seedling image converted into an 8-bit image ready to measure total root surface area.…….page 98
Figure 3.2 Stoolbed lifting process. A: Stoolbeds in the field. B: Rooted shoots carefully unearthed. Panel C: Phenotyping of rooted shoots from a particular genotype……...….page 100
Figure 3.3 A: Hardwood cuttings from the MDX132 family randomly distributed in the two heated bins. B: Genotype bundles of rooted cuttings after spending 6 weeks in the heated bins ready for phenotyping…….……page 101
Figure 3.4 Estimated percentage of deviation from the mean for the haplotypes in the most significant haploblocks, HB30 in linkage group 1, HB5 in linkage group 2 and HB26 in linkage group 17, associated with primary root length in the seedlings from the MDX132 population..……..page 106
Figure 3.5 Estimated percentage of deviation from the mean for the haplotypes in the most significant haploblocks, HB8 at linkage group 5 and HB26 at linkage group 11, associated with rooting ability in the stoolbeds in the MDX132 population……..….page 107

Figure 3.6 A: Correlation matrix showing Spearman's correlation coefficient of the phenotypic data from the hardwood cutting experiment traits B: Correlation matrix showing Spearman's correlation coefficient of the phenotypic data from the root architecture traits in the seedlings and the root architecture traits measured in the last time point of the rhizotrons experiment detailed in Chapter 4..……..page 109

Chapter 4

Figure 4.1 Details of the root system architecture experiment. A: Rhizoboxes in the glasshouse compartment. B: Image of a rooted rootstock collected from stoolbeds. C: Custom-made imaging rig used for root systems phenotyping. D: Root systems from vigorous (left) and dwarfing (right) genotypes at the end of the experiment….page 122
Figure 4.2 Diagram representing some of the root measurements taken from apple rootstocks grown in rhizoboxes……..….page 124
Figure 4.3 The imaging analysis pipeline detailing the steps and programs used during the imaging analysis of the root architecture traits in the MDX132 population (GD x M.9 cross)……..…….page 125
Figure 4.4 Effect of dwarfing on initial root surface area in rootstocks collected from stoolbeds……..…….…….page 129
Figure 4.5 Tree height of apple trees with different combinations of root bark QTL per time point……...page 131
Figure 4.6 Trunk diameter above the graft union of apple trees with different combinations of root bark QTL per time point……..…….page 133
Figure 4.7 Trunk diameter below the graft union of rootstocks with different combinations of root bark QTL per time point……..….page 134
Figure 4.8 Total root length (square transformed) of grafted rootstocks with different combinations of root bark QTL per time point…..……..….page 138
Figure 4.9 Maximum root diameter of grafted rootstocks with different combinations of root bark QTL per time point.……...page 140
Figure 4.10 Mean root diameter (logarithmically transformed) of grafted rootstocks with different combinations of root bark QTL per time point…..……...page 141
Figure 4.11 Maximum root system depth of grafted rootstocks with different combinations of root bark QTL per time point.……..….page 143

Figure 4.12 Total convex hull area of grafted rootstocks with different combinations of root bark QTL per time point……..……..…….page 144
Figure 4.13 Biplots of the principal component analysis (PCA) of 5 root traits from 39 genotypes in rhizoboxes with different combinations of root bark QTL per time point……..…….page 148
Figure 4.14 Principal component analysis of 5 root traits among 39 apple rootstock genotypes grown in rhizoboxes per time point.…..…….page 149
Figure 4.15 Effect of root bark QTL on; A: Root bark percentage, B: Wet canopy weights, C: Wet root weights and D: Root-to-shoot ratios……..page 153
Figure 4.16 Correlation matrix showing Spearman's correlation coefficients of initial root surface area, root bark percentage, canopy and root wet weight and for all the root and canopy traits at the end of the experiment……..……..…….page 156

Supplementary Figures

S1 Estimated haplotypes of M.13, Ottawa 3 and non-recombinant rootstocks from RF185 and SP250 plots showing allele sizes for markers included the first multiplex developed in this study……....page 207
S2 Estimated haplotypes of non-recombinant rootstocks from EE207 and VF224 plots showing allele sizes for markers included the first multiplex developed in this study...……..…….page 208

List of Tables

Chapter 2

Table 2.1 Parentage, number of seeds sown, seed germinated and surviving trees of the MCM rootstock populations……..…page 30

Table 2.2 Genome positions, primer sequences, amplicon range (in MCM families), repeat motif, fluorescent dye and multiplex for PCR for the first eight SSR markers used to genotype the MCM rootstock populations…….……..…page 33

Table 2.3 Genome positions, primer sequences, amplicon range (in MCM families), repeat motif, fluorescent dye and multiplex for PCR for the second batch of SSR markers used to genotype the MCM rootstock populations.…….……page 35

Table 2.4 Location, planting year, parentage and number of trees sampled per scion from trials RF185, VF224, EE207 and SP250 that were used to fine-map the root bark QTL……page 41

Table 2.5 Family name, pedigree and number of seedlings of the new pre-existing progenies examined to identify further recombinants……..…page 43

Table 2.6 Parentage and dwarfing degree of rootstocks used for SNP analysis in Chromosome 5 QTL region to test the recombination hypothesis……..…page 50

Table 2.7 Family name, parentage, number of seedlings, percentage of outcrosses, final number of seedlings and recombinants in *Rb1* and *Rb2* regions in the rootstock populations after screening the first batch of markers……..……..…page 56

Table 2.8 Family name, newly coded name, parentage and number of useful recombinants in *Rb1* and *Rb2* QTL regions in each rootstock population…...…page 57

Table 2.9 Family name, parentage, number of seedlings, percentage of outcrosses, final number of seedlings and total number of recombinant genotypes and useful recombinant genotypes in *Rb1* and *Rb2* QTL regions for the NH seedlings…..page 76

Table 2.10 . Predicted vigour versus actual vigour of rootstocks from the breeding trials according to the presence or absence of the *Rb1* and *Rb2* haplotypes.…page 81

Table 2.11 Type III analysis of variance table for fixed effects of the root bark percentage analysis in EE207 and SP250 plots. Significant p-values in bold…….……..…page 84

Chapter 3

Table 3.1 QTL table summarising the location of the QTL, 2lnBF, QTL region and variance explained by each QTL for primary root length in seedlings and percentage of rooting in 2019 and 2020……..…page 105
Table 3.2 Summary table of the means and ANOVA of primary root length and total root surface area in seedlings; percentage of rooted cuttings, average numbers of roots and root length in cuttings per fixed variable……..……..…page 111

Chapter 4

Table 4.1 Number of genotypes in each dwarfing class based on the presence or absence of the *Rb1* and *Rb2* QTL and the predicted vigour...……..…page 120
Table 4.2 Summary table of the means and ANOVA of tree height, trunk diameter above graft union and tree diameter below graft union per fixed variable including *Rb1*, *Rb2*, time point, block and interactions.……..…page 135
Table 4.3 Summary table of the means and ANOVA of total root length, maximum root diameter, mean root diameter, root system depth and total convex hull area per fixed variable including Rb1, Rb2, time point, block and their interactions.……page 145
Table 4.4 Eigenvalues, percentage of variance explained by each PC and cumulative variance per time point. For each trait, the largest variable loading score crossing the two components appears in bold ……..…..…page 150
Table 4.5 Summary table of statistics for the first two PC of root traits affected by the *Rb1*, *Rb2*, *Rb1* x *Rb2* interaction and block per time point ……..……..…page 151
Table 4.6 Summary table of the means and ANOVA of root bark percentage, wet canopy weight, wet root weight and root-to-shoot ratio per fixed variable including *Rb1, Rb2,* block and *Rb1 x Rb2* interaction ……page 154

Supplementary Tables

S1 Rootstocks cultivars and selections from breeding trials RF185, EE207, SP250 and VF224 used for fine mapping the root bark QTL, scion grafted, root bark percentage, standard deviation and dwarfing level based on the evaluation of breeders.……page 209
S2 Estimated marginal means (EMMs) for linear mixed model of each rootstock per scion for root bark percentage in trial EE207……page 211
S3 Comparison test between scions within each rootstock for root bark percentage in trial EE207……..……...page 212
S4 Estimated marginal means (EMMs) for linear mixed model of each rootstock per scion for root bark percentage in trial SP250……page 213
S5 Comparison test between scions within each rootstock for root bark percentage in trial SP250.……..……...…page 214
S6 Linkage group, QTL provenance and location in the GD genome of the most significant haploblock associated with primary root length in seedlings and percentage of rooting in the stoolbeds in the MDX132 population……..……..…page 215
S7 ANOVA table of fixed effects for the initial root surface area (logarithmic transformed).……..……page 216
S8 Estimated marginal means (EMMs) of the ANOVA for each root bark QTL group for initial root surface area in the root architecture experiment……..…page 216
S9 Multiple comparison test of root bark QTL for initial root surface area in the root architecture experiment……...……..…page 217
S10 Estimated marginal means (EMMs) for linear mixed model of each root bark QTL group within each time point for tree height in the root architecture experiment……...…page 218
S11 Multiple comparison test of root bark QTL groups within each time point for tree height in the root architecture experiment……..……..…page 219
S12 Estimated marginal means (EMMs) for linear mixed model of each block for trunk diameter above the graft union in the root architecture experiment……page 221
S13 Multiple comparison test of blocks for trunk diameter above the graft union in the root architecture experiment ……..……..…page 221

S14 Estimated marginal means (EMMs) for linear mixed model of each root bark QTL group within each time point for trunk diameter above the graft union in the root architecture experiment ……..……..…page 222
S15 Multiple comparison test of root bark QTL groups within each time point for trunk diameter above the graft union in the root architecture experiment.……..…page 223
S16 Estimated marginal means (EMMs) for linear mixed model of each root bark QTL group within each time point for trunk diameter below the graft union in the root architecture experiment ……..……..…page 223
S17 Multiple comparison test of root bark QTL groups within each time point for trunk diameter below the graft union in the root architecture experiment.……..…page 226
S18 Estimated marginal means (EMMs) for linear mixed model of each root bark QTL group within each time point for total root length in the root architecture experiment.……..……..…page 228
S19 Multiple comparison test of root bark QTL groups within each time point for total root length in the root architecture experiment ……..……..…page 229
S20 Multiple comparison test of time point for maximum root diameter in the root architecture experiment.……..……..……..…page 231
S21 Estimated marginal means (EMMs) for linear mixed model of each root bark QTL group within each time point for maximum root diameter in the root architecture experiment.……..……..…page 232
S22 Multiple comparison test of root bark QTL groups within each time point for maximum root diameter in the root architecture experiment ……..……..…page 233
S23 Multiple comparison test of time point for mean root diameter in the root architecture experiment.……..……..…page 235
S24 Estimated marginal means (EMMs) for linear mixed model of each root bark QTL group within each time point for mean root diameter in the root architecture experiment.……..……..…page 236
S25 Multiple comparison test of root bark QTL groups within each time point for mean root diameter in the root architecture experiment ……..……..…page 237
S26 Multiple comparison test of block for maximum root depth in the root architecture experiment. ……..……page 239
S27 Estimated marginal means (EMMs) for linear mixed model of each root bark QTL group within each time point for maximum root depth in the root architecture experiment.…..……page 240

S28 Multiple comparison test of root bark QTL groups within each time point for maximum root depth in the root architecture experiment ……..……page 241
S29 Multiple comparison test of block for convex hull area in the root architecture experiment. ……..…….……page 243
S30 Estimated marginal means (EMMs) for linear mixed model of each root bark QTL group within each time point for convex hull area in the root architecture experiment.……..……..…page 244
S31 Multiple comparison test of root bark QTL groups within each time point for convex hull area in the root architecture experiment.……..……..…page 245
S32 Estimated marginal means (EMMs) of the ANOVA for each root bark QTL group for root bark percentage in the root architecture experiment…..……..……page 247
S33 Multiple comparison test of root bark QTL groups for root bark percentage in the root architecture experiment…….……..……page 247
S34 Estimated marginal means (EMMs) of the ANOVA for each root bark QTL group for wet canopy in the root architecture experiment.…….……page 248
S35 Multiple comparison test of root bark QTL groups for wet canopy weight in the root architecture experiment……..…….……page 248
S36 Estimated marginal means (EMMs) of the ANOVA for each root bark QTL group for wet root weight in the root architecture experiment ……page 249
S37 Multiple comparison test of root bark QTL groups for wet canopy weight in the root architecture experiment ……..…….……page 250
S38 Estimated marginal means (EMMs) of the ANOVA for each root bark QTL group for wet root-to-shoot ratio in the root architecture experiment ……..……page 250
S39 Multiple comparison test of root bark QTL groups for root-to-shoot ratio in the root architecture experiment.……..……..…page 250

Abbreviations

2ln(BF)	Two times the natural logarithm of Bayes Factors
ABA	Abscisic acid
ANOVA	Analysis of Variance
AR	Adventitious roots
BAP	6-Benzilaminopurine
BR	Brassinosteroids
Chr	Chromosome
CK	Cytokinin
cM	centiMorgans
ChuII	Convex hull area
DNA	Deoxyribonucleic Acid
dNTP	Deoxyribonucleotide Triphosphates
EMM	Estimated Marginal Means
GA	Gibberellins
GD	Golden Delicious
GWAS	Genome wide association study
HWC	Hardwood cuttings
IBA	Indole-3-butyric acid
IAA	Indole-3-acetic acid
Indel	Insertion or Deletion
IRSA	Initial root surface area
IRSC	International Rosaceae SNP Consortium
LG	Linkage group
MCMC	Markov Chain Monte Carlo
NCBI	National Centre for Biotechnology Information
NGS	Next Generation Sequencing
NIAB EMR	National Institute of Agricultural Botany East Malling Research
NPA	N-1-naphthylphthalamic acid
PCA	Principal Component Analysis
PCR	Polymerase Chain Reaction
PNG	Portable Network Graphics

PRL	Primary root length
QTL	Quantitative Trait Locus
REML	Restricted maximum likelihood
RB	Root bark
SNP	Single Nucleotide Polymorphism
SSR	Simple Sequence Repeats
TCSA	Trunk cross-sectional area
TRL	Total root length
TRSA	Total root surface area
V P	Total phenotypic variance
V QTL	Additive variance of a QTL

Chapter 1. General introduction

1.1 Apple and apple rootstocks

1.1.1 Overview of apple production

Apples have been cultivated since ancient times and are among the most economically important fruit crops with more than 7500 known cultivars and twenty-five reported species of Malus. Around 5 million hectares of apples are grown worldwide, with more than 93 million tonnes of fruits produced in 2021 (Faostat, 2021). Apples are the second most produced top fruit globally, behind bananas with an annual production of approximately 124 million tons (Faostat, 2021). In the past 40 years, global apple production has increased by 190%, mainly attributed to a higher productivity per hectare since the area utilised for apple production has only increased by approximately 35% during the same period (Faostat, 2021).

Apples are primarily grown in temperate areas due to the chilling requirements for the initiation of blossoming (Heide and Prestrud, 2005). The top three apple-producing countries in the world are China, Turkey and the United States, collectively contributing to approximately 60% of the total global apple production. Notably, China stands out as the largest producer, accounting for 49% of the world's apple production. The United Kingdom ranks 31st on the global list of apple producers, with approximately 460,000 tonnes of apple production (Faostat, 2021).

1.1.2 Origin of modern apples

The cultivated apple, *Malus domestica* Borkh, belongs to the Rosaceae family, and the subfamily Maloideae*,* which also includes other tree-fruit species like pears, quince, loquat and medlar (Evans and Campbell, 2002). Phylogenetic analysis revealed that *Malus sieversii* is the progenitor of the cultivated apple (Velasco *et al.*, 2010) although other species like *Malus sylvestris* Mill are considered a major secondary contributor in Europe (Harris *et al.*, 2002; Coart *et al.*, 2003, 2006; Harrison and Harrison, 2011; Cornille *et al.*, 2012). The wild apple progenitor *Malus sieversii* was found in the Tian Shan Mountains, specifically in Kazakhstan, and was dispersed

to West Europe through the Silk Road, allowing the hybridization and introgression of wild crabapple varieties originating from different regions, including Siberia (*Malus baccata (L.) Borkh.*), the Caucasus (*Malus orientalis Uglitz.*) and Europe (*Malus sylvestris Mill.*) (Cornille *et al.*, 2014; Duan *et al.*, 2017). Over thousands of years, humans selected and cultivated apples with desirable traits, leading to improved taste, texture and size. A type of apple that resembles the modern cultivated apple we know today emerged in the Near East approximately by 4,000 BC. The domesticated apple was later brought to Europe and North Africa by the Greeks and Romans, and from there, it spread to various parts of the world (Juniper *et al.*, 1998).

1.1.3. Genomic resources in apple

The first draft of the apple genome was generated in 2010 after sequencing of Golden Delicious which was a breakthrough for the development of new varieties. In 2017, a high-quality *de novo* assembled genome and methylome was generated using a double haploid of 'Golden Delicious'. This high-quality genome was developed by combining long reads (Pacbio) and short sequencing reads (Illumina), providing a crucial tool for future genetic studies in apples (Daccord *et al.*, 2017).

Several single nucleotide polymorphisms (SNPs) arrays have been developed specifically for apples. The IRSC apple Infinium ® II 8K array became available in 2012. The low-quality apple genome (from 2010), together with low-coverage re-sequenced data from 27 apple cultivars were used to develop this array (Chagné *et al.*, 2012). Shortly after, a 20K Illumina apple array was developed using re-sequencing data from 13 apple cultivars, one accession of *M. micromalus* and two double haploid accessions derived from 'Golden Delicious' (Bianco *et al.*, 2014). The array consisted of 18019 SNPs, over 14000 newly discovered and 3305 SNPs from the 8K IRSC chip.

In 2016, the Axiom® Apple 480K array was generated after high-depth resequencing of 63 different cultivars and the two double haploids used for the 20K array (Bianco *et al.*, 2016). It became a suitable tool for Genome Wide-Association Studies (GWAS) thanks to the high percentage of well-distributed and robust SNPs (Bianco *et al.*, 2016).

1.1.4 Apple rootstocks

1.1.4.1 Benefits of the use of rootstocks

Grafting is an ancient method of vegetative and asexual plant propagation. This technique is typically carried out by joining two distinct parts of a plant: the upper portion, referred to as the 'scion,' and the lower part known as the 'rootstock' or 'stock' (Goldschmidt, 2014). Rootstocks are defined as the part of the tree containing the root system and have been used in temperate fruit trees for more than 2000 years (Webster, 1995b). Rootstocks confer many characteristics to scions and have always been selected for a wide range of desirable traits such as pest and disease resistance, cold hardiness, good soil anchorage, reduced suckering as well as precocity and tree size (Pilcher *et al.*, 2008). Furthermore, tree root systems play a crucial role in nutrient uptake and adaptation to water deficit (Marguerit *et al.*, 2012). For all of these reasons, the choice of an appropriate rootstock is fundamental to orchard success.

With the increasing global demand for food, rootstock selection is gaining more importance since rootstocks with improved root systems can contribute to a better adaptation to drought periods and resistance to plant pathogens and therefore, impact yield (Jensen *et al.*, 2012; Marguerit *et al.*, 2012; Tamura, 2012).

1.1.4.2 Rootstock-induced dwarfing

Dwarfing rootstocks significantly impact the architecture and development of the scion. They reduce both the number and length of internodes, contribute to an early cessation of growth and a smaller trunk cross-sectional area, leading to an overall reduction of the tree size (Costes and Lauri, 1995; Atkinson and Else, 2001; Seleznyova *et al.*, 2003; Pilcher *et al.*, 2008). Furthermore, dwarfing rootstocks induce a higher proportion of buds to flower and precocity (Maggs, 1955; Webster, 1995a). For all of these reasons, dwarfing rootstocks are essential to intensive production methods since they contribute to a greater yield per unit area and crop more and earlier (Robinson, 2007).

1.1.4.3 Main breeding programs and commonly used rootstocks

Apple is one of a number of species that benefit from dwarfing rootstocks and growers have been utilising them for many decades. In fact, as far back as the early 19th

century, rootstock cultivars such as 'English Paradise' and 'Doucin Stock' were identified for their ability to dwarf apple trees and promote early fruit-bearing (Lindley, 1827).

At the beginning of the twentieth century, apple rootstocks from around the world were collected, classified into nine types from I to IX and described at the East Malling Research Station (UK) (Hatton, 1917). Subsequently, additional rootstocks were added to the initial nine although most of them are not commercially available (Hatton, 1917). The dwarfing rootstock 'Malling 9' was part of the original collection. 'Malling 9' ('M.9'), also called 'Jaune de Metz', 'Yellow Metz', 'Yellow Paradise of Metz' and 'Dieudonne', was selected as a chance seedling in France in 1879. M.9 has become the most widely used dwarfing rootstock despite also having drawbacks including poor soil anchorage and fireblight (*Erwinia amylovora*) susceptibility (Ferree *et al.*, 1993; Norelli *et al.*, 2003). A few years later, controlled crosses using M.9 as a parent generated the commonly known rootstocks M.26 and M.27 (Preston, 1967).

A few decades later, a new series of rootstocks was produced in collaboration with the John Innes Centre, located at Merton (UK). ‘Northern Spy’ was used as a parent in this programme as a source of resistance to woolly apple aphid (Erwinia Armilonova) (Preston, 1955). The rootstocks generated in this programme were named the Malling Merton series. Among these rootstocks, it is worth highlighting M.M.106, a moderately vigorous rootstock, and the vigorous M.M.111 which are commonly used in apple cider orchards due to their good anchorage and productivity (Preston, 1955, 1966; Webster *et al.*, 2000).

The Cornell Geneva breeding programme, which started in the 1960s in the New York State Experimental Station in Geneva, aimed mainly to generate rootstocks resistant to fireblight (*Erwinia amylovora*) and crown rot (*Phytophthora cactorum*). Like many other breeding programmes around the world, Malling series rootstocks were used as a parent and were crossed with Robusta 5 in this case. There is a wide variety in size in these roostocks with an improved winter hardiness. The most known are G.202, G.11, G.41 and G.30 (Robinson *et al.*, 2003).

Other important and known rootstocks from Canada such as Ottawa 3, St Jean Morden (SJM series) and SJP84 series were developed by crossing Malling rootstocks with other materials (Khanizadeh *et al.*, 2011a, 2011b). The B series rootstocks from the former Soviet Union, the P series from Poland and the JM series from Japan also released some widely known rootstocks such as Budagovsky 9, P22 and JM7 which also were generated by crossing M series rootstocks and their native material (Zagaja, 1981; Russo *et al.*, 2008; Soejima *et al.*, 2010).

Figure 1.1 shows a classification in six levels of rootstocks from the Malling series, the Malling Merton series, the Cornell Geneva breeding program as well as other rootstocks commonly used in the orchards.

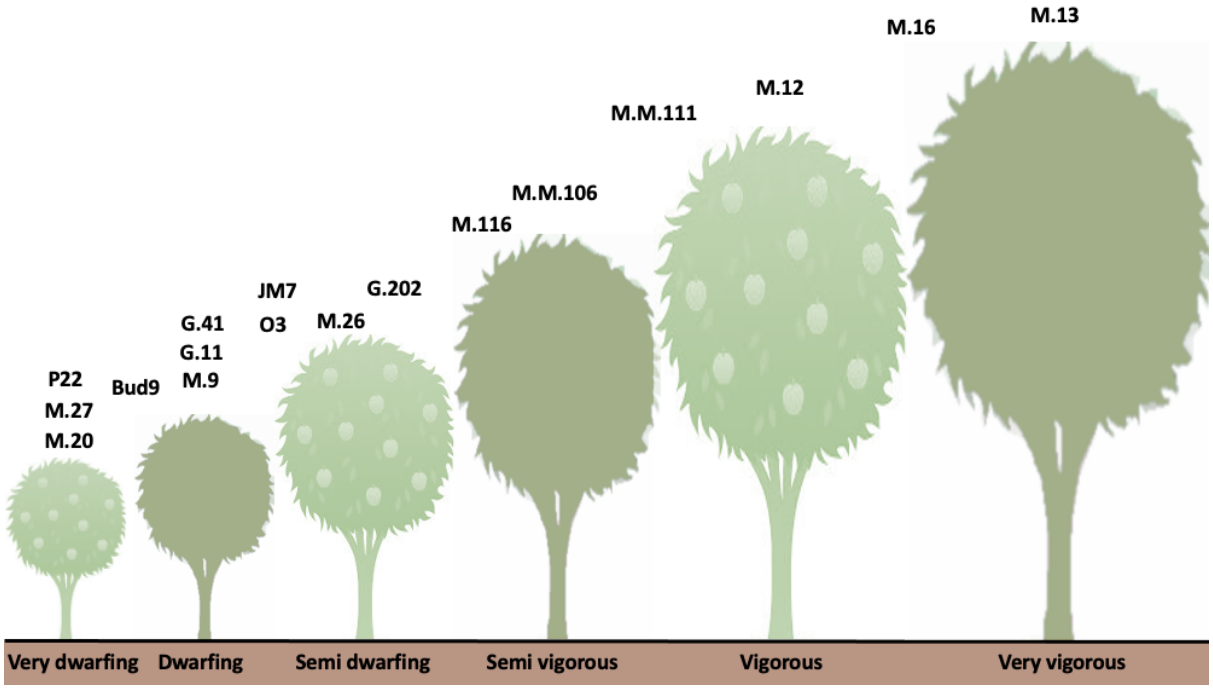

Figure 1.1. Apple rootstocks classified in the six traditionally used dwarfing categories.

1.1.5 Rootstock-scion mechanisms that regulate dwarfing in apple rootstocks

The impact of rootstocks in apple cultivation remains a subject of extensive research and review, given their significant influence on tree physiology and fruit production. Throughout the years, numerous hypotheses have been proposed to elucidate the mechanism behind rootstock-induced dwarfing, but none have provided a complete explanation for the observed effects. Some of the main theories that have been

proposed to explain this complex mechanism are related to hormonal changes, the redistribution of assimilates and the absorption and distribution of water and nutrients.

1.1.5.1 Hormonal regulation

Phytohormones play a crucial role in both vegetative and reproductive growth and are essential for facilitating communication between the root and shoot. One of the most important phytohormones is auxin, a plant growth hormone that directly participates in many biological processes, including cell elongation, differential growth, tissue patterning, and embryogenesis (Sauer *et al.*, 2013). Auxins are produced in leaf primordia and young leaves within plants. They are then transported in a basipetal direction, moving from the upper part of the plant down towards the roots (Morris *et al.*, 2004; Kerr and Bennett, 2007).

In 1981, Lochard and Schneider (1981) hypothesised that dwarfing apple rootstocks could be distinguished by having bark with a reduced capacity for auxin transport compared to more vigorous rootstocks. Subsequent studies have shown that auxin transport capacity is significantly lower in dwarfing rootstocks compared to vigorous rootstocks (Soumelidou *et al.*, 1994; Kamboj *et al.*, 1997a, 1997b). Li *et al.*, (2012) observed that when an apple scion was grafted onto dwarfing rootstock, there was a significant reduction in the expression of the auxin transporter gene PIN1. This reduction led to an insufficient supply to the roots of indole-3-acetic acid (IAA), the most common hormone of the auxin class, ultimately resulting in a dwarfed growth phenotype. Different expression patterns of the auxin efflux carrier gene MdPIN1b in dwarfing versus vigorous rootstocks have been also reported (Gan *et al.*, 2018). It has also been seen that when the IAA transport inhibitor, N-1-naphthylphthalamic acid (NPA), was injected into the stems of vigorous apple trees, these trees reduced the length of the shoots and their architecture was more similar to dwarfing rootstocks (Hooijdonk *et al.*, 2010).

Furthermore, Song et al., (2016) observed that IAA levels of apple trees grafted on dwarfing rootstocks were lower than in vigorous rootstocks, likely a result of reduced expression levels of the auxin synthesis gene *MdYUCCA10a*. Expression in both leaves and roots of the size-controlling rootstock was significantly reduced compared to the taller and stronger rootstocks. This reduced auxin biosynthesis resulted in a

decreased amount of indole-3-acetic acid (IAA) being transported from the shoot to the roots which impacts the root production of additional hormones like cytokinins and gibberellins, which are subsequently transported to the shoot through the xylem. In summary, the reduced synthesis and transport of auxins to the root system of dwarfing rootstocks affect the production of cytokinins and gibberellins and consequently would have an impact on root and shoot growth.

Among cytokinins (CKs) is worth mentioning zeatin which is one of the main active types of cytokinin that is primarily synthesised in the roots and promote cell division, plant growth and development (Carr, 1966; Torrey, 1976; Aloni *et al.*, 2006). Dwarfing rootstocks have been shown to have lower levels of cytokinins compared to vigorous rootstocks (Jones, 1986; Kamboj *et al.*, 1999a). Li *et al.*, (2012) observed that both levels of the cytokinin zeatin, an expression of the isopentenyl transferase gene (*IPT3*), essential for cytokinin biosynthesis, were lower in dwarfing apple rootstocks compared to invigorating rootstocks. Similarly, greater expression of the *MdIPT5* gene in invigorating apple rootstocks led to a greater amount of zeatin, promoting cell division and internode elongation (Feng *et al.*, 2017; Yan *et al.*, 2022). Meanwhile, lower expression of *MdIPT5* in dwarfing rootstocks reduced the production of zeatin and may be responsible for the reduced internode length in size-controlling rootstocks (Feng *et al.*, 2017; Yan *et al.*, 2022). Moreover, Hooijdonk *et al.*, (2010) found that the application of 6-benzylaminopurine (BAP), a synthetic cytokinin, to dwarfing rootstocks, promoted the formation of secondary shoots.

The amount of cytokinin is also linked to the auxin status of the plant. Cytokinin production and translocation in the xylem are dependent on the amount of auxins synthesized in the shoots and subsequently reaching the roots (Lochard and Schneider, 1981). In summary, the low expression of CK genes in the root systems will limit the supply of cytokinins received by the scion, decreasing auxin concentration, and resulting in a permanent reduction in tree growth and overall vigour.

Gibberellins (GAs) are plant hormones that can be found in shoots and root tips as well as in developing flowers and seeds and play a significant role in promoting key aspects of growth, including seed germination, leaf expansion, stem elongation, flowering, and fruit development (Davies, 1995; Silverstone *et al.*, 1997; Bulley *et al.*,

2005). An early study demonstrated that a dwarfing interstock reduced the uptake of the xylem-applied GAs compared to invigorating rootstocks (Richards *et al.*, 1986). More recently, Tworkoski and Fazio, (2016) also found lower levels of GAs in roots and xylem exudates of dwarfing apple rootstocks compared to vigorous. Suppression of GA2ox expression, a gene encoding a gibberellin biosynthetic enzyme, decreased GA levels in the scion, resulting in stem height reductions. This dwarfing effect was alleviated by the exogenous application of GA3 (Bulley *et al.*, 2005). The Gibberellin Insensitive Dwarf1 (GID1c) acts as a receptor of GAs and induces the degradation of DELLA repressor protein (Griffiths *et al.*, 2006; Schwechheimer, 2011). It was found that the expression of GID1c was lower in dwarfing rootstocks and the GA3 treatment promoted GID1c expression in dwarfing rootstocks, resulting in elevated GA levels and subsequently increasing plant height, leaf growth and numbers of internodes and roots (Hao *et al.*, 2019). This supports the idea that reductions in gibberellin production in roots, followed by less transport to shoots, decrease tree height and the number of internodes, ultimately resulting in a dwarf-like phenotype.

Abscisic acid (ABA), commonly associated with abiotic stress responses is usually produced in the roots and transported to the leaves via xylem or quickly synthesised in the leaves. It is essential for physiological processes including leaf senescence, seed germination, stomatal closure and water relation, bud dormancy and growth inhibition (Rudnicki, 1969; Borkowska and Powell, 1982; Zeevaart and Creelman, 1988; Davies, 1995; Sharp and LeNoble, 2002; Osakabe *et al.*, 2014; Lee *et al.*, 2021). It has been reported that dwarfing mutants of apples have higher levels of ABA (Jindal *et al.*, 1974; Kamboj *et al.*, 1999b). Elevated levels of ABA lead to reduced hydraulic conductivity in dwarfing rootstocks, negatively affecting tree growth and yield (Tworkoski and Fazio, 2015). Briefly, high concentrations of ABA act as a growth inhibitor by suppressing the accumulation of other phytohormones resulting in a reduction of growth.

Brassinosteroids (BR) are a type of steroid plant hormone that control root and shoot growth, vascular differentiation and flowering and are widely spread in all actively growing tissues of plants (Fujioka and Yokota, 2003; Bajguz *et al.*, 2020; Li and He, 2020). Exogenous application of BR induced growth of both roots and shoots on apple trees and led to an increase in auxin levels while decreasing ABA and GA3 levels

(Mao *et al.*, 2017). Additionally, overexpression of the MdWRKY9 transcription factor facilitates the dwarfing effect by directly inhibiting the transcription of the brassinosteroid synthetase MdDWF4, thereby reducing the production of BR (Zheng *et al.*, 2018). Overexpression of MdNAC1, a transcription factor that regulates both ABA synthesis and brassinosteroids, induced a dwarfing phenotype (Jia *et al.*, 2018). In summary, dwarfing rootstocks are characterised by low levels of BR and rising levels of BR could potentially induce the expression and transport of auxins.

All these hormonal changes have been proposed as potential mechanisms through which rootstocks influence the vigour of the scion by altering the chemical signalling between roots and shoots. IAA, CK, GA and BR promote plant growth and are generally found in low levels in dwarfing genotypes. In contrast, high transcript levels of ABA pathways, which act as growth inhibitors, are detected in dwarfing rootstocks (Figure 1.2).

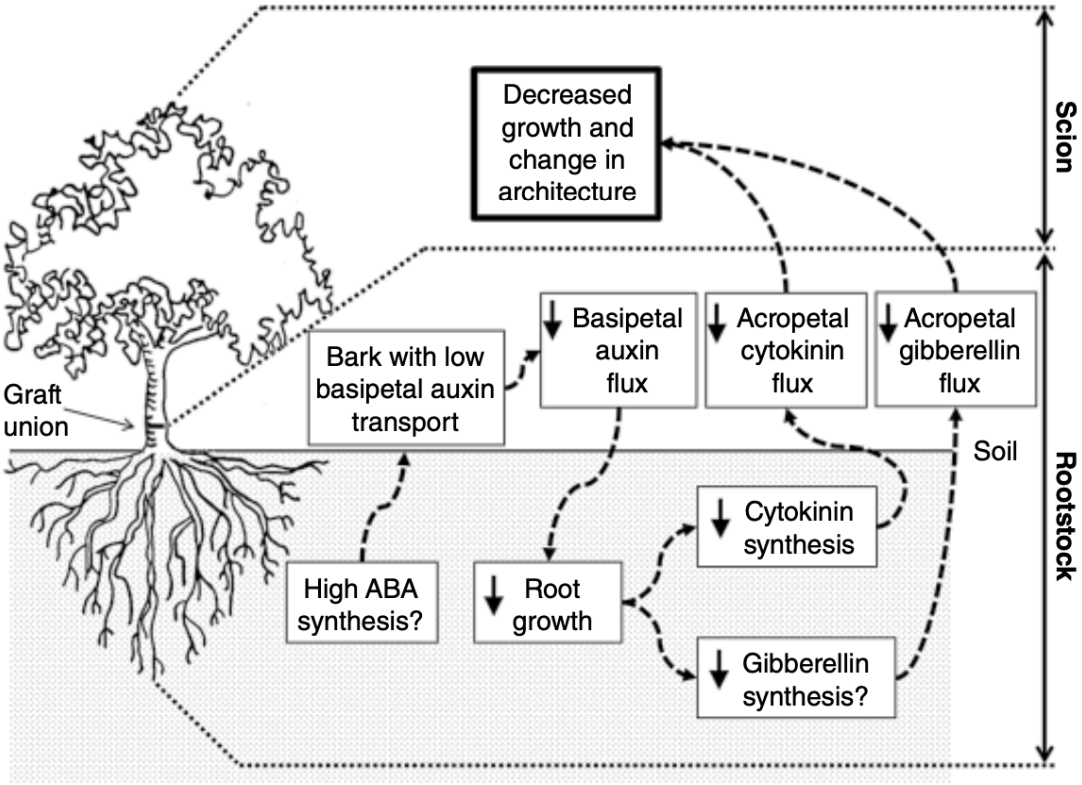

Figure 1.2. Diagram describing the hormonal interactions between rootstock and scion that may explain rootstock-induced dwarfing (Basile and DeJong, 2018).

1.1.5.2 Water uptake and anatomical characteristics

The hydraulic conductivity of the root system can impact shoot growth by regulating the supply of water to the above-ground plant parts. However, its role in rootstock-induced vigour remains a topic of debate.

Early studies revealed that dwarfing apple rootstocks exhibited roots with smaller xylem vessel size, fewer wood fibres, more wood parenchyma and wood ray cells per unit area, and a higher ratio of bark to wood. Additionally, the xylem-to-phloem ratio was smaller in dwarfing rootstocks when compared to those more vigorous. As a result, it was hypothesised that dwarfing apple rootstocks may have inherent anatomical features that directly impact their hydraulic properties (Beakbane and Thompson, 1940, 1947; Beakbane, 1956). Atkinson *et al.*, (2001, 2003) observed that the hydraulic conductivity of grafted apples increased with vigour in the scion, graft union and rootstock and followed the percentage of functional xylem area. Moreover, the differences persisted even when the hydraulic conductivity was normalized by the xylem cross-sectional area. These observations suggested that dwarfing rootstocks not only exhibit reduced xylem area but may also alter anatomical features on the scion as the positive correlation between functional xylem area rootstock vigour was also observed in the scions. Water-stressed trees on vigorous rootstocks grew better than trees on dwarfing rootstocks as they were able to increase the number and diameter of xylem vessels, whereas dwarfing rootstocks had less plasticity (Bauerle *et al.*, 2011).

In summary, rootstock-induced dwarfing may be due to reduced transport of water, mineral nutrients and solutes from roots to shoots that would affect scion growth. This reduction in water transportation is associated with the xylem, converting the xylem-to-phloem area into a useful tool for breeders to aid in the early selection of rootstocks with size-controlling properties.

1.1.5.3 Assimilates production and distribution

In autumn, photosynthesis products (or photo-assimilates) are transported from leaves to roots where they are transformed into starch reserves that will be used for spring growth (Priestley, 1960). This means any factor affecting the carbohydrate reserves

may impact tree vigour in the following spring (Abusrewil *et al.*, 1983; Mika, 1986; Loescher *et al.*, 1990). This hypothesis proposing an explanation for rootstock-induced dwarfing suggests that the storage or utilization of carbohydrate reserves may differ among different rootstocks due to the limitation of the capacity of assimilation CO_2, reduced transport of carbohydrates from shoots to roots or reduced capacity of storage carbohydrates in the root systems (Basile and DeJong, 2018).

The research regarding the impact of dwarfing apple rootstocks on photosynthesis is inconsistent. In general, lower net photosynthesis rates were recorded in dwarfing rootstocks compared to vigorous rootstocks over the whole season mainly due to the fact that vigorous rootstocks maintain the photosynthetic activity later in the season (Gregory, 1957; Tworkoski and Fazio, 2011). Trees with compact canopies will exhibit lower overall CO^2 assimilation rates and less storage tissues, subsequently leading to smaller storage carbohydrate reserves, in comparison to vigorous trees (DeJong, 2016).

Carbohydrates can be classified into two main categories: soluble carbohydrates such as sucrose and sorbitol which are useful as immediate energy sources and non-soluble carbohydrates such as starch which serve as a long-term energy storage. Dwarfing rootstocks have shown lower starch, sorbitol and sucrose root concentrations compared to vigorous rootstocks (Stutte *et al.*, 1994; Olmstead *et al.*, 2010). Brown *et al.*, (1985) reported that shoots from vigorous apple rootstocks had higher starch, soluble sugar and sorbitol from mid-season to the next spring. However, the differences in the roots were only detected in early winter. Foster et al., (2017) hypothesised that the downregulation of auxin influx transporter in dwarfing rootstocks would reduce the polar transport of auxins and would be connected to a reduction in starch hydrolysis and sugar depletion in spring causing the early termination of the primary axis and sylleptic shoot growth. Another explanation for the reduced mobilisation of assimilates could be that the graft union can act as an area of increased resistance to carbohydrate transportation probably due to morphological anomalies in the phloem (Simons and Chu, 1981, 1984; Simons, 1986). Further research is needed to investigate carbohydrate mobilisation throughout the year in the different parts of the trees to understand this process better.

1.1.5.4 Nutrient uptake and distribution

Phloem and xylem characteristics also influence nutrient uptake and distribution within the plant. Metabolite transport within the phloem is influenced by the dimensions of the sieve tubes and the capacity of the phloem to transport and storage might play a role in determining the vigour of the plant (Beakbane, 1956).

In dwarfing rootstocks, the size and number of sieve tube elements in the phloem are smaller, reducing the transport of photosynthates to the roots and accumulating large concentrations of these metabolites above the graft union (Beakbane, 1956; Rogers and Beakbane, 1957). Similarly, the smaller size and number of xylem vessels of dwarfing rootstocks reduce the nutrient and water transport rates (Tworkoski and Fazio, 2011; Marini and Fazio, 2018). Thus, dwarfing rootstocks are generally characterised by a reduced nutrient uptake either because the roots are not able to properly take up and transport nutrients or the graft union hinders the movement of nutrients.

In support of changes in nutrient transport, Bukovac *et al.*, (1958) reported that the uptake of ^{32}P and ^{45}Ca was smaller in dwarfing rootstocks compared to vigorous rootstocks, although they did not find an accumulation of these nutrients at the graft union level. In a later study, the leaf concentrations of N, Ca, Mg, P and Zn were higher on dwarfing rootstocks. However, the B and Fe concentrations were lower on dwarfing rootstocks compared to invigorating rootstocks (Jones, 1976). Moreover, the net assimilation rate of ungrafted dwarfing and vigorous rootstocks was evaluated under different nitrogen (N) levels and revealed that vigorous rootstocks absorbed N more efficiently, especially under limited N supply conditions (Ruck and Bolas, 1956). However, another study found higher amounts of N, amino acids and carbohydrates in the bark of ungrafted dwarfing rootstocks compared to vigorous (Martin and Williams, 1967). While it seems clear that rootstock vigour governed by anatomical and hormonal changes, plays a role in nutrient uptake, more research is needed to elucidate how rootstock vigour specifically influences nutrient distribution. The use of different cultivars, ungrafted or grafted trees of varying ages and the examination of diverse tissues complicates the comparison of studies (Webster, 2004).

In conclusion, the hormonal theory has traditionally been the most prevalent although none of the theories briefly summarised above completely explain the mechanisms of rootstock-induced dwarfing. Furthermore, it is important to highlight that all these theories are highly influenced by each other and that it is probably the set of several factors that is responsible for this complex mechanism.

1.1.6 Genetic control of rootstock-induced dwarfing in apples

Several studies have focused on performing QTL mapping analysis to identify genes controlling rootstock-induced dwarfing and to develop genetic markers closely linked to dwarfing that will help accelerate the breeding process. The first study conducted by Pilcher et al., (2008) genetically mapped *Dw1* in Chromosome (Chr) 5 using the progeny of a cross between the dwarfing rootstock 'M.9' and *Malus x Robusta 5* (R5) by measuring trunk cross-sectional area (TCSA), a measure for rootstock-induced dwarfing. A later study using a population derived from an Ottawa 3 x R5 cross identified a second QTL linked to rootstock-induced dwarfing, named *Dw2* located in Chr11 (Fazio *et al.*, 2014). One year later, Foster et al., (2015) also identified two major QTL, *Dw1* and *Dw2,* in the same chromosomes using another M.9 x R5 population. In 2016, Harrison et al., (2016b) conducted a QTL mapping analysis for root bark ratio, a primary trait related to dwarfing, using the progeny of a cross of M.27 x M.116 (M432 population) and identified *Rb1* and *Rb2* which colocalized with regions previously associated with dwarfing. Furthermore, this study discovered a third QTL, *Rb3*, located in Chr13.

On the other hand, several transcriptome studies have been conducted to identify overexpressed and underexpressed genes in dwarfing rootstocks and numerous candidate genes for rootstock-induced dwarfing have been subsequently investigated mainly related to hormonal processes as described in section 1.1.5.1. In summary, lower expression of the auxin transport genes *MdPIN1b* and *MdPIN8a* (Zhang *et al.*, 2015; Song *et al.*, 2016; Gan *et al.*, 2018), lower expression of the isopentenyl transferase genes *IPT5b* that participate in the cytokinin synthesis (Feng *et al.*, 2017), the suppression of the MdGA20-oxidase gene that codified an enzyme that participates in the biosynthesis of gibberellins (Zhao *et al.*, 2016), the overexpression of *MdNAC1* (Jia *et al.*, 2018), a transcription factor that regulates brassinosteroids and

ABA synthesis and the overexpression of the *MdWRKY9* transcription factor that inhibits the transcription of the brassinosteroid synthetase *MdDWF4* were associated with the induction of the dwarf phenotype. However, none of these genes are located in the QTL regions linked to rootstock-induced dwarfing in Chromosomes 5 and 11 which suggests that those are secondary consequences of the unknown primary effect.

1.2. Propagation methods in apple rootstocks

Apple rootstocks can be propagated using both sexual and asexual methods. Each of these methods has its own advantages and is suitable for specific purposes.

1.2.1 Sexual propagation method

Seed propagation offers distinct advantages in nurseries, primarily due to its simplicity and cost-effectiveness when compared to vegetative propagation methods. In apples, there are no known viruses transmitted by seeds and therefore, the use of rootstocks propagated by seeds offers clear advantages for nurseries struggling with the propagation of virus-free clonal rootstocks. Moreover, seed propagation also avoids soil-borne diseases transmitted in stoolbeds (Webster, 1995b). However, seedlings can display significant variability in performance when utilised as rootstocks. One evident advantage of transitioning to clonal rootstocks (asexual propagation) is the enhanced uniformity observed in the growth and cropping of the scion (Webster, 1995b).

The seed propagation method is normally used by breeders to develop new varieties. The process involves the cross-pollination of parent trees with desired traits, collecting and germinating the resulting seeds, evaluating the seedlings for desirable traits, and repeating the breeding process over multiple generations to refine and stabilise the desired characteristics. Seed propagation is a crucial method in plant breeding, as it allows for the introduction and combination of various traits in a cost-effective manner, although it requires significant time and effort to develop a stable and commercially viable variety.

1.2.2 Asexual propagation methods

The main objective of asexual propagation is to generate plants that are exact genetic replicas of the original plants by using vegetative organs such as leaves or stems, a process commonly referred to as vegetative propagation methods. There are several types of vegetative propagation methods including softwood cuttings, hardwood cuttings, stooling or layering and micropropagation.

A large part of asexual propagation methods involves adventitious root formation. Adventitious root development is a post-embryonic organogenesis process in which roots are formed from non-root tissues, like leaves and stems. Many plant species can naturally generate adventitious roots although they can also be induced in response to various environmental stresses such as flooding, wounding or nutrient deficiencies (Steffens and Rasmussen, 2016). The development of adventitious roots is crucial for the vegetative propagation methods extensively used in forestry, agricultural and horticultural crops.

1.2.2.1 Softwood cuttings

Softwood cuttings are collected from the current year's growth from healthy branches usually in late spring or early summer when the new year growth is still flexible (Webster, 1995b). Many studies have been conducted to investigate how to improve rooting ability in cuttings. It has been demonstrated that the intense pruning of the ‘mother plant’ from which the cuttings are collected helps to increase the rooting rate (Hartmann and Kester, 1975). Hartmann and Kester (1975) also observed that etiolation or blanching, which consists of covering all or part of the cutting to grow them in the absence of light, improved the rooting ability. Moreover, early studies reported that the application of the hormone indole butyric acid (IBA) in the base of the cutting promotes rooting (Webster, 1995b).

The cuttings should be quickly moved to the rooting place since they desiccate rapidly. These cuttings are typically positioned in heated rooting beds, which facilitate root development. These beds are usually filled with a mixture of sand and peat and may include fogging systems to ensure consistent humidity levels and prevent desiccation

(Webster, 1995b). After rooting, the cuttings may need to continue their growth in a glasshouse until they are large enough to be planted (Wertheim and Webster, 2003).

Softwood cuttings are not commonly used in the propagation of apple rootstocks. Nevertheless, there are studies that have proved their efficacy in some Malling rootstocks such as M.M.106 and M.26 and in Polish rootstocks including P1, P2 and P22 (Hansen, 1990a, 1990b).

1.2.2.2 Hardwood cuttings

Hardwood cuttings are collected in the dormant season after the leaves have fallen in the autumn or before the buds break in the spring. This method is the most commonly used for fruit tree rootstock propagation and many aspects of their propagation process are common to softwood cuttings. The use of IBA hormone solutions has been crucial for both softwood and hardwood cuttings and numerous studies about different concentrations and exposure times have been conducted in apple rootstocks (Delargy and Wright, 1979; Howard, 1985; Dvin *et al.*, 2011). In addition, wounding, which entails splitting the base of the cutting, proved to be especially beneficial for cuttings with inherently limited capacity for root formation (Howard *et al.*, 1984).

Similar to the softwood cuttings, the hardwood cuttings are placed in heated rooting beds. Several studies about the most effective basal temperature to propagate rootstocks have been conducted over the years, indicating that the optimum temperatures ranged between 20°C to 22°C (Howard, 1968; Webster *et al.*, 1990). In addition, physiological factors like the diameter of the cutting, length of the cutting and the healthy state of the mother plant significantly affect the rooting success (Hartmann and Kester, 1975; Webster, 1995b; da Costa *et al.*, 2013).

In general, apple rootstocks such as M.M106, M.26 and M.M.111 propagate well through hardwood cuttings. However, others like M.9 are more difficult to propagate with this method, suggesting that the success of this method significantly varies depending on the genotype (Webster, 1995b).

1.2.2.3 Micropropagation

Micropropagation, also known as tissue culture or in vitro culture, is a valuable technique for establishing large populations of new rootstocks that can be readily transported across international borders since they can easily meet plant importation regulations (Webster, 1995b).

Micropropagation consists of four main stages: establishment, propagation, rooting and acclimatisation (Teixeira da Silva *et al.*, 2019). Micropropagation is based on the capacity of every living cell to replicate the entire organism because it contains all the essential genetic information (Hartmann and Kester, 1975). Explants from the desired plant are collected and thoroughly disinfected before placing them in a culture medium. After 4 to 6 weeks the plants are transferred to another media enriched with cytokinins to promote proliferation of new shoots in the explant, commencing in the multiplication stage. Every 4 to 8 weeks the plants are subcultured and this stage can continue for years (Wertheim and Webster, 2003). In the rooting stage, plants are usually transferred to culture media without cytokinins and IBA and are often grown in light absence to help the rooting development (Welander, 1983; Alvarez *et al.*, 1989). In the acclimatisation step, plantlets are moved from rooting media to pots in a greenhouse where low survival is a problem.

Currently, propagating apple trees through plant tissue culture is not a common method as it is considered too expensive but it is more frequently used with other fruit crops in which the stoolbed propagation does not work well. Nonetheless, research on apple tissue culture has facilitated progress in molecular and applied breeding studies.

1.2.2.4 Stooling and Layering

Stooling and layering are division techniques employed in the propagation of tree rootstocks (Knight *et al.*, 1927). In the spring, mother plants can be planted either in an upright position, known as stooling, or at an angle, called layering. These methods involve the induction of adventitious roots in a section of the rootstock stem while it remains attached to the mother plant. Root formation is typically encouraged by shielding the targeted stem portion from light (which also increases humidity),

achieved through methods such as blanching or etiolation. This is done using a mixture of soil and sawdust or peat or by covering the stems with an opaque material such as plastic. The rooted shoots are collected at the end of autumn or early winter (Webster, 1995b).

One of the main drawbacks of the use of stoolbeds and layering is that shoots are very susceptible to soil-borne diseases (Webster, 1995b). However, stool and layer beds are the most commonly used propagation methods in apples since they offer many advantages such as their ability to be mechanised, the high quality of rooted shoots and their easy and low-cost maintenance (Anderson and Elliott, 1983).

1.3. Root architecture

Root system architecture (RSA) can be described as the spatial distribution of roots (Lynch, 1995; Osmont *et al.*, 2007). RSA contributes to plant hydraulics, anchorage and nutrient uptake (Bohn *et al.*, 2006; Lynch, 2007; Paez-Garcia *et al.*, 2015; Ludlow and Muchow, 1990). Furthermore, roots are essential in pathogen recognition and resistance (Süle and Burr, 1998; Singh *et al.*, 2019). Generally, root systems with a large number of lateral roots at the top of the system can improve the uptake of immobile nutrients like phosphate that remain in the topsoil (White *et al.*, 2013; Lynch and Brown, 2001). On the other hand, those root systems with less branching and deeper roots can forage for water easily, reducing water stress, and providing better soil anchorage (White *et al.*, 2013; Lynch and Brown, 2001).

All the root growth processes are mediated by complex hormone interactions. Cytokinins (CK), in the presence of auxins like indole-acetic acid (IAA), regulate root development, vascular differentiation and lateral root initiation (Aloni *et al.*, 2006). Whereas auxin production and transport influence lateral root development (Ljung, 2013; Ljung *et al.*, 2005; Petersson *et al.*, 2009), cytokinins can inhibit root formation (Werner *et al.*, 2001, 2003). On the other hand, strigolactones (SL) increase root hair elongation, reduce lateral root formation and inhibit adventitious roots (Rasmussen *et al.*, 2013).

1.3.1 The impact of dwarfing rootstocks on root system architecture

Extensive research has been conducted on how rootstock-induced dwarfing affects apple scions, but there has been relatively limited exploration into the consequences of dwarfing on root systems. Some studies have shown that the root systems of dwarfing rootstocks had a reduced root spread area with lower total root density and thinner roots while vigorous rootstocks displayed deeper root systems with higher total root density (De Silva, 1999; Lo Bianco *et al.*, 2003; García-Villanueva *et al.*, 2004; Hou *et al.*, 2012; An *et al.*, 2017b).

Dwarfing rootstocks grown in sandy soils exhibited thinner and shorter primary roots and fewer lateral roots compared to trees growing in organic soils and had better nutrient uptake ability (P, K, Ca, Fe and Zn) (Fan and Yang, 2011). Another study showed that as soil grain size increases, the pattern of root architecture shifts from having clustered lateral roots on the upper section of the primary root to having a long primary root with lateral roots more evenly distributed (Fan and Yang, 2008).

In summary, vigorous rootstocks demonstrate better root growth and adaptability to drought while dwarfing rootstocks are poorly anchored to the soil and are more sensitive to environmental stresses due to smaller root systems (Tworkoski and Fazio, 2015).

1.3.2 Root systems as a breeding target for climate resilience

Breeding resilient rootstocks holds paramount importance in the context of climate change and its profound impacts on agriculture. As the global climate continues to undergo shifts in temperature, precipitation patterns, and the frequency of extreme weather events, the role of resilient rootstocks in fruit tree cultivation becomes increasingly significant. Therefore, breeding efforts should focus on enhancing the resilience of rootstocks to abiotic stresses such as drought, extreme temperatures and poor soil conditions. This can involve selecting rootstock genotypes that have an improved capacity for water and nutrient uptake, as well as the ability to adapt to adverse soil conditions. Developing rootstocks with efficient root systems that can

explore a larger soil volume for resources and maintain stable water uptake under varying environmental conditions is a key objective.

Root angle dictates the direction in which the roots are elongated and, therefore, is a factor that influences the development of shallow or deeper root systems (Kitomi *et al.*, 2015; Uga *et al.*, 2015). Furthermore, total root length substantially impacts the root depth of root systems (Pagès *et al.*, 2012). Therefore, both factors contribute to deep rooting and are key traits for improving anchorage and water uptake in rootstocks. Consequently, several studies have been performed to better understand the genetic control of this complex trait in different species. In poplar, the *PtabZIP1L*, homologous to the Arabidopsis *bZIP1* (leucine zipper transcription factors), induced lateral root growth and drought resistance (Dash *et al.*, 2017). In apples, a study using a “Baleng Crab” x M.9 cross concluded that both root growth angle and total root length are good candidates to investigate deep rooting in apples and might be influenced by *MdPIN11* and *MdDRO1*. *MdPIN11* was a homologous gene for the *AtPIN2* from Arabidopsis which regulates root gravitropism and *MdDRO* homologous gene from the DEEPER ROOTING gene in rice (An *et al.*, 2017a). A later study identified 25 QTL for root angle using leafy cuttings from hybrids derived from the apple rootstocks “Baleng Crab” and M.9 and developed six diagnostic markers linked to root angle that can potentially help to select deep-rooted rootstocks. None of the QTL overlap with the dwarfing QTL suggesting that the root angle could be related to dwarfing but not genetically linked (Zheng *et al.*, 2020).

Although there has been some research focused on traits that will enhance the resilience of rootstocks, additional in-depth studies are required to gain a comprehensive understanding of root systems in trees.

1.4. Challenges in understanding rootstock-induced dwarfing, root system architecture and breeding for resilience: Knowledge gaps

The investigation of the impact of dwarfing on scions has been a well-explored subject, yet the underlying genetic basis remains unknown. Three QTL associated with rootstock-induced dwarfing have been identified although the areas covered by these QTL are quite large and contain hundreds of candidate genes. One of the objectives of this study is to fine-map the dwarfing QTL to narrow down the regions and identify the genes controlling this complex mechanism (Chapter 2). Furthermore, breeding dwarfing rootstocks is complicated since the dwarfing effect is usually lost over generations, therefore new molecular markers strongly linked to rootstock-induced dwarfing are essential to hasten the breeding process. Here I aimed to generate genetic markers associated with dwarfing that could help breeders accelerate the breeding process of new dwarfing rootstocks (Chapter 2).

Another factor to consider in the breeding of new rootstock varieties is their propagation. There are several commercial rootstocks that are difficult to propagate, which although possess numerous advantages, are not widely commercialised since their propagation is a limiting factor. In this PhD thesis, one objective is to perform QTL mapping analysis for rooting ability in apple rootstocks and investigate the impact of dwarfing on different propagation methods (Chapter 3). It is essential to better understand the impact of dwarfing in the root system architecture and how this can be optimised for both productivity and resilience. Rootstocks with improved root systems will be key to better adapting to the future climate and will address various common rootstock problems like root anchorage and nutrient uptake. Consequently, this PhD aimed to investigate the influence of two major dwarfing QTL on root architecture and rooting ability (Chapter 3).

Moreover, there has been limited research on the impact of dwarfing on the root system architecture of apples. Another aim of this project was to investigate how dwarfing influenced root traits such as total root length, maximum root depth or convex hull area that could be desirable for breeding deep-rooted rootstocks since this will improve soil anchorage and adaptability to different climate conditions. This research will help to elucidate if rootstock-induced dwarfing and root system architecture can

be decoupled to generate new rootstocks with improved root systems while maintaining the advantages of dwarfing (Chapter 4).

The findings of this thesis will then be summarised in the final chapter (Chapter 5). The end goal is to better understand the genetic and biological processes associated with rootstock-induced dwarfing and obtain markers closely linked to dwarfing and root traits that will aid the generation of more resilient rootstocks while keeping all the benefits of dwarfing.

Chapter 2. Fine mapping the root bark QTL associated with rootstock-induced dwarfing in apple rootstocks

2.1 Introduction

Rootstock-induced dwarfing is a complex trait influenced by several factors such as environmental conditions, growth parameters and scion variety. Many hypotheses have been proposed to explain dwarfing, most of them related to the altered root-to-shoot and shoot-to-root chemical signalling but the specific genes controlling this mechanism remain unknown.

Numerous QTL mapping studies have been conducted to identify the genes responsible for rootstock-induced dwarfing. Pilcher et al., (2008) were the first to genetically map *Dw1* using the progeny of a cross between the dwarfing rootstock 'M.9' and *Malus x robusta 5* (R5). The authors phenotyped trunk cross-sectional area (TCSA) as a measure for rootstock-induced dwarfing. The associated QTL which they attributed to *Dw1* in this map is located on the top of Chromosome (Chr) 5. The presence of *Dw1* in some vigorous genotypes led to the conclusion that *Dw1* was not solely responsible for the dwarfing effect. Fazio et al., (2014) identified *Dw2*, a new dwarfing locus in Chr11 using a cross of Ottawa 3 x R5, with a similar effect on vigour. QTL for early bearing, rootstock height, tree height, fruit count and flower density were found to roughly colocalize with *Dw1* and *Dw2* QTL (Fazio *et al.*, 2014). A later study using another M.9 x R5 population identified two major QTL. *Dw1* was found to colocalise with the previously published location but *Dw2,* although it was also situated in Chr11, it was placed in a slightly different location than the one reported by Fazio et al., (2014) (Foster *et al.*, 2015). Additionally, four minor-effect QTL were identified in Chromosomes 6, 9, 10 and 12 (Foster *et al.*, 2015). A high proportion of root bark (cortical cells) in the apple rootstock has been previously associated with rootstock-induced dwarfing (Beakbane and Thompson, 1947). In 2016, a QTL map for root bark ratio, a primary trait related to dwarfing, was performed using the progeny of a cross of M.27 x M.116 (M432 population) and identified *Rb1* and *Rb2* which colocalized with

regions previously associated with dwarfing (Harrison *et al.*, 2016b). *Rb1* colocalized with the region identified as controlling dwarfing in Chr5 (Pilcher *et al.*, 2008; Fazio *et al.*, 2014; Foster *et al.*, 2015) and Rb2 was situated in the same area as the *Dw2* identified by Foster *et al.*, (2015). Furthermore, Harrison et al., (2016b) discovered a third QTL, *Rb3*, located in Chr13. Cai et al., (2021) used a hybrid population from a cross of Y.2 (*M. baccata*) x Danxia (*M. x domestica*), respectively, to identify two QTL for tree height and stem diameter in Chr11 that colocalize with *Dw2.* Interestingly, no QTL was identified in Chr5. In addition, three QTL for total flower number and branching flower number were detected, one in Chr2 and two in Chr4 (Cai *et al.*, 2021).

As can be seen from the studies above it is clear that there are two QTL regions on chromosomes 5 and 11 associated with rootstock-induced dwarfing. These regions are quite large and, therefore, contain hundreds of genes. Several rootstock families and breeding selections are used in this chapter to fine-map the rootstock-induced dwarfing QTL.

The specific objectives of this chapter were:

- To fine-map the dwarfing QTL *Rb1* and *Rb2* to ultimately identify the genes responsible for rootstock-induced dwarfing and have a better understanding of this complex mechanism.
- To develop new molecular markers closely linked to dwarfing to assist rootstock breeders in the early identification and selection of dwarfing genotypes.

2.2 Methods

Several rootstock populations and rootstocks from the breeding trials have been used in this chapter to fine-map the *Rb1* and *Rb2* QTL regions. All these datasets have been summarised in Figure 2.1 together with their main use and will be further detailed in this chapter.

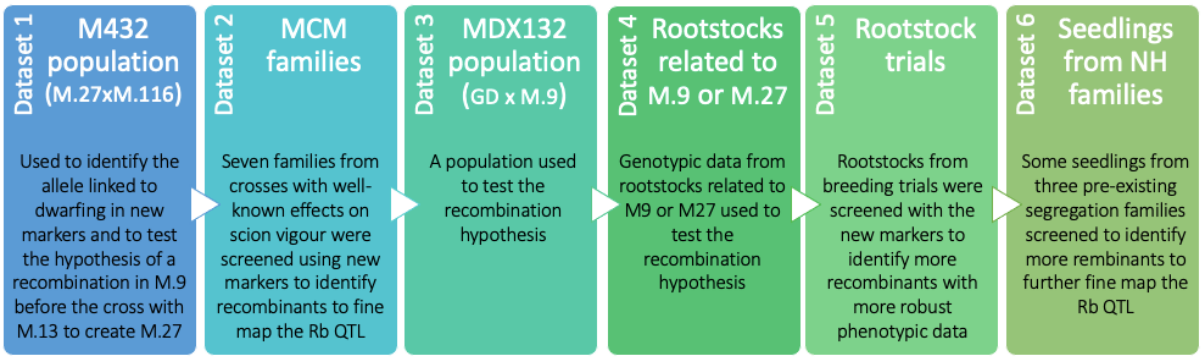

Figure 2.1. Diagram summarising the six datasets used in the fine mapping of the RB QTL and details about the main use of each dataset.

2.2.1. Primers development and identification of dwarfing alleles

2.2.1.1. Single Sequence Repeat (SSR) detection

In preparation for this project, M.9, M.M.106, M.27, M.13 and M.116 rootstock genomes were sequenced using the Illumina HiSeq 2000 platform. DNA libraries were prepared for 100 bp paired-end (PE) generating a minimum of 50X coverage by Nuria Barber. The average insert size of the libraries was 621bp. These rootstocks were selected to be sequenced because they are genetically related and, therefore, the genetic information can be tracked back (Figure 2.2).

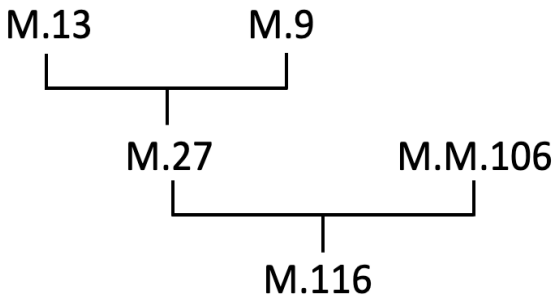

Figure 2.2. Rootstock pedigree used for variant calling

Read quality was checked with FastQC version 0.10.1 (Andrews 2010). Adaptor sequences and low-quality data were removed using fastqc-mcf (Aronesty, 2013). Single-stranded DNA from the bacteriophage PhiX is typically used as quality and calibration control for Illumina sequencing. PhiX sequences were identified and removed from the rootstock sequences aligning them against the PhiX genome using Bowtie 2 version 2.4.4 (Langmead *et al.*, 2009). Reads from each rootstock were then aligned with the doubled-haploid Golden Delicious genome GDDH13 Version 1.1 (Daccord *et al.*, 2017) using BWA-mem version 0.7.15 (Li and Durbin, 2009, 2010; Li, 2013).

SNP markers used for the root bark QTL map (Harrison et al., 2016b) were located in the doubled-haploid Golden Delicious genome GDDH13 Version 1.1 (Daccord *et al.*, 2017) using the commercial software Geneious (version 10.2.3). This allowed me to determine their physical location within the new genome and delimit the region to fine-map.

The root bark QTL regions (Figure 2.3) in the sequenced rootstocks were piled up and variant calling was performed using Samtools version 1.5 (Li *et al.*, 2009). Genetic variants were detected among the sequenced rootstocks including single nucleotide polymorphisms (SNPs), INDELs (insertions or deletions) and Single Sequence Repeats (SSRs) which will be then used as targets for primer design.

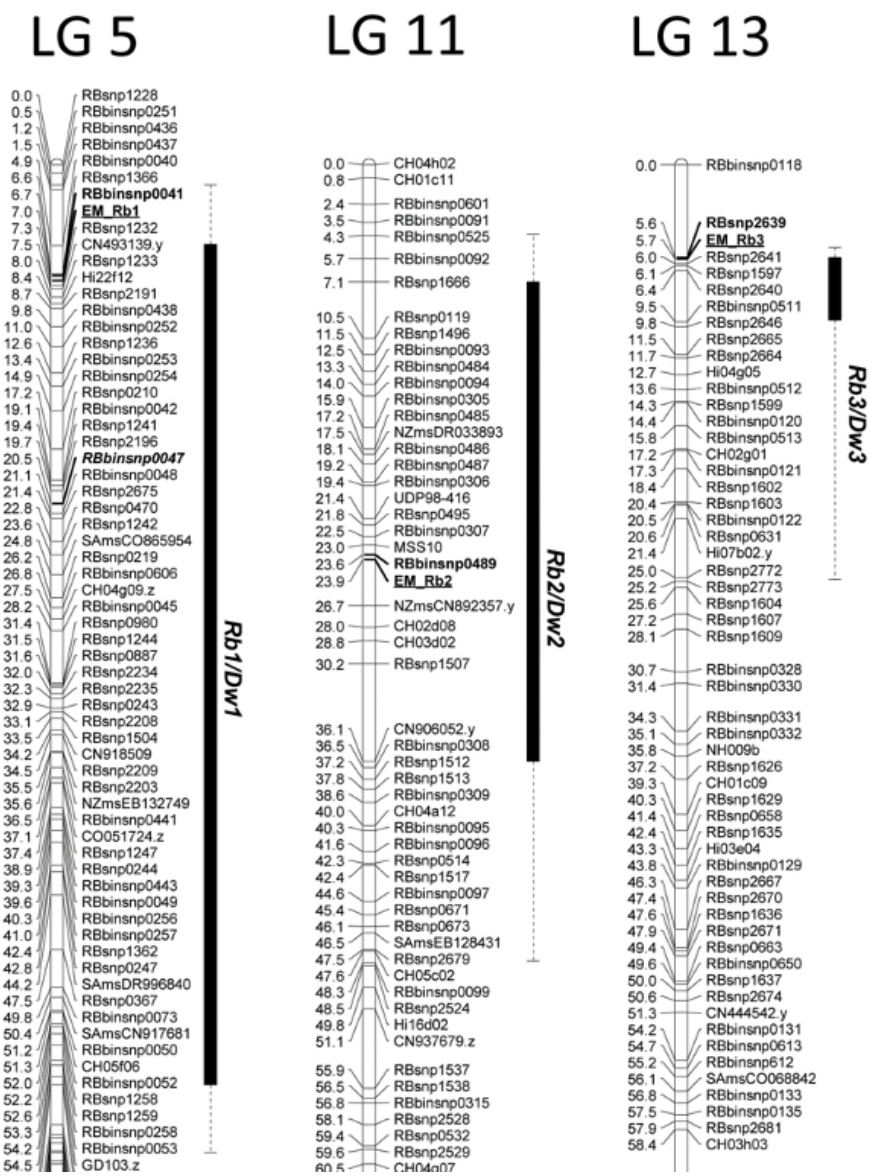

Figure 2.3. Root bark percentage QTL map using M432 population (M.27 x M.116). Markers found to be most significantly linked by (Harrison et al., 2016b) are shown in bold.

2.2.1.2. Primer design

Once genetic regions were delimited, highly polymorphic SSRs along the regions in Chromosomes 5 and 11 were selected as a target for primer design using Primer3 software (Untergasser *et al.*, 2012) available in Geneious. The regions covered by SSRs were slightly larger than the QTL region since it is difficult to find good flanking markers on the edges of the area to fine map. Twenty-seven primer pairs for sixteen loci were tested on M.9, M.27, M.26, M.116 and M.M.106, the parents of the rootstock

populations specially designed for fine mapping the root bark QTL (see details in section 2.2.2.1).

The M13-tailed primer method (Boutin-Ganache *et al.*, 2001) was used to label amplicons for visualization after capillary electrophoresis on a 3130xl genetic analyser (Applied Biosystems). Forward primers were 5'-tailed with the 18bp M13 tail (TGTAAAACGACGGCCAGT). The M13-tailed primer was 5'-fluorescently tagged with 6-FAM, HEX, NED or PET to facilitate multiplexing. Moreover, a 5′GTTT "pigtail" was added to some reverse primers to ensure consistency in amplicon size by reducing the formation of primer-dimers, enhancing specificity and acting as a spacer between the primer and the template during the PCR cycling (Brownstein *et al.*, 1996).

2.2.1.3. DNA extraction, PCR amplification and DNA genotyping by capillary electrophoresis

Leaf samples were collected from M.9, M.27, M.26, M.116 and M.M.106 rootstocks for further DNA extraction. The method chosen for the DNA extraction was Silica Bead Method described in (Edge-Garza et al. 2014). This is a high-throughput and cost-efficient method for extracting DNA from plant leaf samples which makes the sampling process simple and fast since it relies on silica gel beads to desiccate the samples (Edge-Garza et al. 2014).

DNA from the rootstocks mentioned above was used to test the 27 pairs of primers. The PCR reaction was conducted in 13 µl reactions containing 10 ng of gDNA, 1.25 µl of forward primer (2 µM), 1.25 µl of reverse primer (2 µM), 1.25 µl of the dye (2 µM), 6.25 µl of Type-it Multiplex PCR Master Mix from Qiagen and 1 µl of water. Diverse thermal profiles were tested on the primers during the optimisation process. The following touchdown PCR programme was used for all of them since this produced the best results: 95°C for 5 minutes followed by 10 cycles of 95°C for 30 seconds, then 57°C for 90 seconds and 72°C for 45 seconds (annealing temperature was gradually reduced by 0.5°C every cycle). The PCR reaction was continued with 20 cycles of 95°C for 30 seconds, then 52°C for 90 seconds and 72°C for 45 seconds. The reaction was finished with a final elongation step at 60°C for 30 minutes.

PCR products tagged with different dyes were pooled and diluted 1 to 10 with distilled water. The ABI PRISM 3130*xl* Genetic Analyzer was used to determine the exact size of the PCR fragments. Sample preparation for capillary electrophoresis consisted of a mixture of 1.3 µl of PCR dilution plus 9 µl of the electrophoresis mix (8.75 µl of deionized formamide and 0.25 µl of GeneScan(™) 500LIZ(™) from Applied Biosystems). The sample mix was denatured for 3 minutes at 90°C and cooled on ice prior to loading the instrument. Amplicon size analysis was executed using the recommended software, GeneScan version 3.7 and Genotyper version 3.7.

2.2.1.4. Dwarfing allele identification using the M432 population (Dataset 1)

The more polymorphic and easier-to-score SSR markers were selected and tested on germplasm of known phenotype to identify the dwarfing allele(s). DNA from 18 individuals from a previously characterised mapping population (M.27 x M.116 cross) was used. The selected individuals did not show any recombination events in the areas of interest. This population had been previously used for the detection of QTL controlling the root bark ratio (Harrison et al., 2016b), therefore, genotypic and phenotypic information from each individual was available.

In order to identify the alleles linked to dwarfing from markers in Chr5, genotypes with high root bark percentage (above 80%) and presenting the SNPs associated with the RB QTL were selected as an unequivocal dwarfing cohort. In addition, genotypes that did not show the SNPs associated with RB QTL and with a small root bark percentage were selected as vigorous controls. Primers were tested on these individuals following the same PCR protocol and amplicon analysis as described in section 2.2.1.3.

2.2.2. Primer selection and screening on interrelated apple rootstock families

2.2.2.1 MCM rootstock families (Dataset 2)

Seven crosses between interrelated rootstocks with well-characterised effects on scion vigour were made in preparation for this project. I was, at the time, working as a research technician and carried out the controlled pollinations as follows. Apple flowers were collected from the dwarfing and vigorous rootstocks in the 'male' column (Table 2.1); pollen was extracted, desiccated and used to pollinate previously emasculated flowers of the rootstocks in the 'female' column. Ripe apples were collected and their seeds extracted, thoroughly washed and soaked in water for 5-7 days to eliminate exuding germination inhibitors. Only healthy and fully set seeds from each cross were air-dried and stored for later sowing (Table 2.1).

Table 2.1. Parentage, number of seeds sown, seed germinated and surviving trees of the MCM rootstock populations.

Family name	Female	Male	Seeds sown	Seeds germinated	Surviving trees
MCM001	M.9	M.27	150	56	42
MCM002	M.27	M.26	224	117	98
MCM003	M.116	M.27	398	227	184
MCM004	M.27	M.116	184	48	38
MCM005	M.9	M.26	143	52	34
MCM006	M.26	M.27	263	157	140
MCM007	M.M.106	M.27	697	424	335
Total			2059	1081	871

In December 2017, a total of 2059 seeds were sown in trays with a mixture of standard compost, perlite and peat and stored in a cold store at 4°C for 14 weeks. In March 2018, trays were moved to a warm glasshouse at 25/18°C (day/night temperature) and 16/8 h day/night light (achieved with supplementary lighting).

After a few weeks, about 50% of the seeds germinated (see Table 2.1) and were labelled with the code for each cross and an individual seedling number. Seedlings were potted using standard compost containing slow-release fertilizer, grown in pots in a polytunnel. A large number of trees died during the first few weeks after potting, resulting in a final count of 871 surviving trees. In August 2020, after discarding outcrosses, only the 357 trees confirmed to belong to the aforementioned crosses were planted in a 'Deadmans Field' plot at NIAB EMR (Kent, UK).

2.2.2.2. Final primer selection and screening

Eight SSR markers were screened at the same time in the ABI PRISM 3130*xl* Genetic Analyzer to allow for allele variation in previously untested material. In order to multiplex eight primers, four dyes and primers with small and large amplicon sizes in each dye were used.

In this screening, only markers in Chromosomes 5 and 11 were used since the QTL on these regions have a major effect on dwarfing, explaining 53% of the variance as reported by (Harrison et al., 2016b). More individuals were needed to characterise the Chr5 region since this is an area of low recombination with few polymorphic SSRs for which primers of suitable amplicon size could be designed. The *Rb3* region was not included in the first analysis since its effect is not indispensable to cause dwarfing. The initial intention was to screen markers for Rb3 region after the identification of key genotypes. However, this was not executed due to time constraints.

Five loci were selected spanning the whole region in Chr5 and three loci were used to cover the whole length of the dwarfing region in Chr11. Primers for the eight loci were ordered with the forward 5'-fluorescently labelled with different dyes (6-FAM, HEX, NED and PET). Each dye was attached to two different primers and dyes were assigned ensuring that within each dye, amplicon sizes did not overlap. Amplification

of all the primers tested yielded fragments between 127 to 278 bp in length (Table 2.2).

The eight primers detailed in Table 2.2 were mixed and diluted to a final 2 µM concentration and multiplexed in one PCR reaction. These primers were screened on the 871 DNA samples from the progeny of the rootstock crosses developed explicitly for fine mapping (Table 2.1). The PCR reaction was conducted in 13 µl reactions containing 10 ng of gDNA, 1.25 µl of multiplexed primers (2 µM), 6.25 µl of Type it and 3.5 µl of water. The following touchdown PCR programme was used: 95°C for 5 minutes followed by 10 cycles of 95°C for 30 seconds, then 55°C for 90 seconds and 72°C for 30 seconds (annealing temperature was gradually reduced by 0.5°C every cycle). The PCR reaction was continued with 20 cycles of 95°C for 30 seconds, then 50°C for 90 seconds and 72°C for 30 seconds, and a final elongation step at 60°C for 30 minutes. Sample preparation for capillary electrophoresis and amplicon size analysis was performed as detailed in section 2.2.1.3.

Table 2.2. Genome positions, primer sequences, amplicon range (in MCM families), repeat motif, fluorescent dye and multiplex for PCR for the first eight SSR markers used to genotype the MCM rootstock populations.

Marker Name	Chr	Marker position in GD (bp)	Forward primer sequence 5'>3'	Reverse primer sequence 5'>3'	Amplicon size range (bp)	Motif	Dye	Multiplex
CH03a09*	5	41424461	GCCAGGTGTGACTCCTTCTC	CTGCAGCTGCTGAAACTGG	127-131	AG	FAM	Small
MD5002	5	41992706	AACATCGTGCCATGGATCCG	ACCACCATTGTTGCTTGCAA	203-229	AT	HEX	Large
MD5003	5	42191842	ACCTCCAATGCTGAGCTGAA	CCGCCAGCATGCATTTCATT	140-163	AG	HEX	Small
MD5004	5	45680011	TGGGAACTATCTTGTTTCGACT	AGGGTGGGAAACACTTGCTT	249-253	TG	NED	Large
MD5005	5	45829539	GCCGATTGATTTTCCTCTTCCA	GCGTGACTCCCTCTCATTGG	185-203	AG	NED	Small
MD11001	11	6967726	CGGAAATGTCAAATTCGCAACC	TAGCGACTTGTGTGTGTGGG	197-220	AT	PET	Large
MD11002**	11	9834270	CTTTCCCTTTTGCCACCACC	GCAGACACTCACTCACTATCTCTC	140-184	GA	PET	Small
MD11003	11	12737959	GCTCATTTTCTTCTTAAGCAGCC	CCAGTTCCTTACCAAGCAAAATGT	268-278	AT	FAM	Large

* CH03a09 has been already associated with rootstock-induced dwarfing (Pilcher *et al.*, 2008).
** MD11002 amplifies the same locus as the CH02d08 marker that has been previously associated with dwarfing (Fazio *et al.*, 2014) but new primers for this marker have been developed to meet the amplicon size requirements for multiplexing. Original sequences in (Liebhard *et al.*, 2002).

2.2.2.3. Second batch of primers and screening

The first batch of markers was screened on the seven rootstock populations to identify recombinant genotypes. Additional markers were subsequently tested to have as much marker coverage of the QTL regions to detect recombination points. This section summarises this new batch of primers.

Primer pairs for six new markers were ordered with the forward 5'-fluorescently labelled with two different dyes (6-FAM and HEX) and PCR was performed as described in the previous section. Two multiplexes were prepared, one to amplify the two new loci in Chr5 (MCM5006 and MCM5007) and another to amplify the four new loci in Chr11 (MCM11004, MCM11005, MCM11006 and MCM11007) (Table 2.3).

No more than four loci in each region were targeted in this part of the study so only 6-FAM and HEX fluorophores were used since they are cheaper. Each multiplex was tested in the seedlings previously identified as recombinants for the relevant QTL region. The allele(s) linked to dwarfing for these markers were identified following the same procedure described in section 2.2.1.4. PCR conditions, capillary electrophoresis and amplicon analysis were performed as detailed in section 2.2.2.2.

Table 2.3. Genome positions, primer sequences, amplicon range (in MCM families), repeat motif, fluorescent dye and multiplex for PCR for the second batch of SSR markers used to genotype the MCM rootstock populations.

Marker Name	Chr	Marker position in GD (Mb)	Forward primer sequence 5'>3'	Reverse primer sequence 5'>3'	Amplicon size range (bp)	Motif	Dye
MD5006	5	43035949	CCTTCACTTCCTGCCCATCC	GTCGTGGATGCTTTACCCCA	235-247	GA	FAM
MD5007	5	45229790	TGACAGCTCAGCAGTTCTCTG	ACAGCAGGCATTGTTAGGGT	262-296	CT	HEX
MD11004	11	7584542	CCCACTTCTGCTGCACTACA	AGGGGCGTTTTGATATGGGG	191-203	TA	HEX
MD11005	11	8339391	TCACTGGTGGTTCTCGATCG	CGTCGCGTACTCTGATGTCA	116-128	TA	FAM
MD11006	11	10423899	GTTTGTTGTGAAGTGAGTCCCT	TTCGATGTAATGTGGACCCCA	164-177	GT	FAM
MD11007	11	10926735	TGAAATTTTCCGACGAACCTGA	TCGCATCGCCTTCTTCTCTC	153-161	GA	HEX

2.2.3. MCM families phenotyping and data analysis

2.2.3.1. Canopy and root bark measurements

In December 2019, height and trunk diameter were measured in the 357 trees that actually belonged to the MCM crosses and were still alive. Three to ten root segments (2–8 mm in diameter, 50–80 mm in length) were excised from each root system using secateurs, placed into a labelled polythene bag and stored at 4°C before analysis. Each root root fragment was carefully washed using tap water and a scalpel or knife was used to remove a ring of bark (cortex) approximately 2–3 mm in length, leaving behind the stele of the root (Figure 2.4). Digital callipers were used to make pairs of measurements of the root with and without the bark. For each root, the cross-sectional area of the root was calculated as well as the percentage of the total area occupied by the root bark, assuming that the root section was a perfect cylinder. Trees were carefully repotted and plants were retained in case new measurements were needed.

Figure 2.4. Root segments after removing a ring of bark. Green arrow pointing to the area where the stele of the root remains.

2.2.3.2. Data analysis using MCM families

The allele information obtained after genotyping the rootstocks using the markers developed was phased to obtain the tentative haplotypes of each individual. The phasing of haplotypes refers to the process of determining the specific combination of alleles on each of the two homologous chromosomes in an individual's genome. The most likely distribution of alleles was annotated for each haplotype in an Excel document for all the individuals in each cross. The identification of haplotypes will help to detect recombinants by comparing them with the dwarfing haplotype initially identified to better determine the position of the QTL (fine mapping).

Recombinant genotypes are missing a part of the tentative dwarfing haplotype. If they still present the dwarfing phenotype, this would indicate that the region lost during that particular recombination does not contain the dwarfing gene. Conversely, a loss of the phenotypic expression would indicate that the gene responsible for that dwarfing QTL is located within that lost region. Since both, *Rb1* and *Rb2* are needed to cause dwarfing, while evaluating the effect of a recombination at one locus, the other locus always contained a full copy of the dwarfing haplotype with no recombinations.

It has been seen that the proportion of root bark diminishes as the root diameter increases and, therefore, calculating the average root bark percentage per genotype would not be correct. The root bark percentage of each genotype is usually calculated by estimating the root bark percentage of a 7.5 mm diameter root using regression analysis. The number of roots obtained from certain trees was very low to perform an adequate regression analysis to calculate the root bark ratio of a 7.5 mm root, genotypes with less than four roots collected were excluded from the analysis. Tree height, trunk diameter and root bark percentage were included in the recombinant figures 2.14 and 2.15 to help decide whether the recombinant genotype was still dwarfing or not after losing part of the dwarfing haplotype. The number of roots collected per tree was also included in the graphs since normally, in dwarfing trees, it is very difficult to collect a high number of roots. Therefore, the number of roots harvested in each genotype can also be useful to help evaluate the level of dwarfing. The analysis of each recombinant was conducted through a visual assessment, considering all the phenotypic data collectively.

2.2.4 Process to identify the recombination event that occurred during the cross that generated M.27

2.2.4.1 MDX132 (Dataset 3)

The MDX132 family is the progeny of a Golden Delicious (GD) x M.9 cross; 287 seedlings were planted in a 'Deadmans Field' plot at NIAB EMR (Kent, UK) in 2016 (more details in section 3.2.4). This family was used to help identify the dwarfing allele and to confirm the hypothesis of recombination in the cross that generated M.27.

DNA from 148 individuals of the MDX132 mapping population and the parents (GD and M.9) was extracted using the Qiagen DNeasy Kit. The Illumina Infinium® SNP array (also known as the 20K array) was used for genotyping the 150 individuals. The SNP array developed for *Malus spp,* which targets approximately 18k SNPs identified from resequencing 13 apple (*M.* × *domestica*) cultivars and one accession of the crab apple species *M. micromalus* (Bianco *et al.*, 2014). The array contains a total of 18019 SNPs of which 3305 originated from the 8K IRSC chip (Chagné *et al.*, 2012). DNA was prepared according to the manufacturer's recommendations.

The genotypes for each marker were assigned using GenomeStudio Genotyping Module 2.0 (Illumina, San Diego, CA, U.S.A). Automated allele calling was used followed by visual inspection to confirm the clustering of individuals into appropriate classes. Manual clustering was performed for some markers when automated clustering was not satisfactory. ASSisT software (Di Guardo *et al.*, 2015) was used to select only robust markers with a clear cluster separation; 8,700 SNP markers passed this quality control. The low number of filtered SNPs was due to the large number of monomorphic markers in our population which accounted for 35.9% of the total SNPs.

The SNP markers were renamed from 1 to 8700 and coded for linkage map construction according to JoinMap 4.1 conventions as heterozygous in either the father or the mother (<nn × np>, <lm × ll>) or both parents (<hk × hk>) (VAN Ooijen, 2011). A logarithm of odds (LOD) of 4.0 was used to assign markers to different linkage groups. Markers with suspect linkage (recombination frequency estimate >0.6) were removed. Map order was calculated using the maximum likelihood option which calculates both parental maps and an integrated map.

SNP chip data from the MDX132 population (GD x M.9) were used to identify the dwarfing haplotype in the progeny to help with the identification of dwarfing genotypes for the root system architecture experiment (Chapter 4). The data was compared to the SNP chip data from the M432 population (M.27 x M.116), which had previously been used for QTL mapping of root bark ratio (Harrison et al., 2016b). Both M.9 and M.27, are dwarfing rootstocks and M.27 comes from a cross between M.13 (vigorous) and M.9 (dwarfing).

2.2.4.2 SNP calling of rootstocks related to M.9 or M.27 (Dataset 4)

A large number of rootstocks were genotyped in 2014 using the 20K SNP chip as part of a previous study (data not shown). M.9, M.13, M.16, M.26, Ottawa 3, G.30, M.200, R5 and G.41 rootstocks that are derived either from M.9 or M.27 or the parents of a relevant genotype were selected and the SNPs located in the RB QTL regions reanalysed. Automated allele calling was performed followed by visual checking to confirm the clustering of individuals into appropriate classes. Manual clustering was implemented for some markers when automated clustering was not adequate.

2.2.5. Rootstock material from breeding trials to further fine map the RB QTL

2.2.5.1 Rootstocks from breeding trials (Dataset 5)

In April 2018, three apple rootstock trial plots that had been evaluated as part of the East Malling Rootstock Club were excavated using a digger. All these rootstocks in these trials had a dwarfing parent or grandparent; therefore, the dwarfing haplotype(s) could be present in them and their characterisation could contribute to the fine mapping of the root bark QTL and to the validation of the dwarfing markers in different germplasm. Plot RF185 was planted in 2012 and included four selections (M306-6, M306-79 and M306-189) and three rootstock cultivars (M.9, M.M.106 and M.116) as controls. All rootstocks were grafted with Royal Gala as a common scion. The trees available in plot VF224 were planted in March 2010 and included the selections AR10-3-9, AR809-3, AR835-11 and R80. M.M.106 and M.116 rootstocks were used as standard controls. All the rootstocks at the VF224 plot were grafted with Red Falstaff as a scion. In plot EE207 the trees were also planted in March 2010 and the rootstock selections AR852-3, AR839-9, B24, R59 and R104 were assessed with M.26, M.9 and

M.27 as controls. These rootstocks were grafted with two scions, Braeburn and Royal Gala (Table 2.4).

In May 2020, another apple plot named SP250 containing Canadian and Malling rootstocks was grubbed and roots were also collected to identify more recombinants that could help with the fine mapping of the RB QTL. The rootstocks SJM15, SJM188, SJM189, SJP84-5162, SJP84-5231, SJP84-5174 and SJP84-5217 were assessed with M.26, M.27 and M.9 as controls. Most of the rootstocks were grafted with both scions, Gala and Braeburn, but some rootstocks were only grafted with one of them. Details about the number of rootstocks sampled per combination are described in Table 2.4.

Unfortunately, roots could not be obtained from some rootstocks as they were dead or severely damaged. The exact number of rootstocks sampled in each trial is detailed in Table 2.4. Between six and twenty root segments (4–10 mm in diameter, 80–120 mm in length) were excised from each root system using secateurs, placed into a labelled polythene bag and stored at 4°C before analysis. The roots were measured following the same protocol described in section 2.2.3.1.

DNA of these rootstock genotypes was available having been extracted using the Qiagen Dneasy Kit by Dr Suzanne Litthauer (molecular assistant breeder at NIAB EMR). DNA samples were diluted to 5 ng/ul and screened with the first SSR primer multiplex as described in section 2.2.2.2. Recombinant genotypes were screened with the two additional multiplexes for Chr5 and 11 regions as appropriate (see detail in section 2.2.2.3) to identify new recombination points and help narrow down the dwarfing haplotype(s).

Table 2.4. Location, planting year, parentage and number of trees sampled per scion from trials RF185, VF224, EE207 and SP250 that were used to fine-map the root bark QTL.

Plot name	Planting year	Genotype	Pedigree	N. trees sampled Scion A*	N. trees sampled Scion B**
RF185	2012	M.9	Unknown	3	-
RF185	2012	M.M.106	Northern Spy x M.1	4	-
RF185	2012	M.116	M.27 x M.M.106	4	-
RF185	2012	M306-6	AR86-1-20 x M.20	3	-
RF185	2012	M306-79	AR86-1-20 x M.20	4	-
RF185	2012	M306-189	AR86-1-20 x M.20	4	-
VF224	2010	AR10-3-9	M.M106 x M.27	7	-
VF224	2010	AR809-3	R80 x M.26	8	-
VF224	2010	AR835-11	M793 x M.9	7	-
VF224	2010	M.116	M.27 x M.M.106	8	-
VF224	2010	M.M.106	Northern Spy x M.1	8	-
VF224	2010	R80	AR134-31 x AR86-1-22	8	-
EE207	2010	AR852-3	AR362-16 x OP***	5	3
EE207	2010	AR839-9	M.7 x M.27	8	6
EE207	2010	B24	AR10-2-5 x AR86-1-22	5	5
EE207	2010	M.26	M.16 x M.9	8	7
EE207	2010	M.27	M.13 x M.9	8	4
EE207	2010	M.9	Unknown	7	6
EE207	2010	R104	AR134-31 x AR86-1-22	4	3

EE207	2010	R59	AR134-31 x AR86-1-22	7	6
SP250	2014	SJM15	*M. baccata 'Nertchinsk'* x M.9	0	3
SP250	2014	SJM167	*M. baccata 'Nertchinsk'* x M.26	4	4
SP250	2014	SJM188	*M. baccata 'Nertchinsk'* x M.26	3	0
SP250	2014	SJM189	*M. baccata 'Nertchinsk'* x M.26	0	4
SP250	2014	SJP84-5162	*M. robusta 5* x M.27	3	0
SP250	2014	SJP84-5174	*M. robusta 5* x M.27	2	2
SP250	2014	SJP84-5217	*M. robusta 5* x B.57490	4	4
SP250	2014	SJP84-5231	*M. robusta 5* x M.27	0	2
SP250	2014	M.26	M.16 x M.9	4	4
SP250	2014	M.9	Unknown	3	4
SP250	2014	M.M.106	Northern Spy x M.1	4	4

* RF185 rootstocks and VF224 rootstocks were only grafted using one scion, Gala and Red Falstaff, respectively. For EE207 and SP250 plots, scion A was Braeburn.

**Scion B was Royal Gala for rootstocks in EE207 plot and Gala for rootstocks in SP250 plot.

***Open pollination (pollen donor unknown)

2.2.5.2 NH rootstock families (Dataset 6)

A total of 92 seedlings from 3 pre-existing segregating progenies were characterised to identify further recombinants (Table 2.5). In May 2020, leaf material was collected from the seedlings and DNA was extracted using the Silica Bead Method described in (Edge-Garza *et al.*, 2014). DNA was quantified using Nanodrop and then diluted to 5 ng/ul. The first primer multiplex was screened in all the individuals and the multiplexes with extra markers for the Chromosome 5 and 11 regions were tested on relevant recombinants only as described in sections 2.2.2.2 and 2.2.2.3, respectively.

Five to nine root segments (3–10 mm in diameter, 50–120 mm in length) were excised from each root system using secateurs, placed into a labelled polythene bag and

stored at 4°C before analysis. The roots were measured as described in section 2.2.3.1. Tree height was also recorded for these trees.

Table 2.5. Family name, pedigree and number of seedlings of the new pre-existing progenies examined to identify further recombinants.

Family name	Pedigree	Number of seedlings
NH006	M.116 x M.27	25
NH007	M.27 x M.116	36
NH008	M.13 x M.9	31

2.2.5.3 Data analysis for genotypes in datasets 5 and 6

The number of roots available and measured per genotype in dataset 5 (replicated trials) was unsurprisingly higher than for unreplicated seedlings from the progenies in other datasets. The percentage of root bark at a standard root diameter of 7.5 mm was inferred in each genotype using regression analysis. The allele information obtained after genotyping the rootstocks was phased and sorted in an Excel document to help detect recombinants by comparing them with the dwarfing haplotype already identified. The root bark percentage data was used to produce box plot graphs of the recombinant genotypes and the respective controls (Figures 2.16, 2.17 and 2.18). The graphs help to visualise how similar or different the recombinant genotypes found in each plot were when compared to the standards.

The number of roots collected from NH families (Dataset 6) was not very high since the trees needed to be kept alive and harvesting many thick roots could kill the trees. Nevertheless, the percentage of root bark at a standard root diameter of 7.5 mm was also inferred in each genotype using regression analysis. Only recombinant genotypes with more than four roots collected were used for fine mapping.

As in section 2.2.3.2 tree height and root bark percentage were included in the recombinant figure of the NH families (Figure 2.22) to help decide whether the recombinant genotype could still be considered dwarfing without part of the initially-identified dwarfing haplotype. The number of roots collected per tree was also included since in dwarfing trees it is normally very difficult to collect a high number of roots and this information can also be useful to evaluate the level of dwarfing of each recombinant.

For validation analysis, 14 non-recombinant genotypes from the breeding trials programme were used to evaluate the effectiveness of the markers to predict the level of dwarfing. In the absence of *Rb3* information, genotypes that presented dwarfing markers in both haplotypes, *Rb1* and *Rb2* QTL regions, were predicted as dwarfing. Individuals that did not have any dwarfing markers or had only those in the *Rb1* area, were categorised as semi-vigorous. As mentioned before, these rootstocks were carefully evaluated by breeders over several years of phenotypic measurements, including tree height and girth. These measurements together with the root bark percentage estimated using a 7.5 mm root, demonstrated the actual level of dwarfing of these trees.

Linear mixed models fitted by REML were used to analyse the effect of the scion on root bark percentage in EE207 and SP250 plots using the “lme4” package available in R (Bates *et al.*, 2015). The model selection was performed by dropping variables and comparing models with likelihood ratio tests using the ANOVA function. Rootstock, scion and the interaction between rootstock and scion were the fixed variables. The random variable for the EE207 trial analysis was block and for the SP250 trial was row. Post hoc contrasts were performed using the “emmeans” package available in R (Lenth *et al.*, 2018). Graphical outputs were obtained using the “ggplot2” (Wickham, 2016).

2.3 Results

2.3.1. Identifying haplotypes linked to root bark using the M432 population (Dataset 1)

In Harrison et al., (2016b), the QTL associated with root bark percentage spanned unusually large regions of the genome (47.5, 43.2 and 19.4 cM respectively for *Rb1*, *Rb2* and *Rb3*) due to the limited number of recombinations in the areas of interest, particularly in Chr5, and the mapping model chosen.

In this study, visual scrutiny of marker segregation for recombinant individuals in the M432 population was used to narrow the root bark QTL regions associated with dwarfing. After this exercise, the markers flanking the Chr5 QTL (*Rb1*) were RBbinsnp0041 at 6.7 cM and RBbinsnp0047 at 20.5 cM; the Chr11 QTL (*Rb2*) was delimited by UDP98-416 and CH04a12 located at 21.4 cM and 40 cM, respectively. A similar analysis could not be used in QTL in Chr13 since the effect of *Rb3* is additive rather than indispensable to cause the dwarfing phenotype. Furthermore, this QTL was relatively small and flanked by RBsnp2639 at 5.6 cM and RBbinsnp0511 at 25.5 cM (Figure 2.5).

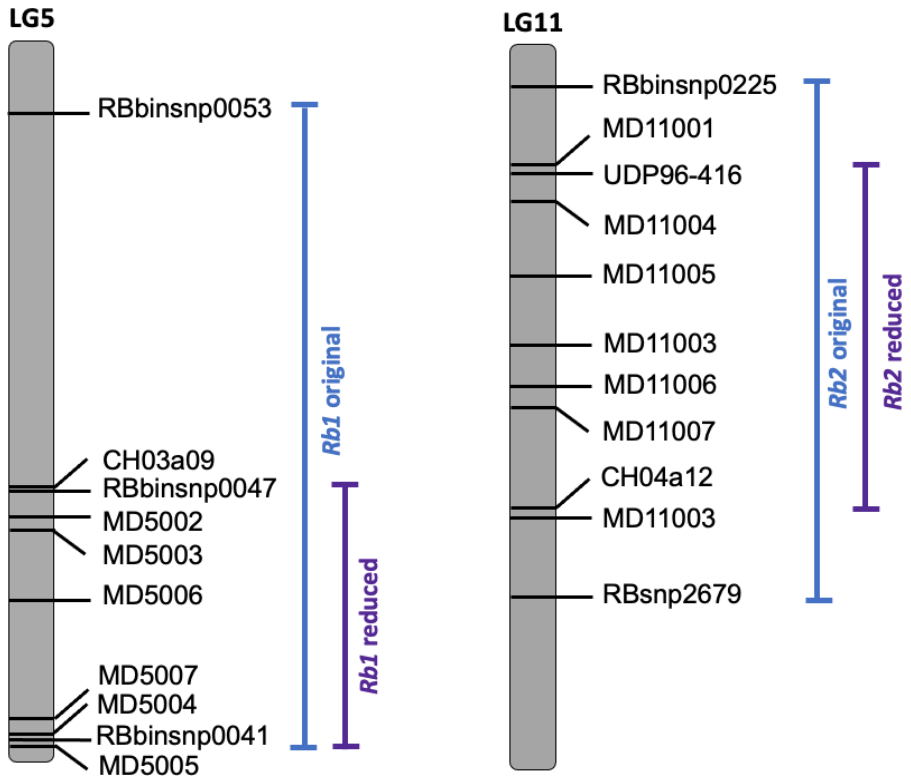

Figure 2.5. Diagram showing key SNP distribution delimiting the *Rb1* and *Rb2* QTL original regions (blue) and the reduced regions (purple) after visually inspecting recombinant genotypes from M432 population. Markers developed in this study spanning the refined regions are also included.

Subsequently, the allele linked to dwarfing in each new flanking marker was identified using M432 root bark percentage data and the presence/absence of the SNPs most significantly associated with increased root bark for each linkage group in (Harrison et al., 2016b). Similarly, alleles amplified by newly designed primers (Table 2.2) were compared with a subset of seedlings with unambiguous phenotypes. For each marker, the common allele present in all individuals classed as unambiguously dwarfing (RB > 80% and carrying the SNP marker with the highest association with the trait) and absent for individuals classed as unambiguously non-dwarfing (RB < 65% and not carrying the SNP associated with the trait) were assigned to the tentative dwarfing haplotypes for Chr5 (Figure 2.6) and Chr11 (Figure 2.7). Given that the selected dwarfing and non-dwarfing genotypes from the M432 progeny did not have any recombiantion event, all the alleles linked to dwarfing in each QTL region belonged to the same haplotype, the dwarfing haplotype. The alleles not associated with dwarfing

formed different haplotypes for Chr5 and 11 regions that were estimated based on the most common combination of alleles in this subset of the M432 population.

Genotype	M432-053		M432-107		M432-127	
RB %	84.6		83.2		82.1	
SNP	Yes		Yes		Yes	
SSR marker	H1	H2	H1	H2	H1	H2
CH03a09	**132**	130	**132**	132	**132**	132
MD5002	**204**	208	**204**	202	**204**	202
MD5003	**141**	162	**141**	150	**141**	150
MD5004	**248**	252	**248**	250	**248**	250
MD5005	**205**	195	**205**	212	**205**	212
Genotype	M432-26		M432-31		M432-75	
RB %	64.2		56.8		62.8	
SNP	No		No		No	
SSR marker	H1	H2	H1	H2	H1	H2
CH03a09	130	132	130	130	130	132
MD5002	208	202	208	208	208	202
MD5003	162	150	162	162	162	150
MD5004	252	250	252	252	252	250
MD5005	195	212	195	195	195	212

Figure 2.6. Summary of allele sizes in 6 non-recombinant individuals with unambiguous dwarfing (top) vs non-dwarfing (bottom) phenotypes from the M432 (M.27 x M.116) population for the five SSR markers in the *Rb1* region (Chr5) developed in this study. Alleles linked to the dwarfing trait are shown in bold. Alleles sizes do not include the M-13 tail although they were first identified using M-13 tagged primers

Genotype	M432-053		M432-107		M432-036	
RB %	84.6		83.2		80.7	
SNP	Yes		Yes		Yes	
SSR marker	H1	H2	H1	H2	H1	H2
MD11001	**212**	**212**	**212**	**212**	**212**	204
MD11002	**142**	**142**	**142**	**142**	**142**	140
MD11003	**272**	**272**	**272**	**272**	**272**	268
Genotype	**M432-011**		**M432-051**		**M432-088**	
RB %	**68.8**		**61.6**		**59.3**	
SNP	**No**		**No**		**No**	
SSR marker	**H1**	**H2**	**H1**	**H2**	**H1**	**H2**
MD11001	197	204	197	204	197	204
MD11002	155	140	155	140	155	140
MD11003	276	268	276	268	276	268

Figure 2.7. Summary of allele sizes in 6 non-recombinant individuals with unambiguous phenotypes, dwarfing (top) vs non-dwarfing (bottom) from the M432 (M.27 x M.116) population for the three SSR markers in the *Rb2* region (Chr11) developed in this study. Genotypes 'M432-053' and 'M432-107' are homozygous for the dwarfing haplotype. Alleles linked to the dwarfing trait are shown in bold. Alleles sizes do not include the M-13 tail although were first identified using M-13 tagged primer.

2.3.2. Fine mapping Step 1 - Recombination in M9 gamete in the M.13 x M.9 cross that generated M27 (Datasets 1, 3 and 4)

2.3.2.1 M.9 and M.27 dwarfing haplotypes

SNP chip data from the MDX132 population (GD x M.9) were compared to the SNP chip data from the M432 population (M.116 x M.27) to identify the dwarfing haplotype for the root architecture experiment (Chapter 4).

Only 3000 SNPs from the 8K array used to genotype the M432 population were present in the 20K array. Unfortunately, the two SNPs with the most significant associations to root bark ratio in Chr5 and Chr13 were not present in the 20K SNP array. Only six SNPs were shared in both arrays in the Chr5 region. A seventh marker was added to the analysis since it was very close to the region and had the same

segregation as the most significant marker. Four shared SNPs were found in the Chr11 QTL region and two in Chr 13.

This study determined the physical position of the SNPs in the dwarfing areas in the Golden Delicious (GD) genome (Daccord *et al.*, 2017). Linkage group 5 was inverted in Harrison et al. (2016b) with respect to the genome alignment which now places the dwarfing region at the end of the Chr5 (between 41.4 and 45.9 Mb).

The dwarfing haplotype in M.27 identified from the segregation of the M432 population was compared to the two possible haplotypes of M.9 (tentatively identified from the segregation of MDX132 family). Three SNPs from the expected dwarfing haplotype in Chr5 were in phase 0 and the other four were in phase 1 (Figure 2.8). M.9 haplotypes identified in the MDX132 family in Chr11 and Chr13 perfectly matched the haplotypes obtained for M.27 in M432.

SNP Name M432	M.27	M.116	Segregation	Phase	cM	M.27 Dw Haplotype	M.27 Non-Dw Haplotype
RBbinsnp0047	AB	BB	lmll	(0-)	20.5	A	B
SNP0210	AB	AA	lmll	(0-)	17.2	B	A
RBbinsnp0253	BB	AB	nnnp	(-0)	13.4	B	B
SNP1236	BB	AB	nnnp	(-0)	12.6	B	B
SNP1233	BB	AB	nnnp	(-0)	8.0	B	B
SNP1232	AA	AB	nnnp	(-0)	7.3	A	A
RBbinsnp0040	AB	AA	lmll	(0-)	4.9	B	A
SNP Name MDX132	**GD**	**M.9**	**Segregation**	**Phase**	**cM**	**M.9 Haplotype 1**	**M.9 Haplotype 0**
SNP1943	AA	AB	nnnp	(-0)	20.5	A	B
SNP0049	AB	AB	hkhk	(11)	17.2	B	A
SNP5999	AA	AB	nnnp	(-1)	13.4	B	A
SNP1185	BB	AB	nnnp	(-0)	12.6	B	A
SNP0946	BB	AB	nnnp	(-1)	8.0	A	B
SNP5892	AA	AB	nnnp	(-1)	7.3	B	A
SNP1613	BB	AB	nnnp	(-1)	4.9	A	B

Figure 2.8. Allele segregation, phase and position in the genome of the SNPs from the M432 and MDX132 populations in the *Rb1* QTL region. SNPs in common highlighted in blue.

2.3.2.2 Using commercial rootstocks derived from M.9 or M.27 to confirm the M.9 to M.27 recombination hypothesis (Dataset 4)

I hypothesised that a recombination event in the *Rb1* region (Chr5) must have occurred in the M.9 pollen grain of the 1934 M.13 x M.9 cross from which M.27 originated. To confirm this hypothesis, seven SNPs in the Chr 5 dwarfing region were examined in four rootstocks derived either from M.9 or M.27 (Table 2.6).

Table 2.6. Parentage and dwarfing degree of rootstocks used for SNP analysis in Chromosome 5 QTL region to test the recombination hypothesis.

Mother	**Dwarfing degree**	**Father**	**Dwarfing degree**	**Progeny**	**Dwarfing degree**
M.16	Vigorous	M.9	Dwarfing	M.26	Semi dwarfing
R5*	Vigorous	Ottawa 3**	Dwarfing	M.200	Dwarfing
R5*	Vigorous	M.9	Dwarfing	G.30	Semi dwarfing
M.27	Very dwarfing	R5	Vigorous*	G.41	Dwarfing

**M. robusta* 5 is only used for breeding and no records have been found of its phenotype as a rootstock. It has been classed as vigorous since it carries none of the alleles linked to *Dw* or *Rb* in previous studies. ** Ottawa 3 originated from a Robin Crab x M.9 cross.

Figure 2.9 shows the SNPs and estimated haplotypes of the parents of M.26 in the Chr5 QTL region associated with dwarfing. M.26 is a semi-dwarfing rootstock generated from a cross between M.16 (vigorous) and M.9 (dwarfing). The dwarfing phenotype must therefore have been inherited from M.9. The estimated M.9 haplotype in M.26 matched with the M.9 haplotype 1 obtained during the genotyping of the MDX132 population (Figure 2.8).

F		M			F		M
M.16	x	M.9	→	M.26	M.16	x	M.9
AA		AB		AA	A		A
AB		AB		BB	B		B
NC		AB		BB	B		B
BB		AB		BB	B		B
BB		AB		AB	B		A
AA		AB		AB	A		B
AA		AB		AA	A		A

Figure 2.9. Expected haplotypes for M.16 and M.9, parents of M.26. In blue, the section that matches the M27 dwarfing haplotype estimated from the M432 population. NC, uncalled SNP.

Ottawa 3 is a dwarfing rootstock originated from a cross between Robin Crab and M.9 (dwarfing), making M.9 a grandparent of M.200. We assume that the dwarfing haplotype would have been transferred from M.9 to Ottawa 3 and finally to M.200. The Ottawa 3 haplotype also matched the M.9 haplotype 1 obtained during the genotyping of the MDX132 population (Figure 2.10). The second SNP from the top in R5 was miscalled as AA and has been corrected to AB.

F		M			F		M
R5	x	Ottawa 3	→	M.200	R5	x	Ottawa 3
BB		A		AB	B		A
A(B)		B		BB	B		B
AB		B		AB	A		B
AB		B		AB	A		B
BB		B		AB	B		A
AA		A		AB	A		B
BB		B		AB	B		A

Figure 2.10. Expected haplotypes for R5 and Ottawa 3, parents of M.200. In blue, the section that matches the M.27 dwarfing haplotype estimated from the M432 population. In green, the corrected allele for R5.

In G.30, a semi-dwarfing rootstock originated from a cross of Robusta 5 (vigorous) and M.9 (dwarfing), the M.9 haplotype inherited by G.30 coincided with the haplotype 1 obtained during the genotyping of the MDX132 population (Figure 2.11).

F		M			F		M
R5	x	M.9	→	G.30	R5	x	M.9
BB		AB		AB	B		A
A(B)		AB		BB	B		B
AB		AB		AB	A		B
AB		AB		AB	A		B
BB		AB		AB	B		A
AA		AB		AB	A		B
BB		AB		AB	B		A

Figure 2.11. Expected haplotypes for R5 and M.9, parents of G.30. In blue, the section that matches the M.27 dwarfing haplotype estimated from the M432 population. In green, the corrected allele for R5.

M.27 rootstock was only genotyped using the 8K SNP chip platform whereas R5 and G.41 were screened using the 20K array. SNP data from both arrays were used in Figure 12 to infer the haplotype of M.27 transferred to G.41. In this case, the M.27 haplotype coincided with the dwarfing haplotype obtained during the genotyping of M432.

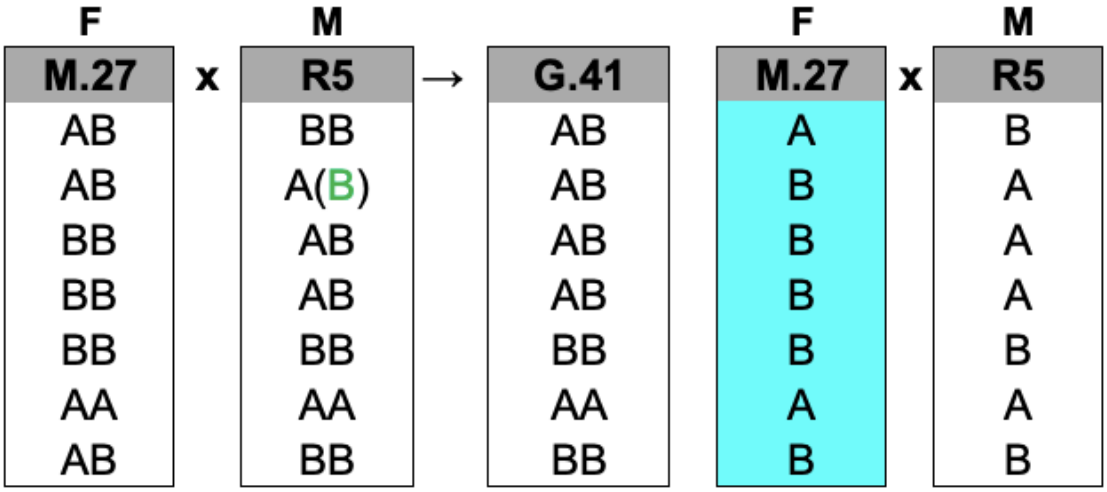

Figure 2.12. Expected haplotypes for M.27 and R5, parents of G.41. In blue, the section that matches the M.27 dwarfing haplotype estimated from the M432 population. In green, the corrected allele for R5.

All these results supported the hypothesis of recombination in the M.9 gamete which produced M.27. In crosses with M.9 as an ancestor, the M.9 haplotypes were consistent, showing only the first four SNPs of the QTL (haplotype 1) in common with the dwarfing haplotype obtained from M.27. However, in M.27 derived genotypes, the dwarfing haplotype completely matched that obtained in the M432 population. Consequently, the recombination took place somewhere between Rbsnp1233 and Rbsnp1236 markers, at 8.0 cM and 12.3 cM, respectively and we can conclude that the region covered by haplotype 0 is not needed for the expression of the dwarfing phenotype. This finding contributed to refine the mapping of the root bark QTL in Chr5 to the area between 41.4 Mb to 45.8 Mb.

2.3.3. Fine mapping Step 2 - MCM rootstock families (Dataset 2)

2.3.3.1 Dwarfing haplotype determination in the parents of the MCM families

The dwarfing haplotype was determined in the parents of the MCM crosses (Table 2.7) so that recombinant genotypes could be identified. Table 7 clearly shows where the recombination of the M.9 haplotype that resulted in the Chr5 allele combination in M.27 occurred resulting in two different dwarfing haplotypes. On the other hand, M.26

(M.16 x M.9) inherited the M.9 *Rb1* haplotype intact. All the markers used in M.26 are homozygous except one, making it almost impossible to distinguish which haplotype is dwarfing in crosses with M.26 as a parent (Figure 2.13).

The amplification of the MD5005 primer was poor in several seedlings from all crosses so this marker was excluded from the analysis for consistency. Since this marker was outside the tighter QTL region identified in this study, we did not aim to replace it or redesign the primers.

	M.27		M.26		M.116		M.M.106		M.9	
Markers Chr5	**H1**	**H2**	**H1**	**H2**	**H1**	**H2**	**H1**	**H2**	**H1**	**H2**
CH03a09	132	130	132	132	132	130	132	128	132	128
MD5002	204	208	204	204	202	208	202	200	204	null
MD5003	141	162	141	141	150	162	150	138	141	150
MD5006	235	245	235	235	247	245	247	245	235	247
MD5007	286	264	276	262	279	266	279	296	276	286
MD5004	248	252	250	250	250	252	250	250	250	248
	M.27		**M.26**		**M.116**		**M.M.106**		**M.9**	
Markers Chr11	**H1**	**H2**	**H1**	**H2**	**H1**	**H2**	**H1**	**H2**	**H1**	**H2**
MD11001	212	197	212	197	212	204	204	220	212	220
MD11004	203	191	203	191	203	null	null	199	203	199
MD11005	128	116	128	116	128	null	null	99	128	124
MD11002	142	155	142	155	142	140	159	140	142	142
MD11006	164	170	164	168	164	170	177	170	164	168
MD11007	159	153	159	157	159	155	161	155	159	161
MD11003	272	276	272	266	272	268	266	268	272	278

Figure 2.13. Estimated haplotypes in the parents of MCM families showing allele sizes for all the markers used in this study. Highlighted in blue, the dwarfing haplotype. In red, allele sizes that are similar to the alleles associated with dwarfing. The thick line indicates the point of the recombination.

2.3.3.2 Identification of recombinant genotypes in MCM rootstocks families

Using the dwarfing haplotypes determined in 2.3.3.1, the genotypes with a recombination event in Chr5 and/or Chr11 were identified. A total of 60 and 84 seedlings were found to carry recombinations in Chr5 and Chr11, respectively; 12 genotypes presented recombinations in both regions.

Even with carefully controlled crosses, there are always some seedlings that do not match the expected pedigree. This could be due to rare selfing, undesired pollen reaching the emasculated flower or to seed mixtures. Unfortunately, the number of outcrosses in four of the families was very high and not many recombinant individuals could be reliably detected in those populations. Once outcrosses were discounted only the seedlings with confirmed parentage were used to identify recombinants. The number of seedlings confirmed as part of the MCM families was 357 (Table 2.8).

The MCM families were renamed from A to G for simplicity. Genotypes within each family are denoted (hereafter) with the corresponding family letter and the genotype number (Table 2.7).

Table 2.7. Family name, parentage, number of seedlings, percentage of outcrosses, final number of seedlings and recombinants in *Rb1* and *Rb2* regions in the rootstock populations after screening the first batch of markers.

Family name	New name	Female	Male	Number of seedlings	% outcrosses	Final number of seedlings	Recombinants in Chr5*	Recombinants in Chr11*
MCM001	A	M.9	M.27	42	9%	38	6	18
MCM002	B	M.27	M.26	98	81%	18	3	8
MCM003	C	M.116	M.27	184	75%	30	5	6
MCM004	D	M.27	M.116	38	94%	2	1	0
MCM005	E	M.9	M.26	34	88%	3	0	1
MCM006	F	M.26	M.27	140	30%	98	19	23
MCM007	G	M.M.106	M.27	335	49%	168	26	28
TOTAL				871		357	60	84

* Recombinants in both regions included.

2.3.3.3 Useful recombinants in MCM rootstocks families

Not all the recombinants identified in the MCM families (A-G families) were useful for fine mapping. As both of the dwarfing QTL, *Rb1* and *Rb2*, are needed to cause the phenotype (Harrison et al., 2016b), recombinant genotypes in one region that did not have a dwarfing haplotype in the other region were discarded for this analysis. In addition, only one copy of the dwarfing haplotype at each locus is needed to cause dwarfing. Consequently, genotypes with two copies of the tentative dwarfing haplotypes presenting recombination in only one of the haplotypes were also discarded since the phenotypic effect of the crossover could not be evaluated. Twelve genotypes had recombinations in both regions and were discounted as it would have been impossible to determine which of the two crossovers was responsible for the non-dwarfing phenotype (Table 2.8). Ultimately, the number of useful recombinants in *Rb1* region was 24 and 33 in *Rb2* region.

Table 2.8. Family name, newly coded name, parentage and number of useful recombinants in *Rb1* and *Rb2* QTL regions in each rootstock population.

Family name	New family name	Female	Male	N. of useful recombinants in Chr5	N. of useful recombinants in Chr11
MCM001	A	M.9	M.27	1	3
MCM002	B	M.27	M.26	3	6
MCM003	C	M.116	M.27	2	2
MCM004	D	M.27	M.116	1	0
MCM005	E	M.9	M.26	0	1
MCM006	F	M.26	M.27	5	11
MCM007	G	M.M.106	M.27	12	10
TOTAL				24	33

2.3.3.4 Fine mapping of Rb1 using MCM families

Root bark percentage (RB%), tree height and trunk diameter were recorded for all the recombinant genotypes found in the *Rb1* QTL region. The number of roots collected per genotype was also recorded since usually, a dwarfing tree does not have many thick roots available for collection and, therefore, a small or large number of roots could be also used as an indicator of the dwarfing degree. The dwarfing level of each genotype (dwarfing vs vigorous) was estimated based on all the phenotypic data available whenever possible. The RB% of the dwarfing rootstocks ranged from 66.6 % to 74.2%. However, in vigorous rootstocks, the RB % range was from 51.3% to 66.6%. Genotypes with intermediate RB % values and/or contradictory phenotypic information were either given a tentative phenotype or classified as inconclusive.

A total of 24 useful recombinant genotypes were identified in the area of interest. As explained before, the number of roots collected in these trees was very small due to the age of the trees and the need to keep them alive. Trees with less than four roots were excluded from the analysis and the final number of genotypes used for fine mapping the *Rb1* QTL was 14 rootstocks. The markers and their corresponding alleles linked to dwarfing are denoted by the name of the marker plus the size of the allele in base pairs as in Figure 2.12.

Genotypes G147 and G335 (M.M.106 x M.27) carried the dwarfing linked allele CH03a09-132 (132bp allele from marker CH03a09) from M.27 and presented root bark ratios of 64.6% and 61.5% (Figure 2.14). These two genotypes carried the non-dwarfing linked alleles for the rest of the markers from M.27, indicating that there must have had a recombination event between CH03a09 and MD5002 in M.27 gametes for the M.M.106 x M.27 cross. The dwarfing level of G147 could not be estimated as the phenotypic data were not conclusive. However, G335 was classified as an invigorating rootstock.

Genotypes A025 (M.9 x M.27) and B055 (M.27 x M.26) had three dwarfing linked alleles CH03a09-132, MD5002-204 and MD5003-141 inherited from M.27. Their root bark percentage was approximately 64%. These two genotypes carried the non-dwarfing linked alleles from M.27 for markers MD5006, MD5007 and MD5004,

suggesting that the recombination point must be located between MD5003 and MD5006 markers in M.27. The dwarfing degree of A025 could not be estimated as according to trunk diameter, tree height and number of roots looked more like a semi or invigorating rootstock but it had a high root bark ratio. B055 showed a fairly thick stem diameter and was second in height in this group of trees, measuring 210 cm and was tentatively classified as vigorous despite its high RB % (Figure 2.14).

Genotypes C017 (M.116 x M.27), C166 (M.116 x M.27), F051 (M.26 x M.27), G210 (M.M.106 x M.27), and B048 (M.27 x M.26) inherited the dwarfing linked alleles CH03a09-132, MD5002-204, MD5003-141 and MD5006-235 from M.27. However, they also carried the non-dwarfing alleles for markers MD5007 and MD5004 from M.27, indicating that the recombination event took place between markers MD5006 and MD5007. The root bark percentage of this group of recombinants ranged from 64.4% and 68.71%. C166 was the tallest tree among all the recombinants, measuring 227 cm in height and was tentatively classified as vigorous since the root bark percentage was high, while G210 displayed the thinnest trunk diameter, measuring 5.18 mm and was clearly a dwarfing rootstock. Additionally, G210 was the shortest tree among the genotypes, reaching a height of 101 cm. The dwarfing level could not be estimated for C017 and B048. Genotype G404 (M.M.106 x M.27) exhibited the lowest root bark percentage at 51.34% and only carried the allele linked to dwarfing MD5004-248 from M.27. The remaining markers had the non-dwarfing alleles from M.27, indicating that a recombination occurred between markers MD5007 and MD5004. G404 was tentatively classified as an invigorating rootstock (Figure 2.14).

The largest root bark percentage was found in genotype G239 (M.M.106 x M.27) with 74.2%. G239 carried only the dwarfing linked alleles from M.27 for markers MD5007-286 and MD5004-248. However, in the rest of the markers, the non-dwarfing allele from M.27 was present, indicating that the recombination took place between MD5006 and MD5007 markers. G239 was considered a dwarfing rootstock. F091 (M.26 x M.27) and G061 (M.M.106 x M.27) had the dwarfing linked alleles for MD5006-235, MD5007-286 and MD5004-248 from M27 and presented RB ratios of 57.85% and 65.76%, respectively. F091 rootstock was categorised as vigorous. Furthermore, G061 exhibited the thickest trunk diameter with 14.74 mm. Determining the extent of dwarfing for this rootstock was challenging due to conflicting indicators. While the root

bark ratio and the number of collected roots suggested a dwarfing potential, it had a notably thick stem and considerable height, therefore, the data were inconclusive. Lastly, genotype F036 (M.26 x M.27) carried the dwarfing linked alleles from M.27 for all the markers except CH03a09 which amplified the allele not associated with dwarfing. This indicated that a crossover occurred between CH03a09 and MD5002 markers in M.27. F026 had 66.9% of root bark, 9.02 mm of trunk diameter and 161 cm in height and was classified as dwarfing (Figure 2.14).

Most of the recombinants examined led to the hypothesis that *Rb1* was located between markers MD5007 and MD5006. This hypothesis will be further dissected in the discussion section 2.4.1.1.

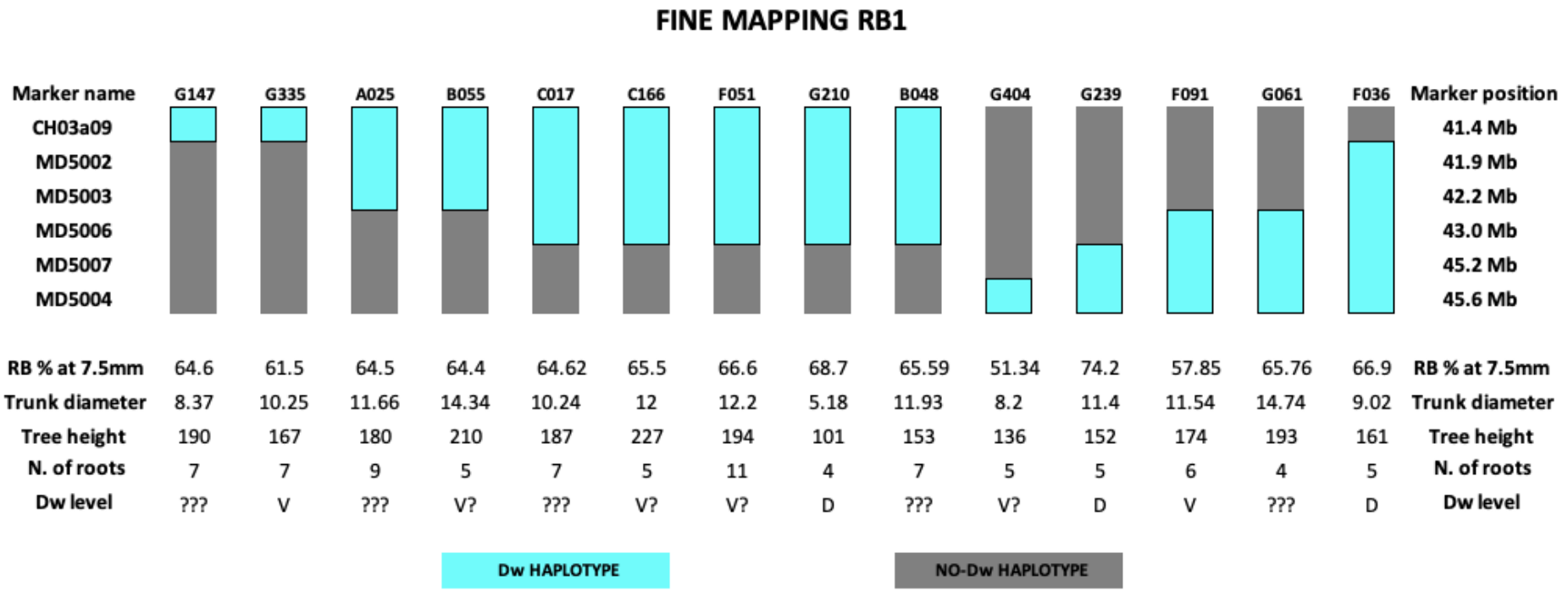

Figure 2.14. Drawing showing genotypes with a recombination event in the *Rb1* QTL region, the RB % at a 7.5 mm root, trunk diameter, tree height, number of roots collected and their estimated dwarfing level (Dw level) based on all the phenotypic information. D: dwarfing; V: vigorous; ?: tentative; ???: inconclusive. Blue denotes the previously defined dwarfing haplotype and grey the non-dwarfing haplotype.

2.3.3.5 Fine mapping of Rb2 using MCM families

Root bark percentage, tree height and trunk diameter were also recorded for the genotypes with a recombination event in the *Rb2* QTL region. The dwarfing level of each genotype was estimated as in section 2.3.3.4. The RB% of the dwarfing rootstocks ranged from 64.2 % to 84.2 %. However, in vigorous rootstocks, the RB % range was from 50.9 % to 64.8 %. Similarly to what happened with recombinants in the *Rb1* region, genotypes with less than four roots collected per tree were excluded from the analysis. The final number of trees used for fine mapping *Rb2* was 20 rootstocks. As in section 2.3.3.4, markers and their corresponding alleles linked to dwarfing are denoted by the name of the marker plus the size of the allele in base pairs as in Figure 2.13.

As can be seen in Figure 2.15, genotypes G198 (M.M.106 x M.27), G303 (M.M.106 x M.27), F050 (M.26 x M.27), F028 (M.26 x M.27) and G019 (M.M.106 x M.27) carried the dwarfing linked allele MD11003-272. All the genotypes inherited this allele from M.27 and in the rest of the markers they carried the alleles not associated with dwarfing from M.27, indicating that in these genotypes the recombination event must have occurred between markers MD11007 and MD11003. The root bark percentage of the aforementioned recombinants ranged from 60.9% to 70.3%. The tallest tree from all the recombinants found in the *Rb2* region was F028, with 217 cm in height and it was categorised as vigorous. G303 was tentatively classified as vigorous since the root bark percentage exhibited an intermediate value. G198 and F050 were both defined as dwarfing rootstocks. The dwarfing degree of G019 could not be estimated since it had RB %, trunk diameter and height typical of dwarfing rootstocks but an unusually high number of collected roots, not very common in dwarfing rootstocks.

G359 (M.M.106 x M.27), G416 (M.M.106 x M.27), and F131 (M.26 x M.27) exhibited the alleles linked to dwarfing in markers MD11007-159 and MD11003-272 from M.27. Similarly, these genotypes carried the alleles not associated with dwarfing from M.27 in the rest of the markers, indicating that the crossover occurred between markers MD11006 and MD11007. The respective root bark measurements for these trees were 84.2, 62.92 and 68.8, with G359 displaying the highest percentage of root bark and the thinnest trunk diameter with 6.57 mm among all the recombinants of this region.

Additionally, F131 was the shortest tree among all the recombinants with 98 cm in height. G359 and F131 were both classified as dwarfing. G416 was tentatively classified as vigorous as it showed intermediate values of RB % and tree height.

Genotypes B030 (M.27 x M.26) and F144 (M.26 x M.27) carried the dwarfing linked alleles in markers MD11002-142, MD11006-164, MD11007-159 and MD11003-272 from M.27. However, for the remaining markers they carried the allele not associated with dwarfing, suggesting that the recombination point was located between MD11005 and MD11002 markers. Their root bark percentage was 81.9% and 67.9%, respectively and were both defined as dwarfing rootstocks. G010 (M.M.106 x M.27) and G310 (M.M.106 x M.27) genotypes carried the alleles linked to dwarfing from M.27 in all the markers except for MD11001 and MD11004 which amplified the non associated with dwarfing alleles. This indicated that the crossover occurred between MD11004 and MD11005. The corresponding root bark percentages were 59.6% and 67.4% for G010 and G310, respectively. G010 was classified as an invigorating rootstock whereas G310 as dwarfing (Figure 2.15).

Genotype B046 (M.27 x M.26) carried the dwarfing linked allele MD11001-212 from M.26. B046 carried the alleles not linked to dwarfing for the rest of the markers from M.26, suggesting that a crossover would have taken place between MD11001 and MD11004 markers in M.26. B046 exhibited 64% of root bark, 13.05 mm of stem diameter and 144 cm of height. The dwarfing degree of this rootstock could not be properly estimated. The rootstock with the lowest root bark percentage was G385 (M.M.106 x M.27), with 50.9% of root bark. This genotype had the alleles linked to dwarfing from M.27 only from markers MD11001-212 and MD11004-203. G385 carried non-dwarfing alleles from M.27 for the rest of the markers. This implies that a recombination event occurred between MD11004 and MD11005 markers. G385 was categorised as a vigorous rootstock (Figure 2.15).

F092 (M.26 x M.27) and A036 (M.9 x M.27) genotypes carried the alleles linked to dwarfing from markers MD11001-212, MD11004-203 and MD11005-128 also inherited from M.27. However, for markers MD11002, MD11006, MD11007 and MD11003 the alleles not associated with dwarfing were amplified, suggesting that the crossover took place between MD11005 and MD11003. The root bark percentage of

these genotypes was 82.2% and 79.3%, respectively, and were both classified as dwarfing (Figure 2.15).

Genotypes F076 (M.26 x M.27), C066 (M.116 x M.27) and E008 (M.9 x M.26) had the dwarfing linked alleles for markers MD11001-221, MD11004-203, MD110005 and MD11002-142. F076 and C066 inherited the alleles linked to dwarfing from M.27. However, E008 inherited the alleles associated with dwarfing from M.9. The alleles in markers MD11006, MD11007 and MD11003 were the ones not associated with dwarfing from their correspondent progenitor. Therefore, the recombination site was located between markers MD11002 and MD11006. Their respective root bark percentage was 73.37%, 64.2% and 81.8% and were all classified as dwarfing rootstocks (Figure 2.15). Genotype A035 (M.9 x M.27) carried the alleles associated with dwarfing for all the markers inherited from M.27 except for marker MD11003 where the allele not linked to dwarfing was present. This indicated that the crossover occurred between MD11007 and MD11003. This rootstock exhibited the thickest stem diameter at 14 mm and 64.8% of root bark. A035 was tentatively classified as vigorous since it showed intermediate values of RB % and tree height (Figure 2.15).

The recombinant genotypes above analysed suggest that there are potentially two genes controlling dwarfing within the *Rb2* QTL region. One in the upper section of the QTL, possibly between markers MD11001 and MD11002 and the other one in the lower section of the QTL, between MD11007 and MD11003 markers. This hypothesis will be further discussed in section 2.4.1.2.

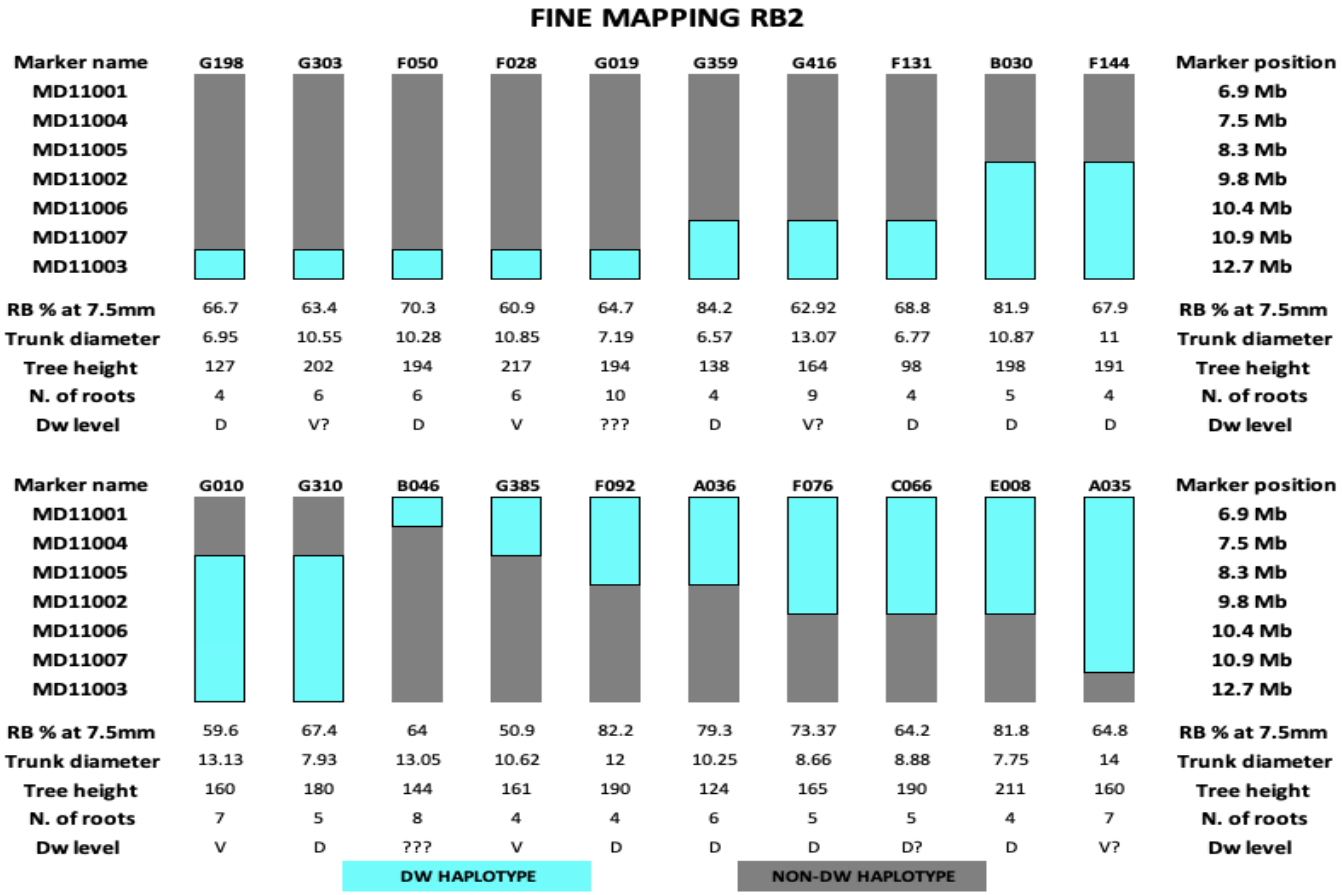

Figure 2.15. Drawing showing genotypes with a recombination event in the *Rb2* QTL region, the RB % at a 7.5 mm root, trunk diameter, tree height, number of roots collected and their estimated dwarfing level (Dw level) based on all the phenotypic information. D: dwarfing; V: vigorous; ?: tentative; ???: inconclusive. Blue denotes the previously defined dwarfing haplotype and grey the non-dwarfing haplotype.

2.3.4 Fine mapping Step 3 - Rootstocks from the breeding trials (Dataset 5)

2.3.4.1 Fine mapping Rb1 and Rb2 using the recombinant genotypes found in the breeding trials

All the markers developed in this study were tested in all the rootstocks available in plots RF185, VF224, EE207 and SP250 (Table 2.4) to identify more recombinant genotypes to refine the fine mapping of the dwarfing regions. Two genotypes with recombinations were identified in RF185, namely M306-79 and M306-189. In the SP250 trial, AR852-3 was the only genotype with a useful recombination. Lastly, in the EE207 trial, SJM189, SJM188, SJM167 and SJP84-5174 showed useful recombinations.

Root bark percentage from the recombinant genotypes together with the respective controls were plotted to visually analyse the level of dwarfing of the recombinant genotypes by comparing the recombinants to the controls. Their effect on scion vigour was evaluated by the breeding team at NIAB after several years of collecting phenotypic information including trunk cross-sectional area, tree height, tree volume and yield among other measurements. The root bark percentage was also used to evaluate the level of dwarfing of the recombinant and compared this to the dwarfing degree observed by breeders.

Recombinants at plot RF185

The experimental rootstock plot RF185 had M.9 (dwarfing), M.116 (semi-invigorating), and M.M.106 (semi-invigorating) as the control rootstocks. The M306-189 and M306-79 genotypes were the two recombinants identified in this trial. M306-189 was classified as highly dwarfing by the breeding team at NIAB with a tree volume of approximately 40% of M.9. The M306-79 genotype was classified as semi-dwarfing being slightly larger than M.9 trees.

M.9 rootstocks had the highest root bark percentage with 69.41% followed by M306-189 trees with 66.12% of root bark on average. According to the root bark information, the M306-189 genotype would have a dwarfing effect on vigour rather than very dwarfing. The extremely small size of the tree might be attributed to a possible incompatibility between the rootstock and the scion. The M306-79 genotype had

59.37% of root bark, closer to that of M.116 genotype with 57.1%. M.M.106 rootstocks had the lowest root bark percentage with 55.79% root bark, as expected. The root bark data also indicated that M306-79 rootstock had a semi-dwarfing effect with root bark percentages between the dwarfing, M.9 and the semi-vigorous, M.116 (Figure 2.16; Supplementary Table S1).

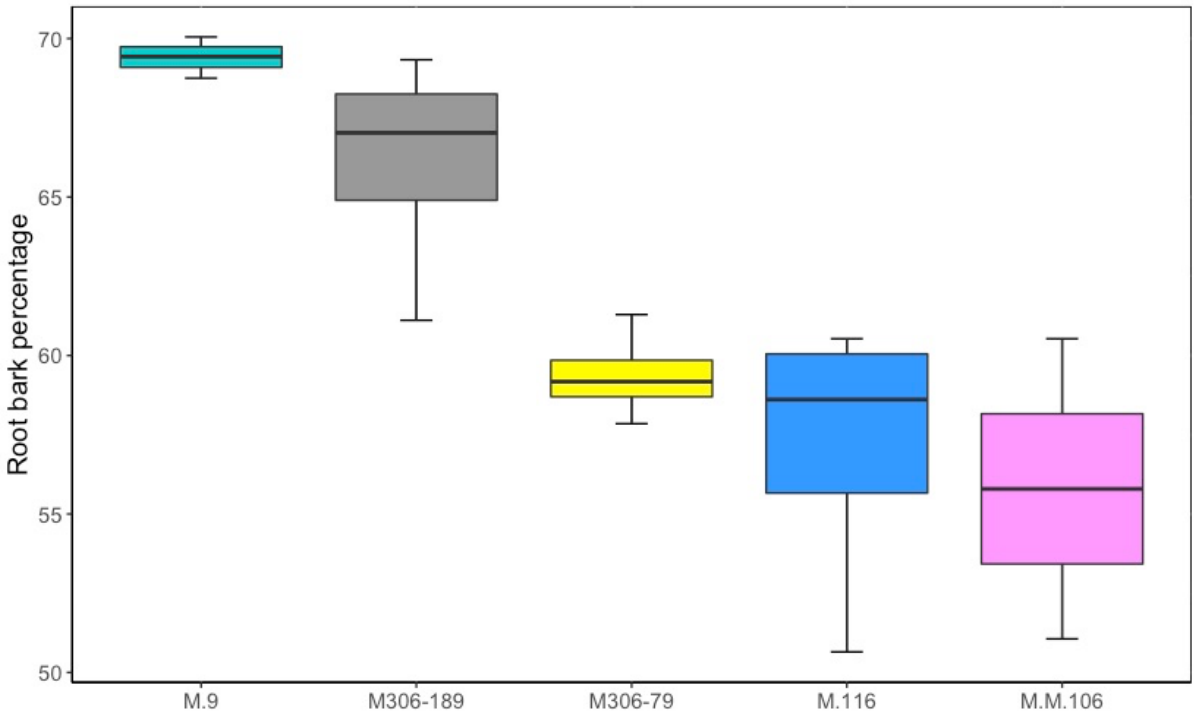

Figure 2.16. Root bark percentage of recombinant genotypes and controls from plot RF185. Centerlines show the medians; whiskers mark the maximum and minimum values, respectively. Upper and lower box boundaries represent the 25th and 75th percentiles, respectively.

Recombinants at plot EE207

In the EE207 plot, M.26 (semi-dwarfing), M.27 (very dwarfing) and M.9 (dwarfing) were the controls. Half of the trees at the EE207 plot were grafted using Braeburn and the remaining half using Royal Gala. AR852-3 was the only genotype that had a useful recombination. The breeding team at NIAB determined that AR852-3 had a semi-dwarfing to semi-vigorous effect on vigour.

AR852-3 rootstocks with Braeburn as scion had an average of 53.09% of root bark while the same rootstocks grafted with Royal Gala had a larger root bark percentage,

64.05% on average. M.26 trees on Braeburn had a 53.05% of root bark, almost identical to the AR852-3 rootstocks on the same scion while M.26 trees on Royal Gala displayed a root bark of 58.56%. The dwarfing degree of AR852-3 observed by the breeders coincided with that observed after measuring the root bark. M.27 showed 67.3% and 70.13% of root bark with Braeburn and Royal Gala, respectively. Finally, M.9 trees exhibited a root bark percentage of 63.07% with Braeburn as the scion, which notably increased to 71.37% when grafted with Royal Gala (Figure 2.17; Supplementary Table S1).

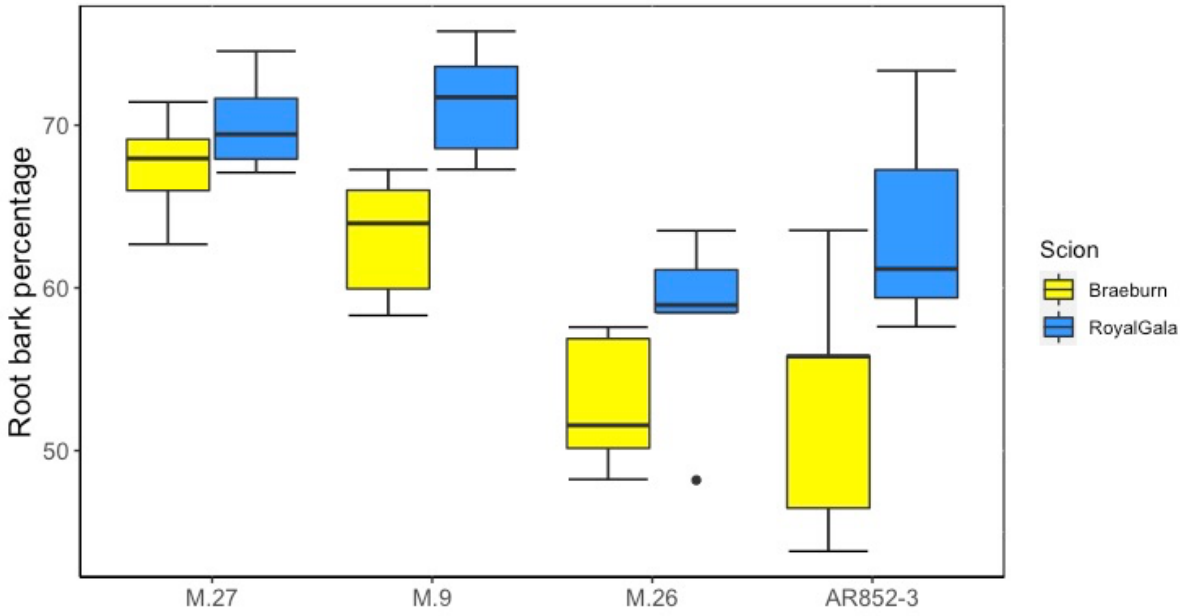

Figure 2.17. Root bark percentage of recombinant genotypes and controls from plot EE207. Centerlines show the medians; whiskers mark the maximum and minimum values, respectively. Upper and lower box boundaries represent the 25th and 75th percentiles, respectively.

Recombinants at plot SP250

Most of the rootstocks planted at the SP250 breeding trial were grafted using two scions, Braeburn and Gala. M.26 (semi-dwarfing), M.9 (dwarfing) and M.M.106 (semi-invigorating) were the control rootstocks available in this plot. Four genotypes had a recombination of interest in this trial. SJM167 with a semi-dwarfing to semi-vigorous effect with trees that were intermediate in size between M.26 and M.M.106. SJM188 rootstocks were only grafted with Braeburn and were classified as semi-dwarfing by breeders. On the other side, SJM189 rootstocks were only grafted using Gala as a

scion and had a dwarfing effect on tree size. SJP84-5174 rootstocks had a semi-dwarfing effect on tree size as observed by breeders with larger trees than M.26.

SJM167 trees grafted with Braeburn had an average root bark percentage of 51.44% whereas M.M.106 trees on the same scion had 51.01% of root bark. However, M.26 trees had 61.98% and 67.56% of root bark with Braeburn and Gala, respectively. The information that breeders collected on this rootstock and that provided by the root bark showed small discrepancies. According to root bark data, SJM167 rootstocks should be clearly classified as semi-vigorous rather than having a semi-dwarfing to semi-vigorous effect. The recombinant SJM188 exhibited an intermediate root bark of 58.24%, very similar to the root bark percentage of the semi-dwarfing M.26 when grafted with Braeburn. The recombinant rootstock SJM189 displayed a 66.04% of root bark which is similar to the 64.72% of root bark of M.9 when grafted with Braeburn, indicating that SJM189 can be also classified as dwarfing based on root bark ratio. Interestingly, the root bark percentage of M.9 rootstocks notably rose to 73.48% when grafted with Gala. In the case of SJP84-5174 trees grafted with Braeburn showed 62.26% of root bark and the same rootstocks grafted with Gala showed an almost identical root bark percentage on average of 62.24%. SJP84-5174 root bark percentage data looked very similar to M.26 data, indicating that this rootstock also has a semi-dwarfing effect on trees (Figure 2.18; Supplementary Table S1).

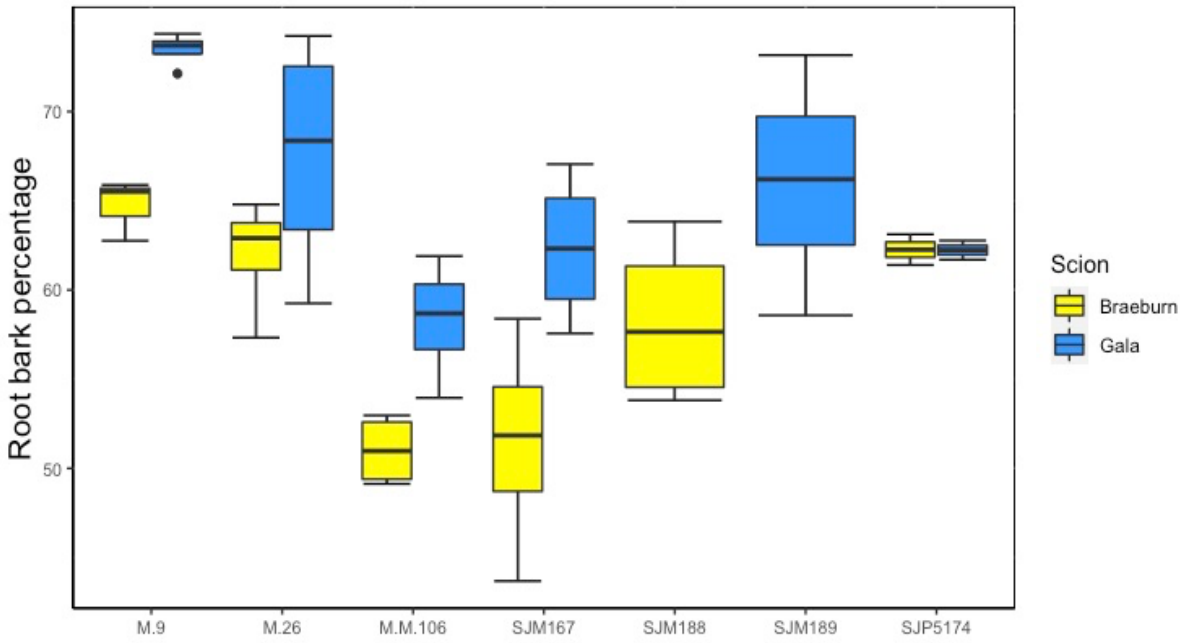

Figure 2.18. Root bark percentage of recombinant genotypes and controls from plot SP250. Centerlines show the medians; whiskers mark the maximum and minimum values, respectively. Upper and lower box boundaries represent the 25th and 75th percentiles, respectively.

2.3.4.2 Recombination locations in the rootstocks from breeding trials

The recombinants identified in RF185, M306-79 (semi-dwarfing) and M306-189 (very dwarfing to dwarfing), were both raised from a cross between AR86-1-20 (semi-vigorous) and the dwarfing M.20 (dwarfing), the latter with unknown parents. AR86-1-20 was generated from an M.M.106 (semi-vigorous) x M.27 (very dwarfing) cross, making them grandparents of the M306 progeny. M306-79 (semi-dwarfing) inherited the Chr5 dwarfing haplotype from M.20 and had a recombination of interest in the *Rb2* QTL (Chr11) either between MD11004 and MD11005 or between MD11005 and MD11002. The precise point of recombination could not be determined in this individual as it is homozygous (98/98) for the marker in the middle, MD11005 (Figure 2.19). Irrespective of the specific recombination site, M306-79 (semi-dwarfing) only displayed the two dwarfing-linked alleles on the upper segment of the region, namely MD11001-212 and MD11004-203.

The recombinant M306-189 (very dwarfing to dwarfing) inherited the dwarfing haplotype in Chr5 from M.20 and, in Chr 11, the non-dwarfing haplotype from AR86-1-20 and haplotype 1 from M.20. M.20 haplotype 1 in Chr11 only carried the dwarfing-linked allele MD11003-272 from an unknown source (Figure 2.19).

In the SP250 trial, AR852-3 (semi-dwarfing to semi-vigorous), reportedly from an M.7 (semi-dwarfing) x M.27 (very dwarfing) cross had a useful recombination in the Chr11 region between markers MD11007 and MD11003. Intriguingly, the examination of allele sizes revealed that the genotype currently held at East Malling as M.7 could not have been the female parent of this selection (Figure 2.19).

		AR86-1-20 (F)		M.20 (M)		M306-079		M306-189	
Markers Chr5	Mb	H1	H2	H1	H2	H1(F)	H2(M)	H1(F)	H2(M)
CH03a09	41.4	128	130	128	132	130	132	128	132
MD5002	41.9	200	208	204	204	200	204	200	204
MD5003	42.2	138	162	150	141	138	141	138	141
MD5006	43.1	245	245	247	235	245	235	245	235
MD5007	45.2	NA	NA	NA	NA	NA	NA	NA	NA
MD5004	45.6	252	250	252	250	250	250	252	250
Markers Chr11	Mb	H1	H2	H1	H2	H1(F)	H2(M)	H1(F)	H2(M)
MD11001	6.9	220	212	199	233	212	233	220	199
MD11004	7.5	198	203	205	210	203	210	198	205
MD11005	8.3	98	NA	98	90	NA	90	98	98
MD11002	9.8	140	142	147	140	140	140	140	147
MD11006	10.4	170	164	170	170	170	170	170	170
MD11007	10.9	155	159	155	155	155	155	155	155
MD11003	12.7	268	272	272	276	268	276	268	272

		M.7 (F)		M.27 (M)		AR852-3	
Markers Chr5	Mb	H1	H2	H1	H2	H1	H2(M)
CH03a09	41.4	123	128	130	132	130	132
MD5002	41.9	197	224	208	204	208	204
MD5003	42.2	150	170	162	141	162	141
MD5006	43.1	NA	NA	245	235	NA	NA
MD5007	45.2	NA	NA	264	286	NA	NA
MD5004	45.6	248	250	252	248	252	248
Markers Chr11	Mb	H1	H2	H1	H2	H1	H2(M)
MD11001	6.9	187	187	197	212	195	197
MD11004	7.5	198	198	191	203	191	191
MD11005	8.3	126	124	116	128	98	116
MD11002	9.8	NA	NA	155	142	147	155
MD11006	10.4	168	168	170	164	162	170
MD11007	10.9	162	162	153	159	157	153
MD11003	12.7	266	278	276	272	276	272

Figure 2.19. Estimated haplotypes of the recombinant rootstocks (in grey) identified in plots RF185 and SP250 showing allele sizes for all the markers used in this study. In green, maternal haplotypes of the recombinant individuals. In yellow, paternal haplotypes of the recombinant individuals. Highlighted in blue, the dwarfing alleles. NA: marker amplification failed. Thick lines indicate recombination sites.

In the EE207 trial, SJM189 (dwarfing), SJM188 (semi-dwarfing) and SJM167 (semi-dwarfing to semi-vigorous) were all generated from a *M. baccata 'Nertchinsk'* (unknown vigour) x M.26 (semi-dwarfing) cross. These three recombinant genotypes had a full copy of the dwarfing haplotype in Chr5 (inherited from M.26) and a recombination in the *Rb2* region in Chr11. SJM189 (very dwarfing to dwarfing) and

SJM188 (semi-dwarfing) only carried the MD11001-212 allele at the top of the *Rb2* area, therefore, a recombination had occurred between markers MD11001 and MD11004. SJM167 (semi-dwarfing to semi-vigorous) had the MD11001-212 and MD11004-203 alleles; thus, the recombination event would have taken place between markers MD11004 and MD11005. On the other hand, SJP84-5174 (semi-dwarfing), reportedly from an R5 (vigorous) x M.27 (very dwarfing) cross had a full copy of the *Rb2* region (Chr11) and a recombination event took place between markers MD5003 and MD5006, in the *Rb1* region (Chr5). Interestingly, allele scores clearly show that M.27 could not have been a parent of this genotype and suggests that M.9 is a more probable pollen source (Figure 2.20).

		M.26 (P)		SJM189		SJM188		SJM167	
Markers Chr5	Mb	H1	H2	H1	H2(M)	H1	H2(M)	H1	H2(M)
CH03a09	41.4	132	132	119	132	119	132	119	132
MD5002	41.9	204	204	198	204	198	204	198	204
MD5003	42.2	141	141	175	141	175	141	175	141
MD5006	43.1	235	235	252	235	252	235	263	235
MD5007	45.2	262	276	272	276	272	276	262	276
MD5004	45.6	250	250	246	250	246	250	236	250
Markers Chr11	Mb	H1	H2	H1	H2(M)	H1	H2(M)	H1	H2(M)
MD11001	6.9	197	212	220	212	220	212	212	212
MD11004	7.5	191	203	191	191	191	191	205	203
MD11005	8.3	116	128	122	116	122	116	116	116
MD11002	9.8	155	142	159	155	159	155	146	155
MD11006	10.4	168	164	174	168	174	168	168	168
MD11007	10.9	157	159	168	157	168	157	161	157
MD11003	12.7	266	272	265	266	265	266	265	266

		M.robusta 5 (F)		M.27 (M)		M.9 (Possible M)		SJP84-5174	
Markers Chr5	Mb	H1	H2	H1	H2	H1	H2	H1(F)	H2(M)
CH03a09	41.4	130	120	130	132	128	132	130	128
MD5002	41.9	null	199	208	204	null	204	199	null
MD5003	42.2	null	140	162	141	150	141	140	150
MD5006	43.1	253	247	245	235	247	235	247	235
MD5007	45.2	261	264	264	286	286	276	264	276
MD5004	45.6	246	250	252	248	248	250	250	250
Markers Chr11	Mb	H1	H2	H1	H2	H1	H2	H1(F)	H2(M)
MD11001	6.9	195	?	197	212	220	212	195	212
MD11004	7.5	189	?	191	203	199	203	189	203
MD11005	8.3	90	98	116	128	124	128	90	128
MD11002	9.8	140	142	155	142	142	142	140	142
MD11006	10.4	164	?	170	164	168	164	164	164
MD11007	10.9	143	167	153	159	161	159	143	159
MD11003	12.7	262	?	276	272	278	272	262	272

Figure 2.20. Estimated haplotypes of the recombinant rootstocks (in grey) identified in the EE207 plot showing allele sizes for all the markers used in this study. In green, maternal haplotypes of the recombinant individuals. In yellow, paternal haplotypes of the recombinant individuals. The dwarfing alleles are highlighted in blue. Thick lines indicate recombination sites.

2.3.4.3 Summary of the recombinants in the breeding trials

Only SJP84-5174 (semi-dwarfing) presented a recombination in the *Rb1* region; it carried the three alleles originally associated with dwarfing MD5006-235, MD5007-276 and MD5004-250. We already know that the region of the last two markers (MD5007 and MD5004) is not part of the *Rb1* QTL region since M.9 and M.27 are both dwarfing and have different alleles in these markers. Therefore, according to this dataset, the dwarfing gene should be now located between markers MD5003 and MD5007 and between 42.2 Mb and 45.2 Mb (Figure 2.21). This colocalizes with the potential location suggested by the MCM recombinants in section 2.3.3.4.

Regarding the Chr11 region, five genotypes had a recombination event in this area. Among them, SJM167 (semi-dwarfing to semi-vigorous) and AR852-3 (semi-dwarfing to semi-vigorous) were unsuitable candidates for the precise mapping of the dwarfing QTL. The SJM189 (very dwarfing to dwarfing) and SJM188 (semi-dwarfing) genotypes only had the dwarfing allele linked to dwarfing for the marker MD110011-212 at the top of the region. This indicated that the dwarfing gene is likely situated at the upper part of the Chr11 region, specifically within the range of 6.9 Mb to 7.5 Mb. M306-079 (semi-dwarfing) exhibited the dwarfing linked alleles for markers MD11001-212 and MD11004-203 at the top, providing further evidence in favour of the hypothesis previously mentioned. Surprisingly, the genotype M306-189 (very dwarfing to dwarfing) which carried the dwarfing linked allele only for the marker MD11003-272 was unequivocally categorised as dwarfing. This finding suggests the presence of an additional dwarfing gene within the *Rb2* QTL, positioned between 10.9 Mb and 12.7 Mb (Figure 2.21). These positions colocalized with the previously suggested locations after the analysis of the MCM families in section 2.3.3.5 and even provided a more precise location for the potential gene in the upper part.

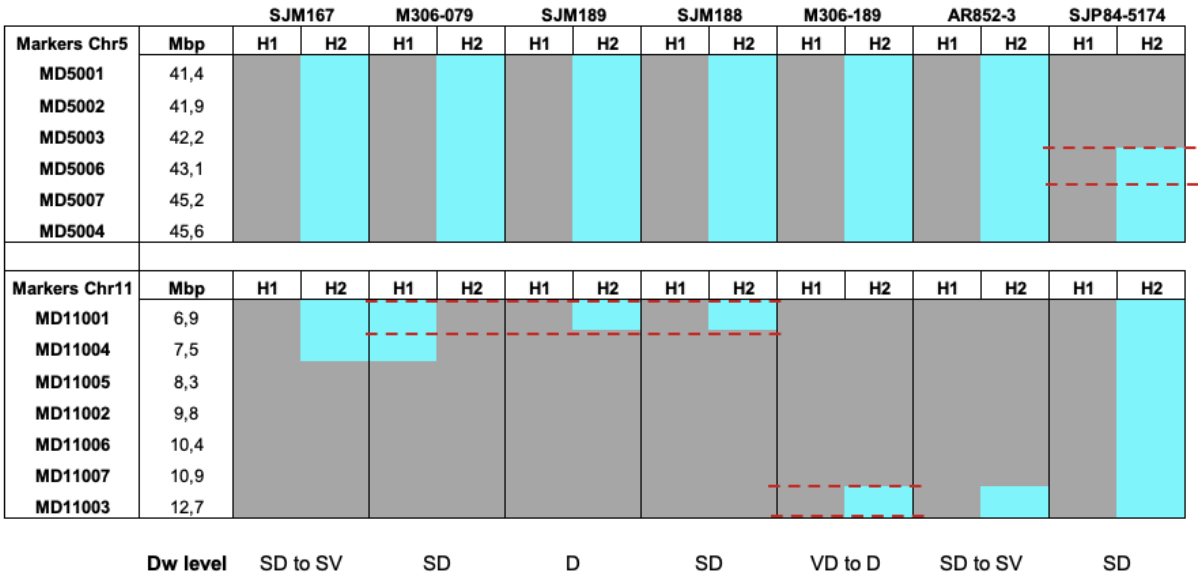

Figure 2.21. Fine mapping summary using the recombinant genotypes from breeding trials. Highlighted in blue the haplotypes containing the dwarfing alleles. In grey, the alleles not associated with dwarfing. Red dashed lines indicate the potential location of the dwarfing genes within each QTL.

2.3.5 Fine mapping Step 4 - NH families (Dataset 6)

2.3.5.1 Identification of recombinant genotypes in the NH families

All the markers developed in this study were tested in the NH progenies to identify more recombinant genotypes to help in the fine mapping of the dwarfing regions (see details in Tables 2.2 and 2.3).

The original number of seedlings belonging to these three populations was much higher but only these seedlings were available at that time. The percentage of outcrosses was calculated based on the number of currently living trees during sampling.

In the *Rb1* QTL region, 16 recombinant genotypes were identified in the NH families and 19 recombinants in the *Rb2* QTL region. As previously explained in section 2.3.3.3, not all the recombinant genotypes found were useful for fine mapping. The number of useful recombinant genotypes was 7 in the *Rb1* region and 6 in the *Rb2* region (Table 2.9).

Table 2.9. Family name, parentage, number of seedlings, percentage of outcrosses, final number of seedlings and total number of recombinant genotypes and useful recombinant genotypes in *Rb1* and *Rb2* QTL regions for the NH seedlings.

Family name	Mother	Father	Number of seedlings	% outcrosses	Final number of seedlings	Recs in Chr5*	Recs in Chr11*	Useful recs in Chr5	Useful recs in Chr11
NH6	M.116	M.27	25	12%	22	7	9	4	3
NH7	M.27	M.116	36	19.4%	29	5	4	3	1
NH8	M.13	M.9	31	35.4%	20	4	6	1	2
Total			92			16	19	7	6

*Including genotypes with recombinations in both regions

2.3.5.2 Fine mapping Rb1 and Rb2 QTL using NH progenies

Root bark percentage and tree height were recorded for all the recombinant genotypes found in the *Rb1* and *Rb2* QTL regions. The number of roots collected per genotype was also recorded since usually, a dwarfing tree does not have many thick roots available for collection and, therefore, a small or large number of roots could be also used as a dwarfing indicator. As in section 2.3.3.4, the dwarfing level of each genotype (dwarfing vs vigorous) was estimated based on all the phenotypic data. The RB% of the dwarfing rootstocks ranged from 64.8 % to 86.9 %. However, in vigorous rootstocks, the RB % range was from 42.02 % to 59.87 %.

The genotypes with a recombination event located in the *Rb1* region are depicted in the upper portion of Figure 2.22. NH6-005 rootstock carried the dwarfing linked alleles for markers MD5006-235, MD5007-286 and MD5004-248 inherited from M.27. For the rest of the markers in the *Rb1* region, NH6-005 carried the non-dwarfing linked alleles. This rootstock displayed a root bark percentage of 64.8% and reached a height of 90 cm and was classified as a dwarfing rootstock. The genotypes NH6-013, NH6-018 and NH8-021 carried the dwarfing linked allele only for the first marker at the top of the region, denoted as CH03a09-132. NH6-013 and NH6-018 inherited the dwarfing linked allele from M.27. However, NH8-021 inherited the CD03a09-132 allele from M.9. Their respective root bark percentage was 55.74%, 58.32% and 58.87%. NH6-013 and NH6-018 were tentatively classified as vigorous since their height was very low compared to the other vigorous trees.

The genotypes NH7-005 and NH7-006 had the dwarfing alleles linked to dwarfing for the four markers at the top of the *Rb1* region from M.27, and therefore, the recombination event was situated between markers MD5006 and MD5007. NH7-005 rootstock had the smallest root bark percentage among this group of recombinants with 42.02% and was also the tallest tree measuring 235 cm in height. Consequently, it was classified as vigorous. Conversely, the NH7-006 genotype exhibited the largest root bark percentage with 86.9% and was also the shortest tree at 60 cm in height. NH-006 was classified as dwarfing. Lastly, the genotypes NH6-022 and NH7-023 carried the dwarfing linked alleles from all the markers except MD5004. Their root bark percentage was 77.64% and 70.13%, respectively. In terms of height, they measured

96 cm and 84 cm, respectively and were both categorised as dwarfing rootstocks (Figure 2.22). All of the above-described recombinants supported the aforementioned hypothesis that the *Rb1* gene was located between MD5006 and MD5007 markers and will be further discussed in section 2.4.1.1.

The individuals from the NH families with a recombination event located in the *Rb2* QTL area are depicted in the lower section of Figure 2.22. The rootstocks NH6-015, NH7-033 and NH8-015 had the dwarfing linked allele only the last marker at the bottom of the dwarfing region, MD11003-272. Their respective root bark was 54.88%, 77.34% and 46.75%. The height of this group of trees was 212 cm, 96 cm and 320 cm, respectively. Notably, the tallest and shortest tree of this group of recombinants, NH7-033 and NH8-015, had the recombination event situated in the same area. Undoubtedly, these genotypes were classified as dwarfing and vigorous, respectively. In addition, NH8-015 is the genotype with the lowest root bark percentage and it was classified as a dwarfing rootstock.

The NH8-017 rootstock carried the dwarfing linked alleles for the first four makers at the top of the *Rb2* QTL region, MD11001-212, MD110004-203, MD11005-128 and MD11002-142 inherited from M.9. It carried the non-dwarfing alleles for the remaining markers and, therefore, the recombination would have taken place between markers MD11002 and MD11006 markers. NH8-017 displayed a root bark percentage of 59.08%, measured 191 cm in height and was classified as an invigorating rootstock. NH6-021 and NH6-023 genotypes had the dwarfing linked alleles for all the markers except the last one inherited from M.27 and M.116, respectively. Consequently, the crossover occurred between MD11007 and MD11003 markers. NH6-021 rootstock had 71.14% of root bark and measured 150 cm in height. NH6-023 exhibited the largest root bark percentage with 84.04% of root bark and reached 185 cm in height. These two genotypes were classified as dwarfing rootstocks (Figure 2.22). All the NH seedlings with a recombination in *Rb2* QTL supported the hypothesis that *Rb2* gene was located between MD11007 and MD11003 and will be further discussed in section 2.4.1.2.

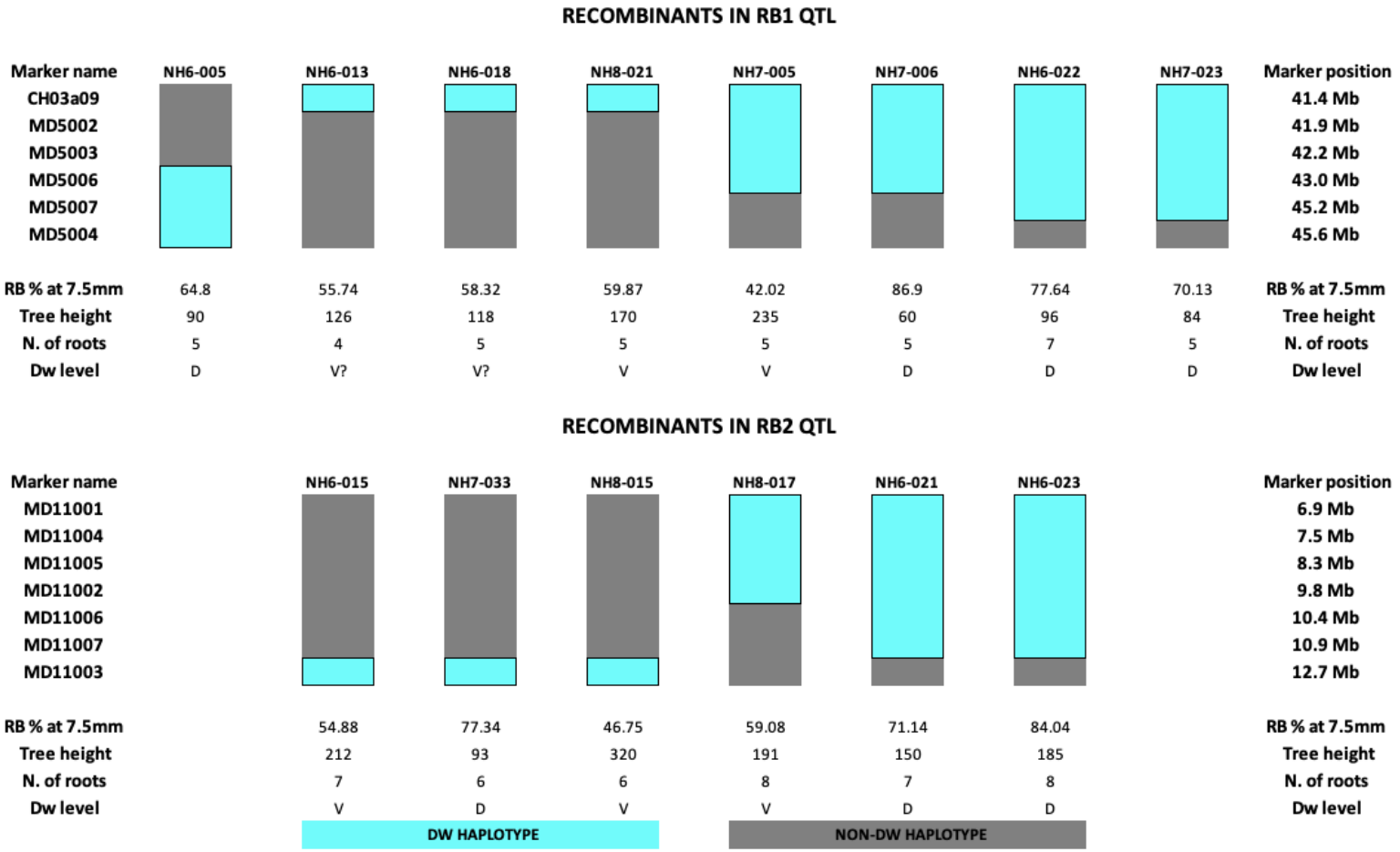

Figure 2.22. Drawing showing genotypes with a recombination event in the *Rb1* QTL region (top) and *Rb2* QTL region (bottom), the RB % at a 7.5 mm root, tree height, number of roots collected and their estimated dwarfing level (Dw level) based on all the phenotypic information. D: dwarfing; V: vigorous; ?: tentative. Blue denotes the previously defined dwarfing haplotype and grey the non-dwarfing haplotype.

2.3.6 Marker validation using rootstocks from the breeding trials

The presence or absence of the dwarfing haplotypes in the *Rb1* and *Rb2* regions was used to predict the vigour of the non-recombinant genotypes available in the breeding trials. Most of the genotype vigour predictions were accurate. Slight discrepancies between the predicted and observed vigour of the rootstocks can be expected due to the challenge of precisely defining the boundaries for each vigour category. It is important to note the absence of *Rb3* information, which despite not being essential to cause dwarfing, plays a role in modulating the degree of dwarfing in certain rootstocks.

Regarding specific cases, the genotype SJP84-5217 was initially projected as dwarfing, but the available phenotypic data indicated a semi-invigorating effect on vigour. Similarly, the AR839-9 rootstock was anticipated to be semi-vigorous due to the lack of dwarfing haplotypes, yet phenotypic data revealed it had a dwarfing to semi-dwarfing impact on vigour. There were also inaccuracies in the vigour predictions for R80, R104, and R59 genotypes. R104 and R59 were both predicted to be semi-vigorous, but their actual characteristics differed; R104 showed traits of dwarfing to semi-dwarfing, while R59 was highly dwarfing. Conversely, the R80 genotype was expected to have a dwarfing effect, but the collected phenotypic information indicated a semi-dwarfing to semi-vigorous vigour effect (Table 2.10; Supplementary Figures S1 and S2; Supplementary Table S1).

Table 2.10. Predicted vigour versus actual vigour of rootstocks from the breeding trials according to the presence or absence of the *Rb1* and *Rb2* haplotypes.

Rootstock	Pedigree	*Rb1* Haplotype	*Rb2* Haplotype	Predicted vigour	Actual vigour
M306-6	AR86-1-20 x M.20	One	None	SV	SV
SJM15	*M. Baccata 'Nertchinsk'* x M.9	One	One	D	VD
SJP84-5162	R5 x M.27	One	One	D	D
SJP84-5217	R5 x B.57490	One	One	D	SV
SJP84-5231	R5 x M.27	One	One	D	D
AR10-3-9	M.M.106 x M.27	None	None	SV	SV
AR809-3	R80 x M.26	Two	One	D	D
AR835-11	M793 x M.9	One	None	SV	SV
R80	AR134-31 x AR86-1-22	One	One	D	SD to SV
AR839-9	M.7 x M.27	None	None	SV	D to SD
B24	AR10-2-5 x AR86-1-22	One	None	SV	SV
R104	AR134-31 x AR86-1-22	None	None	SV	D to SD
R59	AR134-31 x AR86-1-22	One	None	SV	VD

VD: very dwarfing; D: dwarfing; SD: semi-dwarfing; SV: semi-vigorous

2.3.7 Effect of scion on root bark percentage

During the analysis of the recombinant data from the EE207 and SP250 breeding plots, a noteworthy scion effect on root bark percentage was observed, as illustrated in Figures 2.17 and 2.18. To delve deeper into this observation, a linear mixed model was performed, incorporating both rootstock and scion variables. This model aimed to ascertain whether the scion indeed had a significant impact on the root bark percentage.

In the EE207 breeding trial analysis, rootstock, scion and the interaction of both resulted significant in the linear mixed model (p-values = 2.2e-14, 3.1e-06 and 0.0014, respectively; Table 2.11). AR852-3, B24, M.26 and M.9 showed significantly greater root bark percentage when grafted with Royal Gala (Figure 2.23; Supplementary Tables S2 and S3).

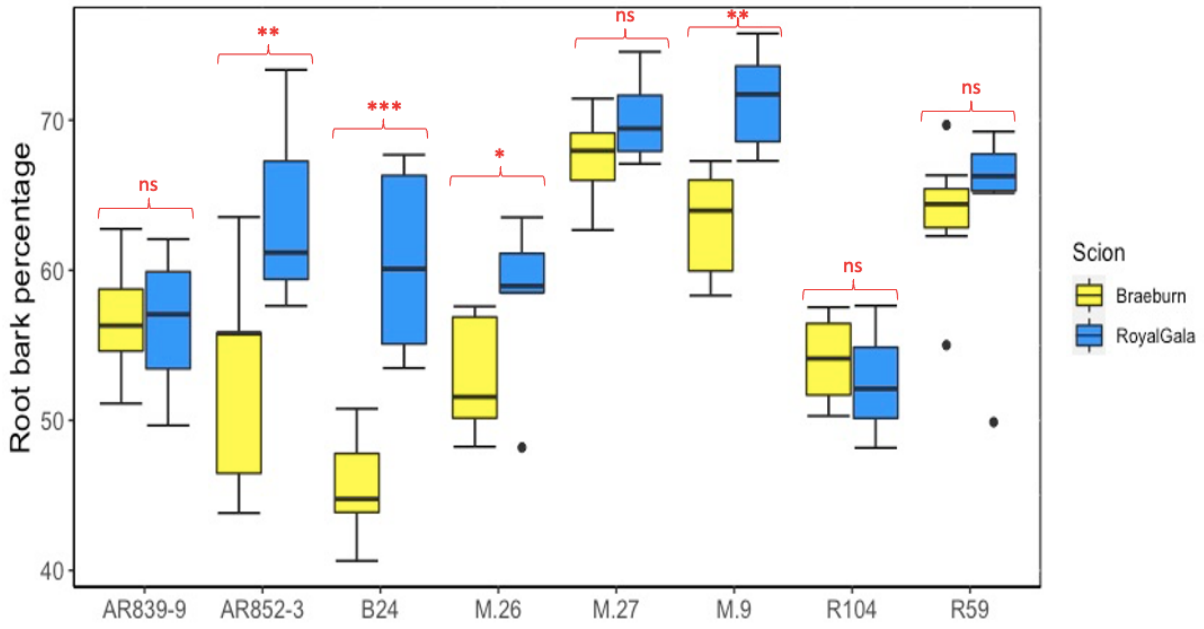

Figure 2.23. Effect of scion on root bark percentage in rootstocks planted at the breeding plot EE207. Centerlines show the medians; whiskers mark the maximum and minimum values, respectively. Upper and lower box boundaries represent the 25th and 75th percentiles, respectively. Mean values and statistics are detailed in Supplementary Tables S2 and S3. *, ** and *** significant at p<0.05, <0.01, <0.001, respectively. ns, no significant differences were detected.

In the SP250 breeding trial, rootstocks that were grafted only with one scion were excluded from the analysis. Rootstock and scion resulted significant (p-value = 1.5e07 and p-value = 0.00025, respectively; Table 2.11). The interaction between rootstock and scion was close to being significant (p-value = 0.0506). M.9, M.M.106 and SJM167 showed significantly greater root bark percentages when grafted with Gala (Figure 2.24; Supplementary Table S4 and S5).

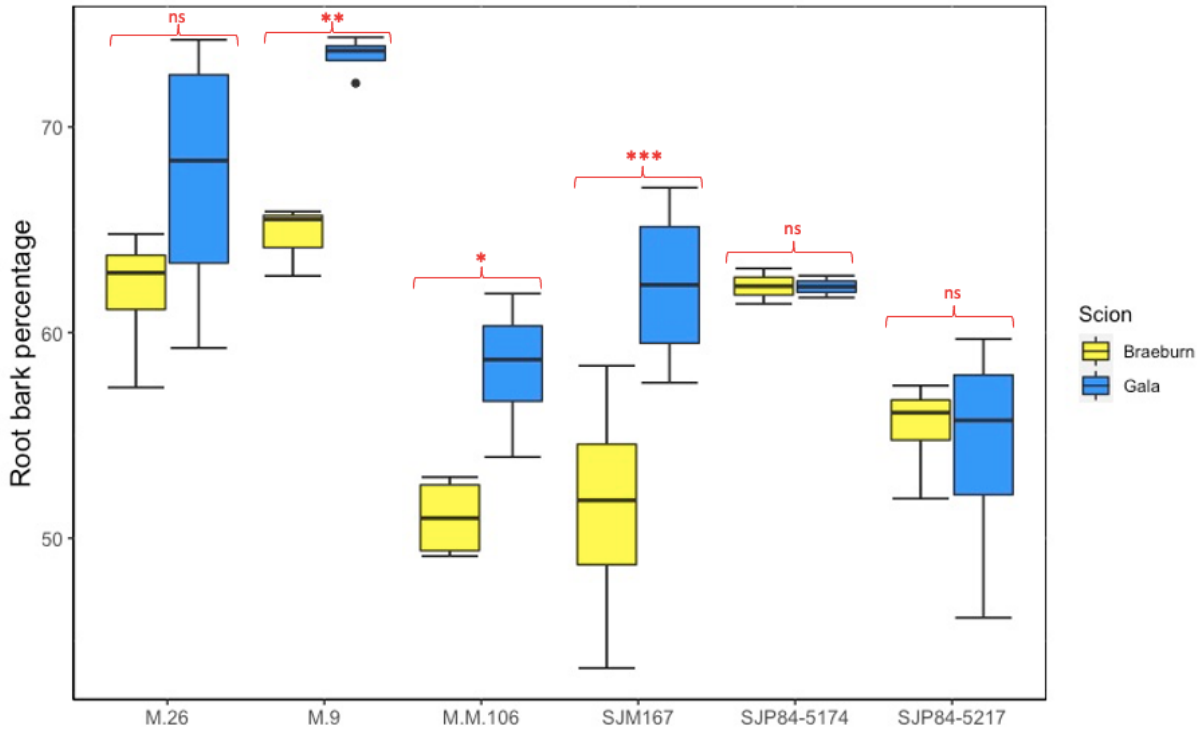

Figure 2.24. Effect of scion on root bark percentage in rootstocks planted at the breeding plot EE207. Centerlines show the medians; whiskers mark the maximum and minimum values, respectively. Upper and lower box boundaries represent the 25th and 75th percentiles, respectively. Mean values and statistics are detailed in Supplementary Tables S4 and S5. *, ** and *** significant at p<0.05, <0.01, <0.001, respectively. ns, no significant differences detected.

Table 2.11. Type III analysis of variance table for fixed effects of the root bark percentage analysis in EE207 and SP250 plots. Significant p-values in bold.

Fixed variable	Sum Sq	Mean Sq	NumDF	DenDF	F value	P value
EE207 analysis						
Rootstock	2943.37	420.48	7	79	18.52	**2.2e-14**
Scion	571.48	571.48	1	79	25.17	**3.1e-06**
Rootstock x Scion	594.86	84.98	7	79	3.74	**0.0014**
SP250 analysis						
Rootstock	1267.31	253.462	5	28.564	16.03	**1.5e-07**
Scion	272.39	272.39	1	29.410	17.23	**0.00025**
Rootstock x Scion	200.48	40.096	5	28.903	2.53	0.0506

2.4 Discussion

2.4.1 Fine mapping of RB QTL associated with rootstock-induced dwarfing

The QTL regions associated with root bark percentage were quite large and, therefore, contained hundreds of candidate genes (Harrison et al., 2016b). In order to fine-map these regions, several SSR markers were developed spanning these areas to identify haplotypes since not knowing the gene controlling this mechanism complicates the development of unique markers closely linked to dwarfing.

Defining a precise threshold for root bark or trunk diameter to determine whether a genotype is dwarfing or not can indeed be challenging. This has made the fine mapping of these regions complicated, as well as the absence of information on the allelic status of *Rb3*. Despite this, considerable progress has been made in reducing these QTL areas.

2.4.1.1 Fine mapping Rb1 QTL

The initial phase of the fine mapping was coincidental, arising from a comparison of M.9 and M.27 dwarfing haplotypes that unexpectedly revealed differences (Figure 2.8). This finding contributed to the fine mapping of the root bark QTL in Chr 5. The fact that M.27 (M.9 x M.13) is significantly more dwarfing than M.9 suggests a contribution to that trait from M.13 even if the phenotype is not expressed in it. This could come from a different locus, indicating another source of dwarfing.

The fine mapping process using MCM populations was more complicated than expected. For one, the number of outcrosses in these families was much higher than expected. Normally, a small percentage of the seeds collected do not belong to the cross possibly due to pollination errors or adverse weather conditions like rainfall occurring shortly after pollination, preventing the correct pollination of the flowers. In the case of the MCM002 and MCM005 families, the problem may have been the use of poor-quality pollen. In both crosses, M.26 pollen from the previous year was employed, which, although expected to be viable, might not have been fully functional. In addition, genotypes that inherited the dwarfing haplotype from M.26 would not be useful as there is homozygosity in most of the markers and some important

recombinations would not be visible (Figure 2.13). Consequently, the number of useful recombinants identified in these families was smaller than expected. Another challenge was the low number of roots collected per tree making it difficult to determine the root bark percentage estimation in a 7.5 mm root. Root collection should be conducted during the winter dormancy period to minimise tree damage. The roots from the MCM families were collected during the winter of 2019/2020 when the trees were barely two years old. It was expected that both the root size and the quantity of roots harvested would be smaller than desired due to the young age of the trees but, at that time, it was the only viable option. Delaying the sampling by a year was not possible within the timeframe of the PhD.

Despite the unexpected problems encountered in the use of the MCM families for the fine mapping of the RB QTL, important information was gathered from the recombinant genotypes. Figure 2.14 shows the recombination site and phenotypic data from all the individuals with useful recombinations in the *Rb1* area. The large number of individuals with an intermediate root bark percentage and the absence of controls in these families made it difficult to establish the level of dwarfing in some individuals.

Genotype G210 was undoubtedly classified as dwarfing as all the phenotypic information proved that. However, genotypes C166 and F051 which had the recombination event in the same site as G210, between MD5006 and MD5007 markers, did not look dwarfing based on the tree height and stem diameter although the root bark percentages were not particularly low. These observations led me to hypothesize that the dwarfing gene must be located between MD5006 and MD5007 markers. G239 was classified as dwarfing and had the recombination situated between markers MD5006 and MD5007 too but it had the lower portion of the dwarfing haplotype instead of the upper portion and supported the aforementioned hypothesis. However, F091 did not support this hypothesis since despite having the dwarfing linked alleles in markers MD5006-235, MD5007-286 and MD5004-248, was categorised as an invigorating rootstock. This discrepancy could be attributed to potential errors in phenotyping resulting from difficulties in measuring thin roots. The genotypes G335 and G404, carrying the dwarfing linked allele for the first and the last marker respectively, were categorised as vigorous and also supported the hypothesis of a recombination event occurring between markers MD5006 and MD5007. Finally,

the F036 genotype, clearly dwarfing according to all phenotypic data, carried the dwarfing linked alleles for all the markers except MD5001, which also supported the formulated hypothesis. Therefore, although the reliability of the data provided by these populations may be weak in some genotypes due to the problems mentioned above, the vast majority of genotypes indicated that the gene responsible for rootstock-induced dwarfing is likely to be located between MD5006 and MD5007 markers (Figure 2.14).

Of the rootstocks from the breeding trials, only genotype SJP84-5174 had a useful recombination in the *Rb1* region. This genotype, which carried the dwarfing linked alleles for the the three markers at the bottom end of the dwarfing haplotype, also supported the previously raised hypothesis (Figure 2.20). The information provided by this genotype was quite reliable since it was replicated and the number of roots collected per tree was quite high as they were eight old trees with well-developed root systems.

Lastly, the recombinants found in the NH families also supported the proposed hypothesis. The genotypes NH6-013, NH6-018 and NH8-021 carried the dwarfing linked allele for the CH03a09-132 and were classified as vigorous trees, despite not being very tall trees. Genotype NH6-005, classified as dwarfing, had the alleles associated with dwarfing in markers MD5006-235, MD5007-286 and MD5004-248 and, therefore, supported our hypothesis. Rootstocks NH7-005 and NH7-006 showed the dwarfing linked alleles in markers CH03a09-132, MD5002-204, MD5003-141 and MD5006-235 were undoubtedly vigorous and dwarfing, respectively. Consequently, both support the formulated hypothesis and are excellent candidates for the further fine mapping of the RB QTL. NH6-022 and NH7-023 carried the alleles associated with dwarfing for all the markers except MD5003 and are clearly dwarfing as expected according to this hypothesis. Despite not being replicated and the number of roots collected was not very large, these populations yield more reliable data than the MCM families since the trees are larger and the size of the phenotyped roots was greater (Figure 2.22).

After this reduction of the RB QTL area, the most significant SNP associated with the *Rb1* QTL located at 45.82 Mb and the SSR marker *Rb1* located at 45.83 Mb were then

situated just outside of the QTL region. This would explain why some dwarfing genotypes screened using the RB SSR markers developed in that study did not have the dwarfing allele (Harrison *et al.,* 2016b). This is the case for Ottawa 3 which did not show the alleles linked to dwarfing in any of the three QTL. Therefore, it was expected to be vigorous but in reality, it had a highly dwarfing effect. It is noteworthy that the RB SSR markers used for this analysis were originally created using the M432 population (M.27 x M.116) as described by Harrison *et al.,* (2016b). Moreover, it is important to remember that this part of the QTL region is different in M.9-derived genotypes as is the case of Ottawa 3 versus M27-derived genotypes. Upon screening the markers developed in this particular study, it was discovered that Ottawa 3, in fact, possessed the dwarfing haplotype within the *Rb1* QTL region (Supplementary Figure S1). This finding could potentially provide an explanation for the observed dwarfing phenotype in Ottawa 3 although the highly dwarfing phenotype would not be explained by the sole presence of the *Rb1* QTL.

In summary, there is considerable evidence to support the theory that the gene responsible for the induction of dwarfing in the *Rb1* region may be located between MD5006 and MD5007 markers, located at 43.0 Mb and 45.2 Mb, respectively. The *Rb1* QTL area has been reduced approximately from 4.4 Mb to 2.2 Mb. In addition, this study provides very valuable genotypes for further fine mapping of the dwarfing region *Rb1* such as G210, NH7-005 and NH7-006. The development of more markers spanning the region between MD5006 and MD5007 markers and the subsequent screening of key genotypes would be key to further fine-mapping this QTL.

2.4.1.2 Fine mapping Rb2 QTL

Within the MCM families, as with *Rb1* QTL, numerous trees exhibited intermediate values that complicated the dwarfing classification. From the five genotypes carrying the dwarfing linked allele only for the MD11003-272 of the *Rb2* QTL, only two genotypes showed clear dwarfing characteristics such as G198 and F050 (Figure 2.15). Consequently, it seemed quite likely that the gene located in this QTL was between the markers MD11003 and MD11007. G359 and F131 rootstock which had the alleles associated with dwarfing for MD11007-159 and MD11003-272 were undoubtedly classified as dwarfing. These genotypes supported the hypothesis

proposing that the gene responsible for dwarfing may be situated between the markers MD11003 and MD11007. However, G416 also carried the dwarfing linked alleles for MD11007-159 and MD11003-272 but did not show dwarfing characteristics. On the other hand, the genotypes B030, F144, G010 and G310 that carried the dwarfing linked alleles for MD11005-128, MD11002-142, MD11006-164, MD11007-159 and MD11003-272 markers, should all be dwarfing if the previous hypothesis is correct but there were some discrepancies. Interestingly, B030, F144 and G310 were classified as dwarfing but G010 was clearly vigorous. Once more, errors in phenotyping may account for these inconsistencies although a second QTL in the same area was also a possibility.

Rootstocks F092 and A036 had the dwarfing linked alleles in the three markers at the top of the region, MD11001-212, MD11004-203 and MD11005-128, and both genotypes were considered as dwarfing. These two genotypes reinforced the theory of a second gene within the *Rb2* region that would be located in the top half of the QTL region. F076, C066 and E008 carried the alleles associated with dwarfing for the four markers at the upper QTL region and were considered dwarfing supporting again the hypothesis of a second gene located at the top of the *Rb2* QTL. Conversely, A035 genotype which had the dwarfing linked alleles for all the markers except the last one at the bottom was not considered dwarfing. A035 supported the first hypothesis raised about which place the dwarfing gene between MD11007 and MD11003 (Figure 2.15). In summary, these MCM families showed favourable arguments to believe that two genes controlling rootstock-induced dwarfing are within the *Rb2* QTL. This was also supported by the literature as the *Dw2* QTL identified by Fazio *et al.*, (2014) is not located exactly in the same place as the *Dw2* mapped by Foster *et al.*, (2015).

In the breeding rootstock trials, the M306-189 genotype carried the allele linked to dwarfing for the last marker at the bottom of the region, MD11003-272, and was undoubtedly classified as very dwarfing. M306-189 was generated from a cross of AR86-1-20 (semi-vigorous) and M.20 (very dwarfing). This line inherited the dwarfing haplotypes from M.20 which also carried the MD11003-272 allele. Therefore, it is undeniable that there must be a gene in that region because both genotypes clearly show high levels of dwarfing and in M306-189, the phenotypic data are quite reliable since the trees were replicated and a large number of roots were collected for analysis.

Moreover, the SJM189 rootstock which also carried the dwarfing linked allele only for the first marker at the top of the QTL region was also classified as dwarfing. This genotype reinforces the hypothesis previously raised about the dwarfing gene located in the upper part of the QTL region and provides a more precise location, between MD11001 and MD11004 markers. SJM188 and M306-079 carried the dwarfing linked alleles for the first and the first two markers at the top of the region, respectively, and were classified as semi-dwarfing also had the first or first two markers at the top of the region but their level of dwarfing is intermediate. The differences in dwarfing levels could be explained by *Rb3* and the different epistatic interactions (Figures 2.19 and 2.20).

All the recombinant genotypes obtained in the NH families situated the dwarfing gene at the bottom of the *Rb2* QTL region, between markers MD11007 and MD11003. Genotype NH7-033 which had the dwarfing-linked allele only for marker MD11003-272 was clearly a dwarfing rootstock. In addition, genotypes NH6-021 and NH6-023, carrying the alleles associated with dwarfing for all the markers except the last one at the bottom of the region, also displayed dwarfing characteristics (Figure 2.22).

This study has generated very valuable genotypes such as G198, F050, A036 and NH7-033 among others that would be enormously useful in the further fine mapping of the *Rb2* QTL.

In summary, the previous findings suggest that there are two genes controlling rootstock-induced dwarfing within the *Rb2* region. The first one is likely located between markers MD11001 and MD11004, from 6.9 Mb to 7.5 Mb and the second gene seems to be located between MD11007 and MD11003 markers, from 10.9 Mb to 12.8 Mb. The *Dw2* QTL mapped by Fazio et al., 2014 was situated between CH02d8 and C13243 markers and the most significant SNP associated with Dw in that area was RosBREEDSNP_SNP_GA_12188459_ Lg11_00240_MAF10_MDP0000713484 _exon1_RosBREEDSNP_SNP_GA_8445216_Lg11__00185_MAF40_531216_exon which is located at 12.1 Mb (Figure 2.25). Other researchers have mapped QTL for interesting traits such as the length and number of sylleptic branches roughly in the same area (Kenis and Keulemans, 2007). However, the QTL mapping carried out by Toshi et al., 2015 placed *Dw2* close to Hi07d11 marker which is distally located from

CH02d08 marker, approximately where MD11001 and MD11004 markers are located. *Rb2* QTL mapped by Harrison et al., (2016b) was also situated in this area and the most significant SNP in that study was RosBREEDSNP_SNP_CA_8702100_Lg11_00735_MAF40_1677605_exon4 which is located at 7.9 Mb (Figure 2.25). QTL for architectural traits such as stem diameter and branching have also been mapped in the same area as CH02d08 (Liebhard *et al.*, 2003; Segura *et al.*, 2009). A recent study also found two QTL for tree height and trunk diameter in the same region in Chr11 (Cai *et al.*, 2021). In conclusion, it seems quite likely that there are two genes responsible for rootstock-induced dwarfing in this region which would explain why it has always been so difficult to map this area.

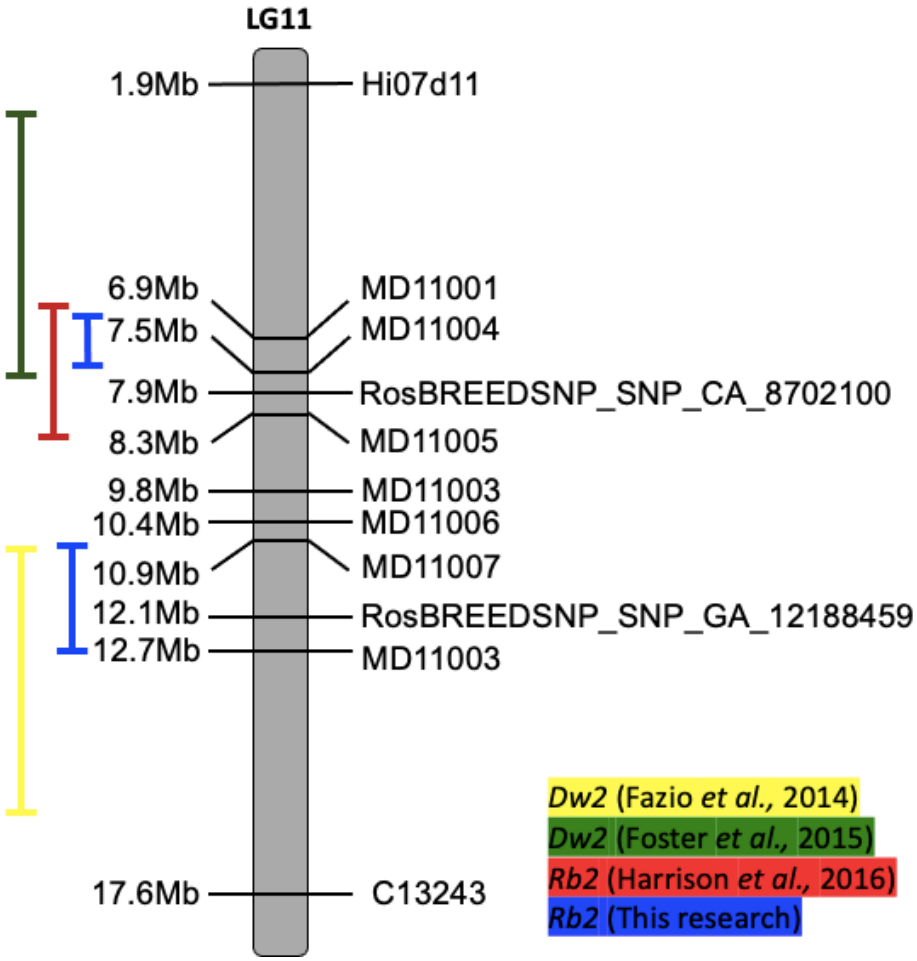

Figure 2.25. Diagram showing the approximate location of *Dw2/Rb2* according to different authors (Fazio et al., 2014; Foster et al., 2015; Harrison et al., 2016b).

2.4.2 Validation of the dwarfing markers developed for this study

This study has generated a large number of markers that have already been used by rootstock breeders at NIAB, UK. The use of markers that are capable of correctly predicting the level of dwarfing of rootstocks can be very beneficial for breeders and help with the early selection of dwarfing genotypes that are currently in demand given their great advantages. The initial idea was to use the non-recombinant genotypes of the MCM families to validate the markers and study all the genotypic classes that should be well represented in these populations. Unfortunately, this was not possible since several allelic combinations were not present in these families due to the large number of outcrosses.

The non-recombinant trees from the breeding trials were used to see if the information provided by the markers coincided with the phenotypic information collected over the years. Nine out of fourteen rootstocks were correctly predicted. In the case of SJP84-5217, the prediction was not accurate. It was predicted as dwarfing since it contained one copy of the dwarfing haplotype in the *Rb1* region and another copy of the dwarfing haplotype in the *Rb2* QTL region. This genotype was generated from a cross of R5 x B.57490. Both dwarfing haplotypes identified in this genotype must have been inherited from B.57490 but we do not have much information about it. One possible explanation could be that M.26 was the parent of B.57490, grandparent of SJP84-5217, and could have inherited the non-dwarfing haplotype from M.26 in the *Rb1* region, which looks almost exactly the same as the dwarfing haplotype due to the homozygosity of the markers, and therefore, SJP84-5217 should be predicted as semi-vigorous. AR839-9 rootstock was predicted as semi-vigorous due to the lack of both dwarfing haplotypes but the phenotypic information revealed that AR839-9 actually had a dwarfing to semi-dwarfing effect on vigour. AR839-9 was generated from a cross of M.7 x M.27 but the markers alleles revealed that neither M.7 nor M.27 were the progenitors of this genotype or neither of the screened rootstocks, suggesting that there might be another source of dwarfing. These discrepancies could also be explained by incompatibility of this rootstock with the scion that could have negatively affected the growth of these trees.

None of the R-series rootstocks available in the breeding trial had the expected vigour. R59 had one copy of the dwarfing haplotype in the *Rb1* region and none of the dwarfing alleles in the *Rb2* area and, therefore, it was expected to be semi-vigorous. However, R59 is a very dwarfing rootstock. The *Rb3* alleles could help to explain this phenotype as the interaction of Rb3 with *Rb1* in the absence of *Rb2* also conferred some dwarfing effect (Harrison et al., 2016b). R80 genotype had the dwarfing haplotypes in *Rb1* and *Rb2* regions but surprisingly R80 is classified as a semi-dwarfing to semi-vigorous rootstock. This could be explained by a double recombination between two neighbouring markers. While such events are not very common, they are not impossible, especially considering that the distance between certain markers is quite large. The genotype R104 did not have any of the dwarfing alleles although is a dwarfing rootstock suggesting that there could be another source of dwarfing. A potential incompatibility between this rootstock and the scion could also explain the dwarfing phenotype of these trees.

The R rootstocks were generated from the AR134-31 x AR86-1-22 cross. AR134-31 was derived from a R5 x M.M.106 cross and AR86-1-22 was generated from the cross of M.27 x M.M.106. Therefore, the only dwarfing ancestor seems to be M.27 which is the grandparent of the R-series rootstocks except for R80 whose pedigree is unclear. Surprisingly, the screening of the markers developed in this study in R5 revealed that some of the dwarfing alleles from the *Rb2* region were present (Figure 2.20). However, it seems that they are not situated in the region most probable for harbouring the genes responsible for causing dwarfism. On the other hand, Foster et al., (2015) reported that a couple of QTL responsible for the overall dwarfing phenotype were surprisingly mapped in R5 despite not being a dwarf rootstock. R5 might indeed be a previously undiscovered potential source of dwarfing that carries one of the genes responsible for dwarfing.

Further research is needed to investigate whether all the dwarfing rootstocks are derived from a unique source of dwarfing. In addition, identifying the dwarfing genes will help to develop markers closely linked to these genes that will assist breeders in the generation of more efficient and resilient rootstocks that are needed to meet the demands of the continuously growing global population.

2.4.3 Effect of scion on root bark percentage

The predominant effect of rootstocks on scions has led most researchers to focus on how rootstocks modify scions and, unfortunately, there has been relatively limited research to investigate how scions influence rootstocks.

The root bark percentage in this study significantly changed depending on the scion when grafted in the same rootstock. This effect also depended on the rootstock-scion combination and seems quite consistent among scions. Gala and Royal Gala, which are similar cultivars, had a greater root bark when grafted on the same rootstock. In contrast, Braeburn consistently displayed the lowest percentage of root bark in both SP250 and EE207 plots. Several researchers already mentioned the effect of scion on belowground traits such as root biomass and root architecture (Li *et al.*, 2016; Harrison *et al.*, 2016a; Valverdi *et al.*, 2019) but the effect of scion on root bark percentage has been reported for the first time in this experiment. Scion also influenced yield, tree volume and tree weight in these trials when evaluated by breeders for the breeding program (data not shown). More research is needed on how scions influence the rootstock-scion complex to better understand how to optimise apple trees to adapt to extreme future conditions.

2.5 Conclusion

In summary, the *Rb1* and *Rb2* QTL areas have been importantly reduced. Furthermore, there is evidence to believe that in *Rb2* QTL region there are two genes controlling rootstock-induced dwarfing which could explain why *Dw2* has been mapped to slightly different regions in Chromosome 11. Moreover, this study has generated useful markers linked to dwarfing that are currently used by breeders as well as genotypes with interesting recombination points and phenotypes that would be useful for further fine mapping the root bark QTL. More research is needed to investigate whether there is more than one source of dwarfing which could explain the discrepancies between the expected and actual vigour of some genotypes.

Chapter 3. Investigating links between seedling roots, adventitious rooting and dwarfing using QTL mapping

3.1 Introduction

A variety of root systems exist in apples (*Malus spp*); the primary root derived from the embryonic radicle and the lateral roots emerging from it are only present in commercial cultivars at the very first stage of the breeding process (Bellini *et al.*, 2014). Thereafter, scion and rootstock genotypes are vegetatively propagated to ensure the multiplication of genetically identical plants. Scion cultivars are very rarely rooted again and instead are propagated by grafting or budding. Rootstocks, on the other hand, can be multiplied in stoolbeds, through hardwood cuttings (most commonly) or in tissue culture. These propagation methods rely on the plants' ability to produce roots from aerial tissues, in this case, apple stems. These are known as adventitious roots and, although they fulfil the same functions as lateral roots (Bellini *et al.*, 2014), their formation is regulated by hormones, with auxins (common in commercial rooting powders) playing a prominent role (Pacurar *et al.*, 2014). In addition, other factors affect adventitious root development including genotype, the physiological state of the mother plant, length and thickness of the shoots on which roots form and environmental conditions such as temperature, light and humidity (Hartmann and Kester, 1975; Webster, 1995b; da Costa *et al.*, 2013).

The propagation method used impacts the root architecture of the trees (Albrecht *et al.*, 2017, 2020; Li *et al.*, 2022). A study using sweet orange trees revealed that rootstocks propagated through vegetative methods often showed larger numbers of longer roots, which were better at resource acquisition when compared to plants grown from seeds (Albrecht *et al.*, 2017). Moreover, another study using grafted sweet orange trees demonstrated that the combination of propagation methods and the rootstock genotype determined the tree growth during the orchard period. These studies indicate that the interaction between genotype and propagation method strongly affects the orchard performance (Albrecht *et al.*, 2020).

QTL mapping has been used to study the genetic control of adventitious root development on several tree species including poplar (Zhang *et al.*, 2009; Ribeiro *et al.*, 2016; Sun *et al.*, 2019), eucalyptus (Grattapaglia *et al.*, 1995; Marques *et al.*, 1999, 2005), oak (Scotti-Saintagne *et al.*, 2005), pine (Shepherd *et al.*, 2006), citrus (Siviero *et al.*, 2003) and pear (Knäbel *et al.*, 2017). In apple, Moriya *et al.*, (2015) identified a QTL controlling adventitious rooting ability in Chromosome 17 using hardwood cuttings.

In this study, the seedlings of the progeny of a GD x M.9 cross (MDX132 family) were characterised to identify QTL for root architecture traits and investigate the correlation between the (primary) root architecture in seedlings and the (adventitious) root architecture in rootstocks propagated using vegetative methods in the experiment detailed in Chapter 4. Early detection of genotypes with specific root architecture has the potential to accelerate the breeding process. Subsequently, the seedlings were planted in the field as stoolbeds to propagate the genotypes. The rooting ability of these rootstocks was phenotyped following propagation in stoolbeds and through hardwood cuttings and QTL mapping conducted to identify genes controlling the production of adventitious roots. The identification of these QTL will allow the development of new markers for rooting ability that will help to generate new rootstocks with improved propagation capabilities. Furthermore, the impact of dwarfing was examined in all these phenotypic traits to understand whether dwarfing influences the root traits investigated in this chapter.

The specific objectives of this chapter were:

- To conduct a QTL mapping analysis for root architecture traits using the seedlings from the MDX132 family and investigate the correlation with the grafted rootstocks used in Chapter 4.
- To perform QTL mapping analyses for rooting ability in the stoolbeds and hardwood cutting experiment using the MDX132 population to identify genes linked to rooting ability and ultimately develop markers for rooting ability.
- To analyse the impact of *Rb1* and *Rb2* on seedlings' root architecture traits and rooting ability for stoolbeds and hardwood cuttings using the MDX132 family.

3.2 Methods

3.2.1. Plant material and genotypic data

The MDX132 population (Golden Delicious x M.9) was used to perform QTL mapping analysis of several root traits. A total of 148 individuals from this population and the parents were genotyped as described in Chapter 2 section 2.2.4.1. Although a linkage map was developed for this population as described in Chapter 2, a haploblock map was used instead for QTL mapping analysis. The haploblock map comprising *circa* 6000 SNPs in 1083 haploblocks was developed by Amanda Karlström (apple breeder at NIAB EMR) using 25 mapping populations and pedigree information for 400 cultivars and breeding selections. The haploblocks were evenly distributed with 1 cM spacing across all chromosomes (Karlström *et al.*, 2022).

3.2.3. Floating seedlings experiment

In November 2014, the seeds of the MDX132 population were planted in germination trays using a mixture of standard compost, perlite and peat and stored in a cold store at 4°C for 14 weeks. The trays were then moved to a warm glasshouse at 25/18°C (day/night temperature) and 16/8 h day/night light (achieved with supplementary lighting).

In April 2015, two months after germination the seedlings were carefully removed from the germination trays and, before planting them in pots, images of the root systems were taken by Nuria Barber (NIAB EMR research assistant). The seedlings were carefully washed with tap water to remove the soil attached to the roots and placed in a 250 x 250 x 20 mm transparent square petri dish filled with water and the root systems were carefully distributed in the plate (Figure 3.1. Panels A and B). A ruler was placed next to the petri dish to have a scale in each image for further calculations. The images were taken using a Canon 1200D camera with an 18-55 mm telephoto lens with a shutter release and mounted on a tripod to avoid movements that would affect the quality of the image.

The imaging analysis was performed using the Fiji plugin available in ImageJ 2.1.0 (Schindelin *et al.*, 2012). Firstly, the scale was set in every image using the ruler visible

in the photos. The images were then cropped to keep only root systems in the image. Primary root length (PRL) was manually traced and measured in 130 genotypes because it was not possible to always find the primary root in every image (Figure 1. Panel C). The photos were then converted into 8-bit black-and-white images and the threshold was adjusted to obtain the black skeleton of the root system to measure the total root surface area (Figure 1. Panel D). The total root surface area (TRSA) was measured in 144 genotypes. No data transformations were needed before the QTL mapping analysis as both the main root length and total root surface area were normally distributed.

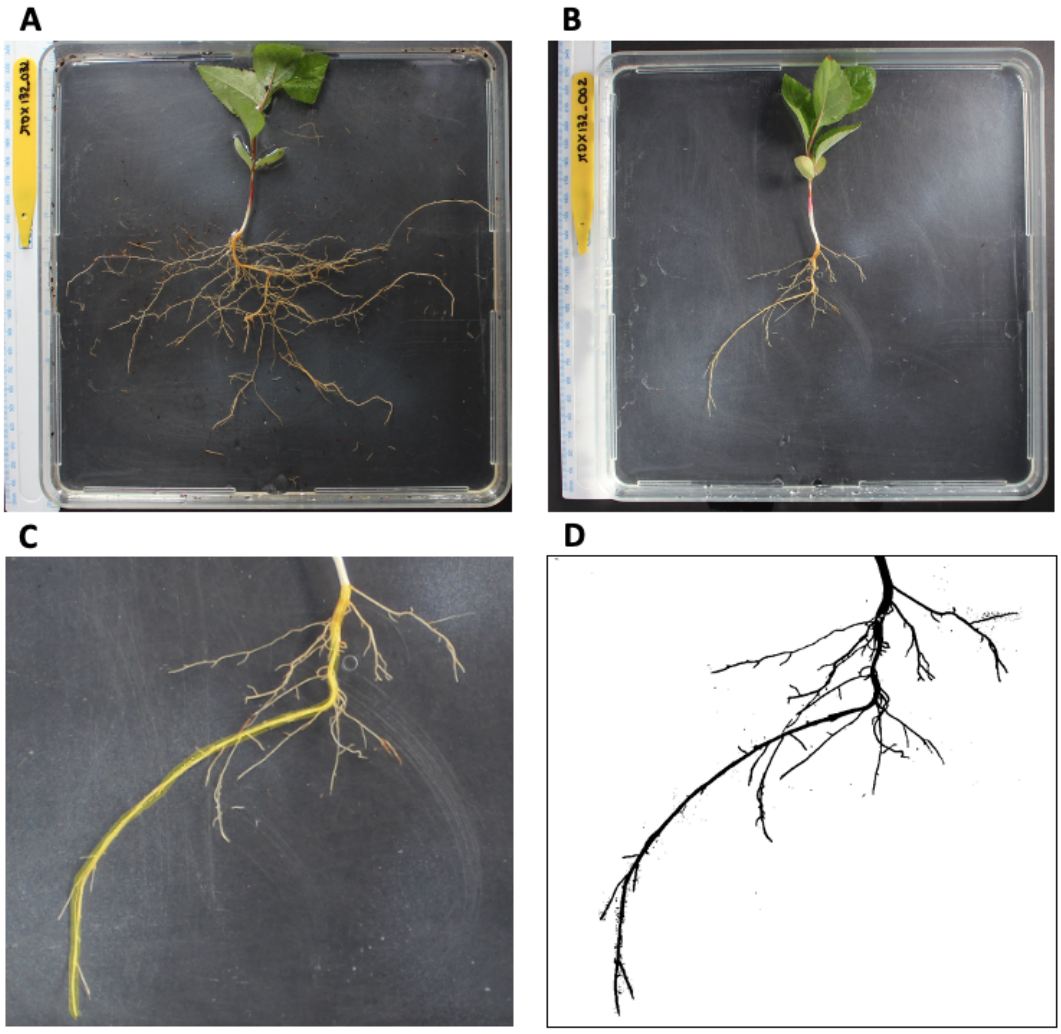

Figure 3.1. Panel A and B: Two MDX132 floating seedlings with different root architecture. Panel C: Cropped seedling image with the main root highlighted in yellow. Panel D: Seedling image converted into an 8-bit image ready to measure total root surface area.

3.2.4. Rootstock propagation experiment

The seedlings from the MDX132 population were grown in pots for a few months and then were planted in “Deadman plot” at NIAB EMR in 2016 as stoolbeds for genotype propagation. In spring 2017, the apple breeder at NIAB EMR, Amanda Karlstrom, cut the trees back to ground level to induce branching. In the spring of 2018, I cut the trees back to ground level again to induce more branching. In mid-June 2018, most of the genotypes had produced several shoots and the trees were earthed up using bottomless 10-litre pots. Pots were filled with moist sawdust to cover about 4-5 inches of the shoots and the remaining 2 inches were filled with soil (Figure 3.2). In August 2018, the grass around this population was treated with herbicide that unfortunately fell directly on some trees, damaging several genotypes that had to be pruned to re-induce healthy growth of new shoots. This reduced the number of genotypes available for the experiment in 2019. In January 2019, the stoolbeds were carefully unearthed and rooted shoots were labeled and stored at 4°C for further measurements. The number of total and rooted shoots was recorded and the proportion of rooted shoots was calculated per genotype to measure rooting ability.

The same procedure was then repeated the following year. The trees were cut back again at the beginning of spring 2019 and stooled using sawdust and soil in June 2019 as previously described. In January 2020, the stoolbeds were again lifted and phenotypic data were recorded as described above.

Genotypes with less than three shoots and those in which the stoolbeds were in bad condition were removed from the analysis. The final number of genotypes included in the analysis in 2019 was 87 and in 2020, 117 genotypes. The number of individuals included in the analysis in 2019 was much smaller due to problems with a herbicide application that caused temporary damage in some individuals and so data is missing for those that were damaged from the first year. The percentage of rooted shoots was transformed using the arcsine method as the data were skewed. The number of shoots in each genotype was used as a cofactor in the analysis.

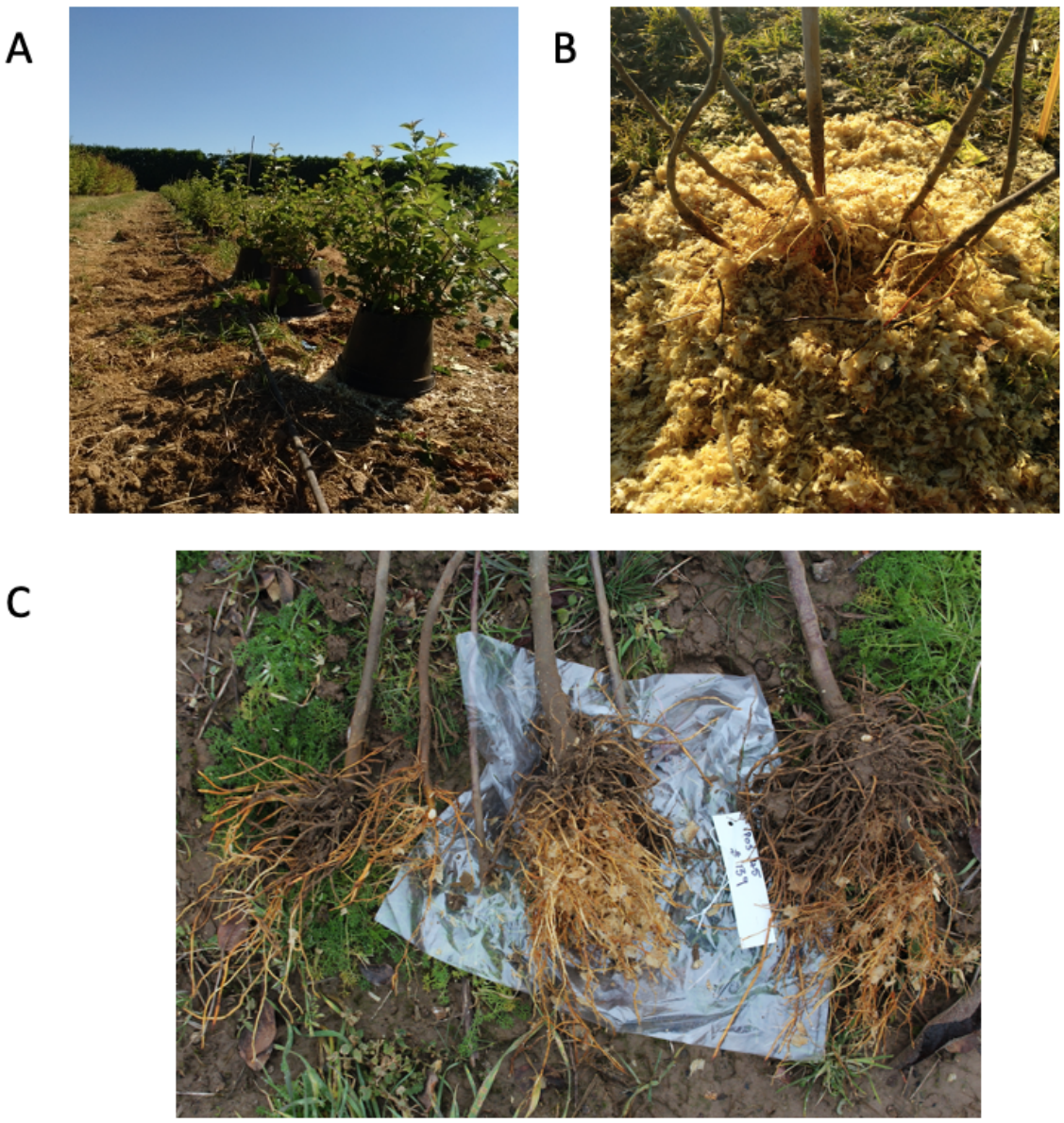

Figure 3.2. Stoolbed lifting process. A: Stoolbeds in the field. B: Rooted shoots carefully unearthed. C: Phenotyping of rooted shoots from a particular genotype.

3.2.5. Hardwood cuttings experiment

In January 2021, first-year shoots were collected from the MDX132 progeny, wrapped in plastic and stored in a cold store at 4°C for future analysis. Four or five cuttings from 122 genotypes were used in the experiment. Some genotypes could not be included in this experiment due to poor quality or the low number of shoots.

The hardwood cuttings that measured between 20 - 30 cm long were prepared by making a couple of 1 cm longitudinal cuts at each side of the cutting using secateurs

in the base of each shoot to allow the hormone solution to penetrate more easily. All the cuttings from the same genotype were wrapped in plastic, leaving the top and bottom of the bundles uncovered. The base of the cuttings were then dipped into an indol-butyric acid solution at a concentration of 2.5 g/L for five seconds. The cuttings were then placed approximately 5-6 cm deep in two bins with sand and heated at 20°C (Figure 3.3. Panel A). The genotypes were randomly distributed in rows in the two bins. After six weeks, the cuttings were removed from the bins and the rooting ability of each genotype was evaluated (Figure 3.3. Panel B). The number of rooted cuttings per genotype as well as the number and length of the roots in each cutting was recorded. The percentage of rooted cuttings per genotype was calculated as well as the average number of roots and the average length of roots per genotype for data analysis. The percentage of rooted cuttings was transformed using the arcsine method and the average number of rooted cuttings was logarithmically transformed as the data were skewed.

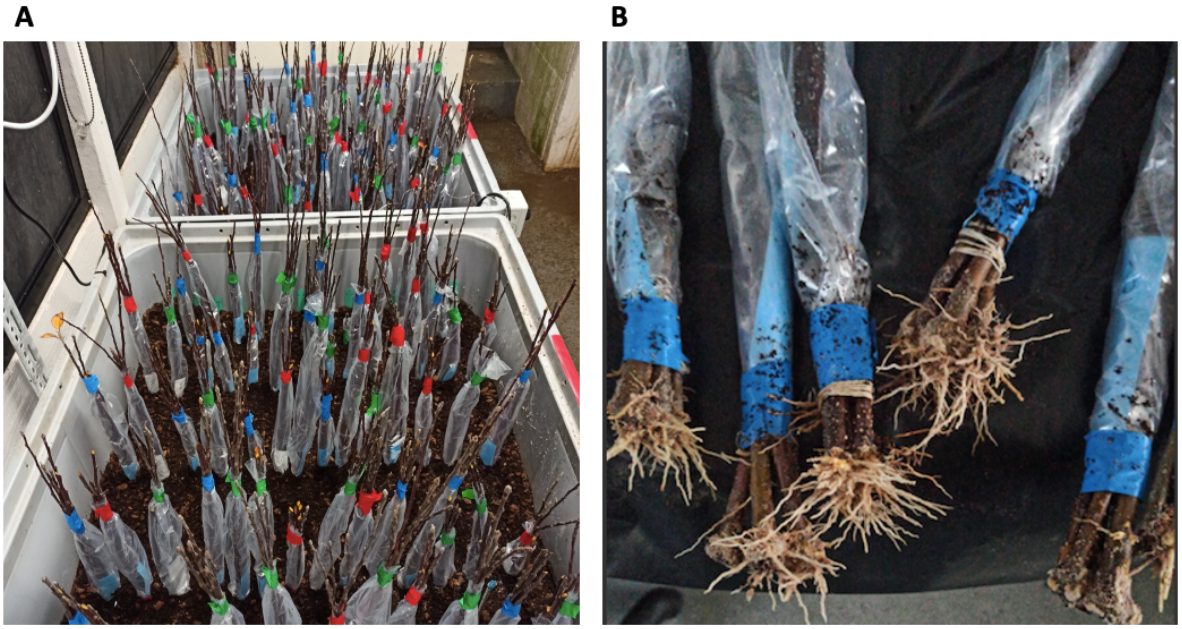

Figure 3.3. A: Hardwood cuttings from the MDX132 family randomly distributed in the two heated bins. B: Genotype bundles of rooted cuttings after spending 6 weeks in the heated bins ready for phenotyping.

3.2.6. QTL analysis

FlexQTL software (accessible at www.flexqtl.nl) using a Markov Chain Monte Carlo (MCMC) simulation was used for QTL mapping as described in the work of Bink *et al.*, (2002, 2008, 2012, 2014). The analyses were conducted using haplotype data, phenotypic data and a consensus genetic linkage map based on 21 full-sib families. QTL effects were set to being additive with a normal prior distribution and a (co) variance matrix with a random, diagonal structure. Each QTL analysis involved an MCMC chain with 200,000 iterations with a thinning factor of 200. The effective sample size was set to 100. Several runs were performed with different starting seeds, maximum number of QTL included in models (5 or 10) and prior expected number of QTL (3 or 5) as recommended to draw reliable and accurate conclusions. The results shown in this chapter are from the FlexQTL™ run with 10 maximum QTL and a prior of 5 QTL.

Two times the natural logarithm of Bayes Factors (2lnBF) obtained from FlexQTL software was used as evidence for the presence and number of QTL. A 2lnBF value greater than 2, 5, or 10 indicated positive, strong, and decisive evidence, respectively (Bink *et al.*, 2008, 2012, 2014). The QTL intervals were defined as regions covered by a continuous set of 2 cM bin intervals with 2lnBF>2. To calculate the proportion of phenotypic variation explained by each QTL the output of the FlexQTL software and the formula; h2= V QTL (additive variance of a QTL) / V P (total phenotypic variance).

3.2.7. Haploblock analysis

The capacity of each haploblock (HB) in the QTL region to account for the observed phenotypic variation was analysed using a linear model using RStudio (R Core Team, 2020). Maternal and paternal haplotypes were tested separately as well as their interaction. The haploblock with the lowest p-value for each QTL was selected for further analysis. The effect of each haplotype within the most significant haploblocks was represented as the percentage of deviation from the mean. The position of the SNPs contained in the most significant haplotypes was located in the Golden Delicious genome (Daccord *et al.*, 2017).

3.2.8. Correlation analysis

A correlation analysis was performed for all the traits analysed in this chapter to investigate the possible relationships between the root architecture of seedlings versus adventitious root architecture from the standard propagation methods of stoolbeds and hardwood cuttings. The correlation matrix was generated using the "corrplot" package available in R (Wei and Simko, 2021). Furthermore, the primary root length and total root surface area of the floating seedlings were correlated with total root length, maximum root system depth and convex hull area measured at the end of the experiment (time point 4) in 39 genotypes grown in rhizoboxes in Chapter 4.

3.2.9. Analysis of the root bark QTL effects on root traits

To understand the impact of dwarfing on the root architecture of seedlings and adventitious rooting, the effect of the RB QTL was analysed in the root architecture traits measured in the seedlings (primary root length and total root surface area) and in the traits measured in the hardwood cuttings (percentage of rooted cutting, average number of roots and average root length). A total of 113 genotypes with no recombination events in the *Rb1* and *Rb2* fine-mapped QTL areas were used for this analysis.

A linear model was used for the analysis of the seedlings' traits using *Rb1, Rb2* and their interaction as fixed variables using RStudio (R Core Team 2020). For the hardwood cutting analysis, a linear mixed model using the "lme4" package available in R (Bates *et al.*, 2015). *Rb1, Rb2* and their interaction as fixed variables and row as a random variable.

3.3 Results

3.3.1 QTL identification

3.3.1.1 Identification of QTL associated with root architecture in floating seedlings

The QTL mapping analysis of the primary root length (PRL) in the floating seedlings identified three QTL with positive evidence on linkage group (LG)1 (2lnBF = 2.2), LG2 (2lnBF = 2.2) and LG17 (2lnBF = 2.3). The variance explained by each QTL ranged from 8.95% to 12.55%. No QTL was identified associated with the total root surface area in the seedlings (Table 3.1).

3.3.1.2 Identification of QTL associated with rooting ability in stoolbeds

The QTL mapping analysis of the stoolbeds dataset found positive evidence (2lnBF = 3.9) for a QTL for rooting ability on LG5 in the 2019 dataset and decisive evidence (2lnBF = 13.2) for the same QTL in the 2020 dataset. There was also positive evidence (2lnBF = 3.8) for a second QTL on LG11 in the 2020 experiment. The variance explained by the QTL located on LG5 was 21.2% in the 2019 experiment and 39.3% in the 2020 experiment. A total of 11.9% of the variance was explained by the QTL identified in LG11 (Table 3.1).

3.3.1.3 Identification of QTL associated with rooting ability in hardwood cuttings

No QTL was identified for the percentage of rooted cuttings, the average number of roots in each cutting and the average root length in the hardwood cutting experiment using the MDX132 progeny (GD x M.9).

Table 3.1. QTL table summarising the location of the QTL, 2lnBF, QTL region and variance explained by each QTL for primary root length in seedlings and percentage of rooting in 2019 and 2020.

Trait	LG	2lnBF for whole LG	QTL region (cM)	% variance explained by each QTL
Primary root length in seedlings	1	2.2	47-59	8.95
	2	2.3	3-27	11.71
	17	2.3	51-61	12.55
% Rooting stoolbeds 2019	5	3.9	6-22	21.2
% Rooting stoolbeds 2020	5	13.2	8-16	39.3
	11	3.8	17-53	11.9

3.3.2 Haploblock analysis

3.3.2.1 Haploblock analysis for primary root length in floating seedlings

The effect of all the haploblocks within the QTL intervals was independently tested. The most significant haploblock identified in the QTL interval in LG1 for primary root length was HB30. Only the paternal haplotype in HB30 was significant in the analysis and, therefore, was inherited from M.9. Rootstocks that carried haplotype 0 from HB30 were associated with a 13.8% increase in PRL compared to the mean. However, genotypes that had haplotype 1 showed a 13.1% decrease in PRL compared to the mean (Figure 3.4 Panel A).

In the QTL identified in LG2, the maternal haplotype in HB5 was the most significant in this region. Genotypes that carried haplotype 0 exhibited a decrease of 15.2% in the PRL compared to the mean. Conversely, those genotypes that had haplotype 1 alleles showed primary roots 17.1% longer than the average (Figure 3.4. Panel B).

In the QTL located in LG17, the paternal haplotype in HB29 was the most significant in this QTL interval. Rootstocks containing haplotype 0 alleles showed an 8.4% increase in PRL compared to the mean. However, the genotypes that carried the haplotype 1 alleles exhibited a reduction of 18.3% in the PRL compared to the mean (Figure 3.4. Panel C).

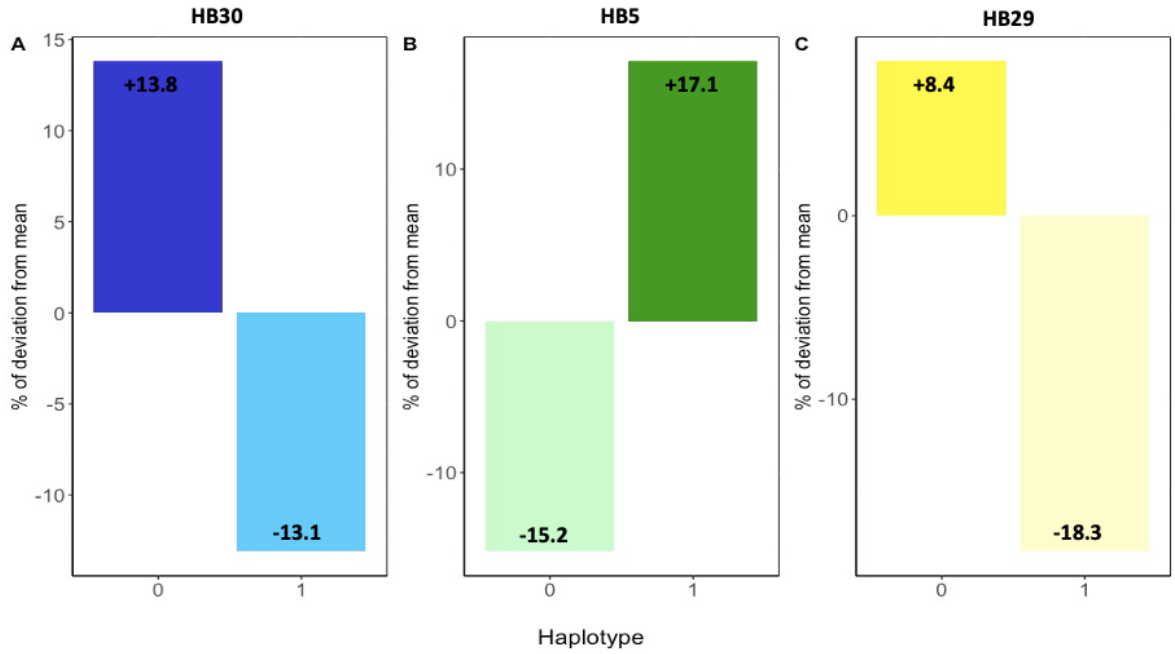

Figure 3.4. Estimated percentage of deviation from the mean for the haplotypes in the most significant haploblocks, HB30 in linkage group 1, HB5 in linkage group 2 and HB26 in linkage group 17, associated with primary root length in the seedlings from the MDX132 population.

3.3.2.2 Haploblock analysis for rooting ability in the stoolbeds

The effect of all the haploblocks within the QTL interval was independently tested. The most significant haploblock identified in the QTL interval in LG5 for rooting ability in 2019 and 2020 was the HB8. Only the paternal haplotype was significant in the model for HB8 in both years, indicating that it was inherited from M.9. HB26 was the most significant haploblock in the QTL interval in LG11 for rooting ability in the 2020 experiment. In this case, the maternal haplotype was the only significant haplotype in the model for HB26, indicating that this QTL was inherited from GD. A haplotype analysis was performed to identify which of the two correspondent haplotypes of the

correspondent parent contributed to better rooting ability in the stoolbeds. The estimated percentage deviation from the mean was calculated for each haplotype in each haploblock. Individuals that carried haplotype 1 from HB8 produced 23.8% and 26.3% of rooted shoots compared to the mean in 2019 and 2020, respectively. However, the presence of haplotype 0 was associated with a 12.9 and 15.5% decrease in rooted shoots compared to the mean. For HB26, haplotype 0 was associated with a 13.1% increase in rooted shoots compared to the mean. Conversely, genotypes that carried haplotype 1 showed a decrease of 11.2% in rooted shoots compared to the mean (Figure 3.5).

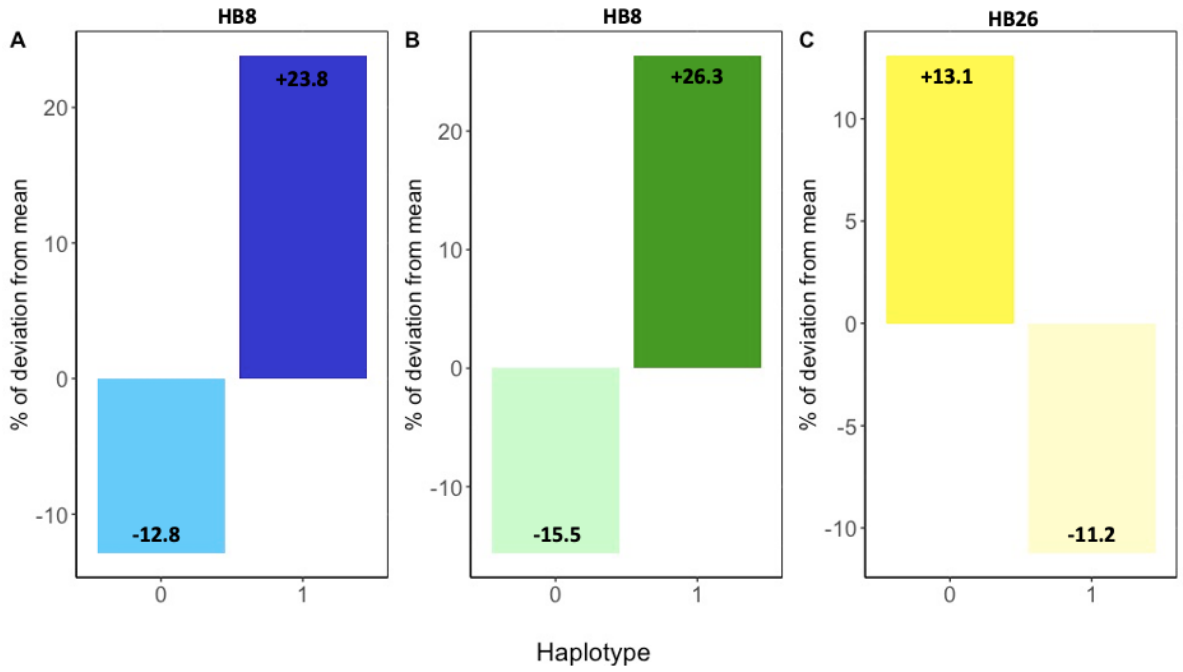

Figure 3.5. Estimated percentage of deviation from the mean for the haplotypes in the most significant haploblocks, HB8 at linkage group 5 and HB26 at linkage group 11, associated with rooting ability in the stoolbeds in the MDX132 population.

3.3.3 Correlation between rooting traits in the MDX132 progeny

Correlation coefficients were calculated for all phenotypic measurements in the three experiments to identify the relationship between all the measured traits. Low to very low correlation values were found between the stoolbeds experiments and the hardwood cutting experiment. The highest correlation was identified between the percentage of rooted shoots in the stoolbeds in 2020 and the hardwood cutting average root length (R=0.18, p-value = 0.07). Very low negative correlations were identified between when comparing HCW average root number with PRL and TRSA in the seedlings (R=-0.15, p-value = 0.13 and R=-0.16, p-value = 0.098, respectively). Similarly, very weak correlations were identified between the seedlings and the stoolbeds experiment with the highest correlation between the TRSA in the seedlings and the percentage of rooting in the stoolbeds in 2020 (R= 0.12, p-value = 0.21). The phenotypic data from the stoolbeds in 2019 and 2020 were not signifiantly correlated (R= 0.21, p-value = 0.052). The traits measured in the hardwood cutting experiment showed a moderate to high correlation between them as expected since those measurements were interrelated. The average root length was significantly correlated to the percentage of rooted cuttings and the average number of roots (R=0.46, p-value = 1.3e-07 and R=0.54, p-value = 2.3e-10, respectively). The percentage of rooted cuttings and the average number of roots were highly correlated (R= 0.71, p-value = 1.7e-19; Figure 3.6. Panel A).

Generally, low correlations were found when comparing the phenotypic measurements of seedlings with the root architecture traits of the same genotypes grafted after being propagated in stoolbeds and grown in rhizotrons as detailed in Chapter 4. The highest correlation value was identified between TRSA in the stoolbeds and total root length in the rhizotrons experiment (R=0.28, p-value = 0.093; Figure 3.6. Panel B).

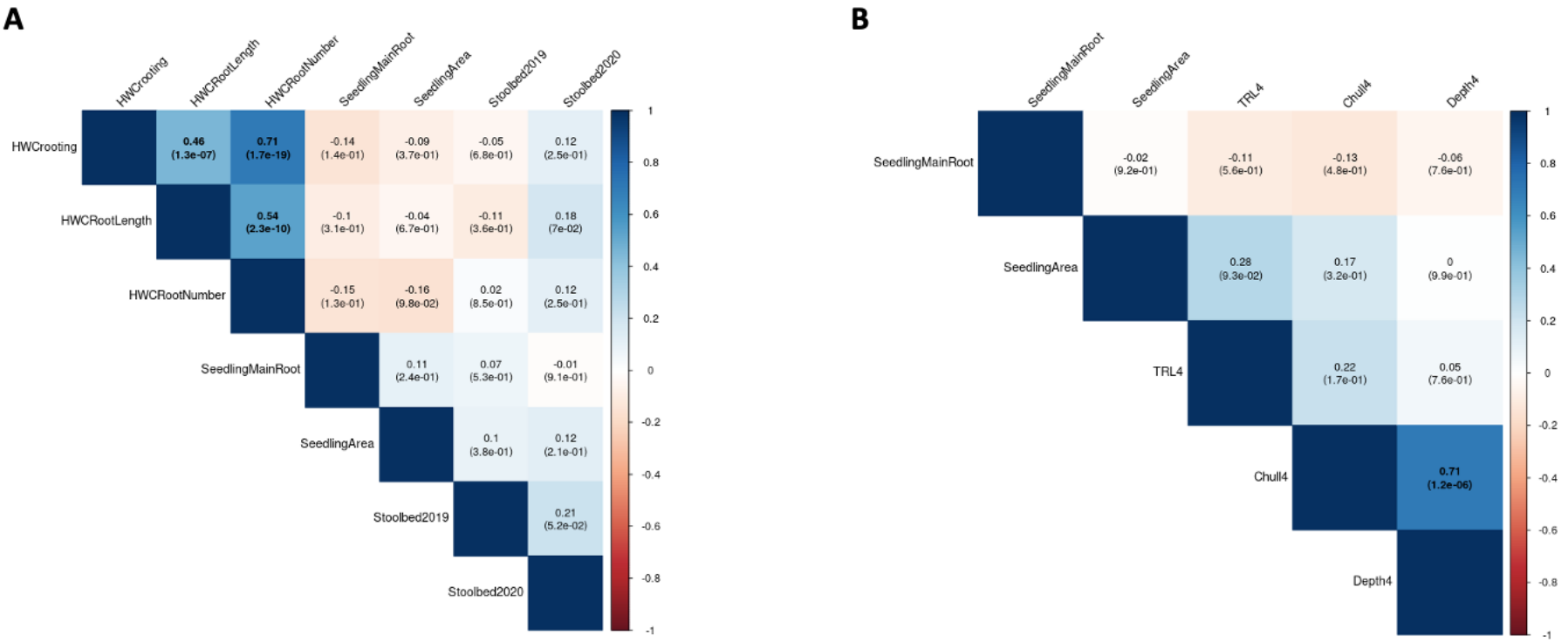

Figure 3.6. A: Correlation matrix showing Spearman's correlation coefficient of the phenotypic data from the hardwood cutting experiment traits (HWCrooting; percentage of rooted cutting, HWCRootLength; average root length per genotype and HWCRootNumber; average root number per genotype), root architecture traits in the seedlings (SeedlingMainRoot; main root length and SeedlingArea; total root surface area) and the percentage of rooted shoots in the stoolbeds in 2019 and 2020 using the MDX132 population. B: Correlation matrix showing Spearman's correlation coefficient of the phenotypic data from the root architecture traits in the seedlings and the root architecture traits (TRL; total root length, Depth; maximum root system depth and Chull; convex hull area) measured in the last time point of the rhizotrons experiment detailed in Chapter 4. Significant correlations and p-values in bold.

3.3.4 Effect of RB QTL on rooting ability in the seedlings' root architecture and the hardwood cuttings experiment

The effect of RB QTL on the seedling root traits was analysed to investigate the impact of dwarfing on initial root architectural traits that could potentially affect growth and seedling survival. The dwarfing effect in rooting ability was also evaluated in the rootstock propagation methods.

Dwarfing did not impact the PRL in the seedlings. However, a significant effect of *Rb1* (p-value = 0.04) on the total root surface area of the seedling was identified (Table 3.1). Seedlings that had the *Rb1* QTL had on average 713±228 mm^2 of root surface area whereas the seedlings that did not carry the *Rb1* QTL had 631± 208 mm^2. No effect of *Rb2* or the interaction term *Rb1 x Rb2* was detected in this analysis (Table 3.2).

The percentage of rooted cuttings in the hardwood cutting experiment was influenced by the presence of the *Rb1* QTL (p-value = 0.04). Interestingly, genotypes that carried the *Rb1* QTL showed a reduced percentage of rooted cuttings. Conversely, dwarfing did not affect either the average number of roots or the average root length in the hardwood cutting experiment (Table 3.2).

Table 3.2. Summary table of the means and ANOVA of primary root length and total root surface area in seedlings; percentage of rooted cuttings, average numbers of roots and root length in cuttings per fixed variable

Fixed variables	Levels	Means				
		Primary root length	**Total root surface area**	**% of rooted cuttings**	**Average number of roots**	**Average root length**
Rb1	**No**	122	631	1.04	0.820	19.1
	Yes	119	713	0.84	0.773	18.8
Rb2	**No**	118	707	0.976	0.772	18.1
	Yes	123	643	0.904	0.822	19.8
ANOVA						
F_{Rb1}		0.10 (0.74)	3.96 (**0.04**)	4.29 (**0.04**)	0.77 (0.38)	0.03 (0.85)
F_{Rb2}		0.14 (0.69)	2.57 (0.11)	0.54 (0.46)	0.86 (0.35)	0.68 (0.41)
$F_{Rb1xRb2}$		0.01 (0.89)	0.79 (0.37)	2.28 (0.13)	3.34 (0.07)	1.03 (0.31)

F_{Rb1}: Rb1 QTL effect; F_{Rb2}: Rb2 QTL effect; $F_{Rb1xRb2}$: Rb1 x Rb2 QTL interaction effect; P-values in brackets and significant p-values in bold.

3.4 Discussion

3.4.1. *Rb1* QTL associated with rootstock-induced dwarfing colocalizes with a QTL identified for rooting ability in the stoolbeds

The identification of QTL associated with rooting ability in stoolbeds would help to better understand the adventitious root production in rootstocks and could be used to select new rootstocks with improved propagation capacity. In this study, two QTL associated with rooting ability were identified in Chr5 and Chr11 which unexpectedly were located in the same chromosomes as *Rb1* and *Rb2*, the QTL associated with rootstock-induced dwarfing (Harrison et al., 2016b). QTL mapping analysis of rooting ability using another population generated from an M.27 x M.116 cross (data not shown) identified several QTL for rooting ability and none of them were located in Chr5 or Chr11, suggesting that the QTL mapped in this study were indeed the rootstock-induce dwarfing QTL.

The QTL linked to (adventitious) rooting ability in Chr5 was identified in the two experiments and was located exactly in the same region as *Rb1*. Furthermore, HB8 resulted in the most significant haploblock in both experiments and was situated approximately at 44.1 Mb which is within the previously fine-mapped region described in Chapter 2 (Supplementary Table S6). QTL mapping analysis for rooting ability on stoolbeds using an M.27 x M.116 cross (data not shown) identified several QTL for rooting ability but none of them was located in Chr5 or Chr11, suggesting that the fact the QTL for rooting ability colocalized with the RB QTL is something specific to this population or experiment. Therefore, it seems that there is an indirect correlation between dwarfing and rooting ability rather than the genes being located in the same region.

One of the hypotheses proposed to explain these findings is based on the substantial impact of dwarfing on the stoolbeds. During the stoolbeds preparation process, the most vigorous genotypes already had fairly tall and mostly lignified shoots. This advanced state of lignification could have potentially hindered the adventitious root formation in these genotypes as the accumulation of lignin has been associated with a reduction in rooting in several plants (Reineke *et al.*, 2002; Singh *et al.*, 2020; Chang

et al., 2023). Conversely, dwarfing genotypes showed softer shoots with less lignin and could have been in a more favourable state for adventitious rooting. Consequently, the data might have been unintentionally skewed. Another possible explanation could be a different way of resource allocation. For instance, in dwarfing rootstocks, the energy could be more readily available for root development rather than being transported to the shoot.

However, *Rb2*, the QTL associated with rooting ability in Chr11 was only identified in the second experiment and roughly colocalised with *Rb2* although the most significant haploblock (HB29) within the QTL area was located approximately at 27 Mb, a little further down in Chr11 than the two proposed QTL associated with dwarfing described in Chapter 2 which were located between 6.9 Mb to 7.5 Mb and from 10.9 Mb to 12.8 Mb (Supplementary Table S6). This could be explained by the fact that the first-year experiment was less reliable due to the smaller number of genotypes included. The area occupied by the QTL is quite large and partially colocalised with *Rb2* although the haplotype with the most significant effect was not located in the same area as the two potential areas mapped for *Rb2*. Moreover, the haplotype linked to a greater rooting ability was segregated from GD. The most likely explanation is that this QTL is, in fact, *Rb2*, even though it is not situated in the exact same region, it is close enough to consider it as the same QTL.

In summary, the strong impact of rootstock-induced dwarfing on rooting on stoolbeds in this population masked any rooting ability QTL that could be present, indicating that dwarfing rootstocks could have a good rooting potential.

3.4.2. Identification of QTL associated with primary root length in rootstock seedlings

Rootstocks with deeper root systems would offer improved capabilities for water and nutrient absorption, better soil anchorage, and thus, enhanced resilience to extreme climatic conditions like floods and droughts. The early identification of genotypes exhibiting favourable root architecture would expedite the breeding process for developing varieties with improved root systems. In this chapter, three QTL associated with PRL were identified in the seedlings with positive evidence (2lnBF > 2). Generally,

most of the studies consider a QTL valid if there is strong evidence within a single experiment, or if they show at least positive evidence in two or more independent phenotyping experiments. Consequently, in order to confirm the existence of these QTL it would be advisable to repeat this experiment using a different population. However, the QTL identified in one population may not be expressed or may have different effects in another population. In addition, the QTL could have different effects in different environments, complicating validation efforts. Therefore, it would be ideal to combine data from multiple populations while minimizing environmental variability to increase the robustness of QTL detection. Furthermore, it has been seen that there is not a strong correlation between root traits measured in this Chapter (3), with the root architecture traits measured in the grafted rootstocks used in Chapter 4, indicating that seedling root architecture seems to be differentially regulated to the root architecture of the rootstocks propagated by stoolbeds in this population. Therefore, these results indicate that seedling rootstocks are not a good prediction tool for future root architecture in apple rootstocks.

3.4.3. Impact of dwarfing on seedlings root architecture, stoolbeds rooting ability and hardwood cutting propagation

Dwarfing undeniably had a significant influence on root production in the stoolbed experiments, with the dwarfing genotypes producing a greater number of roots compared to the vigorous genotypes. Consequently, the QTL identified in the rooting ability experiment were likely the RB QTL as they intriguingly colocalize. As previously mentioned, there seems to be an indirect correlation between rootstock-induced dwarfing and rooting ability due to physiological changes in the shoots mainly caused by dwarfing.

In the hardwood cutting experiment, no QTL was identified to be associated with rooting ability in the MDX132 population, indicating that when the dwarfing effect was controlled by collecting cuttings during the dormant season, they were all in a similar physiological state. However, the statistical analysis of the RB QTL effect on rooting in the hardwood cuttings revealed that *Rb1* had a negative effect on rooting (Table 3.2) and therefore, genotypes that did not have the *Rb1* region produced more roots.

In this case, the reduced rooting rate in dwarfing genotypes may be explained by another physiological factor such as the diameter of the cuttings (not measured), as its effect on rooting has been already reported. Exadaktylou *et al.*, (2009) investigated the rooting in 'Gisela 5' cherry rootstocks using hardwood cuttings and found that the best rooting rates were observed in cuttings with an intermediate diameter. In a study using pear cuttings, same-length cuttings with different diameters were compared and the best rooting was achieved by the cuttings with an intermediate diameter (Lebedev, 2019). The proposed explanation was that the thinnest cuttings could have nutrient deficiencies whereas, in the thickest cuttings, the juvenility could have been reduced (Lebedev, 2019). Verma *et al.*, (2015) reported that in 'Merton 793' apple rootstocks, the thickest cuttings evaluated had the best rooting success whereas very thin cuttings did not develop roots.

The smaller diameter of cuttings could be linked to a reduced content of carbohydrates, which could have a negative impact on the rooting process. Several studies have highlighted the importance of adequate initial carbohydrate content in cuttings to provide the necessary energy reserves for the entire rooting period (Veierskov, 1988; da Costa *et al.*, 2013). Other studies suggest that while carbohydrates themselves may not directly influence rooting, they play a crucial role in the synthesis of auxins, which are plant hormones that are pivotal in the formation of roots (Hartmann and Kester, 1975; Souza and Pereira, 2007). When there is a reduction in the availability of carbohydrates, it can result in a decreased production of auxins, leading to a diminished capacity for root formation. In future studies, measuring both, cutting diameter and carbohydrates, would be a valuable tool to determine their role in rooting.

Another physiological aspect to consider is the hormone interactions occurring in the shoots or cuttings. Cytokinins are plant hormones that are known to inhibit root growth. Dwarfing rootstocks are characterised by a reduced cytokinin synthesis and this could be potentially contributing to a greater rooting ability of dwarfing rooting in stoolbeds. However, the rooting ability of dwarfing rootstocks in the hardwood cutting experiment seems to be diminished and, therefore, investigating the potential fluctuation in hormone levels across the year could shed light on any season variations and their potential correlation with the rooting ability of both cutting and shoots.

3.4.4. Other factors influencing rooting in the different propagation methods

As has been observed in this chapter, various factors affect the rooting capacity of apple rootstocks such as rootstock-induced dwarfing, lignin and the diameter of the cutting. Another factor that significantly impacts adventitious root development is the environmental conditions as demonstrated in previous studies in oak and pear which showed great data variability in experiments repeated 4 years under the same conditions (Scotti-Saintagne *et al.*, 2005; Lebedev, 2019). This would also explain why the correlation between the two stoolbeds experiments was very low since any environmental factor could have affected the rooting experiments.

As occurs in many other traits, genotype has a clear influence on the development of adventitious roots and has been reported in different tree species such as pinus, poplar and hybrid aspen (Panetsos *et al.*, 1994; Stenvall *et al.*, 2004; Zalesny and Wiese, 2006). Consequently, the QTL identified for the primary root trait or the lack of QTL associated with rooting ability in the GD x M.9 population as well as the large impact of dwarfing on some traits could significantly vary using other progenies.

3.5 Conclusion

These results indicate that dwarfing impacts rooting ability in both, hardwood cuttings and stoolbeds. Further investigations are needed to understand which physiological aspects associated with dwarfing influence rooting ability. In addition, no correlation was found between rootstocks seedlings and grafted rootstocks, indicating that the future root architecture of apple rootstocks cannot be predicted using seedling phenotyping. Furthermore, the results presented in this chapter are derived from the study of a single population. It would be essential to study other progenies (ideally families segregating and not segregating for dwarfing traits) and investigate the transferability of these findings to a wider set of germplasm.

Chapter 4. Effect of dwarfing on root system architecture in apple rootstocks

4.1 Introduction

Root systems have great plasticity and root development is modified by a wide range of factors including genetics, soil environment and resource availability (van der Weele *et al.*, 2000; López-Bucio *et al.*, 2003; Hodge, 2004; Malamy, 2005; Koevoets *et al.*, 2016; Karlova *et al.*, 2021). Dwarfing rootstocks impact tree height, trunk diameter, tree architecture, precocity, flowering and yield in the scion and, often, in the rootstock itself and has been widely investigated over the past decades (Atkinson and Else, 2001; Seleznyova *et al.*, 2003; Lauri *et al.*, 2006; Gjamovski and Kiprijanovski, 2011; Amiri *et al.*, 2014; Tworkoski and Fazio, 2015). However, less attention has been paid to the impact of dwarfing on root architecture due to the difficulties in accessing the root systems. Preliminary studies have demonstrated that vigorous rootstocks produced significantly higher root length density, described as the total length of roots within a particular volume of soil, compared to dwarfing rootstocks (De Silva, 1999; An *et al.*, 2017b). Lo Bianco et al., (2003) reported that the vigorous rootstock M.M.106 showed a higher total root density and a more layered vertical distribution of the root system compared to the dwarfing M.9 rootstock. Ma et al., (2013) dwarfing rootstocks as having root systems restricted to a smaller region than the larger and deeper roots of the vigorous rootstocks. Moreover, dwarfing rootstocks show smaller fine root diameters and shorter root lifespans relative to vigorous rootstocks (García-Villanueva *et al.*, 2004; Hou *et al.*, 2012; An *et al.*, 2017b).

The difficulty in accessing root systems complicates progress in this research area. The use of minirhizotrons (tubes with cameras inserted into the soil) or rhizoboxes (planting boxes with transparent windows to observe roots) has facilitated the study of root architecture and root growth dynamics in a non-destructive way. Rhizoboxes are often preferred since they facilitate non-invasive and uninterrupted monitoring of continuous root growth (Mašková and Klimeš, 2019). Typically, rhizoboxes are flat to allow root visualisation via imaging or scanning. Although rhizoboxes cannot be compared to field conditions, they allow us to observe below-ground aspects of root

growth and development that otherwise could not be studied, converting them in an essential tool for root system studies (Lesmes-Vesga *et al.*, 2022).

Early selection of well-rooted rootstocks holds significant potential for reducing the breeding cycle and enhancing breeding efficiency. Despite the advances in the research of apple root systems, further studies are needed to understand the genetic basis of the root spatial distribution in this perennial crop.

In this chapter, 39 genotypes propagated by stoolbeds from a Golden Delicious (GD) x M.9 mapping population with different combinations of the dwarfing root bark QTL (*Rb1* and *Rb2*) were imaged periodically to analyse the effect of dwarfing genetics on root architecture in apple rootstocks. Python scripts specifically designed for this purpose were used to analyse the images automatically providing measurements of important root traits.

The specific objectives of this chapter were:

- To test whether the initial root surface area of rootstocks affects the future root architecture
- To evaluate the impact of dwarfing on important root traits
- To investigate the role of *Rb1* and *Rb2* in the canopy and root traits
- To analyse the correlation between aerial and root traits

4.2 Methods

4.2.1. Genotyping

The MDX132 mapping population (GD x M.9 cross) was used in this experiment, genotyping details are described in section 2.2.4.1. The SNPs data were used to generate a haploblock map as described in section 3.2.1.

4.2.2. Lifting stoolbeds and rooting phenotyping in 2020

The MDX132 population was planted as stoolbeds as described in section 3.2.1. Rootstocks were stooled in June 2018 to conduct the experiment in 2019 but unfortunately, not many genotypes produced well-rooted shoots and, therefore, the experiment was postponed until 2020. In January 2020, stoolbeds were carefully unearthed and rooted shoots were labelled and stored at 4°C for further experiments on root system architecture. The number of roots in each shoot was scored from 1 to 5 (1: 1-2 roots and 5: lots of roots).

4.2.3. Genotype selection for root architecture experiment

SNPs flanking *Rb1* and *Rb2* regions were identified for the improved QTL location from Chapter 2 and individuals with no recombinations in these areas were classified into four groups, depending on the presence or absence of the haplotypes linked to *Rb*1 and *Rb2* respectively (Table 4.1). Although both QTL regions are needed to cause dwarfing, groups with only one of the RB QTL were also included to determine what, if any, individual effect each QTL had on root traits. Genotypes with a minimum root score of 2 were selected for the experiment.

The initial intention of this experiment was to replicate by genotype, but poor rooting of shoots prevented this. Trunk diameter was recorded for the selected genotypes and photos of the roots were also taken before planting the rootstocks in rhizoboxes.

Table 4.1. Number of genotypes in each dwarfing class based on the presence or absence of the *Rb1* and *Rb2* QTL and the predicted vigour

***Rb1* haplotype**	***Rb2* haplotype**	**Number of genotypes**	**Predicted vigour**
No	No	9	Vigorous
Yes	No	10	Vigorous
No	Yes	9	Vigorous
Yes	Yes	12	Dwarfing

4.2.4. Root system architecture rhizoboxes

Non-recombinant and well-rooted genotypes selected for this experiment were grafted at the end of March using Gala graft wood collected from a single Gala tree available at the NIAB EMR. Afterward, grafted trees were planted in rhizoboxes (100 cm x 30 cm x 3 cm) filled with sieved standard compost without slow-release fertilizer to avoid interference with the imaging since the whitish colour of the fertiliser can be confused with roots during image processing. Rhizoboxes were covered with white reflective plastic to prevent roots from direct light.

The rhizoboxes were randomised in 4 blocks and placed in a glasshouse compartment at an inclination of approximately 15° (Figure 4.1. Panel A). Trees were fertigated twice a day for 2 minutes at 8 am and 4 pm using a Dosatron with Universol Green 23-6-10 (N-P-K) fertiliser.

4.2.5. Initial phenotyping

Images of the root systems were taken before grafting using a Canon 1200D camera with an 18-55 mm telephoto lens (Figure 4.1. Panel B). These images were analysed using ImageJ to measure the total root surface area.

Trunk diameter was measured 10 cm below the graft union just after grafting at the end of March. Two measurements were taken using digital callipers, the second one taken at a 90-degree angle to the first. The mean was calculated and used for subsequent analyses.

4.2.6. Canopy phenotyping and imaging

Rhizobox imaging and canopy phenotyping (trunk diameter and height) took place every six weeks from June until October 2020. Trunk diameter was measured as described in the previous section 4.2.5 and tree height was measured using a tape measure.

A homemade imaging rig was set up with 2 Canon 1200D cameras with an 18-55 mm telephoto (using the 18 mm) on a camera slider. The total length of the rhizobox was covered by overlapping the two images. The imaging platform consisted of a Dexion frame where the rhizoboxes were positioned at a fixed distance from the camera. The whole imaging structure was covered by a black cloth and two Manfrotto LED lighting units were used to minimise the variation of the ambient light as much as possible. Images were taken at an f stop of 5.6 to 6.3 at 1/60 using a shutter release (Figure 4.1. Panel C).

4.2.7. Final phenotyping

The last imaging and canopy phenotyping was performed in October 2020. Trees were cut at the graft union level to separate canopy and root systems which were carefully washed with tap water to remove the soil. The root systems were then left to air dry and weighed as well as the above-ground biomass (Figure 4.1. Panel D). Next, 10 to 15 root segments (2-8 mm in diameter, 50-80 mm in length) were excised from each tree using secateurs, placed into a labelled polythene bag and stored at 4°C before root bark analysis. Digital callipers were used to make two of measurements of the root (with and without the bark) as described in Chapter 2 section 2.2.3.1. The percentage of root bark at a standard root diameter of 7.5 mm was then inferred in each genotype using regression analysis.

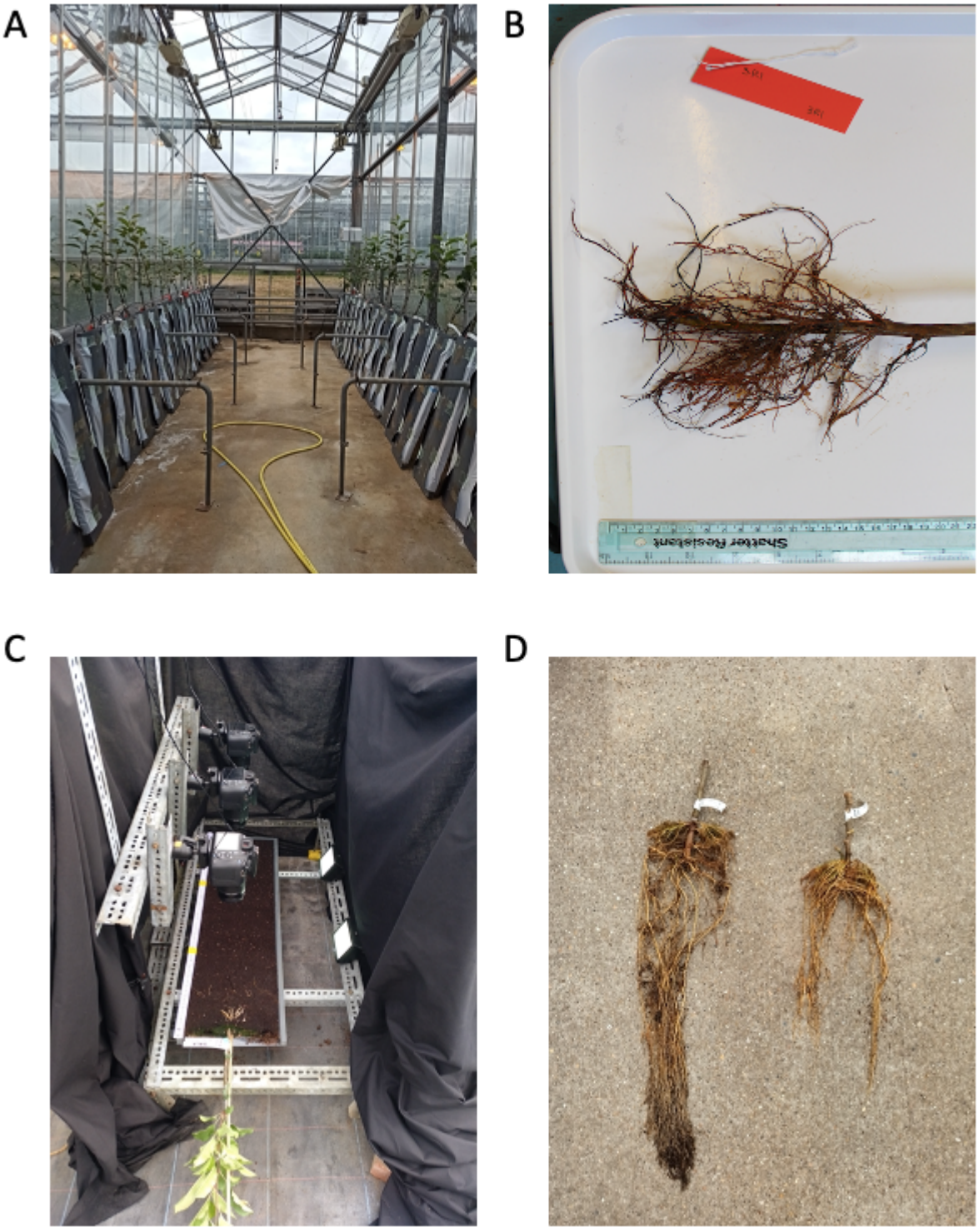

Figure 4.1. Details of the root system architecture experiment. A: Rhizoboxes in the glasshouse compartment. B: Image of a rooted rootstock collected from stoolbeds. C: Custom-made imaging rig used for root systems phenotyping. D: Root systems from vigorous (left) and dwarfing (right) genotypes at the end of the experiment.

4.2.8. Imaging analysis

Chromatic aberrations and lens distortion were corrected using the RawTherapee imaging analysis software version 5.8 (RawTherapee 5.8, 2020). Then, the two photos of each rhizobox were stitched together using the Fiji plug-in available in ImageJ 2.1.0 (Schindelin *et al.*, 2012). Differences in the contrast between the two images were adjusted and a composite image of the rhizobox was created using the montage option and the least square mode. The photos were then exported in PNG format at the best resolution. Afterward, the composite images were reopened using Fiji and the region containing the root information was cropped avoiding the rhizoboxes edges.

Image segmentation, cleaning, re-cropping and root measurements were done using Python scripts developed by Ben Pennington while working at NIAB EMR in 2016 using Python 2.7 (van Rossum, 1995) and that I adapted it to this experiment. In the segmentation script, the photo was converted into a white and black image where the roots were transformed into white pixels and the soil into black pixels. In this script, the number of clusters used to segment the images ranged from 4 to 7. In general, this script worked well using 5 clusters (4 images detecting soil and 1 image for roots). When not completely satisfied with the segmentation of the images, the number of clusters was increased. Occasionally, not all the roots appear clearly in one segmented image. In this case, GIMP version 2.10 (GNU Image Manipulation Programme, 2020) software was used to combine both images to obtain the whole root system in one picture. The segmented images were then cleaned using a cleaning script that removed small blobs of pixels, also known as background noise, that could be mistakenly identified as roots. The size of the blobs was modified in the script depending on how much noise there was in each image. Each image was carefully reviewed and re-cleaned manually using ImageJ if needed. Next, the re-cropping script was used to remove regions of the rhizobox image that contained imaging artefacts.

Finally, the measurement script was utilised to generate an Excel table containing several root measurements such as total root length, mean root diameter, maximum root diameter, maximum root system depth and convex hull area. Graphical outputs

were also produced for each image such as the root diameter distribution of each rhizobox, convex hull figures and skeleton photos (Figures 4.2 and 4.3).

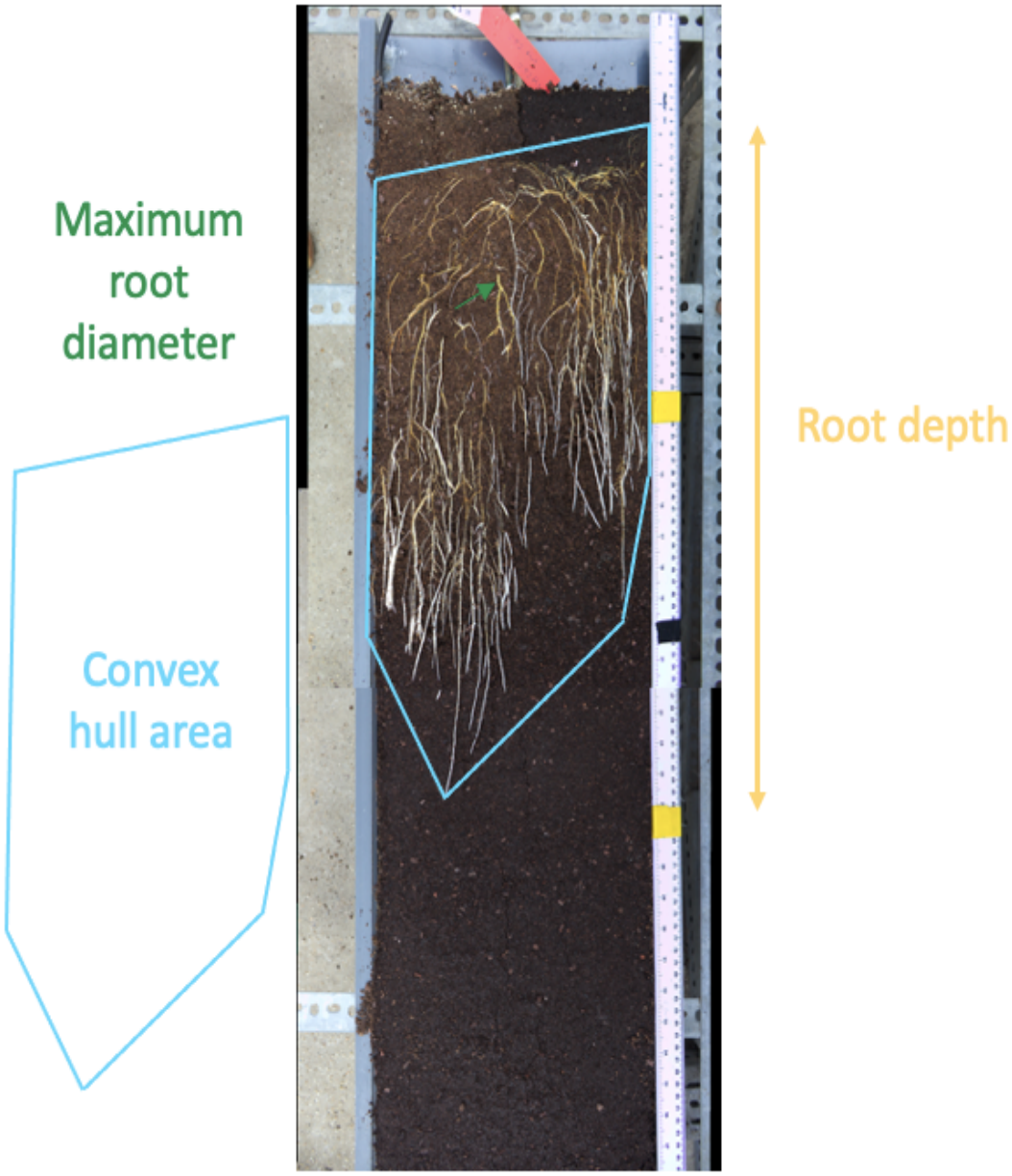

Figure 4.2. Diagram representing some of the root measurements taken from apple rootstocks grown in rhizoboxes.

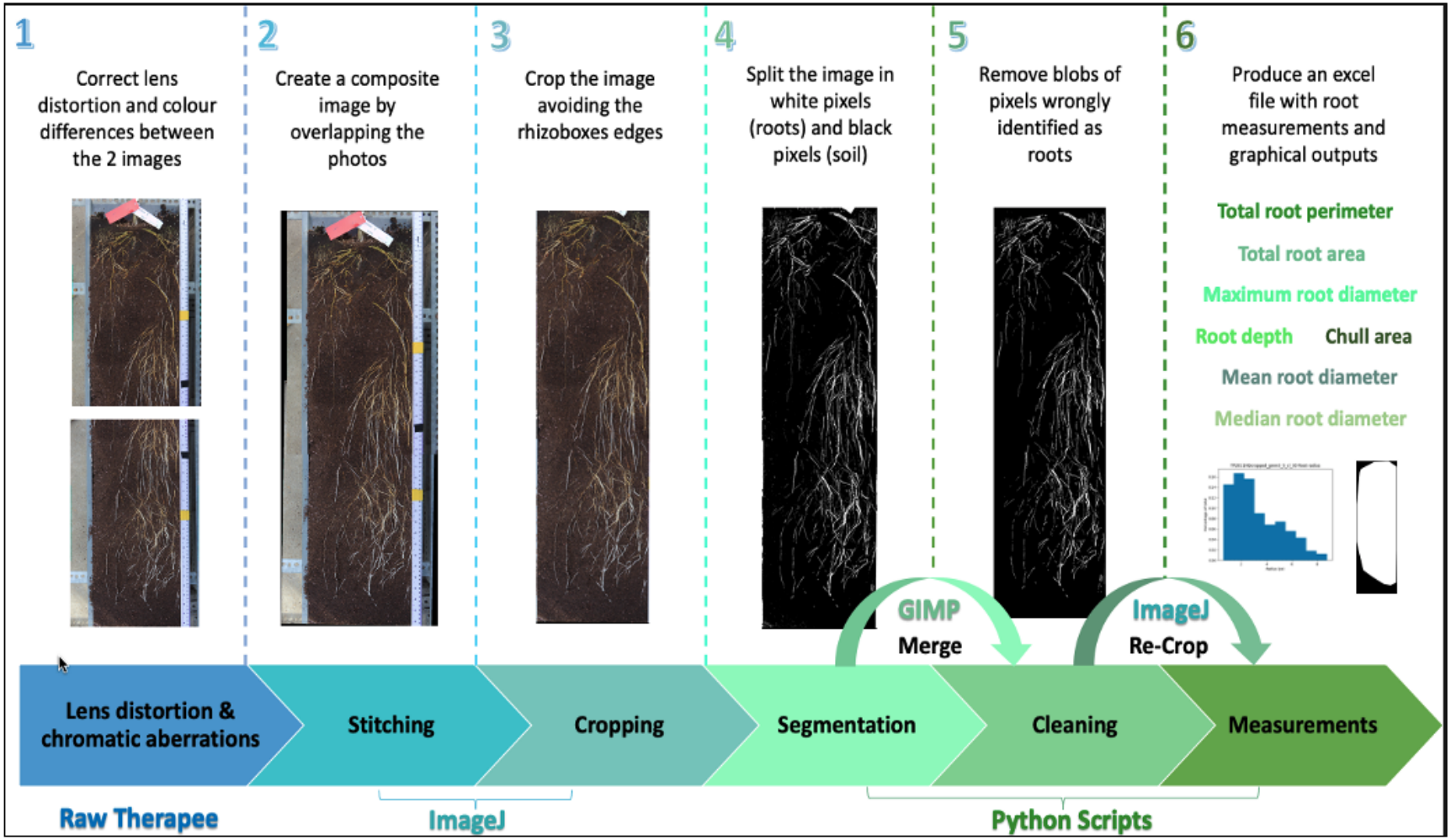

Figure 4.3. The imaging analysis pipeline detailing the steps and programs used during the imaging analysis of the root architecture traits in the MDX132 population (GD x M.9 cross).

4.2.9. Statistical analysis

One-way ANOVA tests and Post hoc tests using Tukey's Honest Significant Differences (Tukey's HSD) were performed for the identification and determination of significant differences in the initial root surface and initial trunk diameter using RStudio (R Core Team 2020). Initial root surface data and initial trunk diameter data were transformed using the logarithmic transformation to improve the distribution of the residuals as they were slightly skewed.

Linear mixed models fitted by REML were used for the canopy data analysis including tree height, trunk diameter above graft union and trunk diameter below graft union and the root traits data analysis including total root length, maximum root diameter, mean root diameter, root system depth and convex hull area using the "lme4" package available in R (Bates *et al.*, 2015). The model selection was performed by dropping variables and comparing models with likelihood ratio tests using the ANOVA function. The best consensus model was chosen for all the analyses. The final model consisted of eight fixed variables: block, time point (TP), *Rb1*, *Rb2*, all the possible interactions of TP, *Rb1* and *Rb2* and genotype as a random variable. Post hoc contrasts were performed using the "emmeans" package available in R (Lenth *et al.*, 2018). Total root length was transformed using the square root transformation and mean root diameter was also transformed using the logarithmic transformation to improve the distribution of the residuals.

All the root traits data were used to perform a principal component analysis (PCA) using the "FactoExtra" package available in R (Kassambara and Mundt, 2020). Linear models were performed at each time point to assess the effect of root bark QTL on each PC.

Correlation coefficients were calculated for initial root surface area (IRSA), root bark percentage (RB%), canopy and root wet weight and for root and canopy traits at the end of the experiment including total root length (TRL), maximum root diameter, mean root diameter, root system depth, convex hull area, tree height, trunk diameter above and below the graft union using the Spearman method. The correlation matrix was generated using the "corrplot" package available in R (Wei and Simko, 2021).

Traits measured at the end of the experiment including root bark percentage, canopy and root bark percentage were analysed using linear models with *Rb1*, *Rb2*, *Rb1* x *Rb2* interaction and block as fixed variables.

Graphical outputs were obtained using the “ggplot2” (Wickham, 2016) and the significance letters were added creating compact letter displays (CLD) of all pairwise comparisons using the “multcomp” and “multcompView” packages available in R (Hothorn *et al.*, 2008; Graves *et al.*, 2019).

4.3. Results

4.3.1. Effect of RB QTL on rootstock traits before planting

The *Rb1* QTL had an impact on the initial root surface in the ungrafted rootstocks at the stoolbeds (F value = 18.97, p-value = 0.0001). However, *Rb2* and the *Rb1* x *Rb2* interaction were not significant (p-value = 0.19 and p-value = 0.12, respectively; Supplementary Table S7). Post hoc tests using Tukey's Honest Significant Differences (Tukey's HSD) were performed using the combined RB QTL information. The group containing both RB QTL was significantly different from the group with none of the RB QTL (p-value = 0.002) and also different from the group with only *Rb2* (p-value = 0.0012; Figure 4.4 and Supplementary Table S9).

The genotypes with both RB QTL had the largest root surface area at the beginning of the experiment, followed by rootstocks with only *Rb1*. No significant differences between *Rb1* and *Rb1Rb2* groups were detected (p-value = 0.1928; Supplementary Table S9). The effect of dwarfing on rooting in the stoolbeds has been discussed in Chapter 3. The initial trunk diameter of the ungrafted rootstocks was not affected by either *Rb1* or *Rb2* (p-value = 0.81 and p-value = 0.83, respectively; Supplementary Table S9).

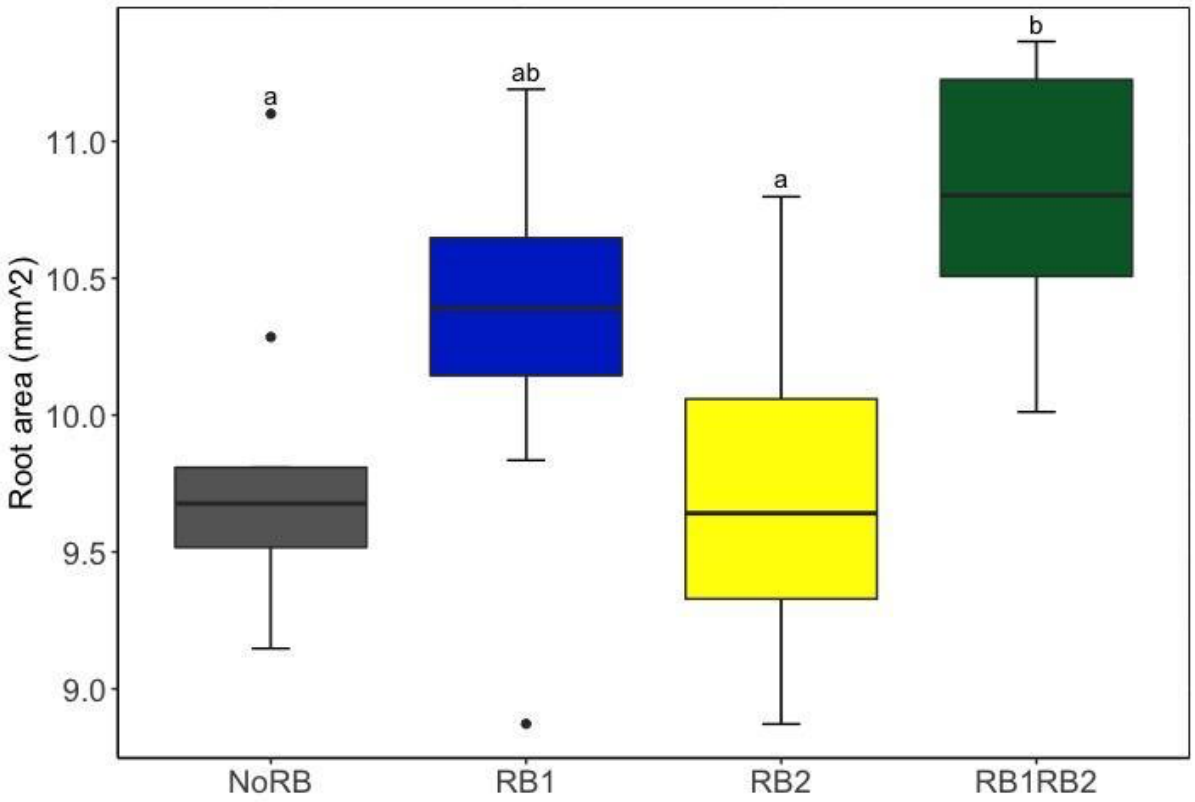

Figure 4.4. Effect of dwarfing on initial root surface area in rootstocks collected from stoolbeds. Centerlines show the medians; whiskers mark the maximum and minimum values, respectively. Upper and lower box boundaries represent the 25th and 75th percentiles, respectively. Different lower-case letters are significantly different ($p<0.05$). Mean values and statistics are detailed in Supplementary Tables S8 and S9.

4.3.2. Effect of RB QTL on canopy traits during the first growing season

4.3.2.1. Tree height

It is widely known that rootstock-induced dwarfing affects tree height among other characteristics, though the exact molecular mechanism is unknown. Tree height together with other canopy traits were measured in this experiment to understand the effect of dwarfing on multiple canopy and root traits and their relationships over time. The effect of the RB QTL on tree height during the first growing season (four time points TPs) was analysed using a linear mixed model fitted by REML. Time point and *Rb1* were the significant fixed variables in the model (p-value < 2.2e-16 and p-value = 0.002051, respectively). Trees with *Rb1* had significantly smaller heights regardless

of the presence of *Rb2*. No effect of block and the interactions of *Rb1*, *Rb2* and TP was observed although the *Rb1* x TP interaction was close to being significant (p-value = 0.06) (Table 4.2).

Emmeans was used to get the model estimated (marginal) means and contrast p-values for the canopy traits. The contrasts were performed using the combined RB QTL information within each time point (TP) and significant differences between dwarfing groups in tree height were detected in TP2, TP3 and TP4. In TP2 and TP3, significant differences were only detected between the groups with no RB QTL and the *Rb1Rb2* group (p-value = 0.0367 and p-value = 0.0157, respectively). In TP4, the differences between NoRb and *Rb1Rb2* groups increased (p-value = 0.001) and the NoRb and *Rb1* group contrast became significantly different (p-value = 0.0156). Moreover, the comparison between *Rb1Rb2* and *Rb2* groups was close to being significant (p-value = 0.051; Figure 4.5; Supplementary Table S11). The differences observed between time points were expected since the trees grew over time.

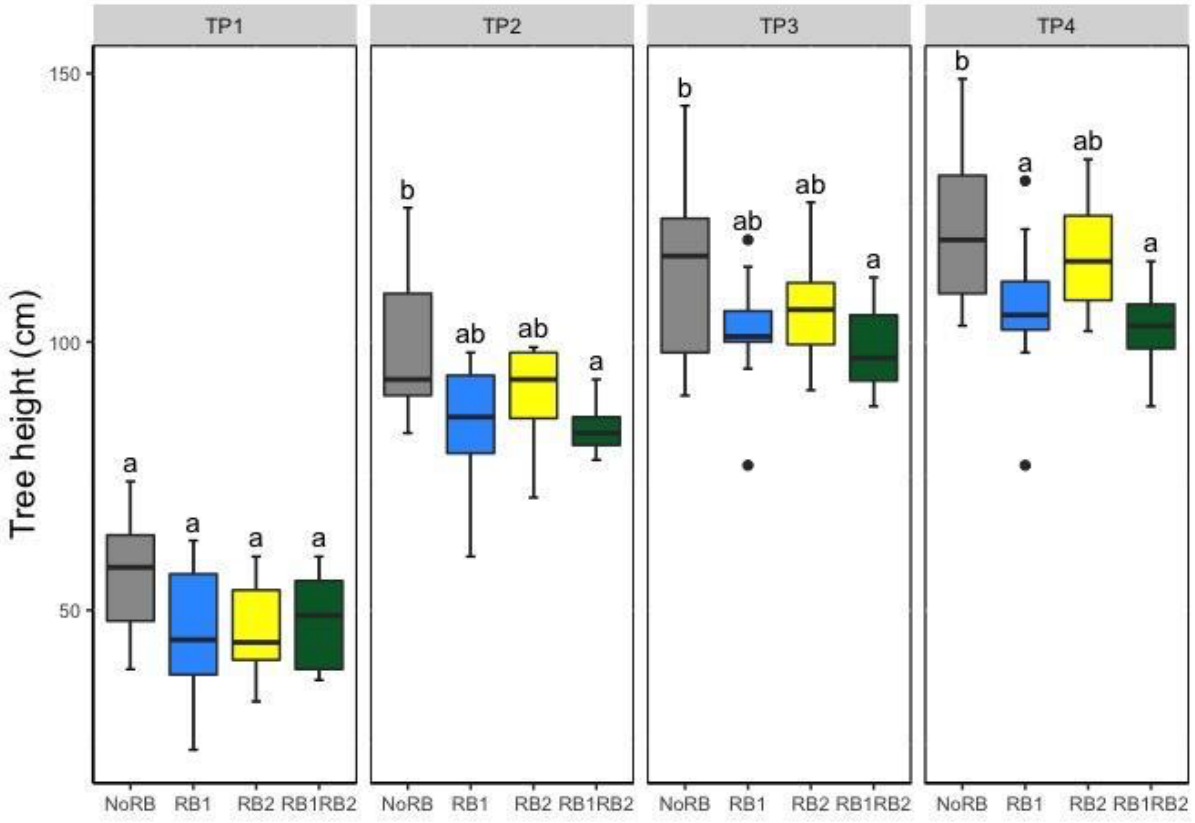

Figure 4.5. Tree height of apple trees with different combinations of root bark QTL per time point. Centerlines show the medians; whiskers mark the maximum and minimum values, respectively. Upper and lower box boundaries represent the 25th and 75th percentiles, respectively. Different lower-case letters are significantly different ($p<0.05$). Mean values and statistics are detailed in Supplementary Tables S10 and S11.

4.3.2.2. Trunk diameter above the graft union

Trunk cross-sectional area (TCSA) is the most common trait associated with rootstock-induced dwarfing. Trees with a high level of dwarfism have a lower TCSA than vigorous trees. In this experiment, the trunk diameter was measured as part of the canopy phenotyping in order to validate this information. *Rb1*, time point, block and the interaction between *Rb1* and time point were significant and, therefore, affected trunk diameter measured 10 cm above the graft union. As previously explained, time point had an effect on trunk diameter since the trees are growing over time (p-value < 2.2e-16; Table 4.2).

Regarding the block effect (p-value = 0.0052), the trunk diameter in block D was slightly smaller than the rest and significant differences were detected when blocks C and D were compared (p-value = 0.0028; Table 4.2 and Supplementary Tables S12 and S13). Trees placed in block D had high sunlight exposure due to the position in which they were located in the glasshouse compartment, which may be why these trees grew slightly less.

The *Rb1* QTL also had a significant effect on trunk diameter (p-value =2.736e-05). However, *Rb2* did not affect trunk diameter above the graft union (p-value = 0.255; Table 4.2). Looking at the different time points, in TP1, significant differences were only detected when comparing the NoRb group with the *Rb1* (p-value = 0.0403). In TP2, the comparison between NoRb and *Rb1* remained significant (p-value = 0.0051) and also significant differences were detected between the NoRb and *Rb1Rb2* groups. (p-value = 0.0121). In TP3, differences were identified between the NoRb against *Rb1* and *Rb1Rb2* groups (p-value = 0.0028 and p-value = 0.0006, respectively) and when comparing *Rb2* with *Rb1* and *Rb1Rb2* groups (p-value = 0.0443 and p-value = 0.0155, respectively). In TP4, the same comparisons as in TP3 were significant but with stronger p-values (Figure 4.6; Supplementary Table S15). The interaction term *Rb1* x TP was also significant (p-value = 0.0003) indicating that the change in trunk diameter was different over time (Table 4.2). In TP1 and TP2, the group with the smallest trunk diameter was *Rb1*, however, from TP3 onward, trees with both QTL had the thinnest trunks. The trunk diameter in the *Rb1Rb2* group increased more slowly than in the other groups. Trees with none of the RB QTL had the largest trunk diameter across all the time points (Figure 4.6; Supplementary Table S15).

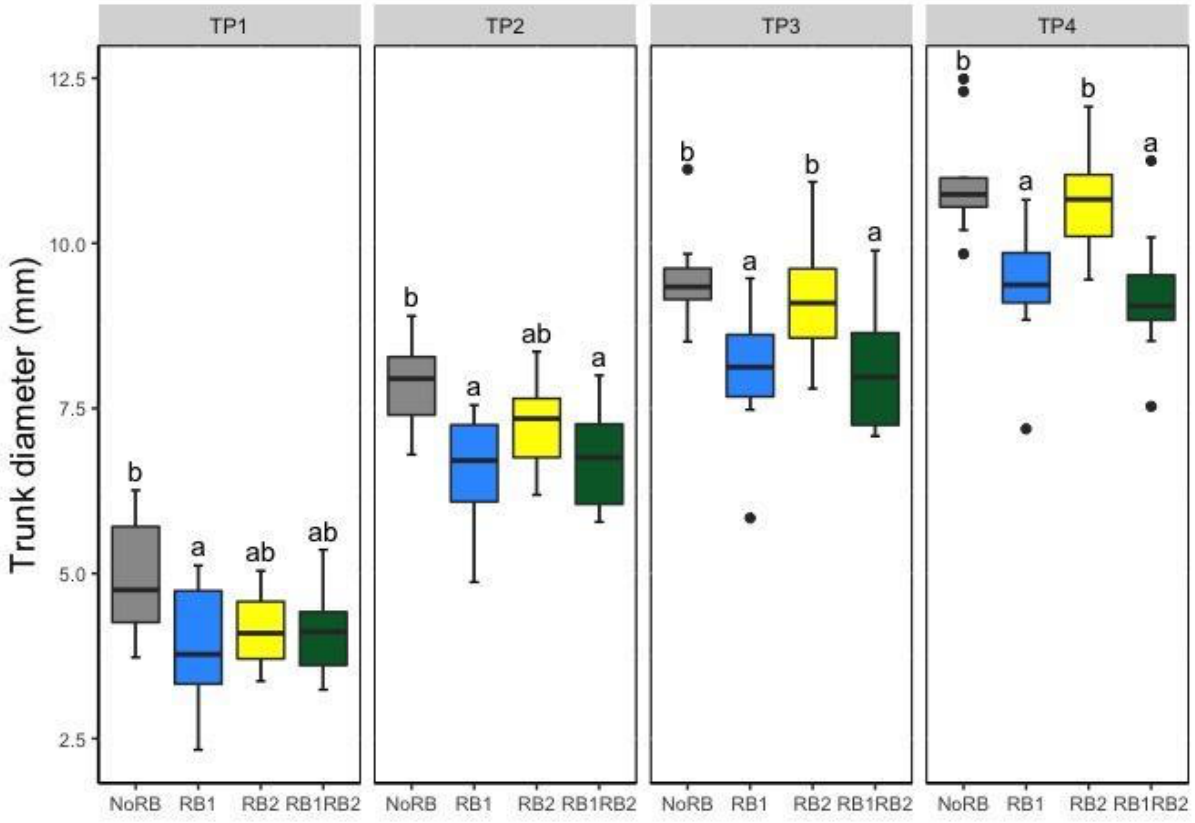

Figure 4.6. Trunk diameter above the graft union of apple trees with different combinations of root bark QTL per time point. Centerlines show the medians; whiskers mark the maximum and minimum values, respectively. Upper and lower box boundaries represent the 25th and 75th percentiles, respectively. Different lower-case letters are significantly different ($p<0.05$). Mean values and statistics are detailed in Supplementary Tables S14 and S15.

4.3.2.3. Trunk diameter below the graft union

In this model, the time point was the only variable affecting the trunk diameter below the graft union (p-value < 2.2e-16; Table 4.2). Interestingly, *Rb1* and *Rb1Rb2* groups had similar means at TP1 and TP2 but in TP3 and TP4 the group with only *Rb1* QTL had the smallest trunk diameter. Moreover, the group with the thickest trunk was *Rb2* in all time points except in TP2 (Supplementary Table S16). Nevertheless, no significant differences were detected when the comparisons between the dwarfing groups were performed (Figure 4.7).

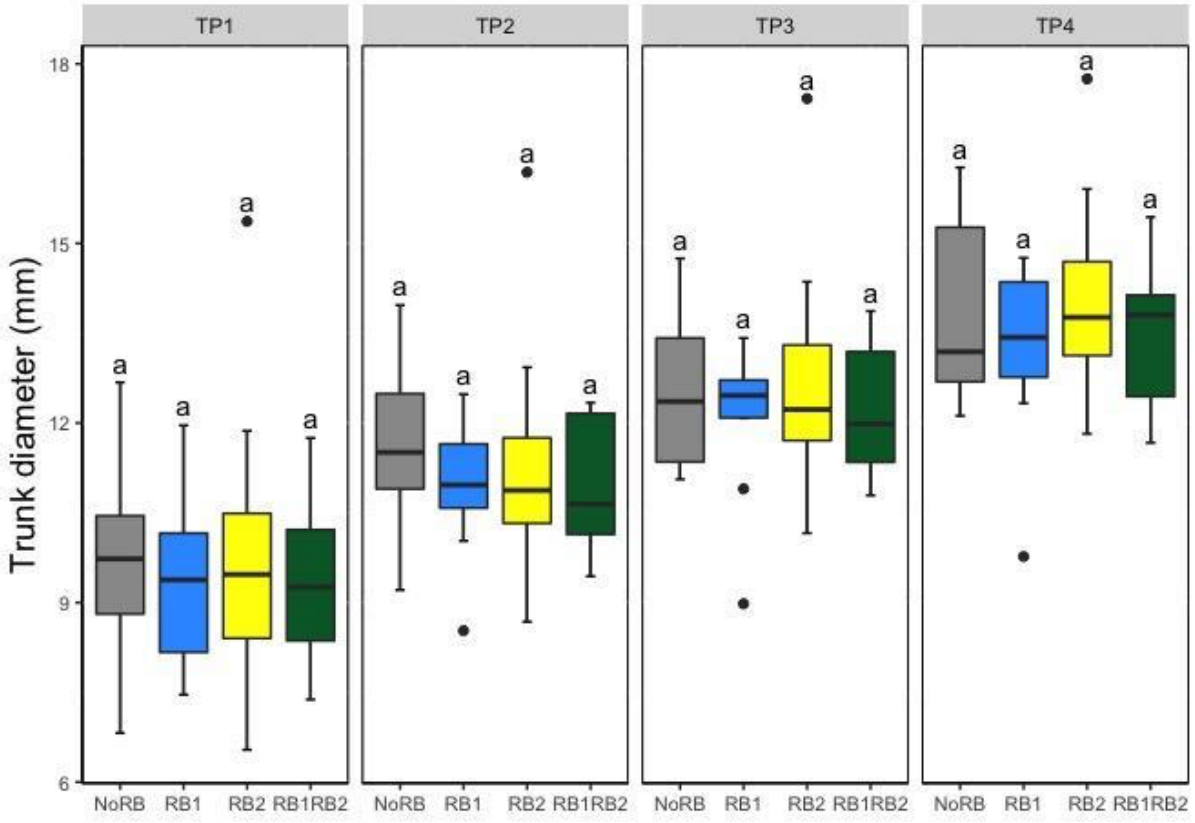

Figure 4.7. Trunk diameter below the graft union of rootstocks with different combinations of root bark QTL per time point. Centerlines show the medians; whiskers mark the maximum and minimum values, respectively. Upper and lower box boundaries represent the 25th and 75th percentiles, respectively. Different lower-case letters are significantly different ($p<0.05$). Mean values and statistics are detailed in Supplementary Tables S16 and S17.

Table 4.2. Summary table of the means and ANOVA of tree height, trunk diameter above graft union and tree diameter below graft union per fixed variable including *Rb1*, *Rb2*, time point, block and interactions.

Fixed variables	Levels	Means		
		Tree Height	Trunk diameter above graft union	Trunk diameter below graft union
Rb1	**No**	93.9	8.04	12.0
	Yes	84.2	7.03	11.5
Rb2	**No**	91.4	7.65	11.7
	Yes	86.7	7.42	11.8
TP	**TP1**	49.3	4.29	9.57
	TP2	89.2	7.11	11.21
	TP3	105.5	8.69	12.42
	TP4	112.1	10.05	13.69
Block	**A**	90.1	7.55	12.0
	B	89.4	7.63	11.7
	C	93.5	8.05	11.9
	D	83.1	6.92	11.4
ANOVA				
F_{Rb1}		11.262 (**0.0020**)	23.911 (**2.736e-05**)	1.152 (0.291)
F_{Rb2}		2.572 (0.118)	1.338 (0.255)	0.076 (0.784)

F_{TP}	452.45 (**<2.2e-16**)	946.29 (**<2.2e-16**)	384.9 (**<2e-16**)
F_{B}	2.2499 (0.1015)	5.1164 (**0.0052**)	0.2966 (0.827)
$F_{Rb1xRb2}$	1.282 (0.265)	1.356 (0.252)	0.296 (0.827)
F_{Rb1xTP}	2.539 (0.0605)	6.728 (**0.0003**)	0.194 (0.899)
F_{Rb2xTP}	0.068 (0.976)	0.093 (0.963)	0.761 (0.518)
$F_{Rb1xRb2xTP}$	0.812 (0.489)	1.546 (0.206)	0.258 (0.855)

F_{Rb1}:Rb1 QTL effect; F_{Rb2}:Rb2 QTL effect; F_{TP}:time point effect; F_{B}:block effect; $F_{Rb1xRb2}$:Rb1 x Rb2 QTL interaction effect; F_{Rb1xTP}:Rb1 QTL x time point interaction effect; F_{Rb2xTP}:Rb2 QTL x time point interaction effect; $F_{Rb1xRb2xTP}$:Rb1 x Rb2 x TP interaction effect. P-values in brackets and significant p-values in bold.

4.3.3. Effect of root bark QTL on root traits

Rootstock breeding has focused extensively on how dwarfing affects the scion, but there is limited knowledge of how it affects root systems. To gain a better understanding of the impact of this complex trait on apple trees, this study assessed how rootstock-induced dwarfing affects critical root system traits. The effect of *Rb1* and *Rb2* on the root traits was analysed using REML analysis.

4.3.3.1. Effect of RB QTL on total root length (TRL)

For the analysis of TRL, time point was the only significant variable in the model (p-value = <2e-16). This is not surprising since the TRL increases over time (Table 4.3).

Emmeans was used to get the model estimated (marginal) means and contrast p-values within each time point. No significant differences between the groups were identified. The mean of the *Rb1Rb2* group was consistently lower than the mean of the other groups from TP2. Additionally, the differences between groups become more evident over time. In TP4, the comparison between NoRb and *Rb1Rb2* groups was close to being significant (p-value=0.06). This suggests that if the experiment had been conducted for a longer duration, there might have been noticeable variations among the dwarfing categories in terms of TRL (Figure 4.8 and Supplementary Tables S18 and S19).

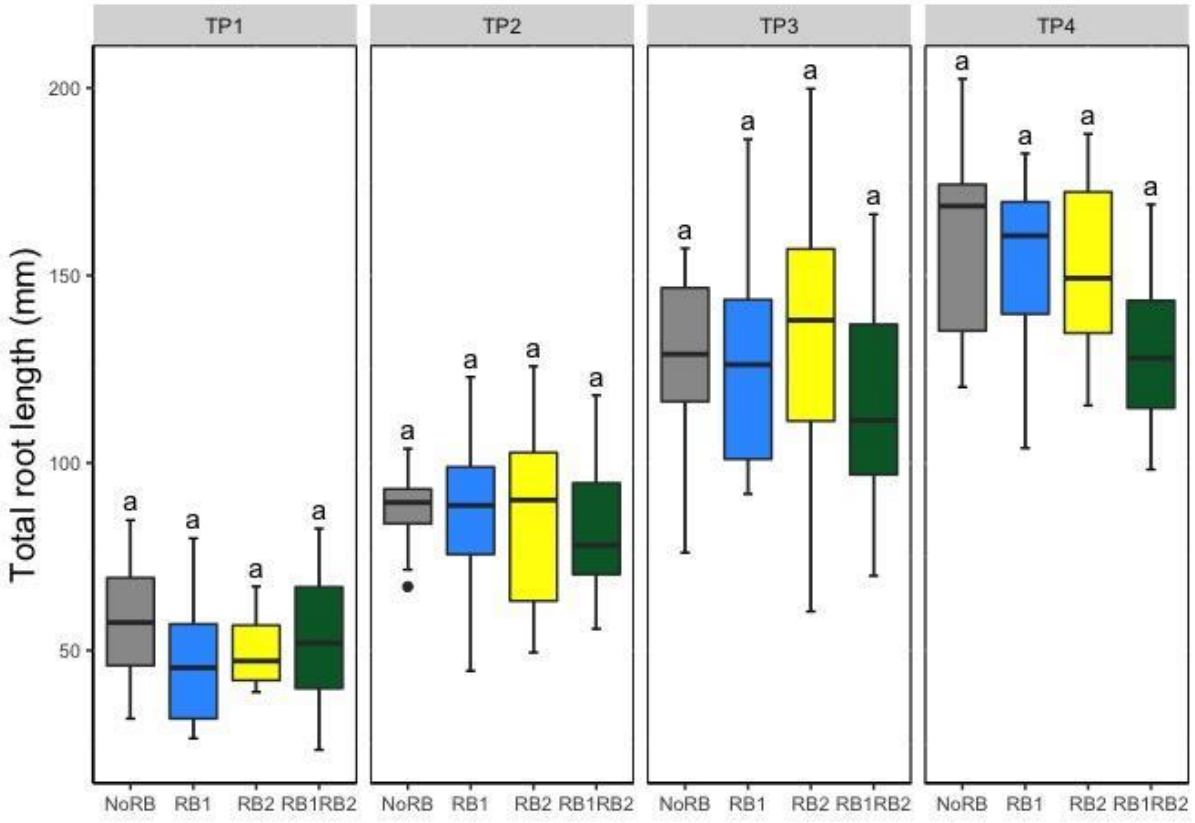

Figure 4.8. Total root length (square transformed) of grafted rootstocks with different combinations of root bark QTL per time point. Centerlines show the medians; whiskers mark the maximum and minimum values, respectively. Upper and lower box boundaries represent the 25th and 75th percentiles, respectively. Different lower-case letters are significantly different ($p<0.05$). Mean values and statistics are detailed in Supplementary Tables S18 and S19.

4.3.3.2. Effect of RB QTL on maximum root diameter

In the case of maximum root diameter, time point was the only significant variable in the model (p-value = 3.67e-13). The maximum root diameter mean for TP1 was 3.08±0.99 mm, while TP4 had the highest mean at 4.57±0.83 mm, indicating that there was an increase in maximum root diameter over time (Table 4.3). In general, the increment in maximum root diameter took place progressively but with a peak of greater thickening between TP1 and TP2 where the differences were significant (p-value = 0.0005; Supplementary Table S20). However, the increase in maximum root diameter occurred differently depending on the RB category, suggesting that the

thickening of the roots may differ among root bark categories. The NoRb QTL rootstocks had a smaller increase in maximum root diameter between TP1 and TP2 compared with the rest of the groups. However, between TP3 and TP4, the maximum root diameter had a sharp increase. The group with *Rb2* alone experienced a significant rise in the maximum diameter of the root between the initial and second time points. Following that, there was a minor increase in the maximum root size between TP2 and TP3. Subsequently, between the third and last time points, there was yet another substantial increase in the maximum root diameter. Rootstocks with only *Rb1* and both QTL exhibited the most significant increase in maximum root diameter between TP1 and TP2. Afterwards, between the second and third time points, there was a slight additional increase in the maximum root diameter for these groups. However, between TP3 and TP4, the *Rb1* group demonstrated a continued increase in maximum root diameter, while the *Rb1Rb2* group experienced a decrease in maximum root diameter (Figure 4.9; Supplementary Table S20).

Although neither *Rb1* nor *Rb2* nor the interactions were significant, the comparisons of RB QTL groups within each time point were still conducted to investigate if differences between root bark categories were detected at any time point. In TP1, significant differences were observed between the NoRb and the *Rb1* groups (p-value = 0.049), with the *Rb1* category showing the lowest maximum root diameter. By the end of the experiment, at TP4, the *Rb1Rb2* group had the lowest mean but was not significantly different from the rest of the groups (Supplementary Table S22; Figure 4.9).

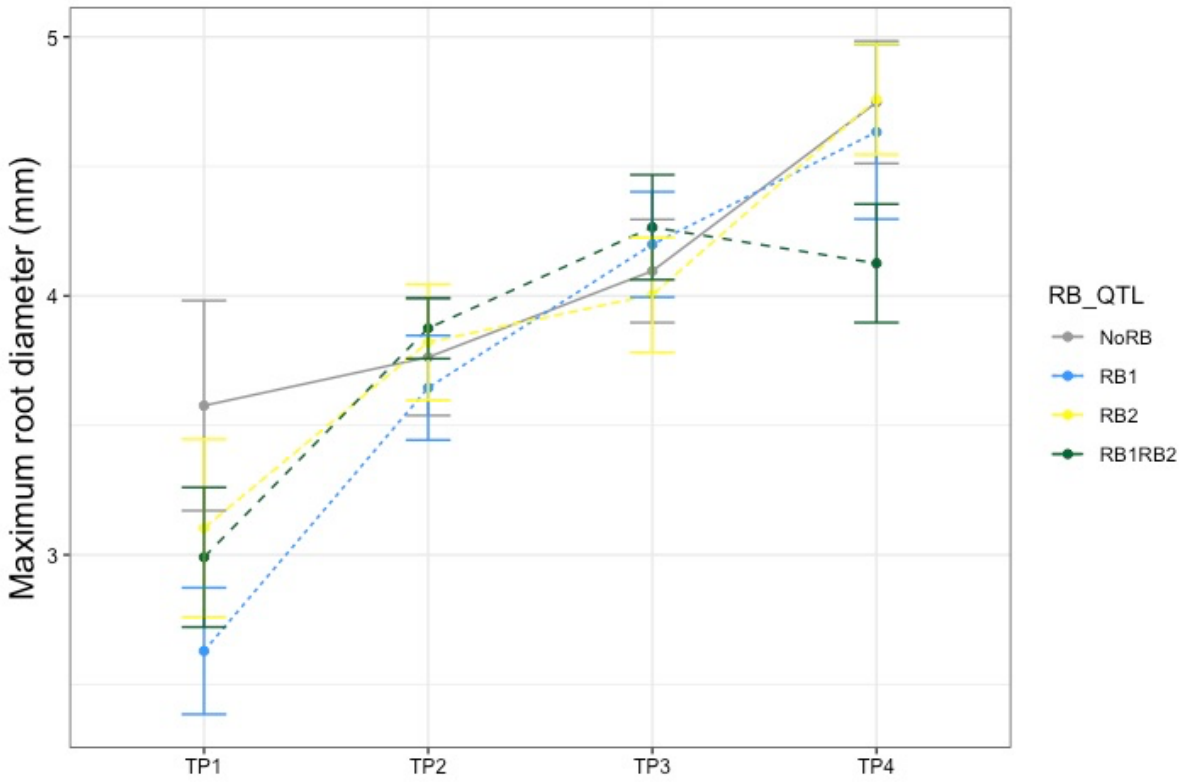

Figure 4.9. Maximum root diameter of grafted rootstocks with different combinations of root bark QTL per time point. Dots represent mean values; Vertical bars indicate the standard errors. Mean values and statistics are detailed in Supplementary Tables S21 and S22).

3.3.3.3. Effect of RB QTL on mean root diameter

As with the maximum root diameter, time point was the sole factor that affected the mean diameter of roots (p-value = 0.012; Table 4.3). When the comparisons between time periods were performed, only the comparison between TP1 and TP2 was found to be statistically significant (p-value = 0.02; Supplementary Table S23). The mean root diameter fluctuated with time and these variations are different depending on the RB categories. Rootstocks lacking any of the RB QTL exhibit a modest increase in mean root diameter between TP1 and TP2. However, in TP3, the mean root diameter decreased, only to experience a significant increase in TP4. Rootstocks containing only *Rb2* that initially had a very small mean root diameter in TP1, underwent a remarkable increase in mean root size in TP2, followed by an important decrease in TP3, and ultimately experienced another substantial increase in mean diameter in

TP4. Rootstocks with either *Rb1* or both QTL, *Rb1Rb2*, showed a dramatic increase in mean root diameter between TP1 and TP2. Subsequently, between the second and third time point, there was a modest decrease in the mean root diameter. Interestingly, there were no variations in mean root diameter between TP3 and TP4 (Supplementary Tables S23 and S24; Figure 4.10).

No significant differences were found when comparing RB QTL groups within each time point (Figure 4.10; Supplementary Table S25). However, it is important to highlight that the *Rb1* and *Rb1Rb2* groups had a smaller mean root size than the rest by the end of the experiment (Supplementary Table S24).

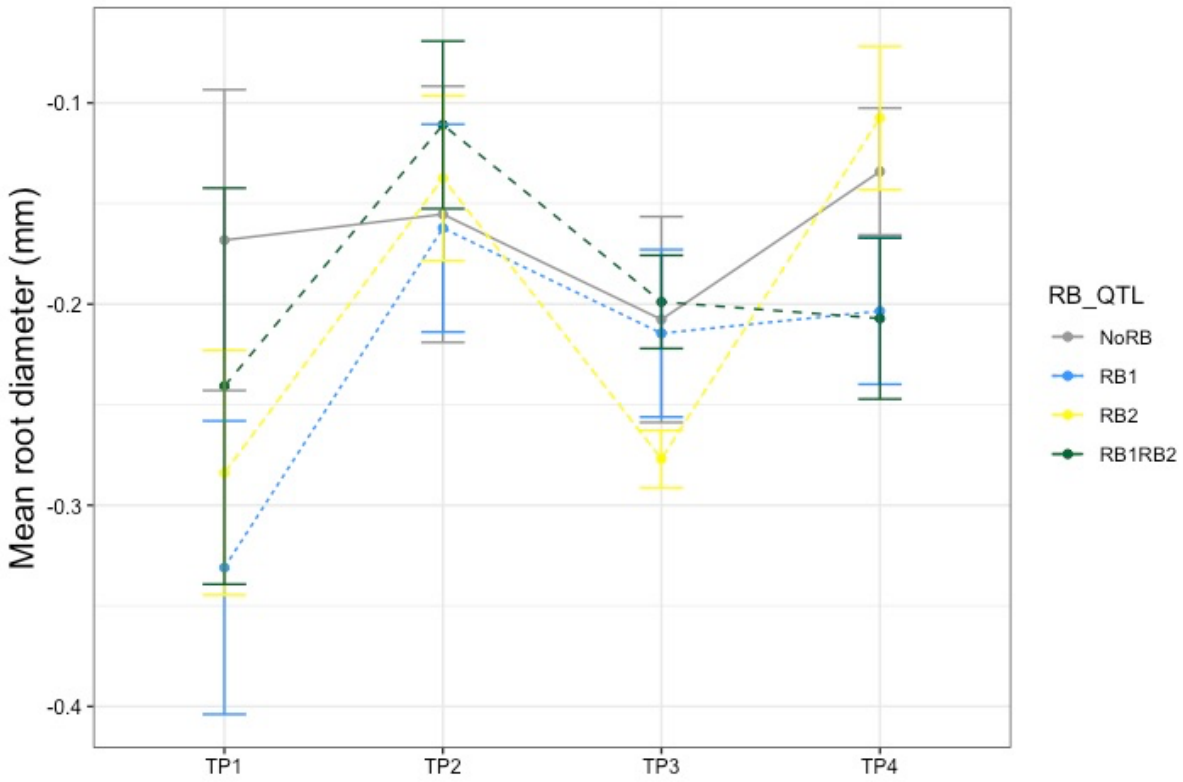

Figure 4.10. Mean root diameter (logarithmically transformed) of grafted rootstocks with different combinations of root bark QTL per time point. Dots represent mean values; Vertical bars indicate the standard errors. Mean values and statistics are detailed in Supplementary Tables S24 and S25).

4.3.3.4. Effect of RB QTL on the total root system depth

The analysis of maximum root system depth area in the apple rootstocks showed that time point, block, and the interaction between *Rb1* x TP were all statistically significant (p-value < 2.2e-16, 4.329e-05 and 0.004, respectively) and therefore, had an effect on root depth (Table 4.3). *Rb1* and the interaction between *Rb1* x *Rb2* x TP are close to being significant (p-value = 0.07 and p-value = 0.06, respectively). Similar to the trunk diameter above the graft union, trees in block D had reduced growth compared to the other blocks. Significant differences were observed when comparing block D with blocks A, B and C (p-values = 0.01, 0.0001 and 0.0002 respectively; Supplementary Table S26).

Despite the fact that *Rb1* and *Rb2* were not significant in the model, comparisons between dwarfing classes were performed within each time point and significant differences between dwarfing groups appeared in TP3. Differences between NoRb and *Rb1Rb2* groups were observed (p-value = 0.0028) and also when comparing *Rb2* and *Rb1Rb2* (p-value = 0.0053; Supplementary Table S28). In TP4, the same comparisons were still significant (p-value = 0.047 and p-value = 0.031) although the p-values were smaller. Moreover, the comparison between *Rb1* and *Rb1Rb2* groups also resulted in significance at the last time point (p-value = 0.016; Figure 4.11).

Interestingly, trees with both RB QTL had the deepest root systems in TP1 with roots reaching an average depth of 332±121 mm and the group of trees with only *Rb2* had the shallowest root systems with an average depth of 307±105 mm. However, this completely changed at TP2 where the *Rb1Rb2* group had the shallowest root system with 570±167 mm mean depth and the *Rb2* group root systems reached a mean depth of 647±183 mm. The *Rb1Rb2* group stayed as the group with the shallowest root systems during the rest of the experiment. Nevertheless, the deepest root systems in TP3 were found in rootstocks with no RB QTL and in TP4 in trees with only *Rb1* but very similar in depth to NoRb and *Rb2* groups (Supplementary Table S27).

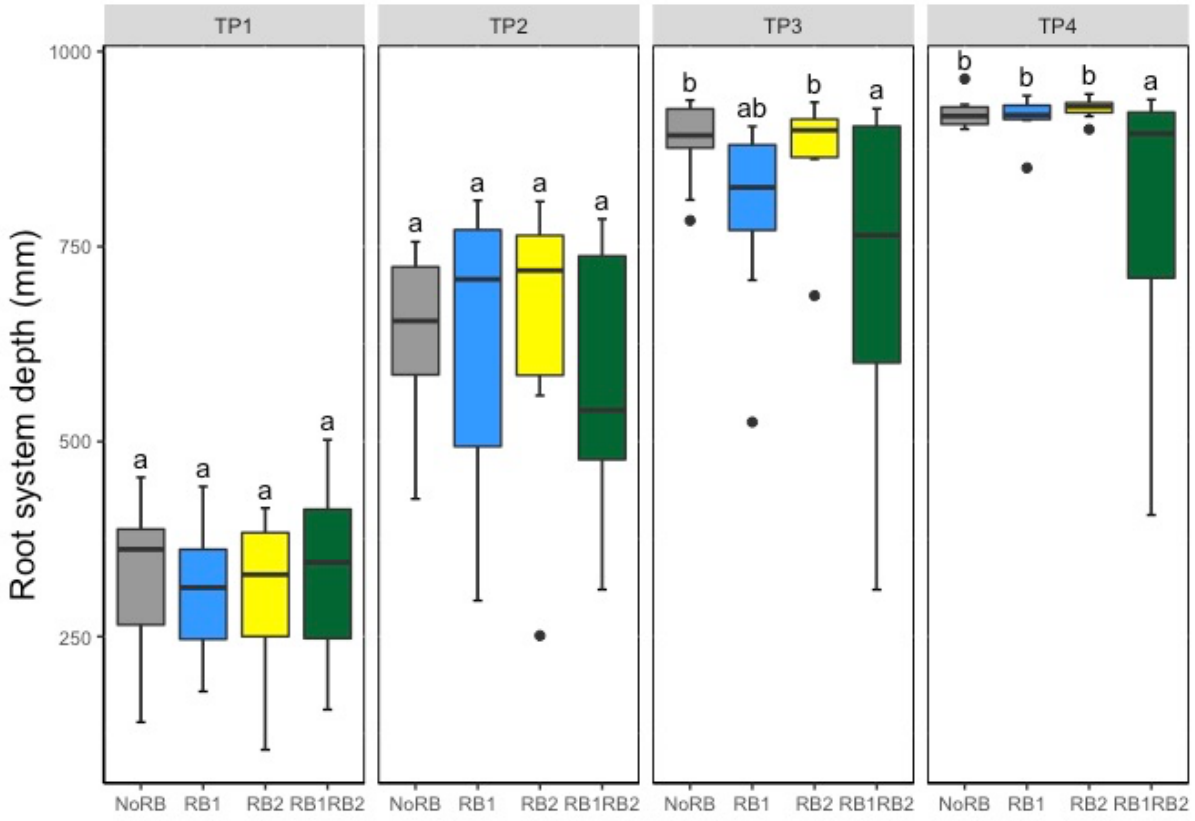

Figure 4.11. Maximum root system depth of grafted rootstocks with different combinations of root bark QTL per time point. Centerlines show the medians; whiskers mark the maximum and minimum values, respectively. Upper and lower box boundaries represent the 25th and 75th percentiles, respectively. Different lower-case letters are significantly different ($p<0.05$). Mean values and statistics are detailed in Supplementary Tables S27 and S28.

4.3.3.5. Effect of RB QTL on convex hull area (chull area)

The effect of the RB QTL on the convex hull area during the first growing season was analysed using REML analysis. Block, time point and the interactions *Rb1* x TP and *Rb1* x *Rb2* x TP were significant in the model (p-value = 6.67e-05, < 2.2e-16, 0.002 and 0.025, respectively; Table 4.3). Regarding the effect of block on the convex hull area, once again, block D had a reduced growth compared to A (p-value = 0.016), B (p-value = 0.0003) and C (p-value = 0.0001; Supplementary Table S29).

Emmean was used to compare the dwarfing classes within each time point. Significant differences in convex hull area between dwarfing categories were observed in TP3, revealing that dwarfing had an impact on the convex hull area in apple rootstocks from the second half of the first growing season. In TP3, significant differences were found when comparing NoRb and *Rb1Rb2* groups (p-value = 0.0051) and between *Rb2* and *Rb1Rb2* groups (p-value = 0.037). The same comparisons resulted in significant differences in TP4 (p-value = 0.012 and p-value = 0.014, respectively) and, in the comparison between *Rb1* and *Rb1Rb2* groups (p-values = 0.0088; Figure 4.12; Supplementary Table S31). Similar to root depth, in TP1 the group with both QTL showed the largest root systems whereas in TP2 exhibited the smallest root area, remaining the smallest for the rest of the experiment (Supplementary Table S30).

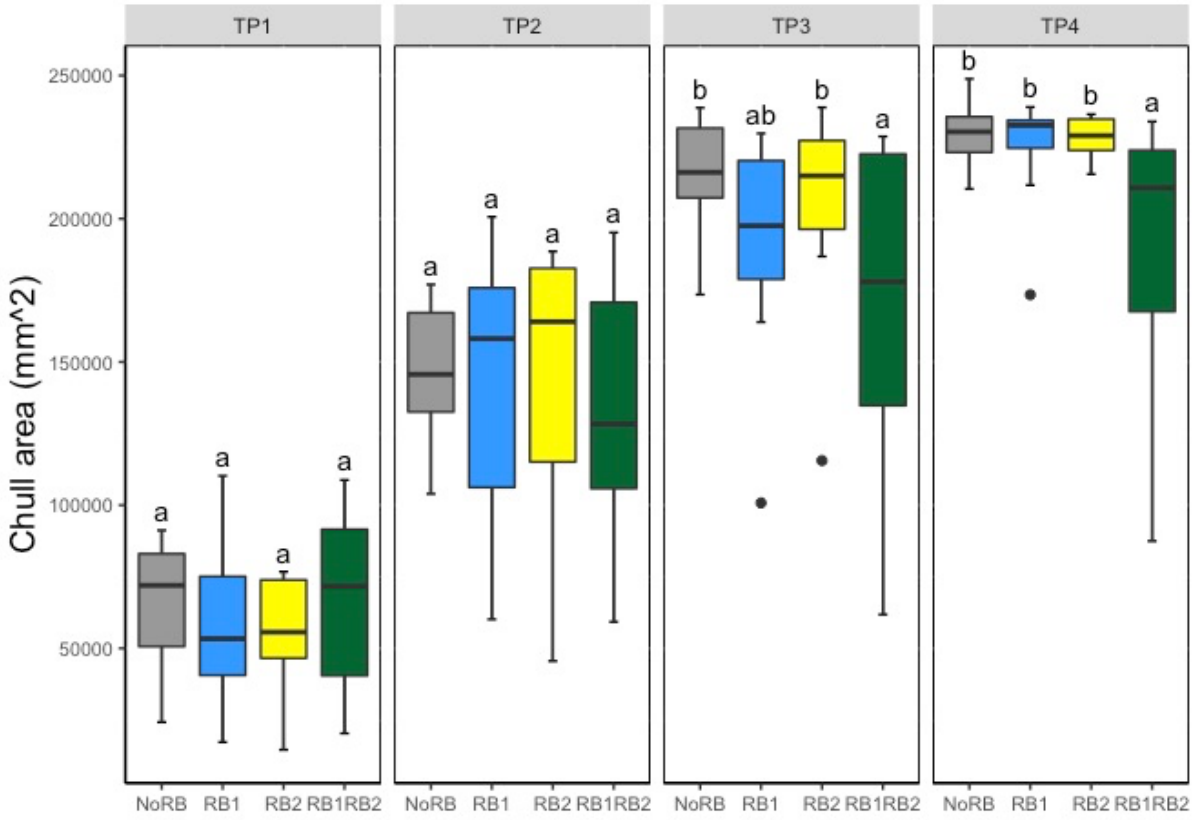

Figure 4.12. Total convex hull area of grafted rootstocks with different combinations of root bark QTL per time point. Centerlines show the medians; whiskers mark the maximum and minimum values, respectively. Upper and lower box boundaries represent the 25th and 75th percentiles, respectively. Different lower-case letters are significantly different ($p<0.05$). Mean values and statistics are detailed in Supplementary Tables S30 and S31.

Table 4.3. Summary table of the means and ANOVA of total root length, maximum root diameter, mean root diameter, root system depth and total convex hull area per fixed variable including Rb1, Rb2, time point, block and their interactions.

		Means				
Fixed variables	**Levels**	**Total root length**	**Maximum root diameter**	**Mean root diameter**	**Root system depth**	**Total convex hull area**
Rb1	**No**	106	3.98	-0.186	688	159649
	Yes	100	3.80	-0.206	638	147580
Rb2	**No**	106	3.92	-0.196	682	159700
	Yes	100	3.87	-0.195	644	147530
TP	**TP1**	51.9	3.08	-0.256	323	61789
	TP2	85.3	3.78	-0.141	622	141328
	TP3	126.3	4.14	-0.224	816	193613
	TP4	149.1	4.57	-0.163	890	217730
Block	**A**	102.4	3.93	-0.200	658	152953
	B	108.9	3.94	-0.161	728	169157
	C	109.7	4.04	-0.175	727	173761
	D	91.6	3.66	-0.246	539	118589
ANOVA						
F_{Rb1}		0.8394 (0.36)	1.687 (0.20)	0.528 (0.46)	3.44 (*0.07*)	2.34 (0.13)

F_{Rb2}	0.741 (0.39)	0.136 (0.71)	0.0008 (0.97)	1.98 (0.16)	2.39 (0.13)
F_{TP}	261.467 (**<2e-16**)	27.382 (**3.67e-13**)	3.727 (**0.012**)	424.72 (**< 2.2e-16**)	470.28 (**< 2.2e-16**)
F_{B}	1.827 (0.16)	1.433 (0.25)	1.894 (0.13)	10.89 (**4.32e-05**)	10.309 (**6.67e-05**)
$F_{Rb1xRb2}$	0.329 (0.57)	0.256 (0.61)	1.349 (0.24)	1.98 (0.16)	1.03 (0.31)
F_{Rb1xTP}	0.986 (0.40)	1.786 (0.15)	1.061 (0.36)	4.66 (**0.004**)	5.22 (**0.002**)
F_{Rb2xTP}	1.337 (0.26)	0.446 (0.72)	0.242 (0.86)	1.08 (0.35)	1.76 (0.15)
$F_{Rb1xRb2xTP}$	1.685 (0.17)	1.308 (0.27)	0.826 (0.48)	2.43 (0.06)	3.23 (**0.025**)

F_{RB1}:Rb1 QTL effect; F_{RB2}:Rb2 QTL effect; F_{TP}:time point effect; F_{B}:block effect; $F_{Rb1xRb2}$:Rb1 x Rb2 QTL interaction effect; F_{Rb1xTP}:Rb1 QTL x time point interaction effect; F_{Rb2xTP}:Rb2 QTL x time point interaction effect; $F_{Rb1xRb2xTP}$:Rb1 x Rb2 x TP interaction effect. P-values in brackets and significant p-values in bold.

4.3.4. Principal component analysis

Principal component analysis for the TRL, maximum root diameter, mean root diameter, root system depth and total convex hull area was performed at every time point to reduce the high dimensional data set.

The first two principal components captured the majority of the variance in this data set at every time point. Principal components with eigenvalues greater than 1 were presented and considered significant. In the TP1 analysis, nearly 90% of the variance was explained by the first two PCs. In the second time point, PC1 represented 50.55% of the variance and the PC2 accounted for 34.8% of the variance. In total, the first two

PCs explained more than 85% of the variance of the root traits data set. Regarding time point 3, a total of 78% of the variance is explained by PC1 and PC2, with PC1 accounting for 51.6% of the variance. At the end of the experiment, in TP4, the cumulative variance explained by the first two PCs was around 75% (Table 4.4). Although the percentage of variance explained by PC1 and PC2 decreased over time, they still accounted for the majority of the variance at the end of the experiment. In general, total root length, convex hull area and root depth contributed the most to PC1 except in TP1 where all the traits had a similar contribution. However, maximum and mean root diameters had the highest contribution to PC2.

In general, the biplots show that root system depth and total convex hull area were strongly correlated at every time point, especially at the end of the experiment. TRL is moderately correlated with these two traits. A strong correlation between maximum root diameter and mean root diameter was observed except in time point 3. No correlation was observed between the maximum and mean root diameter and the total root length, root depth, and convex hull area at any time point (Figure 4.13).

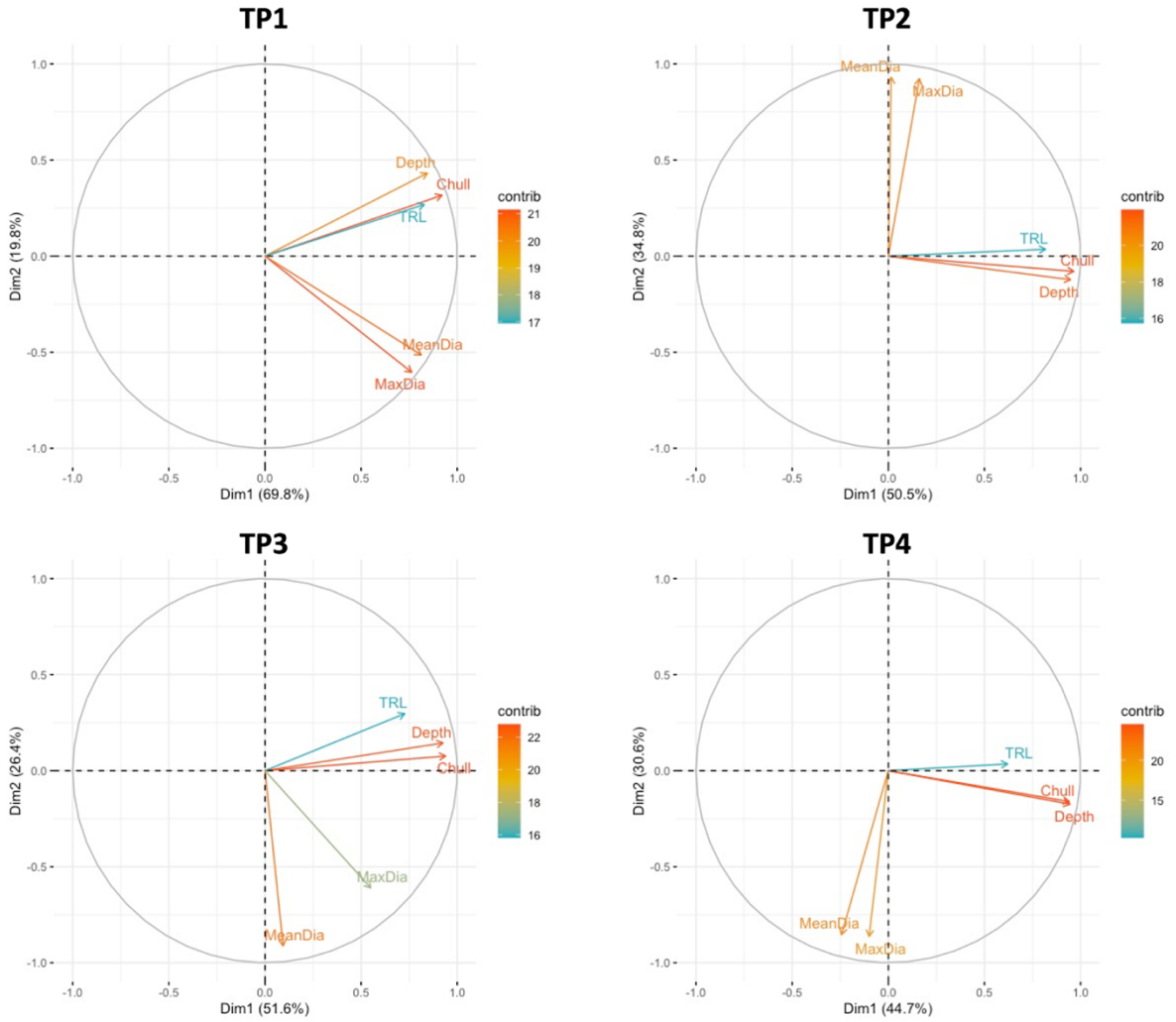

Figure 4.13. Biplots of the principal component analysis (PCA) of 5 root traits from 39 genotypes in rhizoboxes with different combinations of root bark QTL per time point. Traits that group together are correlated to each other whereas traits with arrows on the opposite side are negatively correlated. Variables that are orthogonally located from each other are not correlated. The colour of the arrows represents the contribution to the trait for each PC. Abbreviations stand for: TRL, total root length; MaxDia, maximum root diameter; MeanDia, mean root diameter; Depth, maximum root system depth; Chull, total convex hull area.

Principal components for a total of 39 genotypes were produced for the 5 root traits at every time point. By the end of the first growing season, the green cluster containing genotypes with both RB QTL was clearly separated from the others, indicating that the root systems of trees containing *Rb1* and *Rb2* QTL were phenotypically different from the other trees (Figure 4.14). Linear model analysis of the first two PC's at every time point revealed that *Rb1* had an effect in TP3 in PC1 (p-value < 0.05) and in TP4, in PC1 (p-value < 0.05) and PC2 (p-value < 0.05). However, *Rb2* was only significant in TP4 in PC1 (p-value < 0.05) and the interaction term *Rb1*x*Rb2* was close to being significant in TP4 (p-value < 0.1; Table 4.5). Block was highly significant in PC1 in the first three time points. In summary, this finding confirms the hypothesis that the root architecture of dwarf trees differs from vigorous trees as early as the end of the first season.

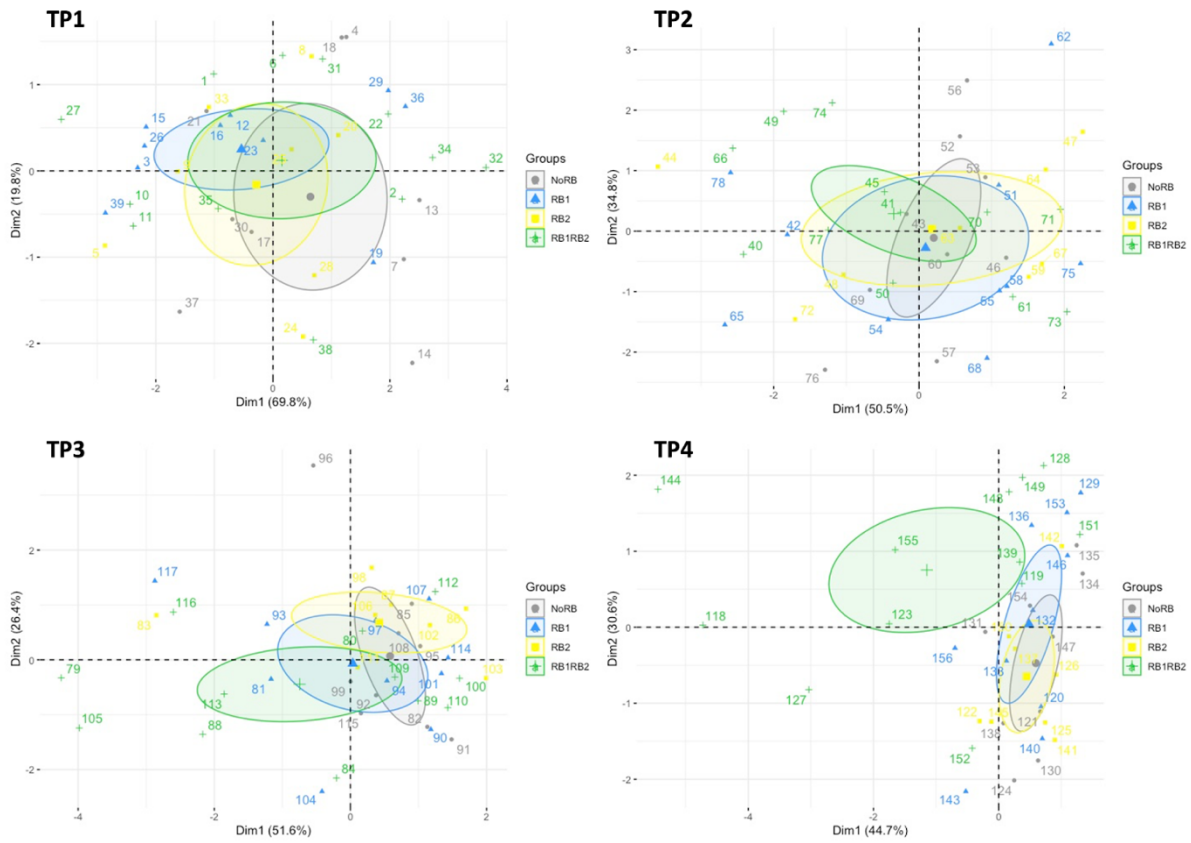

Figure 4.14. Principal component analysis of 5 root traits among 39 apple rootstock genotypes grown in rhizoboxes per time point. The position of each genotype is shown for the principal component PC1 vs. PC2. Genotypes are coloured by root bark QTL classification.

Table 4.4. Eigenvalues, percentage of variance explained by each PC and cumulative variance per time point. For each trait, the largest variable loading score crossing the two components appears in bold.

	TP1		TP2		TP3		TP4	
	PC1	**PC2**	**PC1**	**PC2**	**PC1**	**PC2**	**PC1**	**PC2**
Eigenvalues	3.49	0.99	2.52	1.73	2.58	1.31	2.23	1.53
% Variance	69.83	19.76	50.55	34.79	51.61	26.39	44.66	30.62
% Cumulative	69.83	89.59	50.55	85.34	51.61	78.00	44.66	75.29
TRL	**0.82**	0.26	**0.81**	0.03	**0.72**	0.29	**0.62**	0.03
Max Dia	**0.76**	**-0.60**	0.16	**0.92**	0.55	**-0.61**	-0.09	**-0.86**
Mean Dia	**0.81**	**-0.51**	0.01	**0.93**	0.09	**-0.91**	-0.24	**-0.85**
Depth	**0.84**	0.43	**0.94**	-0.12	**0.92**	0.14	**0.94**	-0.17
Chull	**0.92**	0.31	**0.96**	-0.07	**0.93**	0.07	**0.94**	-0.16

Table 4.5. Summary table of statistics for the first two PC of root traits affected by the *Rb1*, *Rb2*, *Rb1* x *Rb2* interaction and block per time point.

		TP1	TP2	TP3	TP4
		F Value	**F Value**	**F Value**	**F Value**
PC1	***Rb1***	0.55	0.77	**5.18***	**5.22***
	Rb2	0.0009	0.44	1.67	**5.90***
	Rb1xRb2	1.82	0.75	1.17	**3.92 .**
	Block	**7.58*****	**11.17*****	**8.48*****	2.14
PC2	***Rb1***	1.58	0.02	2.91	**7.01***
	Rb2	0.0009	0.76	0.02	0.77
	Rb1xRb2	0.25	0.14	1.80	1.33
	Block	0.83	0.81	0.61	0.97

*. , * , ** and *** significant at p≤ 0.1, 0.05, 0.01 and 0.001 respectively.*

4.3.5. Root bark percentage, canopy and root wet weight and root-to-shoot wet ratio

In October 2020, at the end of the experiment, destructive phenotyping was performed to obtain separated canopy and root system weights and to collect roots for root bark measurements.

Rb1 and *Rb2* had an obvious effect on root bark percentage (p-value = 0.0002 and p-value = 0.029), demonstrating that the selection of genotypes within each dwarfing category was performed correctly. The block effect was close to being significant (p-value = 0.06). The group with both QTL, *Rb1* and *Rb2*, had the highest mean 68.7±5.44% of root bark and showed significant differences when compared with the other three groups. Interestingly, the group with the smallest root bark percentage was

the *Rb2* group with 55.8±7.05% followed by the NoRb group with 57.7±7.43% of root bark. No differences between the NoRb, *Rb1* and *Rb2* groups were detected when the pairwise comparisons were performed (Figure 4.15. Panel A; Table 4.6; Supplementary Tables S32 and S33).

Rb1 did not affect wet canopy weight (p-value = 0.24) neither did wet root weight (p-value = 0.21). Nevertheless, *Rb2* had an effect on both wet canopy and root weights (p-value = 0.007 and p-value = 0.014, respectively). There was no effect of block on these two traits although it was close to being significant in wet root weight (p-value = 0.25 and p-value = 0.059, respectively). The group with both QTL had the lowest canopy wet weight with a mean of 198±28.2 g and the group with none of the QTL had the highest mean with 258±67.8 g. Surprisingly, the *Rb2* group had the second lowest canopy wet weight mean with 201±41.7 g. Pairwise comparisons were done for RB QTL groups on wet canopy and significant differences were only detected when comparing the *Rb1Rb2* group with the group with none of the root bark QTL (p-value = 0.0297; Table 4.6; Supplementary Tables S34 and S35). Interestingly, the contrast between *Rb2* and NoRb groups was nearly significant (p-value = 0.055; Figure 4.15. Panel B). Regarding the analysis of wet root weight, the group of trees containing both dwarfing QTL exhibited the smallest root systems with 205±65.8 g, whereas the group with no RB QTL had the heaviest root systems with an average of 273±77.4 g. Similar to wet canopy weight, *Rb2* group had the second lowest root wet weight mean with 232±42.7 g. No differences between groups in root wet weight were detected, although the NoRb and *Rb1Rb2* comparison was very close to being significant (p-value = 0.0503; Figure 4.15. Panel C; Table 4.6; Supplementary Tables S36 and S37).

The root-to-shoot ratio was calculated by dividing the root wet weight and the shoot wet weight. Trees with a ratio greater than 1 had more roots than shoots whereas trees with a ratio smaller than 1 had more canopy than roots. None of the variables affected the root-to-shoot ratio and therefore, no significant differences between groups were identified (Figure 4.15. Panel D; Table 4.6; Supplementary Tables S38 and S39).

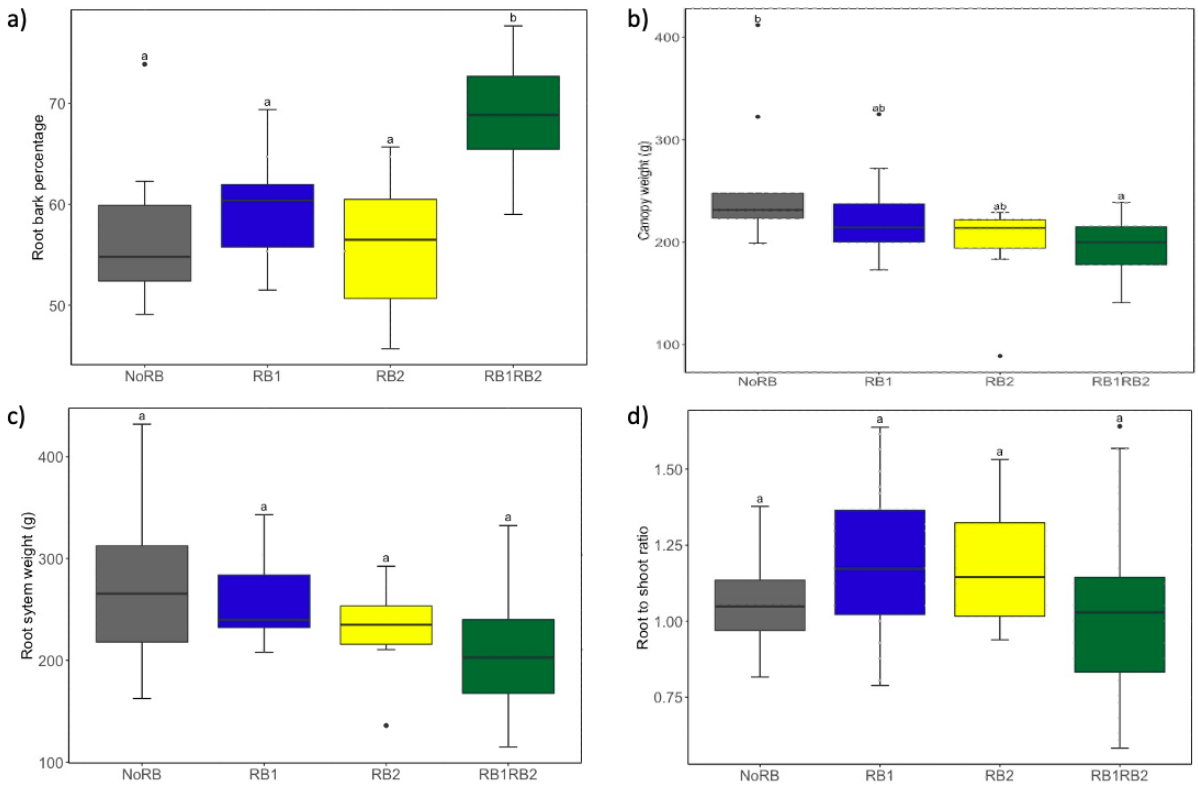

Figure 4.15. Effect of root bark QTL on; A: Root bark percentage, B: Wet canopy weights, C: Wet root weights and D: Root-to-shoot ratios. Centerlines show the medians; whiskers mark the maximum and minimum values, respectively. Upper and lower box boundaries represent the 25th and 75th percentiles, respectively. Different lower-case letters are significantly different ($p<0.05$). Mean values and statistics are detailed in Supplementary Tables S32 to S39.

Table 4.6. Summary table of the means and ANOVA of root bark percentage, wet canopy weight, wet root weight and root-to-shoot ratio per fixed variable including *Rb1, Rb2,* block and *Rb1 x Rb2* interaction.

		Means			
Fixed variables	**Levels**	**Root bark %**	**Wet canopy weight**	**Wet root weight**	**Root-to-shoot ratio**
Rb1	**No**	56.7	230	253	1.12
	Yes	64.0	212	233	1.11
Rb2	**No**	58.5	242	267	1.12
	Yes	62.2	199	219	1.11
Block	**A**	58.0	217	270	1.26
	B	59.4	208	226	1.11
	C	59.1	248	266	1.09
	D	65.0	211	209	1.02
ANOVA					
F_{Rb1}		16.56 (**0.0002**)	1.37 (0.24)	1.59 (0.21)	0.14 (0.71)
F_{Rb2}		5.20 (**0.029**)	8.00 (**0.007**)	6.74 (**0.014**)	0.01 (0.91)
F_B		2.60 (0.06)	1.42 (0.250	2.74 (0.059)	1.58 (0.21)
$F_{Rb1xRb2}$		8.34 (**0.006**)	0.93 (0.34)	0.17 (0.68)	2.75 (0.10)

F_{Rb1}: Rb1 QTL effect; F_{Rb2}: Rb2 QTL effect; F_B: block effect; $F_{Rb1xRb2}$: Rb1 and Rb2 interaction effect. P-values in brackets and significant p-values in bold.

4.3.6. Correlation analysis

Correlation coefficients were calculated for initial root surface area, root bark percentage, canopy and root wet weights and for all the root and canopy traits at the end of the experiment to identify the relationship between traits associated with dwarfing (Figure 4.16). Results showed that among all root traits, convex hull area and depth presented the strongest positive correlation (R=0.71, p-value = 1.2e-06). Mean and maximum root diameter that also displayed a strong direct correlation (R=0.65, p-value = 8.1e-06). Surprisingly, TRL was not strongly correlated with any other root traits but showed a significant negative correlation with IRSA (R=-0.43, p-value = 0.0072) and a direct significant correlation with canopy and roots wet weight (R=0.33, p-value = 0.038 and R=0.52, p-value = 0.0006, respectively). Convex hull area also displayed moderate to strong direct correlations with trunk diameter below the graft union, tree height and canopy wet weights (R=0.58, p-value = 1.6e-04; R=0.54, p-value = 3.7e-04 and R=0.53, p-value = 5.2e-04, respectively). Additionally, convex hull area exhibited a significant inverse correlation with root bark percentage (R=-0.33, p-value = 0.039). Finally, root system depth displayed an intermediate significant positive correlation with trunk diameter above graft union and canopy wet weight (R=0.42, p-value = 0.0091 and R=0.38, p-value = 0.017, respectively; Figure 4.16).

Interestingly, IRSA displayed moderate significant negative correlation with trunk diameter above graft union, tree height and canopy wet weight (R=-0.57, p-value = 1.8e-04; R=-0.41, p-value = 0.0089 and R=-0.35, p-value = 0.03, respectively). Moreover, a significant direct correlation between IRSA and root bark percentage was also observed (R=0.44, p-value = 0.0053). As expected, trunk diameter above the graft union showed a strong direct correlation canopy wet weight and tree height (R=0.67, p-value = 3.2e-06 and R=0.59, p-value = 8.8e-05, respectively), all common traits associated with dwarfing. Moreover, an inverse significant correlation between trunk diameter above graft union and root bark percentage was also observed (R=-0.5, p-value = 0.0013; Figure 4.16).

Lastly, tree height and canopy wet weight displayed a moderate direct correlation (R=0.42, p-value = 0.0086). Canopy wet weight was more strongly correlated with trunk diameter above graft union (R=0.67, p-value = 3.2e-06) than with tree height,

proving that trunk diameter was a better vigour indicator than tree height. Tree height also displayed moderate significant indirect correlation with root bark percentage (R=-0.48, p-value = 0.002; Figure 4.16).

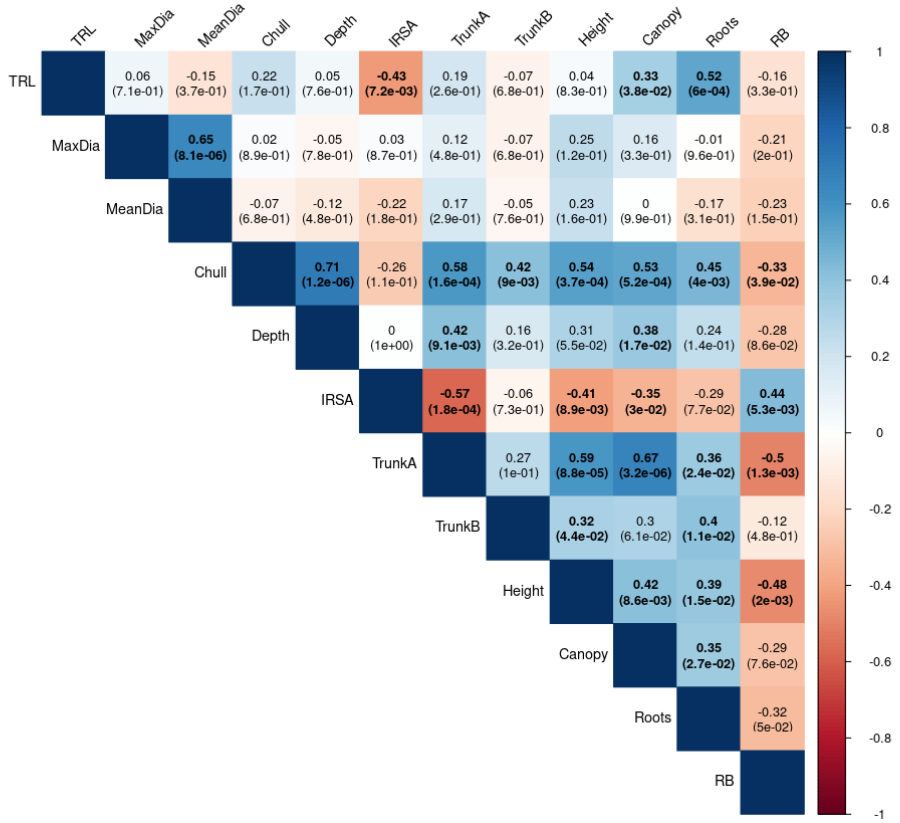

Figure 4.16. Correlation matrix showing Spearman's correlation coefficients of initial root surface area, root bark percentage, canopy and root wet weight and for all the root and canopy traits at the end of the experiment. Significant correlations and p-values in bold. Abbreviations stand for: TRL, total root length; MaxDia, maximum root diameter; MeanDia, mean root diameter; Depth, maximum root system depth; Convex hull, total convex hull area; IRSA, initial root surface area; TrunkA, trunk diameter above graft union; TrunkB, trunk diameter below graft union; Height, tree height; Canopy, canopy wet weight; Roots, root system wet weight and RB, root bark percentage.

4.4 Discussion

4.4.1. Initial root surface area

As previously discussed in Chapter 3, dwarfing had an impact on rooting in the stoolbeds. *Rb1* has a major effect on rooting surface area and is essential to induce rooting in rootstocks. However, *Rb2* alone does not influence rooting in stoolbeds but increases the rooting slightly in the presence of *Rb1*. Interestingly, the *Rb1Rb2* group had the highest amount of roots initially but by the end of the experiment, this group had the lowest total root length (TRL), root depth and convex hull area. The initial amount of roots does not affect the subsequent development of roots in apple rootstocks and it is genetic composition that is a key factor controlling the root architecture.

4.4.2. Canopy traits analysis

Previous research demonstrated that the dwarfing phenotype may take a considerable amount of time to be expressed in some scions and therefore, can only be safely assessed after at least three years of growth (Hatton, 1928). However, in this experiment, using the mapping population of GD x M.9 grafted with Gala, the effect of dwarfing on canopy traits can be seen in the first growing season. In the case of trunk diameter above the graft union, differences in dwarfing groups can be already observed in early June (TP1) and on tree height from mid-July (TP2). Surprisingly, the group with the thinnest trunk in TP1 is the *Rb1* group and is significantly different from the group with none of the QTL, indicating an early dwarfing effect of *Rb1*. By TP2, the group with both RB QTL was also significantly different from the group with no QTL, suggesting that the effect of *Rb2* started to modulate the dwarfing effect on trunk diameter.

The effect of dwarfing on tree height and trunk diameter has been extensively studied (Gjamovski and Kiprijanovski, 2011; Amiri *et al.*, 2014; Tworkoski and Fazio, 2015, 2016; Pilcher *et al.*, 2008; Foster *et al.*, 2015). Two major QTL have been associated with rootstock-induced dwarfing, *Dw1* located on LG5 and *Dw2* located in LG11, both equally controlling tree height and trunk cross-sectional area (Pilcher *et al.*, 2008; Fazio *et al.*, 2014; Foster *et al.*, 2015). As previously discussed in Chapter 2, the root

bark QTL associated with dwarfing, *Rb1* and *Rb2*, co-localise with the regions previously identified as controlling dwarfing, *Dw1* and *Dw2* respectively (Harrison et al., 2016b). Fazio et al., (2014) reported that both *Dw1* and *Dw2* are needed to cause dwarfing and *Dw1* alone did not influence the size of the rootstocks. Nonetheless, Foster et al., (2015) observed that *Dw1* alone influenced the growth, but the combination of *Dw1* and *Dw2* genes has the most important effect on rootstock-induced dwarfing, with *Dw1* having a more pronounced impact than *Dw2*. My research supports the observations of Foster *et al.*, (2015), *Rb1* alone clearly reduced tree height and trunk diameter above the graft union by the end of the experiment and there were significant differences between the *Rb1* group and the group lacking the RB QTL (p-value = 0.0156; p-value = 0.0004; Supplementary Tables S11 and S15). Moreover, despite the increased reduction in tree height and trunk diameter in genotypes with both root bark QTL when compared to those with only *Rb1*, the differences between the two groups were not significant. In conclusion, in this particular experiment *Rb2* may not be indispensable to induce dwarfing on scions in the first year and may act just as an enhancer.

Lastly, the trunk diameter below the graft union was not influenced by the dwarfing QTL *Rb1* and *Rb2*. Interestingly, *Rb1* and *Rb1Rb2* groups had similar means at TP1 and TP2 but in TP3 and TP4 the group with only *Rb1* QTL had the smallest trunk diameter. Moreover, the group with the thickest trunk was *Rb2* in all time points except in TP2 (Supplementary Table S16). Nevertheless, no significant differences were detected when the comparisons between the dwarfing groups were performed (Figure 4.7). This study has validated the impact of the RB QTL on tree height and trunk diameter above the graft union (Harrison et al., 2016b).

4.4.3. Root traits analysis

Most of the studies about apple rootstock dwarfing have focused on the influence of dwarfing in scions but fortunately, in recent years there has been an increase in the research on the impact of dwarfing on root systems (Hou *et al.*, 2012; An *et al.*, 2017b; Ma *et al.*, 2013). Given the importance of climate change and its potential impact on agricultural systems, the development of rootstocks that can thrive under changing

environmental conditions is essential for ensuring sustainable and productive crop production in the future.

The fact that *Rb1*xTP and *Rb1xRb2*xTP are significant (Table 4.3) in the statistical model used for the analysis of maximum root depth and convex hull area indicates that the presence/absence of RB QTL differently impacted these traits over time. In general, at TP1 the rootstocks with both QTL had greater root depth and convex hull area. However, in TP2 the group with both QTL became the group of trees with the weakest root systems. Rootstocks with different combination of RB QTL, resulting in different levels of dwarfing, may have distinct root development patterns, allocating energy to roots or scions at different stages. In the case of dwarfing rootstocks, there could be a tendency to allocate more energy to root development initially, with the intention to subsequently investing this energy in scions. It is noteworthy that the fact that rootstocks with both RB QTL have more roots in TP1 might be attributed to their significantly higher initial root surface area compared to the rest of rootstocks when collected from the stoolbeds (Figure 4.4).

In general, when looking at the impact of dwarfing within each time point, it was observed that root systems of dwarfing genotypes containing either *Rb1* alone or *Rb1* and *Rb2* were shallower and distributed in a smaller area than the root systems of the rest of the genotypes. By the end of the experiment, it seems that both QTL regions are needed to impact the root architecture of the trees, suggesting that the role of *Rb2* in root traits is essential. These findings are in agreement with the studies of Ma *et al.*, (2013) regarding the small region occupied by roots in dwarf apple rootstocks compared to vigorous genotypes. Nonetheless, the differences in TP4 could not be properly assessed since the lack of space in the rhizobox restricted the root growth for some genotypes. A longer experiment with bigger rhizoboxes is needed to fully evaluate the impact of dwarfing on root system depth.

Regarding the TRL, it does not seem to be affected by dwarfing during the first growing season although, by the end of the experiment, the differences between the group with none of the RB QTL and the group with both QTL are close to being significant (p-value = 0.06) suggesting that the impact on TRL could be expressed later, possibly in the second growing season.

In this investigation, dwarfing appeared to have a small impact on the maximum root diameter. In TP1, the group with *Rb1* alone had the lowest maximum root diameter mean and it was significantly different from the group with none of the RB QTL, indicating that *Rb1* has an impact on maximum root diameter at the beginning of the growing season. By the end of the experiment, the roots of the trees with both RB QTL had the smallest maximum root diameter but these were not significantly different from the rest of the groups. In the first growing season, all root bark categories demonstrated an increase in maximum root diameter to a greater or lesser extent. The roots from the NoRb QTL group exhibited a slower thickening initially, followed by a more significant increase towards the end. It is worth noting that the *Rb1Rb2* group was the only category that experienced a reduction in maximum root size between TP3 and TP4. This observation suggests that these particular rootstocks might cease allocating all their energy resources to the root systems by the end of August (TP3) and instead prioritise resource allocation towards the shoots (Figure 4.9).

Previous studies have shown that the mean root diameter is smaller in dwarfing rootstocks compared to vigorous rootstocks (An *et al.*, 2017b; Hou *et al.*, 2012). However, the mean root diameter has not been affected by dwarfing during the experiment presented in this thesis. Nonetheless, towards the end of the experiment genotypes with both root bark QTL had the smallest mean root diameter and this may indicate the start of a trend. Therefore, the effect of dwarfing on mean root diameter could begin to manifest in the next season. The mean root diameter increased and decreased differently depending on the root bark category. From early June (TP1) to mid-July (TP2), all rootstock classes exhibited an increase in mean root diameter, coinciding with a critical period of root thickening. However, by the end of August (TP3), there was a significant decrease in mean root diameter. Towards the end of the experiment, in early October, rootstocks without any RB QTL and rootstocks with *Rb2* alone showed a new increase in mean root diameter. On the other hand, the mean root diameter of *Rb1* and *Rb1Rb2* groups remained unchanged, suggesting that these rootstocks may have ceased root growth by that time. As mentioned earlier, this lack of growth in the roots could indicate a shift in energy allocation towards shoot development rather than root growth. The decrease in mean root diameter in TP3 may

be attributed to the development of new and thinner roots, which reduces the overall mean root diameter and could indicate a root growth peak.

There is a lot of controversy regarding the number of root growth peaks in apples. Root growth peaks vary depending on the rootstocks, their ages and between fruit-bearing and non-bearing trees (An *et al.*, 2017b; Zhou *et al.*, 2022). A study on 13-year-old 'Golden Delicious' apple trees reported three root growth peaks annually, which alternated with shoot growth peaks (Qu and Han, 1983). Other authors affirm that there are two peaks of root growth, one in late spring and the second one in early autumn (Head, 1967; An *et al.*, 2017b). Another study reported a primary peak in new root emergence during late June and early July and an additional smaller peak of root emergence during August to September (Psarras *et al.*, 2000). Moreover, Atkinson and Wilson, (1980) showed that newly grafted M.9 rootstocks only had one root growth peak. Based on the information collected, it is challenging to determine the exact number of root growth peaks occurring during the experiment, as more data is needed before June and in the autumn period. However, it appears evident that there is at least one root growth peak observed in late August. Furthermore, it is noteworthy that the pattern of root growth differs between dwarfing and vigorous rootstocks, indicating variations in their growth dynamics and potentially reflecting their distinct physiological characteristics.

The principal component analysis reinforces the findings regarding the influence of dwarfing on root traits during the first growing season. In TP3, PC1 is affected by *Rb1* and in TP4, PC1 is affected by both QTL and PC2 is affected by *Rb1*. This finding contrasts with the observations made in canopy traits (Section 4.4.2), where the influence of *Rb1* alone was observed. In root traits, however, both RB QTL (*Rb1* and *Rb2*) seem to be necessary to affect root architecture. This suggests that *Rb2* plays a crucial role in shaping root architecture, highlighting its essential contribution to root traits compared to canopy traits in this population.

The impact of dwarfing on canopy traits becomes evident between June and mid-July, indicating observable differences in above-ground growth traits between dwarfing categories. On the other hand, the influence of dwarfing on root traits appears towards the end of the experiment, suggesting that below-ground growth dynamics may take

longer to manifest and become noticeable. Indeed, the observed temporal differences between the effects of dwarfing on canopy traits and root traits can provide valuable insights for designing future studies. The findings suggest the importance of conducting more intensive sampling during the periods when significant changes are occurring. By capturing data during these critical stages, more comprehensive information can be gathered to gain a deeper understanding of the dynamics of both canopy and root growth.

The variability within groups is unequal and is especially higher in the *Rb1Rb2* group, especially in root system depth and convex hull area. This great variability of data could indicate that there may be other genes controlling root architecture in addition to dwarfing. Thus, it would be possible to decouple dwarfing and root architecture and generate new rootstocks with more resilient root systems to adapt to the new climate conditions while conserving all the dwarfing benefits. The great variability of data in the *Rb1Rb2* group may be also due to higher susceptibility to environmental factors in this group. Another hypothesis is that this variation in data may be explained by *Rb3*, a third QTL that modifies the effect of *Rb1* and *Rb2* but unfortunately, there are not enough genotypes within each category to investigate this hypothesis.

Moreover, the lack of replication due to problems with the stoolbeds production is a limitation of this experiment. Without replication, it becomes challenging to determine if the observed effects or findings are specific to the particular sample or if they can be generalised to a broader population. The use of replicates would be very useful to investigate if the large variability in *Rb1Rb2* group.

4.4.4. Final phenotyping analysis

The results obtained in the root bark percentage analysis confirm that the selection of genotypes was performed correctly and that the activity of *Rb1* is dependent on the presence of *Rb2* and vice versa since genotypes with both QTL have a significantly higher root bark percentage than the other groups (Harrison et al., 2016b). Notably, the group with the lowest root bark percentage is *Rb2* (55.8%) instead of the NoRb group (57.7%; Table 4.6).

Previous studies have reported that dwarfing rootstocks have a reduced canopy and root dry matter compared to vigorous rootstocks and, furthermore, dwarfing rootstocks allocate more dry matter to above-ground structures whereas trees on vigorous rootstocks partition more to roots (Stutte *et al.*, 1994; Lo Bianco *et al.*, 2003; Foster *et al.*, 2017). Unfortunately, the dry weights could not be recorded for this experiment since the drying oven was out of service at that time but wet canopy weights were still recorded. Contrary to what has been observed for trunk diameter above the graft union and tree height, *Rb2* was the only QTL that influenced wet canopy and root weights but no effect of *Rb1* was detected (Table 4.6). Notably, despite the observation that interaction between both QTL was not significant statistically, the group with both QTL (*Rb1Rb2*) exhibited the lowest wet canopy weight, which aligns with expectations regarding dry weight. This suggests that there could still be an underlying epistatic mechanism at play and when both QTL are present, the canopy wet weight is the lowest and significantly differs from those rootstocks that do not have any dwarfing QTL (p-value = 0.029; Supplementary Table S35). These findings suggest that the role of *Rb2* on canopy traits could be underestimated if we only look at trunk diameter and tree height and other canopy traits such as leaf area, internodes number and shoot length should be investigated to fully understand the roles of *Rb1* and *Rb2* in canopy traits. Similar to what happens with canopy wet weight, in root wet weight the group with both QTL had the lowest wet root weight but no significant differences between groups were observed. No effect of dwarfing was observed in the root-to-shoot wet weight ratio during this investigation.

4.4.5. Correlation analysis

The length, depth and density of roots are critical factors in determining the tree's ability to absorb water and nutrients from the soil, as well as its anchorage and stability (Parry and Rogers, 1968; Barley, 1970; Li *et al.*, 2019). In this study, IRSA showed a moderate negative correlation with TRL (R=-0.43, p-value = 0.0072; Figure 4,16). Thus, by assessing the rooting performance of rootstock genotypes at an early stage, it may be possible to anticipate their future root architecture and potential impact on plant growth and development.

Convex hull area and root system depth showed a strong correlation with each other. Additionally, both these traits were highly correlated with trunk diameter and tree height, suggesting that they could serve as valuable indicators of root architecture. Interestingly, convex hull area and root system depth were positively correlated with each other, but their correlation with TRL was very low (R=0.71, p-value = 1.2e-06; R=-0.22, p-value = 0.17 and R=-0.05, p-value = 0.76, respectively). This suggests that TRL might not be as strongly associated with dwarfing as other root traits, particularly during the first growing season. Lastly, root bark percentage had a moderate to strong negative correlations with tree height and trunk diameter above the graft union (R=-0.48, p-value = 0.002 and R=-0.50, p-value = 0.0013, respectively). Convex hull area was also significantly correlated with root bark percentage (R=-0.33, p-value = 0.039; Figure 4.16). These four traits are interrelated and could be defined as the best indicators of rootstock-induced dwarfing.

4.5 Conclusion

This study demonstrated that dwarfing rootstocks showed reduced maximum root system depth and total convex hull area compared to vigorous rootstocks by the end of the first growing season. Additionally, the great variability in data in the dwarfing group indicated that dwarfing genotypes are either more susceptible to environmental factors or there are other genes influencing root architecture. This finding opens the possibility of decoupling dwarfing and root architecture. Furthermore, this experiment has also helped to better understand which aspects of the methodology should be considered in future experiments. This would be crucial to capture in detail all the physiological changes associated with rootstock-induced dwarfing and, consequently, obtain a deeper understanding of how this complex mechanism works.

Chapter 5. General discussion

Dwarfing rootstocks reduce the size of the grafted scion and induce a higher proportion of buds to flower. They are essential to intensive production methods, enabling a greater yield per unit area and more uniform cropping earlier in the life of the orchard. However, the genetic control of rootstock-induced dwarfing remains unknown (Atkinson and Else, 2001; Seleznyova *et al.*, 2003).

Several QTL mapping analyses to identify genes controlling rootstock-induced dwarfing have been performed in recent years but the QTL detected are quite large due to the reduced number of observable recombinations in the relevant areas. Three QTL linked to root bark ratio, a primary trait related to rootstock-induced dwarfing, were found in a previous study and established the foundation for the work in this thesis (Harrison et al., 2016b). The QTL were called *Rb1* (Chr 5)*, Rb2* (Chr11) and *Rb3* (Chr13), which after visual scrutiny of recombinant genotypes as described in Chapter 2 section 2.3.1, covered approximately 4.4 Mb, 5.8 Mb and 2 Mb, respectively. This project has focused on the fine mapping of *Rb1* and *Rb2* since their effect is essential to cause dwarfing whereas *Rb3* effect is only additive.

5.1 Key findings

The research presented in this thesis has narrowed the *Rb1* QTL region located in chromosome 5 from 4.4 Mb to 2.2 Mb using the SSR markers specifically developed during this project. The lack of highly polymorphic SSRs has been a challenge for fine-mapping this area.

Despite the challenges, circumstantial evidence unravelled in this thesis may suggest a much smaller region for *Rb1.* This comes from the interesting finding that the QTL mapping for rooting ability in Chapter 3 using the MDX132 population (GD x M.9 cross) identified two QTL in approximately the same regions as *Rb1* and *Rb2*. As previously discussed, there is evidence to believe that these QTL are actually *Rb1* and *Rb2* rather than QTL linked to rooting ability since many physiological aspects linked to dwarfing may have skewed the data. The location of HB8, the most significant haplotype

associated with rooting ability, perfectly colocalized with the previously fine-mapped *Rb1 QTL*, suggesting that the genes that control dwarfing may be located within the HB8 area, between 44.12 Mb to 44.37 Mb (Supplementary Table S6) and *Rb1* could have been fine-mapped even further coincidentally. This finding points us to a very specific region that should be carefully examined in future work using more genetic markers spanning that area.

In addition, two regions linked to rootstock-induced dwarfing have been identified within the *Rb2* region in this study, one located between 6.9 Mb to 7.5 Mb and the second placed between 10.9 Mb to 12.7 Mb. This key finding could offer an explanation for the discrepancies observed in the mapping of *Dw2* on Chromosome 11 by different authors (Fazio *et al.*, 2014; Foster *et al.*, 2015). It also helps to explain the challenges encountered in the fine mapping of this particular region. Tracking the origin of these two QTL regions using a wider set of germplasm would be key to better understand the genetic source of rootstock-induced dwarfing.

One of the greatest achievements of this PhD is the development of multiplexes of primers for highly polymorphic SSR markers that spanned the QTL regions, providing more complete information than the use of single markers. The estimation of dwarfing haplotypes in the *Rb1* and *Rb2* areas has facilitated the early selection of dwarfing rootstocks for breeders and has shed light on some incongruences derived from the use of unique markers that were finally not closely linked to the dwarfing genes.

Another relevant contribution of this thesis has been the generation of genotypes with recombination points situated in key regions. These genotypes exhibit completely opposite phenotypes (very dwarfing vs vigorous) despite showing recombinations in the same areas. Therefore, the screening of new genetic markers spanning the reduced QTL regions on these key genotypes would help to identify a more specific location of the recombination points and, consequently, would contribute to the further refinement of the root bark QTL.

Moreover, the impact of scions on root bark ratio in apple rootstocks has been firstly reported in this thesis. Although most of the studies focused on the impact of rootstocks on scions, it has been seen that understanding the interaction between

scion and rootstock is crucial for optimising fruit tree production, making it a topic widely investigated in several crops. The rootstock-scion interaction can have an effect on the production and distribution of hormones such as auxins, cytokinins, and gibberellins, which play critical roles in root growth and development (Aloni *et al.,* 2010). The quality of the graft union between scion and rootstock affects the efficiency of water and nutrient transport (Cohen *et al.,* 2007, Martinez-Ballesta *et al.,* 2010). Furthermore, the compatibility between scion and rootstock also influences physiological processes like photosynthesis and transpiration (Fullana-Pericàs *et al.,* 2020). Therefore, improved photosynthetic rates in the scion can lead to greater carbohydrate production, which will improve root growth and function. In summary, rootstock-scion communication affects several physiological aspects of the tree such as tree size, growth rate, fruit yield and quality, disease resistance and nutrient and water uptake efficiency (Martinez-Ballesta *et al.,* 2010).

The fact that scions also influence the root morphology of rootstocks in some specific combinations indicates that, the choice of a scion, which previously seemed less relevant to root traits, should in fact also be considered for their impacts on the root funtion and architecture. Therefore, the selection of scion and rootstock must be coordinated to optimise both above and below-ground traits. The mechanism by which the scion modifies rootstock morphology is still an unresolved question which could also be used to further understand the mechanisms underpinning dwarfing.

The advances in understanding how dwarfing differently influences rooting ability in stoolbeds compared to hardwood cuttings have raised questions regarding the potential of dwarfing rootstocks for propagation since dwarfing rootstocks demonstrated excellent performance on stoolbeds whereas in hardwood cuttings showed a diminished rooting ability. Consequently, it will be interesting to determine whether controlling the physiological aspects such as seasonal differences in growth (and hence whether the dwarfing/vigorous physiology is active or reduced due to winter dormancy) will lead to similar results. New populations should be examined in future research to determine if dwarfing and rooting ability are genetically controlled by the same genes.

Interestingly, the impact of dwarfing on scions manifested much earlier than in rootstocks and the impact of each root bark QTL also differed. This would help to better understand the genetic control of dwarfing and will suggest a time frame in which studies on the impact of dwarfing on canopy and root architectural traits should be focused.

Rootstock breeding often involves a trade-off between different traits such as vigour, disease resistance and fruit quality. Developing rootstocks that excel in multiple areas while maintaining resilience remains a challenge. Furthermore, there is little research about dwarfing influence on root systems in rootstocks mainly due to difficulties in accessing root systems. While rhizobox experiments may not perfectly mimic field behaviour, they serve as a powerful tool for preliminary investigations and hypothesis generation, providing controlled and reproducible conditions which can be further validated and applied in field conditions. A few studies have revealed that dwarfing rootstocks often showed shallower root systems compared to vigorous rootstocks (Lo Bianco *et al.*, 2003; Ma *et al.*, 2013). One of the main research questions in this investigation was how dwarfing rootstock influences root system architecture traits that could improve resilience in future climate conditions and whether dwarfing and root architecture can be decoupled. A recent study identified 25 QTL for root angle in apple rootstocks that did not colocalize with the dwarfing QTL, indicating that although dwarfing may influence root angle, it is not genetically controlling it (Zheng *et al.*, 2020). In addition, a study using M.9 and SH.40 apple rootstocks, dwarfing and very dwarfing apple rootstocks respectively, revealed that the SH.40 rootstock exhibited deeper root systems than M.9 despite being more dwarfing. This suggests that there are possibilities for root improvement while keeping a reduced tree size (An et al., 2017a; Ma et al., 2013). In this thesis, dwarfing rootstocks exhibited significantly smaller convex hull area and root system depth compared to vigorous genotypes. Interestingly, the group of rootstocks containing both root bark QTL showed great data variability suggesting that either dwarfing rootstocks are more susceptible to environmental factors or there are other genes controlling root architecture in rootstocks. Consequently, despite the undeniable impact of dwarfing on root architecture, this study suggests that there is an opportunity for enhancing root systems in dwarfing rootstocks.

In addition, the findings of this research could also have a significant potential impact on other high-value perennial crops including cherry, pear and apricot. In pears, a QTL mapping for rootstock-induced dwarfing identified a QTL which is syntenic to *Dw1* in apples demonstrating the high degree of similarity between apple and pear genomes (Knäbel *et al.*, 2015).

In summary, breeding efforts also focus on enhancing the rootstock resilience to abiotic stresses, such as drought, extreme temperatures and poor soil conditions. This can involve selecting rootstock varieties that have an improved capacity for water and nutrient uptake, as well as the ability to adapt to adverse soil conditions using genetic markers tightly linked to the relevant traits. Developing rootstocks with efficient root systems that can explore a larger soil volume for resources and maintain stable water uptake under varying environmental conditions is a key objective. However, breeding for root plasticity, which is the ablity of the plant's root system to change its architecture and growth in response to enviromental stimuli, is a challenge due to its complexity but would be extremely useful for enhancing plant resilience and productivity.

Ultimately, the continuous breeding of rootstocks for resilience plays a vital role in ensuring the sustainability and productivity of orchard systems worldwide, allowing fruit growers to effectively manage various environmental challenges and contribute to the long-term success of the horticultural industry.

5.2 Future directions

5.2.1. Use of SNP markers and *Rb3* to further fine map the root bark QTL

The fine mapping of the *Rb1* and *Rb2* QTL conducted in this study represented an advancement in the discovery of the genes controlling rootstock-induced dwarfing. Due to the lack of highly polymorphic SSR markers especially in the refined *Rb1* area, it would be interesting to look at SNP markers in these problematic areas or specific SSR markers for each genotype to further fine-map the QTL. It is also important to include markers for *Rb3* in future experiments which could contribute to the understanding of incongruences in the predicted versus actual vigour of some

rootstocks. In addition, this study has generated genotypes with recombination events located in relevant regions that would be crucial for narrowing down these areas.

5.2.2. QTLseq analysis to further fine map the root bark QTL

The presence of extreme phenotypes in some of the mapping populations generated during this project raises the possibility of performing QTL-seq, or Quantitative Trait Locus Sequencing. This is a rapid and cost-effective method used to detect the major locus of a certain quantitative trait in a segregating population that can also be used to accelerate the fine mapping of an existing QTL. In this method, bulk segregant analysis (BSA) of contrasting phenotypes, in this case dwarfing versus vigorous rootstsocks, would be combined with next-generation sequencing. This could help to further fine mapping the refined QTL associated with rootstock-induced dwarfing and contribute to the identification of new genetic markers linked to rootstock-induced dwarfing that could accelerate the breeding of new apple rootstocks.

5.2.3. QTL mapping for rooting ability in apple rootstocks

Due to the large effect of dwarfing on rooting ability in the MDX132 population (GD x M.9), it would be interesting to conduct additional rooting ability experiments using other progenies. Future experiments should concentrate on evaluating diverse propagation methods incorporating additional phenotypic data such as cutting or shoot diameter and shoot length. This will help to verify whether rooting ability QTL and rootstock-induced dwarfing QTL actually colocalize or if, on the contrary, the physiological processes associated with dwarfing are influencing the rooting. Moreover, the identification of QTL for rooting ability would help to develop markers linked to this trait that could be deployed into breeding programs to help with the generation of easy-to-propagate rootstocks.

5.2.4. QTL mapping for root traits in apple rootstocks

This study has advanced our understanding of the impact of dwarfing on root traits such as total root length, root system depth and convex hull area. Furthermore, it has also increased our knowledge about the methodology to evaluate root architecture in trees and how this could be improved to better explore tree root systems.

Future investigations should definitely include replicated genotypes (if possible) to discern if the variance within groups is due to genetic or environmental factors. Additionally, future experiments should be ideally conducted for a longer period of time to be able to track further differences in root growth between dwarfing and vigorous rootstocks. Furthermore, it would be interesting to include more time points to capture in detail the root development processes and how these correlate to canopy growth over time in dwarfing versus vigorous rootstocks. Although the root traits measured in the rhizotrons experiment provided valuable insights into how rootstock-induced dwarfing impacts root architecture in apple rootstocks, it would be interesting to measure additional traits such as root branching and root angle in future studies. Root branching and root angle are broadly used in root architecture studies since they directly influence the plant's ability to acquire resources, maintain stability and ultimately affect plant growth and productivity (An *et al.*, 2017a; Liese *et al*., 2017; Zheng *et al*., 2020). Understanding and optimizing these traits could lead to significant improvements in crop performance and resilience. Lastly, the use of bigger rhizoboxes in future experiments would be essential for analysing the root architecture of trees and prevent vigorous genotypes from running out of space before the end of the experiment. All these improvements in methodology should be carefully considered in future research while keeping in mind the time-consuming nature of the phenotyping in this type of experiment.

In summary, future research efforts should focus on identifying QTL for root traits associated with deeper root systems while preserving all the dwarfing benefits. This would aid in the generation of new rootstocks with root systems able to explore larger soil volume looking for water and nutrients and, therefore, will improve rootstock resilience to better adapt to the future climate.

5.2.5. Investigating how the scion-rootstock interaction impacts root morphology and physiology in apple rootstocks in the context of dwarfing

The varying effects of scions on root bark ratio in apple rootstocks highlights the importance of scion selection. Future studies should focus on tracking root morphologycal changes in different combination of rootstocks and scions over time. It would be interesting to investigate if this increase in root bark is also associated with a reduced xylem to phloem ratio and other root morphologycal changes previously

seen in dwarfing rootstocks. Furthermore, it would be relevant to test how the differences in root bark proportion impact the water use efficiency and the transport of hormones and nutrients. This experiment could provide valuable insights into the communication between scions and rootstocks, as well as enhance our understanding of the physiological processes associated with rootstock-indcued dwarfing.

Furthermore, future studies could also explore the genetic and biochemical pathways involved in the rootstock-scion interaction, in order to develop rootstocks that are better tailored to specific scions, thereby improving overall plant health and productivity.

5.2.6. Impact of mycorrhizal inoculation on nutrient uptake and root system architecture

In recent studies, it has been observed that incorporating mycorrhizal fungi into rootstock management practices can significantly improve root architecture and nutrient uptake, leading to more productive trees (Dalla-Costa *et al.,* 2021, Liu *et al.,* 2024). This symbiotic relationship is especially important in sustainable agriculture where reducing chemicals and enhancing the natural plant resilience are key objectives. Investigating the impact of different types of mycorrhizal fungi in nutrient uptake and in root system architecture of commonly used apple rootstocks would be an interesting area to explore in future experiments since its relevance, simplicity and low cost.

References

Abusrewil, G. S., Larsen, F. E. and Fritts, R. (1983). Prestorage and Poststorage Starch Levels in Chemically and Hand-defoliated 'Delicious' Apple Nursery Stock1. *Journal of the American Society for Horticultural Science*, 108 (1), p.20–23. [Online]. Available at: doi:10.21273/JASHS.108.1.20.

Albrecht, U., Bodaghi, S., Meyering, B. and Bowman, K. D. (2020). Influence of rootstock propagation method on traits of grafted sweet orange trees. *HortScience*, 55 (5), p.729–737. [Online]. Available at: doi:10.21273/HORTSCI14928-20.

Albrecht, U., Bordas, M., Lamb, B., Meyering, B. and Bowman, K. D. (2017). Influence of propagation method on root architecture and other traits of young citrus rootstock plants. *HortScience*, 52 (11), p.1569–1576. [Online]. Available at: doi:10.21273/HORTSCI12320-17.

Aloni, R., Aloni, E., Langhans, M. and Ullrich, C. I. (2006). Role of cytokinin and auxin in shaping root architecture: regulating vascular differentiation, lateral root initiation, root apical dominance and root gravitropism. *Annals of Botany*, 97 (5), p.883–893. [Online]. Available at: doi:10.1093/aob/mcl027.

Alvarez, R., Nissen, S. and Sutter, E. G. (1989). Relationship of indole-3-butyric acid and adventitious rooting in M.26 apple (Malus Pumila mill.) shoots cultured in vitro. *Journal of plant growth regulation*, 8 (4), p.263–272. [Online]. Available at: doi:10.1007/BF02021819.

Amiri, M. E., Fallahi, E. and Safi-Songhorabad, M. (2014). Influence of rootstock on mineral uptake and scion growth of 'golden delicious' and 'royal gala' apples. *Journal of plant nutrition*, 37 (1), p.16–29. [Online]. Available at: doi:10.1080/01904167.2013.792838.

Anderson, M. A. and Elliott, A. E. (1983). Stool bed production of clonal apple understocks. *Combined proceedings International Plant Propagators' Society*.

An, H., Dong, H., Wu, T., Wang, Y., Xu, X., Zhang, X. and Han, Z. (2017a). Root growth angle: An important trait that influences the deep rooting of apple rootstocks. *Scientia horticulturae*, 216, p.256–263. [Online]. Available at: doi:10.1016/j.scienta.2017.01.019.

An, H., Luo, F., Wu, T., Wang, Y., Xu, X., Zhang, X. and Han, Z. (2017b). Dwarfing Effect of Apple Rootstocks Is Intimately Associated with Low Number of Fine Roots. *HortScience : a publication of the American Society for Horticultural Science*, 52 (4), p.503–512. [Online]. Available at: doi:10.21273/HORTSCI11579-16.

Aronesty, E. (2013). Comparison of Sequencing Utility Programs. *The open bioinformatics journal*, 7 (1), p.1–8. [Online]. Available at: doi:10.2174/1875036201307010001.

Atkinson, C. J. and Else, M. (2001). Understanding how rootstocks dwarf fruit trees. *Compact Fruit Tree*, (34), p.46–49.

Atkinson, C. J., Else, M. A., Taylor, L. and Dover, C. J. (2003). Root and stem hydraulic conductivity as determinants of growth potential in grafted trees of apple (Malus pumila Mill.). *Journal of Experimental Botany*, 54 (385), p.1221–1229. [Online]. Available at: doi:10.1093/jxb/erg132.

Atkinson, C. J., Else, M. A., Taylor, L. and Webster, A. D. (2001). The rootstock graft union: a contribution to the hydraulics of the worked fruit tree. *Acta horticulturae*, (557), p.117–122. [Online]. Available at: doi:10.17660/ActaHortic.2001.557.14.

Atkinson, D. and Wilson, S. A. (1980). The growth and distribution of fruit tree roots: some consequences for nutrient uptake. *Acta horticulturae*, (92), p.137–150. [Online]. Available at: doi:10.17660/ActaHortic.1980.92.17.

Bajguz, A., Chmur, M. and Gruszka, D. (2020). Comprehensive overview of the brassinosteroid biosynthesis pathways: substrates, products, inhibitors, and connections. *Frontiers in Plant Science*, 11, p.1034. [Online]. Available at: doi:10.3389/fpls.2020.01034.

Barley, K. P. (1970). *The configuration of the root system in relation to nutrient uptake*. In: Advances in Agronomy, 22, Elsevier, p.159–201. [Online]. Available at: doi:10.1016/S0065-2113(08)60268-0.

Basile, B. and DeJong, T. M. (2018). Control of fruit tree vigor induced by dwarfing rootstocks. In: Warrington, I. (ed.), *Horticultural Reviews*, Hoboken, NJ, USA: John Wiley & Sons, Inc., p.39–97. [Online]. Available at: doi:10.1002/9781119521082.ch2.

Bates, D., Mächler, M., Bolker, B. and Walker, S. (2015). Fitting linear mixed-effects models using lme4. *Journal of Statistical Software*, 67 (1), p.1–48. [Online]. Available at: doi:10.18637/jss.v067.i01.

Bauerle, T. L., Centinari, M. and Bauerle, W. L. (2011). Shifts in xylem vessel diameter and embolisms in grafted apple trees of differing rootstock growth potential in response to drought. *Planta*, 234 (5), p.1045–1054. [Online]. Available at: doi:10.1007/s00425-011-1460-6.

Beakbane, A. B. and Thompson, E. C. (1940). Anatomical Studies of Stems and Roots of Hardy Fruit Trees II. The Internal Structure of the Roots of Some Vigorous and Some Dwarfing Apple Rootstocks, and the Correlation of Structure with Vigour. *Journal of Pomology and Horticultural Science*, 17 (2), p.141–149. [Online]. Available at: doi:10.1080/03683621.1940.11513535.

Beakbane, A. B. and Thompson, E. C. (1947). Anatomical studies of stems and roots of hardy fruit trees. IV. the root structure of some new clonal apple rootstocks budded with cox's orange pippin. *Journal of Pomology and Horticultural Science*, 23 (4), p.206–211. [Online]. Available at: doi:10.1080/03683621.1947.11513669.

Beakbane, A. B. (1956). Possible mechanisms of rootstock effect. *Annals of Applied Biology*, 44 (3), p.517–521. [Online]. Available at: doi:10.1111/j.1744-7348.1956.tb02147.x.

Bellini, C., Pacurar, D. I. and Perrone, I. (2014). Adventitious roots and lateral roots: similarities and differences. *Annual review of plant biology*, 65, p.639–666. [Online]. Available at: doi:10.1146/annurev-arplant-050213-035645.

Bianco, L., Cestaro, A., Linsmith, G., Muranty, H., Denancé, C., Théron, A., Poncet, C., Micheletti, D., Kerschbamer, E., Di Pierro, E. A., Larger, S., Pindo, M., Van de Weg, E., Davassi, A., Laurens, F., Velasco, R., Durel, C.-E. and Troggio, M. (2016). Development and validation of the Axiom(®) Apple480K SNP genotyping array. *The Plant Journal*, 86 (1), p.62–74. [Online]. Available at: doi:10.1111/tpj.13145.

Bianco, L., Cestaro, A., Sargent, D. J., Banchi, E., Derdak, S., Di Guardo, M., Salvi, S., Jansen, J., Viola, R., Gut, I., Laurens, F., Chagné, D., Velasco, R., van de Weg, E. and Troggio, M. (2014). Development and validation of a 20K single nucleotide polymorphism (SNP) whole genome genotyping array for apple (*Malus* × domestica Borkh). *Plos One*, 9 (10), p.e110377. [Online]. Available at: doi:10.1371/journal.pone.0110377.

Bink, M. C. A. M., Boer, M. P., ter Braak, C. J. F., Jansen, J., Voorrips, R. E. and van de Weg, W. E. (2008). Bayesian analysis of complex traits in pedigreed plant populations. *Euphytica*, 161 (1–2), p.85–96. [Online]. Available at: doi:10.1007/s10681-007-9516-1.

Bink, M. C. A. M., Jansen, J., Madduri, M., Voorrips, R. E., Durel, C. E., Kouassi, A. B., Laurens, F., Mathis, F., Gessler, C., Gobbin, D., Rezzonico, F., Patocchi, A., Kellerhals, M., Boudichevskaia, A., Dunemann, F., Peil, A., Nowicka, A., Lata, B., Stankiewicz-Kosyl, M., Jeziorek, K., Pitera, E., Soska, A., Tomala, K., Evans, K. M., Fernández-Fernández, F., Guerra, W., Korbin, M., Keller, S., Lewandowski, M., Plocharski, W., Rutkowski, K., Zurawicz, E., Costa, F., Sansavini, S., Tartarini, S., Komjanc, M., Mott, D., Antofie, A., Lateur, M., Rondia, A., Gianfranceschi, L. and van de Weg, W. E. (2014). Bayesian QTL analyses using pedigreed families of an outcrossing species, with application to fruit firmness in apple. *TAG. Theoretical and Applied Genetics. Theoretische und Angewandte Genetik*, 127 (5), p.1073–1090. [Online]. Available at: doi:10.1007/s00122-014-2281-3.

Bink, M. C. A. M., Totir, L. R., ter Braak, C. J. F., Winkler, C. R., Boer, M. P. and Smith, O. S. (2012). QTL linkage analysis of connected populations using ancestral marker and pedigree information. *TAG. Theoretical and Applied Genetics. Theoretische und Angewandte Genetik*, 124 (6), p.1097–1113. [Online]. Available at: doi:10.1007/s00122-011-1772-8.

Bink, M. C. A. M., Uimari, P., Sillanpää, J., Janss, G. and Jansen, C. (2002). Multiple QTL mapping in related plant populations via a pedigree-analysis approach. *TAG. Theoretical and Applied Genetics. Theoretische und Angewandte Genetik*, 104 (5), p.751–762. [Online]. Available at: doi:10.1007/s00122-001-0796-x.

Bohn, M., Novais, J., Fonseca, R., Tuberosa, R. and Grift, T. E. (2006). Genetic evaluation of root complexity in maize. *Acta Agronomica Hungarica*, 54 (3), p.291–303. [Online]. Available at: doi:10.1556/AAgr.54.2006.3.3.

Borkowska, B. and Powell, L. E. (1982). Abscisic acid relationships in dormancy of apple buds. *Scientia horticulturae*, 18 (2), p.111–117. [Online]. Available at: doi:10.1016/0304-4238(82)90124-8.

Boutin-Ganache, I., Raposo, M., Raymond, M. and Deschepper, C. F. (2001). M13-tailed primers improve the readability and usability of microsatellite analyses performed with two different allele-sizing methods. *Biotechniques*, 31 (1), p.24–26, 28. [Online]. Available at: doi:10.2144/01311bm02.

Brownstein, M. J., Carpten, J. D. and Smith, J. R. (1996). Modulation of Non-Templated Nucleotide Addition by*Taq* DNA Polymerase: Primer Modifications that Facilitate Genotyping. *Biotechniques*, 20 (6), p.1004–1010. [Online]. Available at: doi:10.2144/96206st01.

Brown, C. S., Young, E. and Pharr, D. M. (1985). Rootstock and scion effects on the seasonal distribution of dry weight and carbohydrates in young apple trees. *Journal of the American Society for Horticultural Science*, 110 (5), p.696–701. [Online]. Available at: doi:10.21273/JASHS.110.5.696.

Bukovac, M. J., Wittwer, S. H. and Tukey, H. B. (1958). Effect of Stock-Scion Interrelationships on the Transport of^{32} P and^{45} Ca in the Apple. *Journal of Horticultural Science*, 33 (3), p.145–152. [Online]. Available at: doi:10.1080/00221589.1958.11513922.

Bulley, S. M., Wilson, F. M., Hedden, P., Phillips, A. L., Croker, S. J. and James, D. J. (2005). Modification of gibberellin biosynthesis in the grafted apple scion allows control

of tree height independent of the rootstock. *Plant Biotechnology Journal*, 3 (2), p.215–223. [Online]. Available at: doi:10.1111/j.1467-7652.2005.00119.x.

Cai, H., Wang, Q., Gao, J., Li, C., Du, X., Ding, B. and Yang, T. (2021). Construction of a high-density genetic linkage map and QTL analysis of morphological traits in an F1 Malusdomestica × Malus baccata hybrid. *Physiology and molecular biology of plants : an international journal of functional plant biology*, 27 (9), p.1997–2007. [Online]. Available at: doi:10.1007/s12298-021-01069-0.

Carr, D. J. (1966). Metabolic and hormonal regulation of growth and development. *Trends in plant morphogenesis (ed. E. G. CUTTER) London: Longmans, Green & Co*, p.253–283.

Chagné, D., Crowhurst, R. N., Troggio, M., Davey, M. W., Gilmore, B., Lawley, C., Vanderzande, S., Hellens, R. P., Kumar, S., Cestaro, A., Velasco, R., Main, D., Rees, J. D., Iezzoni, A., Mockler, T., Wilhelm, L., Van de Weg, E., Gardiner, S. E., Bassil, N. and Peace, C. (2012). Genome-wide SNP detection, validation, and development of an 8K SNP array for apple. *Plos One*, 7 (2), p.e31745. [Online]. Available at: doi:10.1371/journal.pone.0031745.

Chang, E., Guo, W., Dong, Y., Jia, Z., Zhao, X., Jiang, Z., Zhang, L., Zhang, J. and Liu, J. (2023). Metabolic profiling reveals key metabolites regulating adventitious root formation in ancient Platycladus orientalis cuttings. *Frontiers in Plant Science*, 14, p.1192371. [Online]. Available at: doi:10.3389/fpls.2023.1192371.

Coart, E., VAN Glabeke, S., DE Loose, M., Larsen, A. S. and Roldán-Ruiz, I. (2006). Chloroplast diversity in the genus Malus: new insights into the relationship between the European wild apple (Malus sylvestris (L.) Mill.) and the domesticated apple (Malus domestica Borkh.). *Molecular Ecology*, 15 (8), p.2171–2182. [Online]. Available at: doi:10.1111/j.1365-294X.2006.02924.x.

Coart, E., Vekemans, X., Smulders, M. J. M., Wagner, I., Van Huylenbroeck, J., Van Bockstaele, E. and Roldán-Ruiz, I. (2003). Genetic variation in the endangered wild apple (*Malus sylvestris* (L.) Mill.) in Belgium as revealed by amplified fragment length

polymorphism and microsatellite markers. *Molecular Ecology*, 12 (4), p.845–857. [Online]. Available at: doi:10.1046/j.1365-294X.2003.01778.x.

Cohen, S., Naor, A., Bennink, J., Grava, A., Tyree, M., 2007. Hydraulic resistance components of mature apple trees on rootstocks of different vigours. J. Exp. Bot. 58, 4213–4224.

Cornille, A., Giraud, T., Smulders, M. J. M., Roldán-Ruiz, I. and Gladieux, P. (2014). The domestication and evolutionary ecology of apples. *Trends in Genetics*, 30 (2), p.57–65. [Online]. Available at: doi:10.1016/j.tig.2013.10.002.

Cornille, A., Gladieux, P., Smulders, M. J. M., Roldán-Ruiz, I., Laurens, F., Le Cam, B., Nersesyan, A., Clavel, J., Olonova, M., Feugey, L., Gabrielyan, I., Zhang, X.-G., Tenaillon, M. I. and Giraud, T. (2012). New insight into the history of domesticated apple: secondary contribution of the European wild apple to the genome of cultivated varieties. *PLoS Genetics*, 8 (5), p.e1002703. [Online]. Available at: doi:10.1371/journal.pgen.1002703.

da Costa, C. T., de Almeida, M. R., Ruedell, C. M., Schwambach, J., Maraschin, F. S. and Fett-Neto, A. G. (2013). When stress and development go hand in hand: main hormonal controls of adventitious rooting in cuttings. *Frontiers in Plant Science*, 4, p.133. [Online]. Available at: doi:10.3389/fpls.2013.00133.

Costes, E. and Lauri, P. E. (1995). Processus de croissance en relation avec la ramification sylleptique et la floraison chez le pommier. *J. Bouchon (ed.), Architecture des arbresfruitiers et forestiers. INRA Editions*, 74, p.41–50.

Daccord, N., Celton, J.-M., Linsmith, G., Becker, C., Choisne, N., Schijlen, E., van de Geest, H., Bianco, L., Micheletti, D., Velasco, R., Di Pierro, E. A., Gouzy, J., Rees, D. J. G., Guérif, P., Muranty, H., Durel, C.-E., Laurens, F., Lespinasse, Y., Gaillard, S., Aubourg, S., Quesneville, H., Weigel, D., van de Weg, E., Troggio, M. and Bucher, E. (2017). High-quality de novo assembly of the apple genome and methylome dynamics of early fruit development. *Nature Genetics*, 49 (7), p.1099–1106. [Online]. Available at: doi:10.1038/ng.3886.

Dalla Costa, M., Rech, T. D., Primieri, S., Pigozzi, B. G., Werner, S. S., & Stürmer, S. L. (2021). Inoculation with isolates of arbuscular mycorrhizal fungi influences growth, nutrient use efficiency and gas exchange traits in micropropagated apple rootstock 'Marubakaido'. *Plant Cell, Tissue and Organ Culture (PCTOC)*, *145*(1), 89-99.

Dash, M., Yordanov, Y. S., Georgieva, T., Tschaplinski, T. J., Yordanova, E. and Busov, V. (2017). Poplar PtabZIP1-like enhances lateral root formation and biomass growth under drought stress. *The Plant Journal*, 89 (4), p.692–705. [Online]. Available at: doi:10.1111/tpj.13413.

Davies, P. J. (1995). *Plant Hormones: Physiology, Biochemistry, and Molecular Biology*. Springer Sciences & Business Media.

DeJong, T. M. (2016). Demystifying carbohydrate allocation to storage in fruit trees. *Acta horticulturae*, (1130), p.329–334. [Online]. Available at: doi:10.17660/ActaHortic.2016.1130.49.

Delargy, J. A. and Wright, C. E. (1979). Root formation in cuttings of apple in relation to auxin application and to etiolation. *The New Phytologist*, 82 (2), p.341–347. [Online]. Available at: doi:10.1111/j.1469-8137.1979.tb02659.x.

De Silva, H. (1999). Analysis of distribution of root length density of apple trees on different dwarfing rootstocks. *Annals of Botany*, 83 (4), p.335–345. [Online]. Available at: doi:10.1006/anbo.1999.0829.

Di Guardo, M., Micheletti, D., Bianco, L., Koehorst-van Putten, H. J. J., Longhi, S., Costa, F., Aranzana, M. J., Velasco, R., Arús, P., Troggio, M. and van de Weg, E. W. (2015). ASSIsT: an automatic SNP scoring tool for in- and outbreeding species. *Bioinformatics*, 31 (23), p.3873–3874. [Online]. Available at: doi:10.1093/bioinformatics/btv446.

Duan, N., Bai, Y., Sun, H., Wang, N., Ma, Y., Li, M., Wang, X., Jiao, C., Legall, N., Mao, L., Wan, S., Wang, K., He, T., Feng, S., Zhang, Z., Mao, Z., Shen, X., Chen, X., Jiang, Y., Wu, S., Yin, C., Ge, S., Yang, L., Jiang, S., Xu, H., Liu, J., Wang, D., Qu, C., Wang, Y., Zuo, W., Xiang, L., Liu, C., Zhang, D., Gao, Y., Xu, Y., Xu, K., Chao, T., Fazio, G., Shu, H., Zhong, G.-Y., Cheng, L., Fei, Z. and Chen, X. (2017). Genome re-

sequencing reveals the history of apple and supports a two-stage model for fruit enlargement. *Nature Communications*, 8 (1), p.249. [Online]. Available at: doi:10.1038/s41467-017-00336-7.

Dvin, S. R., Moghadam, E. G. and Kiani, M. (2011). Rooting response of hardwood cuttings of MM111 apple clonal rootstock to indolebutyric acid and rooting media. *Asian Journal of Applied Sciences*, 4 (4), p.453–458. [Online]. Available at: doi:10.3923/ajaps.2011.453.458.

Edge-Garza, D. A., Rowland, T. V., Haendiges, S. and Peace, C. (2014). A high-throughput and cost-efficient DNA extraction protocol for the tree fruit crops of apple, sweet cherry, and peach relying on silica beads during tissue sampling. *Molecular Breeding*, 34 (4), p.2225–2228. [Online]. Available at: doi:10.1007/s11032-014-0160-x.

Evans, R. C. and Campbell, C. S. (2002). The origin of the apple subfamily (Maloideae; Rosaceae) is clarified by DNA sequence data from duplicated GBSSI genes. *American Journal of Botany*, 89 (9), p.1478–1484. [Online]. Available at: doi:10.3732/ajb.89.9.1478.

Exadaktylou, E., Thomidis, T., Grout, B., Zakynthinos, G. and Tsipouridis, C. (2009). Methods to improve the rooting of hardwood cuttings of the ‘gisela 5’ cherry rootstock. *HortTechnology*, 19 (2), p.254–259. [Online]. Available at: doi:10.21273/HORTSCI.19.2.254.

Fan, W. and Yang, H. (2008). Root architecture of apple trees under different soil conditions. *Acta horticulturae*, (767), p.417–422. [Online]. Available at: doi:10.17660/ActaHortic.2008.767.47.

Fan, W. and Yang, H. (2011). Effect of soil type on root architecture and nutrient uptake by roots of young apple rootstocks. *Acta horticulturae*, (903), p.885–890. [Online]. Available at: doi:10.17660/ActaHortic.2011.903.123.

Faostat. (2021). *Food and Agriculture Organization of the United Nations.* . [Online]. Available at: http://www.fao.org/faostat/en/ [Accessed: 22 May 2023].

Fazio, G., Wan, Y., Kviklys, D., Romero, L., Adams, R., Strickland, D. and Robinson, T. (2014). Dw2, a new dwarfing locus in apple rootstocks and its relationship to induction of early bearing in apple scions. *Journal of the American Society for Horticultural Science*, 139 (2), p.87–98. [Online]. Available at: doi:10.21273/JASHS.139.2.87.

Feng, Y., Zhang, X., Wu, T., Xu, X., Han, Z. and Wang, Y. (2017). Methylation effect on IPT5b gene expression determines cytokinin biosynthesis in apple rootstock. *Biochemical and Biophysical Research Communications*, 482 (4), p.604–609. [Online]. Available at: doi:10.1016/j.bbrc.2016.11.080.

Ferree, D. C., Clayton-Greene, K. A. and Bishop, B. (1993). Influence of orchard management system on canopy composition, light distribution, net photosynthesis and transpiration of apple trees. *Journal of Horticultural Science*, 68 (3), p.377–392. [Online]. Available at: doi:10.1080/00221589.1993.11516365.

Foster, T. M., Celton, J.-M., Chagné, D., Tustin, D. S. and Gardiner, S. E. (2015). Two quantitative trait loci, Dw1 and Dw2, are primarily responsible for rootstock-induced dwarfing in apple. *Horticulture Research*, 2, p.15001. [Online]. Available at: doi:10.1038/hortres.2015.1.

Foster, T. M., McAtee, P. A., Waite, C. N., Boldingh, H. L. and McGhie, T. K. (2017). Apple dwarfing rootstocks exhibit an imbalance in carbohydrate allocation and reduced cell growth and metabolism. *Horticulture Research*, 4, p.17009. [Online]. Available at: doi:10.1038/hortres.2017.9.

Fujioka, S. and Yokota, T. (2003). Biosynthesis and metabolism of brassinosteroids. *Annual review of plant biology*, 54, p.137–164. [Online]. Available at: doi:10.1146/annurev.arplant.54.031902.134921.

Fullana-Pericàs, M., Conesa, M. À., Pérez-Alfocea, F., & Galmés, J. (2020). The influence of grafting on crops' photosynthetic performance. *Plant science*, *295*, 110250.

Gan, Z., Wang, Y., Wu, T., Xu, X., Zhang, X. and Han, Z. (2018). MdPIN1b encodes a putative auxin efflux carrier and has different expression patterns in BC and M9

apple rootstocks. *Plant Molecular Biology*, 96 (4–5), p.353–365. [Online]. Available at: doi:10.1007/s11103-018-0700-6.

García-Villanueva, E., Costes, E. and Jourdan, C. (2004). Comparing root and aerial growth dynamics of two apple hybrids ownrooted and grafted on m.9. *Acta horticulturae*, (658), p.61–67. [Online]. Available at: doi:10.17660/ActaHortic.2004.658.5.

Gjamovski, V. and Kiprijanovski, M. (2011). Influence of nine dwarfing apple rootstocks on vigour and productivity of apple cultivar 'Granny Smith.' *Scientia horticulturae*, 129 (4), p.742–746. [Online]. Available at: doi:10.1016/j.scienta.2011.05.032.

Goldschmidt, E. E. (2014). Plant grafting: new mechanisms, evolutionary implications. *Frontiers in Plant Science*, 5, p.727. [Online]. Available at: doi:10.3389/fpls.2014.00727.

Grattapaglia, D., Bertolucci, F. L. and Sederoff, R. R. (1995). Genetic mapping of QTLs controlling vegetative propagation in Eucalyptus grandis and E. urophylla using a pseudo-testcross strategy and RAPD markers. *TAG. Theoretical and Applied Genetics. Theoretische und Angewandte Genetik*, 90 (7–8), p.933–947. [Online]. Available at: doi:10.1007/BF00222906.

Graves, S., Piepho, H. P., Selzer, L. and Dorai-Raj, S. (2019). multcompView: Visualizations of Paired Comparisons. *R package version 0.1-8*. [Online]. Available at: https://cran.r-project.org/web/packages/multcompView/index.html [Accessed: 1 June 2022].

Gregory, F. G. (1957). The place of plant physiology in fruit growing. *Ann. Rept E. Malling Res. Sta.*, 41 (8).

Griffiths, J., Murase, K., Rieu, I., Zentella, R., Zhang, Z.-L., Powers, S. J., Gong, F., Phillips, A. L., Hedden, P., Sun, T. and Thomas, S. G. (2006). Genetic characterization and functional analysis of the GID1 gibberellin receptors in Arabidopsis. *The Plant Cell*, 18 (12), p.3399–3414. [Online]. Available at: doi:10.1105/tpc.106.047415.

Hansen, O. B. (1990a). Rapid production of apple rootstocks by softwood cuttings. *Scientia horticulturae*, 42 (4), p.277–287. [Online]. Available at: doi:10.1016/0304-4238(90)90051-F.

Hansen, O. B. (1990b). The rooting potential of dwarfing apple rootstocks. *Norsk Landbruksforsking*.

Hao, S., Lu, Y., Liu, J., Bu, Y., Chen, Q., Ma, N., Zhou, Z. and Yao, Y. (2019). GIBBERELLIN INSENSITIVE DWARF1 plays an important role in the growth regulation of dwarf apple rootstocks. *HortScience*, 54 (3), p.416–422. [Online]. Available at: doi:10.21273/HORTSCI13685-18.

Harrison, N., Barber-Perez, N., Pennington, B., Cascant-Lopez, E. and Gregory, P. J. (2016a). Root system architecture in reciprocal grafts of apple rootstock-scion combinations. *Acta horticulturae*, (1130), p.409–414. [Online]. Available at: doi:10.17660/ActaHortic.2016.1130.61.

Harrison, N., Harrison, R. J., Barber-Perez, N., Cascant-Lopez, E., Cobo-Medina, M., Lipska, M., Conde-Ruíz, R., Brain, P., Gregory, P. J. and Fernández-Fernández, F. (2016b). A new three-locus model for rootstock-induced dwarfing in apple revealed by genetic mapping of root bark percentage. *Journal of Experimental Botany*, 67 (6), p.1871–1881. [Online]. Available at: doi:10.1093/jxb/erw001.

Harrison, N. and Harrison, R. J. (2011). On the evolutionary history of the domesticated apple. *Nature Genetics*, 43 (11), p.1043–1044; author reply 1044. [Online]. Available at: doi:10.1038/ng.935.

Harris, S. A., Robinson, J. P. and Juniper, B. E. (2002). Genetic clues to the origin of the apple. *Trends in Genetics*, 18 (8), p.426–430. [Online]. Available at: doi:10.1016/s0168-9525(02)02689-6.

Hartmann, H. T. and Kester, D. E. (1975). Plant propagation: principles and practices. 3rd edition. *Plant propagation: principles and practices. 3rd edition.*

Hatton, R. G. (1917). “Paradise” apple socks. *J R Hort Soc*, 42, p.361–399.

Hatton, R. G. (1928). The influence of different root stocks upon the vigour and productivity of the variety budded or grafted thereon. *Journal of Pomology and Horticultural Science*, 6 (1), p.1–28. [Online]. Available at: doi:10.1080/03683621.1928.11513308.

Head, G. C. (1967). Effects of seasonal changes in shoot growth on the amount of unsuberized root on apple and plum trees. *Journal of Horticultural Science*, 42 (2), p.169–180. [Online]. Available at: doi:10.1080/00221589.1967.11514205.

Heide, O. M. and Prestrud, A. K. (2005). Low temperature, but not photoperiod, controls growth cessation and dormancy induction and release in apple and pear. *Tree Physiology*, 25 (1), p.109–114.

Hodge, A. (2004). The plastic plant: root responses to heterogeneous supplies of nutrients. *The New Phytologist*, 162 (1), p.9–24. [Online]. Available at: doi:10.1111/j.1469-8137.2004.01015.x.

Hooijdonk, V., Woolley, D. J., Warrington, I. J. and Tustin, D. S. (2010). Initial alteration of scion architecture by dwarfing apple rootstocks may involve shoot-root-shoot signalling by auxin, gibberellin, and cytokinin. *The Journal of Horticultural Science and Biotechnology*, 85 (1), p.59–65. [Online]. Available at: doi:10.1080/14620316.2010.11512631.

Hothorn, T., Bretz, F. and Westfall, P. (2008). Simultaneous inference in general parametric models. *Biometrical Journal. Biometrische Zeitschrift*, 50 (3), p.346–363. [Online]. Available at: doi:10.1002/bimj.200810425.

Hou, C., Ma, L., Luo, F., Wang, Y., Zhang, X. and Han, Z. (2012). Impact of rootstock and interstems on fine root survivorship and seasonal variation in apple. *Scientia horticulturae*, 148, p.169–176. [Online]. Available at: doi:10.1016/j.scienta.2012.10.008.

Howard, B. H., Harrison-Murray, R. S. and Mackenzie, K. A. D. (1984). Rooting responses to wounding winter cuttings of M.26 apple rootstock. *Journal of Horticultural Science*, 59 (2), p.131–139. [Online]. Available at: doi:10.1080/00221589.1984.11515179.

Howard, B. H. (1968). The Influence Of$_4$ (Indolyl-$_3$) Butyric Acid and Basal Temperature on the Rooting of Apple Rootstock Hardwood Cuttings. *Journal of Horticultural Science*, 43 (1), p.23–31. [Online]. Available at: doi:10.1080/00221589.1968.11514229.

Howard, B. H. (1985). Factors affecting the response of leafless winter cuttings of apple and plum to IBA applied in powder formulation. *Journal of Horticultural Science*, 60 (2), p.161–168. [Online]. Available at: doi:10.1080/14620316.1985.11515615.

Jensen, P. J., Halbrendt, N., Fazio, G., Makalowska, I., Altman, N., Praul, C., Maximova, S. N., Ngugi, H. K., Crassweller, R. M., Travis, J. W. and McNellis, T. W. (2012). Rootstock-regulated gene expression patterns associated with fire blight resistance in apple. *BMC Genomics*, 13, p.9. [Online]. Available at: doi:10.1186/1471-2164-13-9.

Jia, D., Gong, X., Li, M., Li, C., Sun, T. and Ma, F. (2018). Overexpression of a Novel Apple NAC Transcription Factor Gene, MdNAC1, Confers the Dwarf Phenotype in Transgenic Apple (Malus domestica). *Genes*, 9 (5). [Online]. Available at: doi:10.3390/genes9050229.

Jindal, K. K., Dalbro, S., Andersen, A. S. and Poll, L. (1974). Endogenous growth substances in normal and dwarf mutants of cortland and golden delicious apple shoots. *Physiologia Plantarum*, 32 (1), p.71–77. [Online]. Available at: doi:10.1111/j.1399-3054.1974.tb03729.x.

Jones, O. P. (1976). Effect of dwarfing interstocks on xylem sap composition in apple trees: effect on nitrogen, potassium, phosphorus, calcium and magnesium content. *Annals of Botany*, 40 (6), p.1231–1235. [Online]. Available at: doi:10.1093/oxfordjournals.aob.a085243.

Jones, O. P. (1986). Endogenous growth regulators and rootstock/scion interactions in apple and cherry trees. *Acta horticulturae*, (179), p.177–184. [Online]. Available at: doi:10.17660/ActaHortic.1986.179.18.

Juniper, B. E., Watkins, R. and Harris, S. A. (1998). The origin of the apple. *Acta horticulturae*, (484), p.27–34. [Online]. Available at: doi:10.17660/ActaHortic.1998.484.1.

Kamboj, J. S., Blake, P. S., Quinlan, J. D. and Baker, D. A. (1999a). Identification and quantitation by GC-MS of zeatin and zeatin riboside in xylem sap from rootstock and scion of grafted apple trees. *Plant growth regulation*, 28, p.199–205.

Kamboj, J. S., Blake, P. S., Quinlan, J. D., Webster, A. D. and Baker, D. A. (1997a). Recent advances in studies on the dwarfing mechanism of apple rootstocks. *Acta horticulturae*, (451), p.75–82. [Online]. Available at: doi:10.17660/ActaHortic.1997.451.4.

Kamboj, J. S., Browning, G., Blake, P. S., Quinlan, J. D. and Baker, D. A. (1999b). GC-MS-SIM analysis of abscisic acid and indole-3-acetic acid in shoot bark of apple rootstocks. *Plant Growth Regulation*, 28, p.21–27.

Kamboj, J. S., Browning, G., Quinlan, J. D., Blake, P. S. and Baker, D. A. (1997b). Polar transport of [^{3} H]-IAA in apical shoot segments of different apple rootstocks. *Journal of Horticultural Science*, 72 (5), p.773–780. [Online]. Available at: doi:10.1080/14620316.1997.11515570.

Karlova, R., Boer, D., Hayes, S. and Testerink, C. (2021). Root plasticity under abiotic stress. *Plant Physiology*, 187 (3), p.1057–1070. [Online]. Available at: doi:10.1093/plphys/kiab392.

Karlström, A., Gómez-Cortecero, A., Nellist, C. F., Ordidge, M., Dunwell, J. M. and Harrison, R. J. (2022). Identification of novel genetic regions associated with resistance to European canker in apple. *BMC Plant Biology*, 22 (1), p.452. [Online]. Available at: doi:10.1186/s12870-022-03833-0.

Kassambara, A. and Mundt, F. (2020). Factoextra: Extract and Visualize the Results of Multivariate Data Analyses. *R Packase Version 1.0.7*.

Kenis, K. and Keulemans, J. (2007). Study of tree architecture of apple (Malus × domestica Borkh.) by QTL analysis of growth traits. *Molecular Breeding*, 19 (3), p.193–208. [Online]. Available at: doi:10.1007/s11032-006-9022-5.

Kerr, I. D. and Bennett, M. J. (2007). New insight into the biochemical mechanisms regulating auxin transport in plants. *The Biochemical Journal*, 401 (3), p.613–622. [Online]. Available at: doi:10.1042/BJ20061411.

Khanizadeh, S., Groleau, Y., Granger, R., Rousselle, G. L., Privé, J. P. and Embree, C. G. (2011a). St Jean 84 (SJ84) dwarf winter hardy apple rootstocks series . *Acta horticulturae*, (903), p.187–188. [Online]. Available at: doi:10.17660/ActaHortic.2011.903.20.

Khanizadeh, S., Groleau, Y., Granger, R., Rousselle, G. L., Privé, J. P. and Embree, C. G. (2011b). St Jean Morden dwarf winter hardy rootstock series. *Acta horticulturae*, (903), p.191–192. [Online]. Available at: doi:10.17660/ActaHortic.2011.903.22.

Kitomi, Y., Kanno, N., Kawai, S., Mizubayashi, T., Fukuoka, S. and Uga, Y. (2015). QTLs underlying natural variation of root growth angle among rice cultivars with the same functional allele of DEEPER ROOTING 1. *Rice (New York, N.Y.)*, 8, p.16. [Online]. Available at: doi:10.1186/s12284-015-0049-2.

Knäbel, M., Friend, A. P., Palmer, J. W., Diack, R., Gardiner, S. E., Tustin, S., Schaffer, R., Foster, T. and Chagné, D. (2017). Quantitative trait loci controlling vegetative propagation traits mapped in European pear (Pyrus communis L.). *Tree genetics & genomes*, 13 (3), p.55. [Online]. Available at: doi:10.1007/s11295-017-1141-0.

Knäbel, M., Friend, A. P., Palmer, J. W., Diack, R., Wiedow, C., Alspach, P., Deng, C., Gardiner, S. E., Tustin, D. S., Schaffer, R., Foster, T. and Chagné, D. (2015). Genetic control of pear rootstock-induced dwarfing and precocity is linked to a chromosomal region syntenic to the apple Dw1 loci. *BMC Plant Biology*, 15, p.230. [Online]. Available at: doi:10.1186/s12870-015-0620-4.

Knight, R. C., Amos, J., Hatton, R. G. and Witt, A. W. (1927). The vegetative propagation of fruit tree rootstocks. *Rep. East Mail. Res. Station A, 11*, 11, p.11–30.

Koevoets, I. T., Venema, J. H., Elzenga, J. T. M. and Testerink, C. (2016). Roots Withstanding their Environment: Exploiting Root System Architecture Responses to Abiotic Stress to Improve Crop Tolerance. *Frontiers in Plant Science*, 7, p.1335. [Online]. Available at: doi:10.3389/fpls.2016.01335.

Langmead, B., Trapnell, C., Pop, M. and Salzberg, S. L. (2009). Ultrafast and memory-efficient alignment of short DNA sequences to the human genome. *Genome Biology*, 10 (3), p.R25. [Online]. Available at: doi:10.1186/gb-2009-10-3-r25.

Lauri, P. E., Maguylo, K. and Trottier, C. (2006). Architecture and size relations: an essay on the apple (Malus x domestica, Rosaceae) tree. *American Journal of Botany*, 93 (3), p.357–368. [Online]. Available at: doi:10.3732/ajb.93.3.357.

Lebedev, V. (2019). The Rooting of Stem Cuttings and the Stability of uidA Gene Expression in Generative and Vegetative Progeny of Transgenic Pear Rootstock in the Field. *Plants*, 8 (8). [Online]. Available at: doi:10.3390/plants8080291.

Lee, Y., Do, V. G., Kim, S., Kweon, H. and McGhie, T. K. (2021). Cold stress triggers premature fruit abscission through ABA-dependent signal transduction in early developing apple. *Plos One*, 16 (4), p.e0249975. [Online]. Available at: doi:10.1371/journal.pone.0249975.

Lenth, R., Singmann, H., Love, J., Buerkner, P. and Herve, M. (2018). Package "Emmeans." *R package version 4.0-3*.

Lesmes-Vesga, R. A., Cano, L. M., Ritenour, M. A., Sarkhosh, A., Chaparro, J. X. and Rossi, L. (2022). Rhizoboxes as rapid tools for the study of root systems of prunus seedlings. *Plants*, 11 (16). [Online]. Available at: doi:10.3390/plants11162081.

Liebhard, R., Gianfranceschi, L., Koller, B., Ryder, C. D., Tarchini, R., Van De Weg, E. and Gessler, C. (2002). Development and characterisation of 140 new microsatellites in apple (Malus x domestica Borkh.). *Molecular Breeding*.

Liebhard, R., Koller, B., Patocchi, A., Kellerhals, M., Pfammatter, W., Jermini, M. and Gessler, C. (2003). Mapping quantitative field resistance against apple scab in a

“fiesta” x “discovery” progeny. *Phytopathology*, 93 (4), p.493–501. [Online]. Available at: doi:10.1094/PHYTO.2003.93.4.493.

Liese, R., Alings, K., & Meier, I. C. (2017). Root branching is a leading root trait of the plant economics spectrum in temperate trees. *Frontiers in Plant Science*, *8*, 245427.

Lindley, J. (1827). *The Pomological magazine; or, Figures and descriptions of the most important varieties of fruit cultivated in Great Britain*. J. Ridgway.

Li, G., Ma, J., Tan, M., Mao, J., An, N., Sha, G., Zhang, D., Zhao, C. and Han, M. (2016). Transcriptome analysis reveals the effects of sugar metabolism and auxin and cytokinin signaling pathways on root growth and development of grafted apple. *BMC Genomics*, 17, p.150. [Online]. Available at: doi:10.1186/s12864-016-2484-x.

Li, H. and Durbin, R. (2009). Fast and accurate short read alignment with Burrows-Wheeler transform. *Bioinformatics*, 25 (14), p.1754–1760. [Online]. Available at: doi:10.1093/bioinformatics/btp324.

Li, H. and Durbin, R. (2010). Fast and accurate long-read alignment with Burrows-Wheeler transform. *Bioinformatics*, 26 (5), p.589–595. [Online]. Available at: doi:10.1093/bioinformatics/btp698.

Li, H., Handsaker, B., Wysoker, A., Fennell, T., Ruan, J., Homer, N., Marth, G., Abecasis, G., Durbin, R. and 1000 Genome Project Data Processing Subgroup. (2009). The Sequence Alignment/Map format and SAMtools. *Bioinformatics*, 25 (16), p.2078–2079. [Online]. Available at: doi:10.1093/bioinformatics/btp352.

Li, H., Si, B., Ma, X. and Wu, P. (2019). Deep soil water extraction by apple sequesters organic carbon via root biomass rather than altering soil organic carbon content. *The Science of the Total Environment*, 670, p.662–671. [Online]. Available at: doi:10.1016/j.scitotenv.2019.03.267.

Li, H. (2013). Aligning sequence reads, clone sequences and assembly contigs with BWA-MEM. *arXiv*. [Online]. Available at: doi:10.48550/arxiv.1303.3997.

Li, H. L., Zhang, H., Yu, C., Ma, L., Wang, Y., Zhang, X. Z. and Han, Z. H. (2012). Possible roles of auxin and zeatin for initiating the dwarfing effect of M9 used as apple rootstock or interstock. *Acta physiologiae plantarum / Polish Academy of Sciences, Committee of Plant Physiology Genetics and Breeding*, 34 (1), p.235–244. [Online]. Available at: doi:10.1007/s11738-011-0822-9.

Li, L., Deng, X., Zhang, T., Tian, Y., Ma, X. and Wu, P. (2022). Propagation Methods Decide Root Architecture of Chinese Fir: Evidence from Tissue Culturing, Rooted Cutting and Seed Germination. *Plants*, 11 (19). [Online]. Available at: doi:10.3390/plants11192472.

Li, Z. and He, Y. (2020). Roles of brassinosteroids in plant reproduction. *International Journal of Molecular Sciences*, 21 (3). [Online]. Available at: doi:10.3390/ijms21030872.

Liu, C. Y., Guo, X. N., Dai, F. J., & Wu, Q. S. (2024). Mycorrhizal Symbiosis Enhances P Uptake and Indole-3-Acetic Acid Accumulation to Improve Root Morphology in Different Citrus Genotypes. *Horticulturae*, *10*(4), 339.

Ljung, K., Hull, A. K., Celenza, J., Yamada, M., Estelle, M., Normanly, J. and Sandberg, G. (2005). Sites and regulation of auxin biosynthesis in Arabidopsis roots. *The Plant Cell*, 17 (4), p.1090–1104. [Online]. Available at: doi:10.1105/tpc.104.029272.

Ljung, K. (2013). Auxin metabolism and homeostasis during plant development. *Development*, 140 (5), p.943–950. [Online]. Available at: doi:10.1242/dev.086363.

Lochard, R. G. and Schneider, G. W. (1981). Stock and scion growth relationships and the dwarfing mechanism in apple. In: Janick, J. (ed.), *Horticultural Reviews*, Hoboken, NJ, USA: John Wiley & Sons, Inc., p.315–375. [Online]. Available at: doi:10.1002/9781118060766.ch7.

Loescher, W. H., McCamant, T. and Keller, J. D. (1990). Carbohydrate reserves, translocation, and storage in woody plant roots. *HortScience*, 25 (3), p.274–281. [Online]. Available at: doi:10.21273/HORTSCI.25.3.274.

Lo Bianco, R., Policarpo, M. and Scariano, L. (2003). Effects of rootstock vigour and in-row spacing on stem and root growth, conformation and dry-matter distribution of young apple trees. *The Journal of Horticultural Science and Biotechnology*, 78 (6), p.828–836. [Online]. Available at: doi:10.1080/14620316.2003.11511705.

López-Bucio, J., Cruz-Ramírez, A. and Herrera-Estrella, L. (2003). The role of nutrient availability in regulating root architecture. *Current Opinion in Plant Biology*, 6 (3), p.280–287. [Online]. Available at: doi:10.1016/S1369-5266(03)00035-9.

Ludlow, M. M. and Muchow, R. C. (1990). A Critical Evaluation of Traits for Improving Crop Yields in Water-Limited Environments. In: *Advances in agronomy volume 43*, Advances in Agronomy, 43, Elsevier, p.107–153. [Online]. Available at: doi:10.1016/S0065-2113(08)60477-0.

Lynch, J. P. and Brown, K. M. (2001). Topsoil foraging – an architectural adaptation of plants to low phosphorus availability. *Plant and Soil*.

Lynch, J. P. (1995). Root architecture and plant productivity. *Plant Physiology*, 109 (1), p.7–13. [Online]. Available at: doi:10.1104/pp.109.1.7.

Lynch, J. P. (2007). Roots of the Second Green Revolution. *Australian journal of botany*, 55 (5), p.493. [Online]. Available at: doi:10.1071/BT06118.

Maggs, D. H. (1955). The inception of flowering in some apple rootstock varieties. *Journal of Horticultural Science*, 30 (4), p.234–241. [Online]. Available at: doi:10.1080/00221589.1955.11513846.

Malamy, J. E. (2005). Intrinsic and environmental response pathways that regulate root system architecture. *Plant, Cell & Environment*, 28 (1), p.67–77. [Online]. Available at: doi:10.1111/j.1365-3040.2005.01306.x.

Mao, J., Zhang, D., Li, K., Liu, Z., Liu, X., Song, C., Li, G., Zhao, C., Ma, J. and Han, M. (2017). Effect of exogenous Brassinolide (BR) application on the morphology, hormone status, and gene expression of developing lateral roots in Malus hupehensis. *Plant growth regulation*, 82 (3), p.391–401. [Online]. Available at: doi:10.1007/s10725-017-0264-5.

Marguerit, E., Brendel, O., Lebon, E., Van Leeuwen, C. and Ollat, N. (2012). Rootstock control of scion transpiration and its acclimation to water deficit are controlled by different genes. *The New Phytologist*, 194 (2), p.416–429. [Online]. Available at: doi:10.1111/j.1469-8137.2012.04059.x.

Marini, R. P. and Fazio, G. (2018). Apple rootstocks: history, physiology, management, and breeding. In: Warrington, I. (ed.), *Horticultural Reviews*, Hoboken, NJ, USA: John Wiley & Sons, Inc., p.197–312. [Online]. Available at: doi:10.1002/9781119431077.ch6.

Ma, L., Hou, C. W., Zhang, X. Z., Li, H. L., Han, D. G., Wang, Y. and Han, Z. H. (2013). Seasonal growth and spatial distribution of apple tree roots on different rootstocks or interstems. *Journal of the American Society for Horticultural Science*, 138 (2), p.79–87. [Online]. Available at: doi:10.21273/JASHS.138.2.79.

Marques, C. M., Carocha, V. J., Pereira de Sá, A. R., Oliveira, M. R., Pires, A. M., Sederoff, R. and Borralho, N. M. G. (2005). Verification of QTL linked markers for propagation traits in Eucalyptus. *Tree genetics & genomes*, 1 (3), p.103–108. [Online]. Available at: doi:10.1007/s11295-005-0013-1.

Marques, C. M., Vasquez-Kool, J., Carocha, V. J., Ferreira, J. G., O'Malley, D. M., Liu, B. H. and Sederoff, R. (1999). Genetic dissection of vegetative propagation traits in Eucalyptus tereticornis and E. globulus. *TAG. Theoretical and Applied Genetics. Theoretische und Angewandte Genetik*, 99 (6), p.936–946. [Online]. Available at: doi:10.1007/s001220051400.

Martin, G. C. and Williams, M. W. (1967). Comparison of some biochemical constituents of EM IX and XVI bark. *HortScience*, 2 (4), p.154. [Online]. Available at: doi:10.21273/HORTSCI.2.4.154.

Martínez-Ballesta, M. C., Alcaraz-López, C., Muries, B., Mota-Cadenas, C., & Carvajal, M. (2010). Physiological aspects of rootstock–scion interactions. *Scientia Horticulturae*, *127*(2), 112-118.

Mašková, T. and Klimeš, A. (2019). The effect of rhizoboxes on plant growth and root: shoot biomass partitioning. *Frontiers in Plant Science*, 10, p.1693. [Online]. Available at: doi:10.3389/fpls.2019.01693.

Mika, A. (1986). Physiological responses of fruit trees to pruning. In: Janick, J. (ed.), *Horticultural Reviews*, Wiley, p.337–378. [Online]. Available at: doi:10.1002/9781118060810.ch9.

Moriya, S., Iwanami, H., Haji, T., Okada, K., Yamada, M., Yamamoto, T. and Abe, K. (2015). Identification and genetic characterization of a quantitative trait locus for adventitious rooting from apple hardwood cuttings. *Tree genetics & genomes*, 11 (3). [Online]. Available at: doi:10.1007/s11295-015-0883-9.

Morris, D., Friml, J. and Zažímalová, E. (2004). Hormones in plant growth and development. E1. The Transport of Auxins. *P.J. Davies (ed.), Plant Hormones: Biosynthesis, Signal Transduction, Action! Kluwer, Dordrecht.*, p.437–479.

Norelli, J. L., Holleran, H. T., Johnson, W. C., Robinson, T. L. and Aldwinckle, H. S. (2003). Resistance of Geneva and Other Apple Rootstocks to*Erwinia amylovora*. *Plant disease*, 87 (1), p.26–32. [Online]. Available at: doi:10.1094/PDIS.2003.87.1.26.

Olmstead, M. A., Lang, N. S. and Lang, G. A. (2010). Carbohydrate profiles in the graft union of young sweet cherry trees grown on dwarfing and vigorous rootstocks. *Scientia horticulturae*, 124 (1), p.78–82. [Online]. Available at: doi:10.1016/j.scienta.2009.12.022.

Osakabe, Y., Yamaguchi-Shinozaki, K., Shinozaki, K. and Tran, L.-S. P. (2014). ABA control of plant macroelement membrane transport systems in response to water deficit and high salinity. *The New Phytologist*, 202 (1), p.35–49. [Online]. Available at: doi:10.1111/nph.12613.

Osmont, K. S., Sibout, R. and Hardtke, C. S. (2007). Hidden branches: developments in root system architecture. *Annual review of plant biology*, 58, p.93–113. [Online]. Available at: doi:10.1146/annurev.arplant.58.032806.104006.

Pacurar, D. I., Perrone, I. and Bellini, C. (2014). Auxin is a central player in the hormone cross-talks that control adventitious rooting. *Physiologia Plantarum*, 151 (1), p.83–96. [Online]. Available at: doi:10.1111/ppl.12171.

Paez-Garcia, A., Motes, C. M., Scheible, W.-R., Chen, R., Blancaflor, E. B. and Monteros, M. J. (2015). Root traits and phenotyping strategies for plant improvement. *Plants*, 4 (2), p.334–355. [Online]. Available at: doi:10.3390/plants4020334.

Pagès, L., Bruchou, C. and Garré, S. (2012). Links between root length density profiles and models of the root system architecture. *Vadose Zone Journal*, 11 (4), p.vzj2011.0152. [Online]. Available at: doi:10.2136/vzj2011.0152.

Panetsos, K., Scaltsoyiannes, A. and Alizoti, P. (1994). Effect of genotype and cutting type on the vegetative propagation of the pine hybrid (Pinus brutia (Ten) × Pinus halepensis (Mill)). *Annales des Sciences Forestières*, 51 (5), p.447–454. [Online]. Available at: doi:10.1051/forest:19940502.

Parry, M. S. and Rogers, W. S. (1968). Dwarfing interstocks: their effect on the field performance and anchorage of apple trees. *Journal of Horticultural Science*, 43 (2), p.133–146. [Online]. Available at: doi:10.1080/00221589.1968.11514240.

Petersson, S. V., Johansson, A. I., Kowalczyk, M., Makoveychuk, A., Wang, J. Y., Moritz, T., Grebe, M., Benfey, P. N., Sandberg, G. and Ljung, K. (2009). An auxin gradient and maximum in the Arabidopsis root apex shown by high-resolution cell-specific analysis of IAA distribution and synthesis. *The Plant Cell*, 21 (6), p.1659–1668. [Online]. Available at: doi:10.1105/tpc.109.066480.

Pilcher, R. L. R., Celton, J. M., Gardiner, S. E. and Tustin, D. S. (2008). Genetic Markers Linked to the Dwarfing Trait of Apple Rootstock 'Malling 9.' *Journal of the American Society for Horticultural Science*.

Preston, A. P. (1955). Apple Rootstock Studies : Malling-Merton Rootstocks. *Journal of Horticultural Science*, 30 (1), p.25–33. [Online]. Available at: doi:10.1080/00221589.1955.11513825.

Preston, A. P. (1966). Apple Rootstock Studies: Fifteen Years' Results with Malling-Merton Clones. *Journal of Horticultural Science*, 41 (4), p.349–360. [Online]. Available at: doi:10.1080/00221589.1966.11514181.

Preston, A. P. (1967). Apple rootstock studies: fifteen years' results with some M.IX crosses. *Journal of Horticultural Science*, 42 (1), p.41–50. [Online]. Available at: doi:10.1080/00221589.1967.11514191.

Priestley, C. A. (1960). Seasonal changes in the carbohydrate resources of some six-year-old apple trees. *Annual Report East Malling Research Station 1959*.

Psarras, G., Merwin, I. A., Lakso, A. N. and Ray, J. A. (2000). Root growth phenology, root longevity, and rhizosphere respiration of field grown `mutsu' apple trees on `malling 9' rootstock. *Journal of the American Society for Horticultural Science*, 125 (5), p.596–602. [Online]. Available at: doi:10.21273/JASHS.125.5.596.

Rasmussen, A., Depuydt, S., Goormachtig, S. and Geelen, D. (2013). Strigolactones fine-tune the root system. *Planta*, 238 (4), p.615–626. [Online]. Available at: doi:10.1007/s00425-013-1911-3.

Reineke, R. A., Hackett, W. P. and Smith, A. G. (2002). Lignification Associated with Decreased Adventitious Rooting Competence of English Ivy Petioles. *Journal of environmental horticulture*, 20 (4), p.236–239. [Online]. Available at: doi:10.24266/0738-2898-20.4.236.

Ribeiro, C. L., Silva, C. M., Drost, D. R., Novaes, E., Novaes, C. R. D. B., Dervinis, C. and Kirst, M. (2016). Integration of genetic, genomic and transcriptomic information identifies putative regulators of adventitious root formation in Populus. *BMC Plant Biology*, 16, p.66. [Online]. Available at: doi:10.1186/s12870-016-0753-0.

Richards, D., Thompson, W. K. and Pharis, R. P. (1986). The Influence of Dwarfing Interstocks on the Distribution and Metabolism of Xylem-Applied [3H]Gibberellin A4 in Apple. *PLANT PHYSIOLOGY*, 82 (4), p.1090–1095. [Online]. Available at: doi:10.1104/pp.82.4.1090.

Robinson, T. L., Aldwinckle, H., Fazio, G. and Holleran, T. (2003). The geneva series of apple rootstocks from cornell: performance, disease resistance, and commercialization. *Acta horticulturae*, (622), p.513–520. [Online]. Available at: doi:10.17660/ActaHortic.2003.622.56.

Robinson, T. L. (2007). Effects of tree density and tree shape on apple orchard performance. *Acta horticulturae*, (732), p.405–414. [Online]. Available at: doi:10.17660/ActaHortic.2007.732.61.

Rogers, W. S. and Beakbane, A. B. (1957). Stock and scion relations. *Annual Review of Plant Physiology*, 8 (1), p.217–236. [Online]. Available at: doi:10.1146/annurev.pp.08.060157.001245.

van Rossum, G. (1995). Python reference manual. *Centrum voor Wiskunde en Informatica Amsterdam.*

Ruck, H. C. and Bolas, B. D. (1956). Studies in the comparative physiology of apple rootstocks. *Annals of Botany*, 20 (1), p.57–68. [Online]. Available at: doi:10.1093/oxfordjournals.aob.a083515.

Rudnicki, R. (1969). Studies on abscisic acid in apple seeds. *Planta*, 86 (1), p.63–68. [Online]. Available at: doi:10.1007/BF00385304.

Russo, N. L., Aldwinckle, H. S., Robinson, T. L. and Fazio, G. (2008). Budagovsky 9 rootstock: Uncovering a novel resistance to fire blight . *Acta horticulturae*, (793), p.321–324. [Online]. Available at: doi:10.17660/ActaHortic.2008.793.47.

R Core Team. (2020). R: a language and environment forstatistical computing. *R Foundation for Statistical Computing, Vienna, Austria*. [Online]. Available at: URL https://www.R-project.org/. [Accessed: 20 November 2023].

Sauer, M., Robert, S. and Kleine-Vehn, J. (2013). Auxin: simply complicated. *Journal of Experimental Botany*, 64 (9), p.2565–2577. [Online]. Available at: doi:10.1093/jxb/ert139.

Schindelin, J., Arganda-Carreras, I., Frise, E., Kaynig, V., Longair, M., Pietzsch, T., Preibisch, S., Rueden, C., Saalfeld, S., Schmid, B., Tinevez, J.-Y., White, D. J., Hartenstein, V., Eliceiri, K., Tomancak, P. and Cardona, A. (2012). Fiji: an open-source platform for biological-image analysis. *Nature Methods*, 9 (7), p.676–682. [Online]. Available at: doi:10.1038/nmeth.2019.

Schwechheimer, C. (2011). Gibberellin signaling in plants - the extended version. *Frontiers in Plant Science*, 2, p.107. [Online]. Available at: doi:10.3389/fpls.2011.00107.

Scotti-Saintagne, C., Bertocchi, E., Barreneche, T., Kremer, A. and Plomion, C. (2005). Quantitative trait loci mapping for vegetative propagation in pedunculate oak. *Annales des Sciences Forestières*, 62 (4), p.369–374. [Online]. Available at: doi:10.1051/forest:2005032.

Segura, V., Durel, C.-E. and Costes, E. (2009). Dissecting apple tree architecture into genetic, ontogenetic and environmental effects: QTL mapping. *Tree genetics & genomes*, 5 (1), p.165–179. [Online]. Available at: doi:10.1007/s11295-008-0181-x.

Seleznyova, A. N., Thorp, T. G., White, M., Tustin, S. and Costes, E. (2003). Application of architectural analysis and AMAPmod methodology to study dwarfing phenomenon: the branch structure of “Royal Gala” apple grafted on dwarfing and non-dwarfing rootstock/interstock combinations. *Annals of Botany*, 91 (6), p.665–672. [Online]. Available at: doi:10.1093/aob/mcg072.

Sharp, R. E. and LeNoble, M. E. (2002). ABA, ethylene and the control of shoot and root growth under water stress. *Journal of Experimental Botany*, 53 (366), p.33–37. [Online]. Available at: doi:10.1093/jexbot/53.366.33.

Shepherd, M., Huang, S., Eggler, P., Cross, M., Dale, G., Dieters, M. and Henry, R. (2006). Congruence in QTL for adventitious rooting in Pinus elliottii × Pinus caribaea hybrids resolves between and within-species effects. *Molecular Breeding*, 18 (1), p.11–28. [Online]. Available at: doi:10.1007/s11032-006-9006-5.

Silverstone, A. L., Chang, C., Krol, E. and Sun, T. P. (1997). Developmental regulation of the gibberellin biosynthetic gene GA1 in Arabidopsis thaliana. *The Plant Journal*, 12 (1), p.9–19. [Online]. Available at: doi:10.1046/j.1365-313x.1997.12010009.x.

Simons, R. K. and Chu, M. C. (1981). Morphological and anatomical characteristics of graft unions in apple trees on dwarfing rootstocks. *Acta horticulturae*, (114), p.198–199. [Online]. Available at: doi:10.17660/ActaHortic.1981.114.27.

Simons, R. K. and Chu, M. C. (1984). Tissue development within the graft union as related to dwarfing in apple. *Acta horticulturae*, (146), p.203–210. [Online]. Available at: doi:10.17660/ActaHortic.1984.146.22.

Simons, R. K. (1986). Graft-union characteristics as related to dwarfing in apple (malus domestica borkh.). *Acta horticulturae*, (160), p.57–66. [Online]. Available at: doi:10.17660/ActaHortic.1986.160.6.

Singh, J., Fabrizio, J., Desnoues, E., Silva, J. P., Busch, W. and Khan, A. (2019). Root system traits impact early fire blight susceptibility in apple (Malus × domestica). *BMC Plant Biology*, 19 (1), p.579. [Online]. Available at: doi:10.1186/s12870-019-2202-3.

Singh, V., Zemach, H., Shabtai, S., Aloni, R., Yang, J., Zhang, P., Sergeeva, L., Ligterink, W. and Firon, N. (2020). Proximal and distal parts of sweetpotato adventitious roots display differences in root architecture, lignin, and starch metabolism and their developmental fates. *Frontiers in Plant Science*, 11, p.609923. [Online]. Available at: doi:10.3389/fpls.2020.609923.

Siviero, A., Cristofani, M. and Machado, M. A. (2003). QTL mapping associated with rooting stem cuttings from Citrus sunki vs. Poncirus trifoliata hybrids. *Cropp Breeding and Applied Biotechnology*, 3 (1), p.83–88. [Online]. Available at: doi:10.12702/1984-7033.v03n01a12.

Soejima, J., Yoshida, Y., Haniuda, T., Bessho, H., Tsuchiya, S., Masuda, T., Komori, S., Sanada, T., Ito, Y., Sadamori, S. and Kashimura, Y. (2010). *New dwarfing apple rootstocks “JM 1”, “JM 7” and “JM 8”.*

Song, C., Zhang, D., Zhang, J., Zheng, L., Zhao, C., Ma, J., An, N. and Han, M. (2016). Expression analysis of key auxin synthesis, transport, and metabolism genes in different young dwarfing apple trees. *Acta physiologiae plantarum / Polish Academy of Sciences, Committee of Plant Physiology Genetics and Breeding*, 38 (2), p.43. [Online]. Available at: doi:10.1007/s11738-016-2065-2.

Soumelidou, K., Morris, D. A., Battey, N. H., Barnett, J. R. and John, P. (1994). Auxin transport capacity in relation to the dwarfing effect of apple rootstocks. *Journal of Horticultural Science*, 69 (4), p.719–725. [Online]. Available at: doi:10.1080/14620316.1994.11516505.

Souza, A. V. and Pereira, A. M. S. (2007). Enraizamento de plantas cultivadas in vitro. *Revista Brasileira de Plantas Medicinais, [s. l.],* 9 (4), p.103–117.

Steffens, B. and Rasmussen, A. (2016). The physiology of adventitious roots. *Plant Physiology*, 170 (2), p.603–617. [Online]. Available at: doi:10.1104/pp.15.01360.

Stenvall, N., Haapala, T. and Pulkkinen, P. (2004). Effect of Genotype, Age and Treatment of Stock Plants on Propagation of Hybrid Aspen (*Populus tremula* × *Populus tremuloides*) by Root Cuttings. *Scandinavian Journal of Forest Research*, 19 (4), p.303–311. [Online]. Available at: doi:10.1080/02827580410024115.

Stutte, G. W., Baugher, T. A., Walter, S. P., Leach, D. W., Glenn, D. M. and Tworkoski, T. J. (1994). Rootstock and Training System Affect Dry-matter and Carbohydrate Distribution in `Golden Delicious' Apple Trees. *Journal of the American Society for Horticultural Science*, 119 (3), p.492–497. [Online]. Available at: doi:10.21273/JASHS.119.3.492.

Süle, S. and Burr, T. J. (1998). The effect of resistance of rootstocks to crown gall (Agrobacterium spp.) on the susceptibility of scions in grape vine cultivars. *Plant Pathology*, 47 (1), p.84–88. [Online]. Available at: doi:10.1046/j.1365-3059.1998.00205.x.

Sun, P., Jia, H., Zhang, Y., Li, J., Lu, M. and Hu, J. (2019). Deciphering Genetic Architecture of Adventitious Root and Related Shoot Traits in Populus Using QTL

Mapping and RNA-Seq Data. *International Journal of Molecular Sciences*, 20 (24). [Online]. Available at: doi:10.3390/ijms20246114.

Tamura, F. (2012). Recent advances in research on japanese pear rootstocks. *Journal of the Japanese Society for Horticultural Science*, 81 (1), p.1–10. [Online]. Available at: doi:10.2503/jjshs1.81.1.

Teixeira da Silva, J. A., Gulyás, A., Magyar-Tábori, K., Wang, M.-R., Wang, Q.-C. and Dobránszki, J. (2019). In vitro tissue culture of apple and other Malus species: recent advances and applications. *Planta*, 249 (4), p.975–1006. [Online]. Available at: doi:10.1007/s00425-019-03100-x.

Torrey, J. G. (1976). Root hormones and plant growth. *Annual Review of Plant Physiology*, 27 (1), p.435–459. [Online]. Available at: doi:10.1146/annurev.pp.27.060176.002251.

Tworkoski, T. and Fazio, G. (2011). Physiological and morphological effects of size-controlling rootstocks on “fuji” apple scions. *Acta horticulturae*, (903), p.865–872. [Online]. Available at: doi:10.17660/ActaHortic.2011.903.120.

Tworkoski, T. and Fazio, G. (2015). Effects of Size-Controlling Apple Rootstocks on Growth, Abscisic Acid, and Hydraulic Conductivity of Scion of Different Vigor. *International Journal of Fruit Science*, 15 (4), p.369–381. [Online]. Available at: doi:10.1080/15538362.2015.1009973.

Tworkoski, T. and Fazio, G. (2016). Hormone and growth interactions of scions and size-controlling rootstocks of young apple trees. *Plant growth regulation*, 78 (1), p.105–119. [Online]. Available at: doi:10.1007/s10725-015-0078-2.

Uga, Y., Kitomi, Y., Yamamoto, E., Kanno, N., Kawai, S., Mizubayashi, T. and Fukuoka, S. (2015). A QTL for root growth angle on rice chromosome 7 is involved in the genetic pathway of DEEPER ROOTING 1. *Rice (New York, N.Y.)*, 8, p.8. [Online]. Available at: doi:10.1186/s12284-015-0044-7.

Untergasser, A., Cutcutache, I., Koressaar, T., Ye, J., Faircloth, B. C., Remm, M. and Rozen, S. G. (2012). Primer3--new capabilities and interfaces. *Nucleic Acids Research*, 40 (15), p.e115. [Online]. Available at: doi:10.1093/nar/gks596.

Valverdi, N. A., Cheng, L. and Kalcsits, L. (2019). Apple Scion and Rootstock Contribute to Nutrient Uptake and Partitioning under Different Belowground Environments. *Agronomy*, 9 (8), p.415. [Online]. Available at: doi:10.3390/agronomy9080415.

VAN Ooijen, J. W. (2011). Multipoint maximum likelihood mapping in a full-sib family of an outbreeding species. *Genetics research*, 93 (5), p.343–349. [Online]. Available at: doi:10.1017/S0016672311000279.

Veierskov, B. (1988). Relations between carbohydrates and adventitious root formation. *Advances in plant sciences series (USA)*.

Velasco, R., Zharkikh, A., Affourtit, J., Dhingra, A., Cestaro, A., Kalyanaraman, A., Fontana, P., Bhatnagar, S. K., Troggio, M., Pruss, D., Salvi, S., Pindo, M., Baldi, P., Castelletti, S., Cavaiuolo, M., Coppola, G., Costa, F., Cova, V., Dal Ri, A., Goremykin, V., Komjanc, M., Longhi, S., Magnago, P., Malacarne, G., Malnoy, M., Micheletti, D., Moretto, M., Perazzolli, M., Si-Ammour, A., Vezzulli, S., Zini, E., Eldredge, G., Fitzgerald, L. M., Gutin, N., Lanchbury, J., Macalma, T., Mitchell, J. T., Reid, J., Wardell, B., Kodira, C., Chen, Z., Desany, B., Niazi, F., Palmer, M., Koepke, T., Jiwan, D., Schaeffer, S., Krishnan, V., Wu, C., Chu, V. T., King, S. T., Vick, J., Tao, Q., Mraz, A., Stormo, A., Stormo, K., Bogden, R., Ederle, D., Stella, A., Vecchietti, A., Kater, M. M., Masiero, S., Lasserre, P., Lespinasse, Y., Allan, A. C., Bus, V., Chagné, D., Crowhurst, R. N., Gleave, A. P., Lavezzo, E., Fawcett, J. A., Proost, S., Rouzé, P., Sterck, L., Toppo, S., Lazzari, B., Hellens, R. P., Durel, C.-E., Gutin, A., Bumgarner, R. E., Gardiner, S. E., Skolnick, M., Egholm, M., Van de Peer, Y., Salamini, F. and Viola, R. (2010). The genome of the domesticated apple (Malus × domestica Borkh.). *Nature Genetics*, 42 (10), p.833–839. [Online]. Available at: doi:10.1038/ng.654.

Verma, P., Chauhan, P. S., Chandel, J. S. and Thakur, M. (2015). Effect of the size of cuttings (length and diameter) on rooting in cuttings of apple clonal rootstock Merton

793. *Journal of Applied and Natural Science*, 7 (2), p.602–605. [Online]. Available at: doi:10.31018/jans.v7i2.652.

Webster, A. D., Tobutt, K. and Evans, K. (2000). *Breeding and Evaluation of New Rootstocks for Apple, Pear and Sweet Cherr*. In: 6 February 2000, International dwarf fruit association.

Webster, A. D. (1995a). Rootstock and interstock effects on deciduous fruit tree vigour, precocity, and yield productivity. *New Zealand journal of crop and horticultural science*, 23 (4), p.373–382. [Online]. Available at: doi:10.1080/01140671.1995.9513913.

Webster, A. D. (1995b). Temperate fruit tree rootstock propagation. *New Zealand journal of crop and horticultural science*, 23 (4), p.355–372. [Online]. Available at: doi:10.1080/01140671.1995.9513912.

Webster, A. D. (2004). Vigour mechanisms in dwarfing rootstocks for temperate fruit trees. *Acta horticulturae*, (658), p.29–41. [Online]. Available at: doi:10.17660/ActaHortic.2004.658.1.

Webster, C. A., Howard, B. H. and Harrison-Murray, R. S. (1990). Factors involved in the rooting response of apple winter cuttings to high basal temperatures. *Journal of Horticultural Science*, 65 (1), p.7–14. [Online]. Available at: doi:10.1080/00221589.1990.11516021.

van der Weele, C. M., Spollen, W. G., Sharp, R. E. and Baskin, T. I. (2000). Growth of Arabidopsis thaliana seedlings under water deficit studied by control of water potential in nutrient-agar media. *Journal of Experimental Botany*, 51 (350), p.1555–1562. [Online]. Available at: doi:10.1093/jexbot/51.350.1555.

Wei, T. and Simko, V. (2021). *R package "corrplot": Visualization of a Correlation Matrix. (Version 0.92)*. [Online]. Available at: https://taiyun.github.io/corrplot/ [Accessed: 29 October 2023].

Welander, M. (1983). In vitro rooting of the apple rootstock M 26 in adult and juvenile growth phases and acclimatization of the plantlets. *Physiologia Plantarum*, 58 (3), p.231–238. [Online]. Available at: doi:10.1111/j.1399-3054.1983.tb04174.x.

Werner, T., Motyka, V., Laucou, V., Smets, R., Van Onckelen, H. and Schmülling, T. (2003). Cytokinin-deficient transgenic Arabidopsis plants show multiple developmental alterations indicating opposite functions of cytokinins in the regulation of shoot and root meristem activity. *The Plant Cell*, 15 (11), p.2532–2550. [Online]. Available at: doi:10.1105/tpc.014928.

Werner, T., Motyka, V., Strnad, M. and Schmülling, T. (2001). Regulation of plant growth by cytokinin. *Proceedings of the National Academy of Sciences of the United States of America*, 98 (18), p.10487–10492. [Online]. Available at: doi:10.1073/pnas.171304098.

Wertheim, S. J. and Webster, A. D. (2003). Propagation and nursery tree quality. In: Ferree, D. C. and Warrington, I. J. (eds.), *Apples: botany, production and uses*, Wallingford: CABI, p.125–151. [Online]. Available at: doi:10.1079/9780851995922.0125.

White, P. J., George, T. S., Gregory, P. J., Bengough, A. G., Hallett, P. D. and McKenzie, B. M. (2013). Matching roots to their environment. *Annals of Botany*, 112 (2), p.207–222. [Online]. Available at: doi:10.1093/aob/mct123.

Wickham, H. (2016). *ggplot2 - Elegant Graphics for Data Analysis*. 2nd ed. Cham: Springer International Publishing. [Online]. Available at: doi:10.1007/978-3-319-24277-4.

Yan, T., Mei, C., Song, H., Shan, D., Sun, Y., Hu, Z., Wang, L., Zhang, T., Wang, J. and Kong, J. (2022). Potential roles of melatonin and ABA on apple dwarfing in semi-arid area of Xinjiang China. *PeerJ*, 10, p.e13008. [Online]. Available at: doi:10.7717/peerj.13008.

Zagaja, S. W. (1981). Performance of two apple cultivars on p series dwarf rootstocks. *Acta horticulturae*, (114), p.162–169. [Online]. Available at: doi:10.17660/ActaHortic.1981.114.22.

Zalesny, R. S. and Wiese, A. H. (2006). Date of shoot collection, genotype, and original shoot position affect early rooting of dormant hardwood cuttings of populus. *Silvae genetica*, 55 (1–6), p.169–182. [Online]. Available at: doi:10.1515/sg-2006-0024.

Zeevaart, J. A. D. and Creelman, R. A. (1988). Metabolism and physiology of abscisic acid. *Annual review of plant physiology and plant molecular biology*, 39 (1), p.439–473. [Online]. Available at: doi:10.1146/annurev.pp.39.060188.002255.

Zhang, B., Tong, C., Yin, T., Zhang, X., Zhuge, Q., Huang, M., Wang, M. and Wu, R. (2009). Detection of quantitative trait loci influencing growth trajectories of adventitious roots in Populus using functional mapping. *Tree genetics & genomes*, 5 (3), p.539–552. [Online]. Available at: doi:10.1007/s11295-009-0207-z.

Zhang, H., An, H. S., Wang, Y., Zhang, X. Z. and Han, Z. H. (2015). Low expression of PIN gene family members is involved in triggering the dwarfing effect in M9 interstem but not in M9 rootstock apple trees. *Acta physiologiae plantarum / Polish Academy of Sciences, Committee of Plant Physiology Genetics and Breeding*, 37 (5), p.104. [Online]. Available at: doi:10.1007/s11738-015-1851-6.

Zhao, K., Zhang, F., Yang, Y., Ma, Y., Liu, Y., Li, H., Dai, H. and Zhang, Z. (2016). Modification of Plant Height via RNAi Suppression of MdGA20-ox Gene Expression in Apple. *Journal of the American Society for Horticultural Science*, 141 (3), p.242–248. [Online]. Available at: doi:10.21273/JASHS.141.3.242.

Zheng, C., Shen, F., Wang, Y., Wu, T., Xu, X., Zhang, X. and Han, Z. (2020). Intricate genetic variation networks control the adventitious root growth angle in apple. *BMC Genomics*, 21 (1), p.852. [Online]. Available at: doi:10.1186/s12864-020-07257-8.

Zheng, X., Zhao, Y., Shan, D., Shi, K., Wang, L., Li, Q., Wang, N., Zhou, J., Yao, J., Xue, Y., Fang, S., Chu, J., Guo, Y. and Kong, J. (2018). MdWRKY9 overexpression confers intensive dwarfing in the M26 rootstock of apple by directly inhibiting brassinosteroid synthetase MdDWF4 expression. *The New Phytologist*, 217 (3), p.1086–1098. [Online]. Available at: doi:10.1111/nph.14891.

Zhou, S., Shen, Z., Yin, B., Liang, B., Li, Z., Zhang, X. and Xu, J. (2022). Effects of dwarfing interstock length on the growth and fruit of apple tree. *Horticulturae*, 9 (1), p.40. [Online]. Available at: doi:10.3390/horticulturae9010040.

Supplementary data

		M.13		Ottawa 3		M306-006	
Markers Chr5	**Mb**	**H1**	**H2**	**H1**	**H2**	**H1**	**H2**
CH03a09	41.4	132	130	132	138	132	128
MD5002	41.9	204	208	204	220	204	200
MD5003	42.2	141	162	141	162	141	138
MD5006	43.1	235	245	NA	NA	NA	NA
MD5007	45.2	264	264	NA	NA	NA	NA
MD5004	45.6	252	252	250	248	250	252
Markers Chr11	**Mb**	**H1**	**H2**	**H1**	**H2**	**H1**	**H2**
MD11001	6.9	197	197	186	220	220	233
MD11004	7.5	191	191	NA	NA	NA	NA
MD11005	8.3	116	116	NA	NA	NA	NA
MD11002	9.8	155	155	145	142	140	140
MD11006	10.4	168	170	NA	NA	NA	NA
MD11007	10.9	158	153	NA	NA	NA	NA
MD11003	12.7	265	276	266	278	268	276

		SJM15		SJP84-5231		SJP84-5162		SJP84-5217	
Markers Chr5	**Mb**	**H1**	**H2**	**H1**	**H2**	**H1**	**H2**	**H1**	**H2**
CH03a09	41.4	132	120	132	120	132	120	132	130
MD5002	41.9	204	199	204	199	204	199	204	null
MD5003	42.2	141	175	141	140	141	140	141	null
MD5006	43.1	NA	NA	NA	NA	NA	NA	NA	NA
MD5007	45.2	NA	NA	NA	NA	NA	NA	NA	NA
MD5004	45.6	250	236	248	246	250	246	250	250
Markers Chr11	**Mb**	**H1**	**H2**	**H1**	**H2**	**H1**	**H2**	**H1**	**H2**
MD11001	6.9	212	212	195	212	195	212	null	212
MD11004	7.5	NA	NA	NA	NA	NA	NA	NA	NA
MD11005	8.3	NA	NA	NA	NA	NA	NA	NA	NA
MD11002	9.8	146	142	140	142	140	142	142	142
MD11006	10.4	NA	NA	NA	NA	NA	NA	NA	NA
MD11007	10.9	NA	NA	NA	NA	NA	NA	NA	NA
MD11003	12.7	272	272	262	272	262	272	null	272

Supplementary Figure S1. Estimated haplotypes of M.13, Ottawa 3 and non-recombinant rootstocks from RF185 and SP250 plots showing allele sizes for markers included the first multiplex developed in this study. The dwarfing alleles are highlighted in blue. NA: marker not tested. Thick lines indicate recombination sites.

		AR835-11		R104		R59		R80	
Markers Chr5	Mb	H1	H2	H1	H2	H1	H2	H1	H2
CH03a09	41.4	132	130	132	120	132	128	132	132
MD5002	41.9	204	208	202	199	204	200	204	204
MD5003	42.2	141	162	150	140	141	138	141	150
MD5006	43.1	NA	NA	NA	NA	NA	NA	NA	NA
MD5007	45.2	NA	NA	NA	NA	NA	NA	NA	NA
MD5004	45.6	250	250	250	250	248	250	250	250
Markers Chr11	Mb	H1	H2	H1	H2	H1	H2	H1	H2
MD11001	6.9	200	220	204	null	195	204	195	212
MD11004	7.5	NA	NA	NA	NA	NA	NA	NA	NA
MD11005	8.3	NA	NA	NA	NA	NA	NA	NA	NA
MD11002	9.8	139	142	159	142	140	159	155	142
MD11006	10.4	NA	NA	NA	NA	NA	NA	NA	NA
MD11007	10.9	NA	NA	NA	NA	NA	NA	NA	NA
MD11003	12.7	275	278	266	null	262	266	270	272

		B24		AR10-3-9		AR839-9		AR809-3	
Markers Chr5	Mb	H1	H2	H1	H2	H1	H2	H1	H2
CH03a09	41.4	132	132	132	130	128	132	132	132
MD5002	41.9	204	212	202	208	200	202	204	204
MD5003	42.2	141	152	150	162	138	150	141	141
MD5006	43.1	NA	NA	NA	NA	NA	NA	NA	NA
MD5007	45.2	NA	NA	NA	NA	NA	NA	NA	NA
MD5004	45.6	248	250	250	252	250	250	250	250
Markers Chr11	Mb	H1	H2	H1	H2	H1	H2	H1	H2
MD11001	6.9	218	220	197	204	204	220	195	212
MD11004	7.5	NA	NA	NA	NA	NA	NA	NA	NA
MD11005	8.3	NA	NA	NA	NA	NA	NA	NA	NA
MD11002	9.8	138	140	155	159	159	140	155	142
MD11006	10.4	NA	NA	NA	NA	NA	NA	NA	NA
MD11007	10.9	NA	NA	NA	NA	NA	NA	NA	NA
MD11003	12.7	266	268	276	266	268	266	270	272

Supplementary Figure S2. Estimated haplotypes of non-recombinant rootstocks from EE207 and VF224 plots showing allele sizes for markers included the first multiplex developed in this study. The dwarfing alleles are highlighted in blue. NA: marker not tested. Thick lines indicate recombination sites.

Supplementary Table S1. Rootstocks cultivars and selections from breeding trials RF185, EE207, SP250 and VF224 used for fine mapping the root bark QTL, scion grafted, root bark percentage, standard deviation and dwarfing level based on the evaluation of breeders.

Trial	Rootstock	Scion	RB%±SD	Dw level*
RF185	M.9	Gala	69.4±0.65	D
	M.116	Gala	57.1±4.51	SV
	M.M106	Gala	55.8±4.73	SV
	M306-6	Gala	58.5±0.99	SV
	M306-79	Gala	59.4±1.43	SD
	M306-189	Gala	66.1±3.58	VD to D
EE207	M.27	Braeburn	67.3±3.16	VD
	M.27	Royal Gala	70.1±3.31	VD
	M.9	Braeburn	63.1±3.66	D
	M.9	Royal Gala	71.3±3.38	D
	M.26	Braeburn	53.1±3.63	SV
	M.26	Royal Gala	58.6±4.94	SV
	AR852-3	Braeburn	53.1±7.96	SD to SV
	AR852-3	Royal Gala	64.1±8.25	SD to SV
	AR839-9	Braeburn	56.5±3.64	D to SD
	AR839-9	Royal Gala	56.5±4.74	D to SD
	B24	Braeburn	45.6±3.87	SV
	B24	Royal Gala	60.5±6.41	SV
	R104	Braeburn	54.0±3.37	D to SD
	R104	Royal Gala	52.6±4.75	D to SD
	R59	Braeburn	63.7±4.50	VD

	R59	Royal Gala	64.1±7.14	VD
SP250	M.9	Braeburn	64.7±1.71	D
	M.9	Gala	73.5±0.95	D
	M.26	Braeburn	62.0±3.25	SD
	M.26	Gala	67.6±6.85	SD
	M.M.106	Braeburn	51.0±1.98	SV
	M.M.106	Gala	58.3±3.39	SV
	SJM167	Braeburn	51.4±6.13	SD to SV
	SJM167	Gala	62.3±4.26	SD to SV
	SJM188	Braeburn	58.2±4.75	SD
	SJM189	Gala	66.0±6.26	D
	SJP84-5217	Braeburn	54.7±2.81	SV
	SJP84-5217	Gala	54.3±5.92	SV
	SJP84-5174	Braeburn	62.3±1.21	SD
	SJP84-5174	Gala	62.2±0.75	SD
	SJP84-5162	Braeburn	63.8±4.80	D
	SJP84-5231	Gala	79.8±3.74	D
	SJM15	Gala	61.9±10.1	VD
VF224	M.116	Red Falstaff	56.1±2.42	SV
	M.M.106	Red Falstaff	51.9±2.80	SV
	AR10-3-9	Red Falstaff	56.6±4.51	SV
	AR809-3	Red Falstaff	60.0±2.09	D
	AR835-11	Red Falstaff	57.4±3.15	SV
	R80	Red Falstaff	57.2±2.69	SD to SV

* Dwarfing level asigned by breeder after several year of phenotyping traits associated with rootstock-induced dwarfing such as trunk cross-sectional area, tree volume, tree height and yield. VD: very dwarfing; D: dwarfing; SD: semi-dwarfing; SV: semi-vigorous.

EFFECT OF SCION ON ROOT BARK PERCENTAGE IN EE207 AND SP250 TRIALS

Supplementary Table S2. Estimated marginal means (EMMs) for linear mixed model of each rootstock per scion for root bark percentage in trial EE207. Degrees of freedom method: Kenward-roger. Confidence level used: 0.95

Rootstock	Scion	emmean	SE	df	Lower.CL	Upper.CL
AR839-9	**Braeburn**	56.5	1.51	76.2	53.5	59.5
AR839-9	**Royal Gala**	56.5	1.97	77.0	52.6	60.4
AR852-3	**Braeburn**	53.1	2.16	79.0	48.8	57.4
AR852-3	**Royal Gala**	64.0	2.79	79.0	58.5	69.6
B24	**Braeburn**	45.6	2.16	79.0	41.3	49.9
B24	**Royal Gala**	60.5	2.16	76.2	56.2	64.8
M26	**Braeburn**	53.0	1.59	78.0	49.9	56.2
M26	**Royal Gala**	58.6	1.81	77.5	54.9	62.2
M27	**Braeburn**	67.3	1.68	79.0	63.9	70.7
M27	**Royal Gala**	70.1	2.41	79.0	65.3	74.9
M9	**Braeburn**	63.1	1.81	79.0	59.5	66.7
M9	**Royal Gala**	71.4	1.96	79.0	67.5	75.3
R104	**Braeburn**	54.0	2.42	79.0	49.2	58.8
R104	**Royal Gala**	52.6	2.79	79.0	47.1	58.2
R59	**Braeburn**	63.7	1.81	79.0	60.1	67.3
R59	**Royal Gala**	64.1	1.96	79.0	60.2	68.0

Supplementary Table S3. Comparison test between scions within each rootstock for root bark percentage in trial EE207. Degrees-of-freedom method: kenward-roger.

Rootstock	Contrast	estimate	SE	df	t.ratio	p.value
AR839-9	**Braeburn - RG**	0.0447	2.48	76.7	0.018	0.9857
AR852-3	**Braeburn - RG**	-10.9567	3.52	79.0	-3.109	**0.0026**
B24	**Braeburn - RG**	-14.9660	3.05	78.2	-4.906	**<0.0001**
M26	**Braeburn - RG**	-5.5083	2.41	77.8	-2.282	**0.0252**
M27	**Braeburn - RG**	-2.8300	2.94	79.0	-0.963	0.3384
M9	**Braeburn - RG**	-8.3062	2.66	79.0	-3.120	**0.0025**
R104	**Braeburn - RG**	1.3822	3.69	79.0	0.374	0.7092
R59	**Braeburn - RG**	-0.4812	2.66	79.0	-0.181	0.8571

RG: Royal Gala

Supplementary Table S4. Estimated marginal means (EMMs) for linear mixed model of each rootstock per scion for root bark percentage in trial SP250. Degrees of freedom method: Kenward-roger. Confidence level used: 0.95

Rootstock	Scion	emmean	SE	df	Lower.CL	Upper.CL
M26	**Braeburn**	62.1	2.08	30.9	57.9	66.3
M26	**Gala**	67.5	2.08	30.9	63.2	71.7
M9	**Braeburn**	64.7	2.42	31.0	59.7	69.6
M9	**Gala**	73.6	2.08	30.9	69.3	77.8
MM106	**Braeburn**	51.1	2.08	30.9	46.9	55.4
MM106	**Gala**	58.2	2.08	30.9	54.0	62.5
SJM167	**Braeburn**	51.4	2.08	30.9	47.2	55.7
SJM167	**Gala**	62.4	2.08	30.9	58.2	66.7
SJP84-5174	**Braeburn**	62.0	2.96	31.0	56.0	68.0
SJP84-5174	**Gala**	62.5	2.98	31.0	56.4	68.5
SJP84-5217	**Braeburn**	55.6	2.08	30.9	51.3	59.8
SJP84-5217	**Gala**	54.3	2.08	30.9	50.1	58.5

Supplementary Table S5. Comparison test between scions within each rootstock for root bark percentage in trial SP250. Degrees-of-freedom method: kenward-roger.

Rootstock	Contrast	estimate	SE	df	t.ratio	p.value
M26	**Braeburn - Gala**	-5.385	2.86	27.7	-1.880	0.0706
M9	**Braeburn - Gala**	-8.912	3.13	28.4	-2.843	**0.0082**
MM106	**Braeburn - Gala**	-7.105	2.86	27.7	-2.481	**0.0195**
SJM167	**Braeburn - Gala**	-11.005	2.91	29.4	-3.788	**0.0007**
SJP84-5174	**Braeburn - Gala**	-0.454	4.24	30.8	-0.107	0.9153
SJP84-5217	**Braeburn - Gala**	1.265	2.86	27.6	0.442	0.6622

Supplementary Table S6. Linkage group, QTL provenance and location in the GD genome of the most significant haploblock associated with primary root length in seedlings and percentage of rooting in the stoolbeds in the MDX132 population.

Trait	LG	Most significant HB	QTL provenance	Location of most significant HB in the GD genome (Mb)
Primary root length in seedlings	1	HB30	M.9	28.0 to 28.38
	2	HB5	GD	2.60 to 2.89
	17	HB29	M.9	21.92 to 21.93
% Rooting stoolbeds 2019	5	HB8	M.9	44.12 to 44.37
% Rooting stoolbeds 2020	5	HB8	M.9	44.12 to 44.37
	11	HB26	GD	27.0 to 27.49

INITIAL ROOT SURFACE AREA

Supplementary Table S7. ANOVA table of fixed effects for the initial root surface area (logarithmic transformed). Significant p-values in bold.

	Df	Sum Sq	Mean Sq	F value	Pr(>F)
Rb1	1	6.41	6.41	18.97	**0.0001**
Rb2	1	0.60	0.60	1.78	0.19
Rb1 x Rb2	1	0.83	0.83	2.46	0.12
Residuals	35	11.82	0.33		

Supplementary Table S8. Estimated marginal means (EMMs) of the ANOVA for each root bark QTL group for initial root surface area in the root architecture experiment. Confidence level used: 0.95.

RB QTL	emmean	SE	df	Lower.CL	Upper.CL
NoRb	9.80	0.194	35	9.40	10.2
Rb1	10.30	0.184	35	9.93	10.7
Rb2	9.71	0.205	35	9.30	10.1
Rb1Rb2	10.81	0.168	35	10.47	11.1

Supplementary Table S9. Multiple comparison test of root bark QTL for initial root surface area in the root architecture experiment. P value adjustment: tukey method for comparing a family of 4 estimates. Significant p-values in bold.

contrast	estimate	SE	df	t.ratio	p.value
NoRb – *Rb1*	-0.5012	0.267	35	-1.877	0.2563
NoRb – *Rb2*	0.0836	0.282	35	0.296	0.9908
NoRb – *Rb1Rb2*	-1.0091	0.256	35	-3.937	**0.0020**
Rb1* – *Rb2	0.5848	0.276	35	2.121	0.1663
Rb1* – *Rb1Rb2	-0.5079	0.249	35	-2.041	0.1928
Rb2 – Rb1Rb2	-1.0927	0.265	35	-4.119	**0.0012**

TREE HEIGHT

Supplementary Table S10. Estimated marginal means (EMMs) for linear mixed model of each root bark QTL group within each time point for tree height in the root architecture experiment. Results are averaged over the levels of: block. Degrees of freedom method: Kenward-roger. Confidence level used: 0.95

Time point	RB QTL group	emmean	SE	df	Lower.CL	Upper.CL
TP1	**NoRb**	56.8	3.81	75.3	49.3	64.4
TP1	***Rb1***	45.7	3.62	75.2	38.5	52.9
TP1	***Rb2***	46.4	4.03	75.7	41.9	55.0
TP1	***Rb1Rb2***	48.4	3.29	75.7	38.3	54.4
TP2	**NoRb**	97.8	3.81	75.3	90.3	105.4
TP2	***Rb1***	84.9	3.62	75.2	77.7	92.1
TP2	***Rb2***	90.1	4.03	75.7	82.1	98.2
TP2	***Rb1Rb2***	84.0	3.29	75.7	77.4	90.6
TP3	**NoRb**	114.2	3.81	75.3	106.6	121.8
TP3	***Rb1***	102.3	3.62	75.2	95.1	109.5
TP3	***Rb2***	106.9	4.03	75.7	98.8	113.9
TP3	***Rb1Rb2***	98.8	3.29	75.7	92.2	105.3
TP4	**NoRb**	122.6	3.81	75.3	115.0	130.2
TP4	***Rb1***	106.5	3.62	75.2	99.3	113.7
TP4	***Rb2***	116.4	4.03	75.7	108.3	124.4
TP4	***Rb1Rb2***	102.8	3.29	75.7	96.2	109.3

Supplementary Table S11. Multiple comparison test of root bark QTL groups within each time point for tree height in the root architecture experiment. Results are averaged over the levels of: Block. Degrees-of-freedom method: kenward-roger. P value adjustment: tukey method for comparing a family of 4 estimates. Significant p-values in bold.

TP	contrast	estimate	SE	df	t.ratio	p.value
TP1	**NoRb – *Rb1***	11.159	5.26	75.1	2.121	0.1560
TP1	**NoRb – *Rb1Rb2***	8.429	5.04	75.5	1.674	0.3445
TP1	**NoRb – *Rb2***	10.417	5.55	75.5	1.888	0.2420
TP1	***Rb1* – *Rb1Rb2***	-2.730	4.89	75.5	-0.558	0.9440
TP1	***Rb1* – *Rb2***	-0.689	5.42	75.5	-0.127	0.9993
TP1	***Rb1Rb2* – *Rb2***	2.042	5.20	75.7	0.392	0.9794
TP2	**NoRb – *Rb1***	12.959	5.26	75.1	2.463	0.0743
TP2	**NoRb – *Rb1Rb2***	13.846	5.04	75.5	2.750	**0.0367**
TP2	**NoRb – *Rb2***	7.721	5.55	75.5	1.392	0.5083
TP2	***Rb1* – *Rb1Rb2***	0.886	4.89	75.5	0.181	0.9979
TP2	***Rb1* – *Rb2***	-5.239	5.42	75.5	-0.967	0.7684
TP2	***Rb1Rb2* – *Rb2***	-6.125	5.20	75.7	-1.177	0.6432
TP3	**NoRb – *Rb1***	11.893	5.26	75.1	2.260	0.1168
TP3	**NoRb – *Rb1Rb2***	15.429	5.04	75.5	3.064	**0.0157**
TP3	**NoRb – *Rb2***	7.304	5.55	75.5	1.317	0.5553
TP3	***Rb1* – *Rb1Rb2***	3.536	4.89	75.5	0.723	0.8876

TP3	***Rb1 – Rb2***	-4.589	5.42	75.5	-0.847	0.8317
TP3	***Rb1Rb2 – Rb2***	-8.125	5.20	75.7	-1.561	0.4068
TP4	**NoRb – *Rb1***	16.137	5.26	75.1	3.067	**0.0156**
TP4	**NoRb – *Rb1Rb2***	19.873	5.04	75.5	3.947	**0.0010**
TP4	**NoRb – *Rb2***	6.248	5.55	75.5	1.126	0.6745
TP4	***Rb1 – Rb1Rb2***	3.736	4.89	75.5	0.764	0.8703
TP4	***Rb1 – Rb2***	-9.889	5.42	75.5	-1.826	0.2694
TP4	***Rb1Rb2 – Rb2***	-13.625	5.20	75.7	-2.618	0.0511

TRUNK DIAMETER ABOVE GRAFT UNION

Supplementary Table S12. Estimated marginal means (EMMs) for linear mixed model of each block for trunk diameter above the graft union in the root architecture experiment. Results are averaged over the levels of: *Rb1, Rb2* and TP. Degrees of freedom method: Kenward-roger. Confidence level used: 0.95.

Block	emmean	SE	df	Lower.CL	Upper.CL
A	7.55	0.203	32	7.13	7.96
B	7.63	0.203	32	7.22	8.04
C	8.05	0.213	32	7.61	8.48
D	6.92	0.203	32	6.50	7.33

Supplementary Table S13. Multiple comparison test of blocks for trunk diameter above the graft union in the root architecture experiment. Results are averaged over the levels of: *Rb1, Rb2* and TP. Degrees-of-freedom method: kenward-roger. P value adjustment: tukey method for comparing a family of 4 estimates. Significant p-values in bold.

contrast	estimate	SE	df	t.ratio	p.value
A – B	-0.0836	0.286	32	-0.292	0.9912
A – C	-0.4999	0.293	32	-1.704	0.3383
A – D	0.6300	0.285	32	2.211	0.1420
B – C	-0.4163	0.293	32	-1.419	0.4973
B – D	0.7136	0.286	32	2.491	0.0806
C – D	1.1299	0.293	32	3.852	**0.0028**

Supplementary Table S14. Estimated marginal means (EMMs) for linear mixed model of each root bark QTL group within each time point for trunk diameter above the graft union in the root architecture experiment. Results are averaged over the levels of: block. Degrees of freedom method: Kenward-roger. Confidence level used: 0.95.

Time point	RB QTL group	emmean	SE	df	Lower.CL	Upper.CL
TP1	**NoRb**	4.92	0.257	63.6	4.41	5.44
TP1	***Rb1***	3.96	0.244	63.5	3.47	4.44
TP1	***Rb2***	4.15	0.272	63.9	3.61	4.69
TP1	***Rb1Rb2***	4.11	0.222	63.9	3.67	4.56
TP2	**NoRb**	7.83	0.257	63.6	7.31	8.34
TP2	**Rb1**	6.60	0.244	63.5	6.11	7.08
TP2	**Rb2**	7.28	0.272	63.9	6.73	7.82
TP2	**Rb1Rb2**	6.75	0.222	63.9	6.31	7.19
TP3	**NoRb**	9.44	0.257	63.6	8.93	9.96
TP3	***Rb1***	8.14	0.244	63.5	7.65	8.63
TP3	***Rb2***	9.12	0.272	63.9	8.58	9.67
TP3	***Rb1Rb2***	8.04	0.222	63.9	7.60	8.48
TP4	**NoRb**	10.93	0.257	63.6	10.42	11.45
TP4	***Rb1***	9.42	0.244	63.5	8.93	9.90
TP4	***Rb2***	10.65	0.272	63.9	10.11	11.20
TP4	***Rb1Rb2***	9.22	0.222	63.9	8.77	9.66

Supplementary Table S15. Multiple comparison test of root bark QTL groups within each time point for trunk diameter above the graft union in the root architecture experiment. Results are averaged over the levels of: Block. Degrees-of-freedom method: kenward-roger. P value adjustment: tukey method for comparing a family of 4 estimates. Significant p-values in bold.

TP	contrast	estimate	SE	df	t.ratio	p.value
TP1	**NoRb – *Rb1***	0.9682	0.355	63.4	2.726	**0.0403**
TP1	**NoRb – *Rb1Rb2***	0.8122	0.340	63.7	2.391	0.0892
TP1	**NoRb – *Rb2***	0.7726	0.374	63.7	2.064	0.1759
TP1	***Rb1* – *Rb1Rb2***	-0.1560	0.330	63.7	-0.473	0.9648
TP1	***Rb1* – *Rb2***	-0.1956	0.365	63.7	-0.535	0.9501
TP1	***Rb1Rb2* – *Rb2***	0.0396	0.351	63.9	0.113	0.9995
TP2	**NoRb – *Rb1***	1.2315	0.355	63.4	3.467	**0.0051**
TP2	**NoRb – *Rb1Rb2***	1.0780	0.340	63.7	3.173	**0.0121**
TP2	**NoRb – *Rb2***	0.5509	0.374	63.7	1.472	0.4601
TP2	***Rb1* – *Rb1Rb2***	-0.1535	0.330	63.7	-0.465	0.9664
TP2	***Rb1* – *Rb2***	-0.6806	0.365	63.7	-1.862	0.2545
TP2	***Rb1Rb2* – *Rb2***	0.5271	0.351	63.9	1.501	0.4427
TP3	**NoRb – *Rb1***	1.3000	0.355	63.4	3.660	**0.0028**
TP3	**NoRb – *Rb1Rb2***	1.4008	0.340	63.7	4.123	**0.0006**
TP3	**NoRb – *Rb2***	0.3179	0.374	63.7	0.849	0.8306
TP3	***Rb1* – *Rb1Rb2***	0.1008	0.330	63.7	0.306	0.9900

TP3	***Rb1 – Rb2***	-0.9821	0.365	63.7	-2.688	**0.0443**
TP3	***Rb1Rb2 – Rb2***	1.0829	0.351	63.9	3.085	**0.0155**
TP4	**NoRb – *Rb1***	1.5160	0.355	63.4	4.268	**0.0004**
TP4	**NoRb – *Rb1Rb2***	1.7158	0.340	63.7	5.051	**<0.0001**
TP4	**NoRb – *Rb2***	0.2791	0.374	63.7	0.746	0.8781
TP4	***Rb1 – Rb1Rb2***	0.1998	0.330	63.7	0.606	0.9299
TP4	***Rb1 – Rb2***	-1.2368	0.365	63.7	-3.385	**0.0066**
TP4	***Rb1Rb2 – Rb2***	1.4367	0.351	63.9	4.092	**0.0007**

TRUNK DIAMETER BELOW GRAFT UNION

Supplementary Table S16. Estimated marginal means (EMMs) for linear mixed model of each root bark QTL group within each time point for trunk diameter below the graft union in the root architecture experiment. Results are averaged over the levels of: block. Degrees of freedom method: Kenward-roger. Confidence level used: 0.95.

Time point	RB QTL group	emmean	SE	df	Lower.CL	Upper.CL
TP1	**NoRb**	9.64	0.542	38.3	8.54	10.7
TP1	***Rb1***	9.33	0.515	38.2	8.28	10.4
TP1	***Rb2***	9.94	0.573	38.3	8.78	11.1
TP1	***Rb1Rb2***	9.38	0.468	38.3	8.43	10.3
TP2	**NoRb**	11.56	0.542	38.3	10.46	12.7
TP2	***Rb1***	10.93	0.515	38.2	9.89	12.0
TP2	***Rb2***	11.39	0.573	38.3	10.23	12.5
TP2	***Rb1Rb2***	10.95	0.468	38.3	10.00	11.9
TP3	**NoRb**	12.61	0.542	38.3	11.51	13.7
TP3	***Rb1***	12.08	0.515	38.2	11.04	13.1
TP3	***Rb2***	12.79	0.573	38.3	11.63	14.0
TP3	***Rb1Rb2***	12.21	0.468	38.3	11.27	13.2
TP4	**NoRb**	13.83	0.542	38.3	12.73	14.9
TP4	***Rb1***	13.25	0.515	38.2	12.21	14.3
TP4	***Rb2***	14.18	0.573	38.3	13.02	15.3
TP4	***Rb1Rb2***	13.50	0.468	38.3	12.55	14.4

Supplementary Table S17. Multiple comparison test of root bark QTL groups within each time point for trunk diameter below the graft union in the root architecture experiment. Results are averaged over the levels of: Block. Degrees-of-freedom method: kenward-roger. P value adjustment: tukey method for comparing a family of 4 estimates.

TP	contrast	estimate	SE	df	t.ratio	p.value
TP1	**NoRb – *Rb1***	0.3176	0.750	38.2	0.424	0.9741
TP1	**NoRb – *Rb1Rb2***	0.2659	0.716	38.3	0.371	0.9823
TP1	**NoRb – *Rb2***	-0.2949	0.789	38.3	-0.374	0.9819
TP1	***Rb1* – *Rb1Rb2***	-0.0516	0.696	38.3	-0.074	0.9999
TP1	***Rb1* – *Rb2***	-0.6125	0.771	38.3	-0.795	0.8563
TP1	***Rb1Rb2* – *Rb2***	0.5608	0.740	38.3	0.758	0.8727
TP2	**NoRb – *Rb1***	0.6312	0.750	38.2	0.842	0.8341
TP2	**NoRb – *Rb1Rb2***	0.6109	0.716	38.3	0.853	0.8288
TP2	**NoRb – *Rb2***	0.1730	0.789	38.3	0.219	0.9962
TP2	***Rb1* – *Rb1Rb2***	-0.0203	0.609	38.3	-0.029	1.0000
TP2	***Rb1* – *Rb2***	-0.4582	0.771	38.3	-0.595	0.9331
TP2	***Rb1Rb2* – *Rb2***	0.4379	0.740	38.3	0.592	0.9339
TP3	**NoRb – *Rb1***	0.5323	0.750	38.2	0.710	0.8925
TP3	**NoRb – *Rb1Rb2***	0.3970	0.716	38.3	0.554	0.9448
TP3	**NoRb – *Rb2***	-0.1834	0.789	38.3	-0.232	0.9955
TP3	***Rb1* – *Rb1Rb2***	-0.1353	0.696	38.3	-0.194	0.9973
TP3	***Rb1* – *Rb2***	-0.7157	0.771	38.3	-0.929	0.7896

TP3	***Rb1Rb2* – *Rb2***	0.5804	0.740	38.3	0.784	0.8610
TP4	**NoRb – *Rb1***	0.5783	0.750	38.2	0.771	0.8669
TP4	**NoRb – *Rb1Rb2***	0.3329	0.716	38.3	0.465	0.9663
TP4	**NoRb – *Rb2***	-0.3509	0.789	38.3	-0.445	0.9703
TP4	***Rb1* – *Rb1Rb2***	-0.2455	0.696	38.3	-0.353	0.9847
TP4	***Rb1* – *Rb2***	-0.9292	0.771	38.3	-1.206	0.6269
TP4	***Rb1Rb2* – *Rb2***	0.6837	0.740	38.3	0.924	0.7921

TOTAL ROOT LENGTH

Supplementary Table S18. Estimated marginal means (EMMs) for linear mixed model of each root bark QTL group within each time point for total root length in the root architecture experiment. Results are averaged over the levels of: block. Degrees of freedom method: Kenward-roger. Confidence level used: 0.95

TP	RB QTL group	emmean	SE	df	Lower.CL	Upper.CL
TP1	**NoRb**	56.3	8.00	70.3	40.3	72.3
TP1	***Rb1***	48.2	7.59	70.2	33.0	63.3
TP1	***Rb2***	50.0	8.46	70.6	33.1	66.9
TP1	***Rb1Rb2***	52.9	6.91	70.6	39.2	66.7
TP2	**NoRb**	86.0	8.00	70.3	70.0	101.9
TP2	***Rb1***	87.9	7.59	70.2	72.8	103.1
TP2	***Rb2***	84.9	8.46	70.6	68.1	101.8
TP2	***Rb1Rb2***	82.5	6.91	70.6	68.7	96.3
TP3	**NoRb**	126.7	8.00	70.3	110.8	142.7
TP3	***Rb1***	128.8	7.59	70.2	113.7	144.0
TP3	***Rb2***	134.0	8.46	70.6	117.1	150.9
TP3	***Rb1Rb2***	115.6	6.91	70.6	101.8	129.4
TP4	**NoRb**	158.6	8.00	70.3	142.6	174.5
TP4	***Rb1***	154.1	7.59	70.2	138.9	169.2
TP4	***Rb2***	151.5	8.46	70.6	134.7	168.4
TP4	***Rb1Rb2***	132.2	6.91	70.6	118.4	146.0

Supplementary Table S19. Multiple comparison test of root bark QTL groups within each time point for total root length in the root architecture experiment. Results are averaged over the levels of: Block. Degrees-of-freedom method: kenward-roger. P value adjustment: tukey method for comparing a family of 4 estimates. Significant p-values in bold.

TP	contrast	estimate	SE	df	t.ratio	p.value
TP1	**NoRb – *Rb1***	8.10	11.0	70.1	0.734	0.8833
TP1	**NoRb – *Rb1Rb2***	3.35	10.6	70.4	0.317	0.9889
TP1	**NoRb – *Rb2***	6.31	11.6	70.5	0.542	0.9483
TP1	***Rb1* – *Rb1Rb2***	-4.76	10.3	70.4	-0.463	0.9668
TP1	***Rb1* – *Rb2***	-1.79	11.4	70.4	-0.157	0.9986
TP1	***Rb1Rb2* – *Rb2***	-2.97	10.9	70.6	-0.271	0.9929
TP2	**NoRb – *Rb1***	-1.96	11.0	70.1	-0.177	0.9980
TP2	**NoRb – *Rb1Rb2***	3.46	10.6	70.4	0.327	0.9878
TP2	**NoRb – *Rb2***	1.04	11.6	70.5	0.089	0.9997
TP2	***Rb1* – *Rb1Rb2***	5.42	10.3	70.4	0.528	0.9520
TP2	***Rb1* – *Rb2***	3.00	11.4	70.4	0.264	0.9935
TP2	***Rb1Rb2* – *Rb2***	2.42	10.9	70.6	0.222	0.9961
TP3	**NoRb – *Rb1***	-2.09	11.0	70.1	-0.189	0.9976
TP3	**NoRb – *Rb1Rb2***	11.11	10.6	70.4	1.051	0.7204
TP3	**NoRb – *Rb2***	-7.30	11.6	70.5	-0.627	0.9230
TP3	***Rb1* – *Rb1Rb2***	13.20	10.3	70.4	1.285	0.5751

TP3	***Rb1 – Rb2***	-5.21	11.4	70.4	-0.458	0.9678
TP3	***Rb1Rb2 – Rb2***	18.41	10.9	70.6	1.685	0.3392
TP4	**NoRb – *Rb1***	4.49	11.0	70.1	0.407	0.9771
TP4	**NoRb – *Rb1Rb2***	26.39	10.6	70.4	2.497	*0.0691*
TP4	**NoRb – *Rb2***	7.05	11.6	70.5	0.606	0.9299
TP4	***Rb1 – Rb1Rb2***	21.90	10.3	70.4	2.133	0.1527
TP4	***Rb1 – Rb2***	2.56	11.4	70.4	0.225	0.9959
TP4	***Rb1Rb2 – Rb2***	19.34	10.9	70.6	1.770	0.2961

MAXIMUM ROOT DIAMETER

Supplementary Table S20. Multiple comparison test of time point for maximum root diameter in the root architecture experiment. Results are averaged over the levels of: *Rb1, Rb2* and block. Degrees-of-freedom method: kenward-roger. P value adjustment: tukey method for comparing a family of 4 estimates. Significant p-values in bold.

contrast	estimate	SE	df	t.ratio	p.value
TP1 - TP2	-0.701	0.171	105	-4.108	**0.0005**
TP1 - TP3	-1.066	0.171	105	-6.242	**<0.0001**
TP1 - TP4	-1.492	0.171	105	-8.734	**<0.0001**
TP2 - TP3	-0.365	0.171	105	-2.135	0.1489
TP2 - TP4	-0.790	0.171	105	-4.627	**0.0001**
TP3 - TP4	-0.426	0.171	105	-2.492	0.0671

Supplementary Table S21. Estimated marginal means (EMMs) for linear mixed model of each root bark QTL group within each time point for maximum root diameter in the root architecture experiment. Results are averaged over the levels of: block. Degrees of freedom method: Kenward-roger. Confidence level used: 0.95.

TP	RB QTL group	emmean	SE	df	Lower.CL	Upper.CL
TP1	**NoRb**	3.57	0.257	134	3.06	4.08
TP1	***Rb1***	2.65	0.244	134	2.17	3.13
TP1	***Rb2***	3.10	0.272	134	2.57	3.64
TP1	***Rb1Rb2***	2.99	0.222	134	2.55	3.43
TP2	**NoRb**	3.76	0.257	134	3.25	4.27
TP2	***Rb1***	3.66	0.244	134	3.18	4.15
TP2	***Rb2***	3.82	0.272	134	3.28	4.36
TP2	***Rb1Rb2***	3.88	0.222	134	3.44	4.31
TP3	**NoRb**	4.09	0.257	134	3.58	4.60
TP3	***Rb1***	4.22	0.244	134	3.74	4.70
TP3	***Rb2***	4.00	0.272	134	3.47	4.54
TP3	***Rb1Rb2***	4.26	0.222	134	3.83	4.70
TP4	**NoRb**	4.74	0.257	134	4.23	5.25
TP4	***Rb1***	4.65	0.244	134	4.17	5.13
TP4	***Rb2***	4.76	0.272	134	4.22	5.30
TP4	***Rb1Rb2***	4.13	0.222	134	3.69	4.57

Supplementary Table S22. Multiple comparison test of root bark QTL groups within each time point for maximum root diameter in the root architecture experiment. Results are averaged over the levels of: Block. Degrees-of-freedom method: kenward-roger. P value adjustment: tukey method for comparing a family of 4 estimates. Significant p-values in bold.

TP	contrast	estimate	SE	df	t.ratio	p.value
TP1	**NoRb – *Rb1***	0.9234	0.354	134	2.607	**0.0493**
TP1	**NoRb – *Rb1Rb2***	0.5803	0.339	134	1.710	0.3228
TP1	**NoRb – *Rb2***	0.4678	0.374	134	1.251	0.5958
TP1	***Rb1* – *Rb1Rb2***	-0.3431	0.330	134	-1.041	0.7258
TP1	***Rb1* – *Rb2***	-0.4556	0.365	134	-1.248	0.5976
TP1	***Rb1Rb2* – *Rb2***	0.1125	0.351	134	0.321	0.9886
TP2	**NoRb – *Rb1***	0.0938	0.354	134	0.265	0.9935
TP2	**NoRb – *Rb1Rb2***	-0.1170	0.339	134	-0.345	0.9859
TP2	**NoRb – *Rb2***	-0.0632	0.374	134	-0.169	0.9983
TP2	***Rb1* – *Rb1Rb2***	-0.2108	0.330	134	-0.640	0.9190
TP2	***Rb1* – *Rb2***	-01570	0.365	134	-0.430	0.9732
TP2	***Rb1Rb2* – *Rb2***	-0.0538	0.351	134	-0.153	0.9987
TP3	**NoRb – *Rb1***	-0.1268	0.354	134	-0.358	0.9842
TP3	**NoRb – *Rb1Rb2***	-0.1741	0.339	134	-0.513	0.9559
TP3	**NoRb – *Rb2***	0.0872	0.374	134	0.233	0.9955
TP3	***Rb1* – *Rb1Rb2***	-0.0473	0.330	134	-0.143	0.9989

TP3	***Rb1 – Rb2***	0.2140	0.365	134	0.586	0.9362
TP3	***Rb1Rb2 – Rb2***	-0.2612	0.351	134	-0.744	0.8791
TP4	**NoRb – *Rb1***	0.0904	0.354	134	0.255	0.9942
TP4	**NoRb – *Rb1Rb2***	0.6168	0.339	134	1.817	0.2699
TP4	**NoRb – *Rb2***	-0.0163	0.374	134	-0.044	1.000
TP4	***Rb1 – Rb1Rb2***	0.5264	0.330	134	1.597	0.3839
TP4	***Rb1 – Rb2***	-0.1066	0.365	134	-0.292	0.9913
TP4	***Rb1Rb2 – Rb2***	0.6330	0.351	134	1.803	0.2765

MEAN ROOT DIAMETER

Supplementary Table S23. Multiple comparison test of time point for mean root diameter in the root architecture experiment. Results are averaged over the levels of: *Rb1, Rb2* and block. Degrees of freedom method: Kenward-roger. P value adjustment: tukey method for comparing a family of 4 estimates. Significant p-values in bold.

contrast	estimate	SE	df	t.ratio	p.value
TP1 - TP2	-0.1145	0.0389	105	-2.941	**0.0206**
TP1 - TP3	-0.0315	0.0389	105	-0.808	0.8504
TP1 - TP4	-0.0929	0.0389	105	-2.388	0.0856
TP2 - TP3	0.0830	0.0389	105	2.133	0.1494
TP2 - TP4	0.0215	0.0389	105	0.553	0.9455
TP3 - TP4	-0.0615	0.0389	105	-1.580	0.3945

Supplementary Table S24. Estimated marginal means (EMMs) for linear mixed model of each root bark QTL group within each time point for mean root diameter in the root architecture experiment. Results are averaged over the levels of: block. Degrees of freedom method: Kenward-roger. Confidence level used: 0.95.

TP	RB QTL group	emmean	SE	df	Lower.CL	Upper.CL
TP1	**NoRb**	-0.172	0.0567	137	-0.284	-0.0598
TP1	***Rb1***	-0.325	0.0538	137	-0.432	-0.2191
TP1	***Rb2***	-0.284	0.0601	137	-0.403	-0.1651
TP1	***Rb1Rb2***	-0.241	0.0491	137	-0.338	-0.1438
TP2	**NoRb**	-0.159	0.0567	137	-0.271	-0.0470
TP2	***Rb1***	-0.157	0.0538	137	-0.263	-0.0503
TP2	***Rb2***	-0.137	0.0601	137	-0.256	-0.0186
TP2	***Rb1Rb2***	-0.111	0.0491	137	-0.208	-0.0139
TP3	**NoRb**	-0.211	0.0567	137	-0.324	-0.0993
TP3	***Rb1***	-0.209	0.0538	137	-0.315	-0.1026
TP3	***Rb2***	-0.277	0.0601	137	-0.396	-0.1581
TP3	***Rb1Rb2***	-0.199	0.0491	137	-0.296	-0.1019
TP4	**NoRb**	-0.138	0.0567	137	-0.250	-0.0257
TP4	**Rb1**	-0.198	0.0538	137	-0.304	-0.0915
TP4	**Rb2**	-0.107	0.0601	137	-0.226	0.0114
TP4	**Rb1Rb2**	-0.207	0.0491	137	-0.304	-0.1101

Supplementary Table S25. Multiple comparison test of root bark QTL groups within each time point for mean root diameter in the root architecture experiment. Results are averaged over the levels of: Block. Degrees-of-freedom method: kenward-roger. P value adjustment: tukey method for comparing a family of 4 estimates. Significant p-values in bold.

TP	contrast	estimate	SE	df	t.ratio	p.value
TP1	**NoRb – *Rb1***	0.15349	0.0782	137	1.962	0.2077
TP1	**NoRb – *Rb1Rb2***	0.06880	0.0750	137	0.917	0.7956
TP1	**NoRb – *Rb2***	0.11190	0.0826	137	1.354	0.5302
TP1	***Rb1* – *Rb1Rb2***	-0.08469	0.0728	137	-1.163	0.6512
TP1	***Rb1* – *Rb2***	-0.04159	0.0807	137	-0.516	0.9553
TP1	***Rb1Rb2* – *Rb2***	-0.04310	0.0776	137	-0.556	0.9449
TP2	**NoRb – *Rb1***	-0.00243	0.0782	137	-0.031	1.0000
TP2	**NoRb – *Rb1Rb2***	-0.04827	0.0750	137	-0.644	0.9176
TP2	**NoRb – *Rb2***	-0.02168	0.0826	137	-0.262	0.9936
TP2	***Rb1* – *Rb1Rb2***	-0.04584	0.0728	137	-0.629	0.9224
TP2	***Rb1* – *Rb2***	-0.01925	0.0807	137	-0.239	0.9952
TP2	***Rb1Rb2* – *Rb2***	-0.02658	0.0776	137	-0.343	0.9861
TP3	**NoRb – *Rb1***	-0.00245	0.0782	137	-0.031	1.0000
TP3	**NoRb – *Rb1Rb2***	-0.01256	0.0750	137	-0.168	0.9983
TP3	**NoRb – *Rb2***	0.06547	0.0826	137	-0.369	0.9828
TP3	***Rb1* – *Rb1Rb2***	-0.01011	0.0728	137	-0.139	0.9990

TP3	***Rb1 – Rb2***	0.06792	0.0807	137	0.842	0.8343
TP3	***Rb1Rb2 – Rb2***	-0.07804	0.0776	137	-1.006	0.7463
TP4	**NoRb – *Rb1***	0.06006	0.0782	137	0.768	0.8689
TP4	**NoRb – *Rb1Rb2***	0.06922	0.0750	137	0.923	0.7926
TP4	**NoRb – *Rb2***	-0.03049	0.0826	137	-0.369	0.9828
TP4	***Rb1 – Rb1Rb2***	0.00916	0.0728	137	0.126	0.9993
TP4	***Rb1 – Rb2***	-0.09055	0.0807	137	-1.122	0.6764
TP4	***Rb1Rb2 – Rb2***	0.09971	0.0776	137	1.285	0.5739

MAXIMUM ROOT DEPTH

Supplementary Table S26. Multiple comparison test of block for maximum root depth in the root architecture experiment. Results are averaged over the levels of: *Rb1, Rb2* and TP. Degrees of freedom method: Kenward-roger. P value adjustment: tukey method for comparing a family of 4 estimates. Significant p-values in bold.

contrast	estimate	SE	df	t.ratio	p.value
A – B	-69.167	37.8	32	-1.831	0.2777
A – C	-68.540	38.7	32	-1.772	0.3049
A – D	119.559	37.6	32	3.183	**0.0163**
B – C	0.627	38.7	32	0.016	1.0000
B – D	188.726	37.8	32	4.997	**0.0001**
C – D	188.099	38.7	32	4.864	**0.0002**

Supplementary Table S27. Estimated marginal means (EMMs) for linear mixed model of each root bark QTL group within each time point for maximum root depth in the root architecture experiment. Results are averaged over the levels of: block. Degrees of freedom method: Kenward-roger. Confidence level used: 0.95.

TP	RB QTL group	emmean	SE	df	Lower.CL	Upper.CL
TP1	**NoRb**	329	35.6	74.3	258	400
TP1	***Rb1***	324	33.8	74.2	257	392
TP1	***Rb2***	307	37.7	74.6	232	382
TP1	***Rb1Rb2***	332	30.8	74.6	271	393
TP2	**NoRb**	632	35.6	74.3	561	703
TP2	***Rb1***	640	33.8	74.2	573	708
TP2	***Rb2***	647	37.7	74.6	572	723
TP2	***Rb1Rb2***	570	30.8	74.6	508	631
TP3	**NoRb**	877	35.6	74.3	806	948
TP3	***Rb1***	810	33.8	74.2	743	877
TP3	***Rb2***	872	37.7	74.6	797	947
TP3	***Rb1Rb2***	705	30.8	74.6	644	767
TP4	**NoRb**	915	35.6	74.3	844	986
TP4	***Rb1***	929	33.8	74.2	862	997
TP4	***Rb2***	927	37.7	74.6	852	1002
TP4	***Rb1Rb2***	790	30.8	74.6	728	851

Supplementary Table S28. Multiple comparison test of root bark QTL groups within each time point for maximum root depth in the root architecture experiment. Results are averaged over the levels of: Block. Degrees-of-freedom method: kenward-roger. P value adjustment: tukey method for comparing a family of 4 estimates. Significant p-values in bold.

TP	contrast	estimate	SE	df	t.ratio	p.value
TP1	**NoRb – *Rb1***	4.68	49.2	74.0	0.095	0.9997
TP1	**NoRb – *Rb1Rb2***	-2.84	47.1	74.4	-0.060	0.9999
TP1	**NoRb – *Rb2***	22.41	51.9	74.5	0.0432	0.9728
TP1	***Rb1* – *Rb1Rb2***	-7.52	45.7	74.4	-0.164	0.9984
TP1	***Rb1* – *Rb2***	17.72	50.7	74.4	0.350	0.9852
TP1	***Rb1Rb2* – *Rb2***	-25.24	48.7	74.6	-0.519	0.9544
TP2	**NoRb – *Rb1***	-7.99	49.2	74.0	-0.162	0.9985
TP2	**NoRb – *Rb1Rb2***	62.64	47.1	74.4	1.330	0.5470
TP2	**NoRb – *Rb2***	-15.08	51.9	74.5	-0.291	0.9914
TP2	***Rb1* – *Rb1Rb2***	70.63	45.7	74.4	1.544	0.4168
TP2	***Rb1* – *Rb2***	-7.09	50.7	74.4	-0.140	0.9990
TP2	***Rb1Rb2* – *Rb2***	77.72	48.7	74.6	1.597	0.3867
TP3	**NoRb – *Rb1***	66.54	49.2	74.0	1.352	0.5333
TP3	**NoRb – *Rb1Rb2***	171.20	47.1	74.4	3.635	**0.0028**
TP3	**NoRb – *Rb2***	4.24	51.9	74.5	0.082	0.9998
TP3	***Rb1* – *Rb1Rb2***	104.66	45.7	74.4	2.288	0.1101

TP3	***Rb1 – Rb2***	-62.30	50.7	74.4	-1.230	0.6100
TP3	***Rb1Rb2 – Rb2***	166.96	48.7	74.6	3.430	**0.0053**
TP4	**NoRb – *Rb1***	-14.53	49.2	74.0	-0.295	0.9910
TP4	**NoRb – *Rb1Rb2***	124.92	47.1	74.4	2.653	**0.0471**
TP4	**NoRb – *Rb2***	-12.05	51.9	74.5	-0.232	0.9956
TP4	***Rb1 – Rb1Rb2***	139.45	45.7	74.4	3.049	**0.0164**
TP4	***Rb1 – Rb2***	2.49	50.7	74.4	0.049	1.0000
TP4	***Rb1Rb2 – Rb2***	136.97	48.7	74.6	2.814	**0.0311**

CONVEX HULL AREA

Supplementary Table S29. Multiple comparison test of block for convex hull area in the root architecture experiment. Results are averaged over the levels of: *Rb1, Rb2* and TP. Degrees-of-freedom method: kenward-roger. P value adjustment: tukey method for comparing a family of 4 estimates. Significant p-values in bold.

contrast	estimate	SE	df	t.ratio	p.value
A – B	-16204	10903	32	-1.486	0.4573
A – C	-20808	11164	32	-1.864	0.2635
A – D	34364	10845	32	3.169	**0.0168**
B – C	-4603	11165	32	-0.412	0.9760
B – D	50569	10903	32	4.638	**0.0003**
C – D	55172	11164	32	4.942	**0.0001**

Supplementary Table S30. Estimated marginal means (EMMs) for linear mixed model of each root bark QTL group within each time point for convex hull area in the root architecture experiment. Results are averaged over the levels of: block. Degrees of freedom method: Kenward-roger. Confidence level used: 0.95

TP	RB QTL group	emmean	SE	df	Lower.CL	Upper.CL
TP1	**NoRb**	64101	9905	66.1	44327	83876
TP1	***Rb1***	62415	9402	66.0	43643	81187
TP1	***Rb2***	54555	10476	66.4	33642	75468
TP1	***Rb1Rb2***	66086	8553	66.4	49010	83161
TP2	**NoRb**	143943	9905	66.1	124169	163718
TP2	***Rb1***	145845	9402	66.0	127073	164617
TP2	***Rb2***	144085	10476	66.4	123172	164998
TP2	***Rb1Rb2***	131439	8553	66.4	114364	148514
TP3	**NoRb**	211174	9905	66.1	191399	230948
TP3	***Rb1***	194198	9402	66.0	175426	212970
TP3	***Rb2***	203173	10476	66.4	182260	224086
TP3	***Rb1Rb2***	165906	8553	66.4	148830	182981
TP4	**NoRb**	227695	9905	66.1	207920	247469
TP4	***Rb1***	228228	9402	66.0	209456	247000
TP4	***Rb2***	228470	10476	66.4	207558	249383
TP4	***Rb1Rb2***	186527	8553	66.4	169451	203602

Supplementary Table S31. Multiple comparison test of root bark QTL groups within each time point for convex hull area in the root architecture experiment. Results are averaged over the levels of: Block. Degrees-of-freedom method: kenward-roger. P value adjustment: tukey method for comparing a family of 4 estimates. Significant p-values in bold.

TP	contrast	estimate	SE	df	t.ratio	p.value
TP1	**NoRb – *Rb1***	1686	13680	65.9	0.123	0.9993
TP1	**NoRb – *Rb1Rb2***	-1984	13087	66.2	-0.152	0.9987
TP1	**NoRb – *Rb2***	9546	14417	66.3	0.662	0.9109
TP1	***Rb1* – *Rb1Rb2***	-3671	12711	66.2	-0.289	0.9915
TP1	***Rb1* – *Rb2***	7860	14076	66.2	0.558	0.9439
TP1	***Rb1Rb2* – *Rb2***	-11531	13524	66.4	-0.853	0.8290
TP2	**NoRb – *Rb1***	-1901	13680	65.9	-0.139	0.9990
TP2	**NoRb – *Rb1Rb2***	12504	13087	66.2	0.956	0.7750
TP2	**NoRb – *Rb2***	-141	14417	66.3	-0.010	1.0000
TP2	***Rb1* – *Rb1Rb2***	14406	12711	66.2	1.133	0.6704
TP2	***Rb1* – *Rb2***	1760	14076	66.2	0.125	0.9993
TP2	***Rb1Rb2* – *Rb2***	12646	13524	66.4	0.935	0.7861
TP3	**NoRb – *Rb1***	16975	13680	65.9	1.241	0.6034
TP3	**NoRb – *Rb1Rb2***	45268	13087	66.2	3.459	**0.0051**
TP3	**NoRb – *Rb2***	8001	14417	66.3	0.555	0.9449
TP3	***Rb1* – *Rb1Rb2***	28293	12711	66.2	2.226	0.1269

TP3	***Rb1 – Rb2***	-8975	14076	66.2	-0.638	0.9195
TP3	***Rb1Rb2 – Rb2***	37267	13524	66.4	2.756	**0.0370**
TP4	**NoRb – *Rb1***	-534	13680	65.9	-0.039	1.0000
TP4	**NoRb – *Rb1Rb2***	41168	13087	66.2	3.146	**0.0129**
TP4	**NoRb – *Rb2***	-776	14417	66.3	-0.054	0.9999
TP4	***Rb1 – Rb1Rb2***	41702	12711	66.2	3.281	**0.0088**
TP4	***Rb1 – Rb2***	-242	14076	66.2	-0.017	1.0000
TP4	***Rb1Rb2 – Rb2***	41944	13524	66.4	3.101	**0.0147**

ROOT BARK PERCENTAGE

Supplementary Table S32. Estimated marginal means (EMMs) of the ANOVA for each root bark QTL group for root bark percentage in the root architecture experiment. Results are averaged over the levels of: Block. Confidence level used: 0.95.

Block	emmean	SE	df	Lower.CL	Upper.CL
NoRb	57.7	1.99	32	53.6	61.7
Rb1	59.4	1.89	32	55.5	63.2
Rb2	55.8	2.10	32	51.5	60.1
Rb1Rb2	68.7	1.72	32	65.2	72.2

Supplementary Table S33. Multiple comparison test of root bark QTL groups for root bark percentage in the root architecture experiment. Results are averaged over the levels of: Block. P value adjustment: tukey method for comparing a family of 4 estimates. Significant p-values in bold.

contrast	estimate	SE	df	t.ratio	p.value
NoRb - *Rb1*	-1.71	2.75	32	-0.620	0.9250
NoRb - *Rb2*	1.85	2.90	32	0.639	0.9185
NoRb - *Rb1Rb2*	-11.02	2.63	32	-4.192	**0.0011**
Rb1 - Rb2	3.56	2.83	32	1.258	0.5956
Rb1 - Rb1Rb2	-9.31	2.55	32	-3.648	**0.0049**
Rb2 - Rb1Rb2	-12.87	2.71	32	-4.742	**0.0002**

WET CANOPY WEIGHT

Supplementary Table S34. Estimated marginal means (EMMs) of the ANOVA for each root bark QTL group for wet canopy in the root architecture experiment. Results are averaged over the levels of: Block. Confidence level used: 0.95.

Block	emmean	SE	df	Lower.CL	Upper.CL
NoRb	258	15.6	32	227	290
Rb1	226	16.5	32	193	260
Rb2	201	14.8	32	171	231
Rb1Rb2	198	13.5	32	170	225

Supplementary Table S35. Multiple comparison test of root bark QTL groups for wet canopy weight in the root architecture experiment. Results are averaged over the levels of: Block. P value adjustment: tukey method for comparing a family of 4 estimates. Significant p-values in bold.

contrast	estimate	SE	df	t.ratio	p.value
NoRb - *Rb1*	32.28	22.7	32	1.421	0.4962
NoRb - *Rb2*	57.55	21.6	32	2.665	0.0553
NoRb - *Rb1Rb2*	60.55	20.6	32	2.935	**0.0297**
Rb1 - Rb2	25.28	22.2	32	1.139	0.6684
Rb1 - Rb1Rb2	28.27	21.3	32	1.327	0.5529
Rb2 - Rb1Rb2	2.99	20.0	32	0.149	0.9988

WET ROOT WEIGHT

Supplementary Table S36. Estimated marginal means (EMMs) of the ANOVA for each root bark QTL group for wet root weight in the root architecture experiment. Results are averaged over the levels of: Block. Confidence level used: 0.95.

Block	emmean	SE	df	Lower.CL	Upper.CL
NoRb	273	19.2	32	234	312
Rb1	261	20.2	32	220	302
Rb2	232	18.2	32	195	269
Rb1Rb2	205	16.5	32	171	238

Supplementary Table S37. Multiple comparison test of root bark QTL groups for wet canopy weight in the root architecture experiment. Results are averaged over the levels of: Block. P value adjustment: tukey method for comparing a family of 4 estimates. Significant p-values in bold.

contrast	estimate	SE	df	t.ratio	p.value
NoRb - *Rb1*	12.1	27.9	32	0.436	0.9718
NoRb - *Rb2*	40.9	26.5	32	1.545	0.4235
NoRb - *Rb1Rb2*	68.5	25.3	32	2.707	0.0503
Rb1 - Rb2	28.8	27.2	32	1.058	0.7172
Rb1 - Rb1Rb2	56.3	26.1	32	2.157	0.1573
Rb2 - Rb1Rb2	27.6	24.6	32	1.122	0.6792

WET ROOT-TO-SHOOT RATIO

Supplementary Table S38. Estimated marginal means (EMMs) of the ANOVA for each root bark QTL group for wet root-to-shoot ratio in the root architecture experiment. Results are averaged over the levels of: Block. Confidence level used: 0.95.

Block	emmean	SE	df	Lower.CL	Upper.CL
NoRb	1.06	0.0851	32	0.887	1.23
Rb1	1.19	0.0899	32	1.004	1.37
Rb2	1.19	0.0808	32	1.022	1.35
Rb1Rb2	1.04	0.0734	32	0.890	1.19

Supplementary Table S39. Multiple comparison test of root bark QTL groups for root-to-shoot ratio in the root architecture experiment. Results are averaged over the levels of: Block. P value adjustment: tukey method for comparing a family of 4 estimates. Significant p-values in bold.

contrast	estimate	SE	df	t.ratio	p.value
NoRb - *Rb1*	-0.126469	0.124	32	-1.022	0.7380
NoRb - Rb2	-0.126743	0.118	32	-1.077	0.7056
NoRb - *Rb1Rb2*	0.021229	0.112	32	0.189	0.9976
Rb1 - Rb2	-0.000275	0.121	32	-0.002	1.0000
Rb1 - Rb1Rb2	0.147697	0.116	32	1.273	0.5863
Rb2 - Rb1Rb2	0.147972	0.109	32	1.356	0.5355